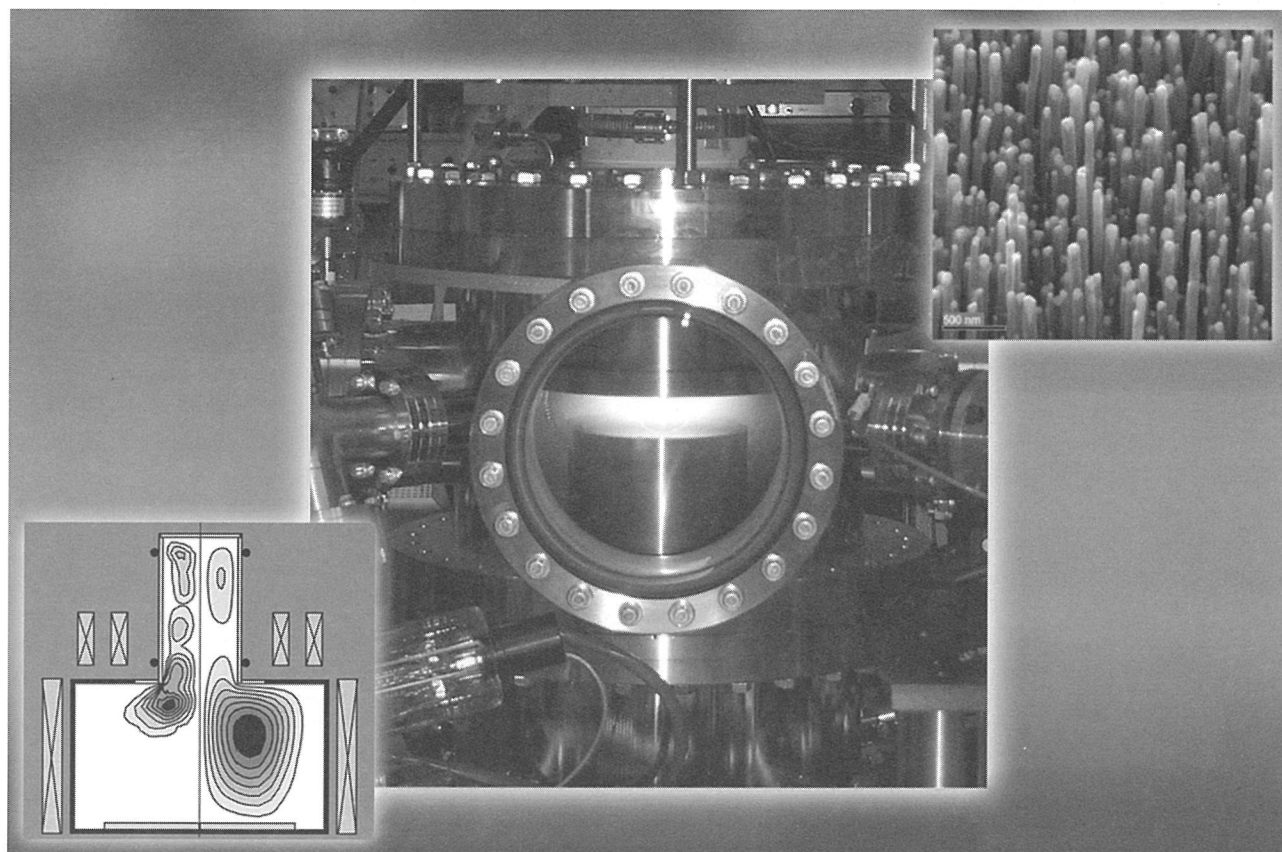


BULLETIN

OF THE AMERICAN PHYSICAL SOCIETY

PROGRAM OF THE 56th ANNUAL
GASEOUS ELECTRONICS CONFERENCE



October 2003
Volume 48, No. 6

October 21–24, 2003
San Francisco, California

BULLETIN

OF THE AMERICAN PHYSICAL SOCIETY

Coden BAPSA6
Series II, Vol. 48, No. 6

ISSN: 0003-0503
October 2003

APS COUNCIL 2003

President

Myriam P. Sarachik,* *City College of New York-CUNY*

President-Elect

Helen R. Quinn,* *Stanford University (SLAC)*

Vice President

Marvin L. Cohen,* *University of California, Berkeley*

Executive Officer

Judy R. Franz,* *University of Alabama, Huntsville (on leave)*

Treasurer

Thomas McIlrath,* *University of Maryland (emeritus)*

Editor-in-Chief

Martin Blume,* *Brookhaven National Laboratory*

Past-President

William F. Brinkman,* *Bell Labs-Lucent Technologies (Ret.)*

General Councillors

Jonathan A. Bagger,* Janet Conrad, Stuart Freedman,* Frances Houle, Gerald Mahan, Margaret Murnane,* Cherry Ann Murray,* Philip Phillips,* Laura Smoliar, Jin-Joo Song

International Councillor

T. Maurice Rice

Chair, Nominating Committee

Susan Seestrom

Chair, Panel on Public Affairs

John Ahearne

Division, Forum and Section Councillors

Kate Kirby (*Atomic, Molecular & Optical Physics*), Robert Eisenberg (*Biological*), Sylvia Ceyer (*Chemical*), Allen Goldman* (*Condensed Matter Physics*), Steven White (*Computational*), Harry Swinney (*Fluid Dynamics*), Peter Zimmerman (*Forum on Education*), Stuart Wolf (*Forum on Industrial and Applied Physics*), Gloria Lubkin (*Forum on History of Physics*), James Vary (*Forum on International Physics*), Ed Gerjuoy (*Forum on Physics and Society*), Timothy P. Lodge (*Polymer Physics*), J.H. Eberly (*Laser Science*), G. Slade Cargill, III* (*Materials*), Bunny C. Clark (*Nuclear*), Sally Dawson, Peter Meyers (*Particles & Fields*), Stephen Holmes (*Physics of Beams*), James Drake (*Plasma*), Gian Vidali (*New York Section*), Joe Hamilton (*Southeast Section*)

*Members of the APS Executive Board

ADVISORS

Representatives from other Societies

Charles H. Holbrow, *AAPT*; Marc Brodsky, *AIP*

International Advisors

Gerardo C. Puente, *Mexican Physical Society*;
Bela Joos, *Canadian Association of Physicists*

Editor: Donna M. Baudrau, CMP

Meetings Abstracts Coordinator:

Laura Walsh

APS MEETINGS DEPARTMENT

One Physics Ellipse

College Park, MD 20740-3844

Telephone: (301) 209-3286

FAX: (301) 209-0866

Donna Baudrau, *Director of Meetings & Conventions*

Terri Gaier, *Senior Meeting Planner*

Daren Dean, *Meeting Planner*

Don Wise, *Registrar*

Staff Representatives

Alan Chodos, *Associate Executive Officer*; Irving Lerch, *Director of International Affairs*; Fredrick Stein, *Director of Education and Outreach*; Robert L. Park, *Director, Public Information*; Michael Lubell, *Director, Public Affairs*; Stanley Brown, *Editorial Director*; Charles Muller, *Director, Journal Operations*; Michael Stephens, *Controller and Assistant Treasurer*

Administrator for Governing Committees

Ken Cole

The *Bulletin of the American Physical Society* is published 11X in 2003—March, April, May, July (2X), October (3X), November (2X), and December—by the American Physical Society through the American Institute of Physics. It contains information about meetings of the Society, including abstracts of papers to be presented, as well as transactions of past meetings. Reprints of papers can be obtained only by writing directly to the authors.

The *Bulletin* is delivered, on subscription, by Periodicals mail. Complete volumes are also available on microfilm. **APS Members** may subscribe to individual issues, or for the entire year. **Nonmembers** may subscribe to the *Bulletin* at the following rates: Domestic \$635; Foreign Surface \$660; Air Freight \$680. Information on prices, as well as subscription orders, renewals, and address changes, should be addressed as follows: **For APS Members**—Membership Department, American Physical Society, One Physics Ellipse, College Park, MD 20740-3844. **For Nonmembers**—Circulation and Fulfillment Division, The American Institute of Physics, Suite 1N01, 2 Huntington Quadrangle, Melville, NY 11747-4502. Allow at least 6 weeks advance notice. For address changes, please send both the old and new addresses, and, if possible, include a mailing label from a recent issue. Requests from subscribers for missing issues will be honored without charge only if received within 6 months of the issue's actual date of publication.

The *Bulletin of the American Physical Society* (ISSN: 0003-0503) is published eleven times a year for the American Physical Society by the American Institute of Physics. 2003 subscription rate is \$635 for domestic nonmembers. Postmaster: Send address changes to *Bulletin of the American Physical Society*, AIP, Suite 1N01, 2 Huntington Quadrangle, Melville, NY 11747-4502. Periodicals postage paid at Huntington Station, NY, and additional mailing offices.

BULLETIN

OF THE AMERICAN PHYSICAL SOCIETY

Vol. 48, No. 6, October 2003

56th Annual Gaseous Electronics Conference

TABLE OF CONTENTS

General Information	3
Special Sessions and Events	3
<i>Sessions</i>	3
<i>Presentation Formats</i>	4
<i>GEC Student Award for Excellence</i>	4
Registration	5
Banquet and Reception	5
E-mail and Other Business Services	5
Audio-Visual Equipment	5
Dining Options	5
Guest Program	5
Call for Nominations for GEC General and Executive Committees	5
<i>GEC 2003 Executive Committee</i>	6
<i>Conference Secretary</i>	6
Please Note	6
Epitome	7
Main Text	10
<i>Tuesday, October 21, 2003</i>	10

<i>Wednesday, October 22, 2003</i>	37
<i>Thursday, October 23, 2003</i>	60
<i>Friday, October 24, 2003</i>	80
Author Index	90
Map	At End of Issue

56th Annual Gaseous Electronics Conference
October 21–24, 2003
NASA Ames Research Center
San Francisco, California

GENERAL INFORMATION

Welcome to the 56th Annual Gaseous Electronics Conference (GEC) of the American Physical Society (APS). The GEC 2003 program includes the GEC Foundation Talk and the annual GEC Student Award for Excellence. Oral sessions with both invited and contributed papers and three poster sessions will address a broad range of topics. The Cathedral Hill Hotel in downtown San Francisco will serve as headquarters for the conference.

SPECIAL SESSIONS AND EVENTS

The GEC Executive Committee is pleased to announce the *Foundation Talk* at GEC 2003. The talk will be given by Prof. John Coburn, University of California, Berkeley, and is entitled, "The evolution of plasma etching in microelectronic manufacturing". The GEC Foundation Talk is a plenary session at each GEC. Its aim is to present a cogent overview of a topical area and to put it into context for the very cross-disciplinary audience that attends the GEC. The talk covers both introductory material to guide students and newcomers, as well as cutting edge work from the speaker's own experience to engage the expert.

Two special workshops are planned. The first workshop, *Special Session: Trends in Plasma Etching*, will be held during lunchtime on Tuesday, October 21, 2003. This workshop will highlight the present state of the art in plasma etching as it pertains to the semiconductor industry. This session will have a special format where a select number of talks will focus on the present technologies and challenges of semiconductor etching processes and how the plasma research community can contribute to furthering the state of the art. A discussion period will follow, giving all audience members a chance to question the speakers and discuss issues. All GEC participants are invited to attend. This workshop is organized by Drs. Deepak Bose and Brett Cruden, Eloret Corporation.

The second workshop, *Thermal Plasma Workshop*, will be held during lunchtime on Thursday, October 23, 2003. A special emphasis of this workshop will be plasma modeling, with an invited presentation by Armelle Vardelle, ENSIL and University of Limoges, on "Three-dimensional, time-dependent models of thermal arcs". The purpose of the workshop will be to compare different approaches for theoretical descriptions of so-called thermal plasmas and the relative merits of each of the approaches, as well as the associated numerical simulation techniques. A further purpose is to raise interest in unresolved issues that ask for creative approaches in further research. All GEC attendees are invited to attend the workshop and participate in the discussion. A box lunch will be available for purchase at both workshops. This workshop is organized by Prof. Joachim Heberlein, University of Minnesota.

SESSIONS

- Reception and Registration (*Session AM*)
- Dusty Plasmas (*Session BT1*)
- Atmospheric Pressure Glow Discharges (*Session BT2*)
- Carbon Nanotube Growth (*Session CT1*)
- Capacitively Coupled Plasmas (*Session CT2*)
- Workshop: Trends in Plasma Etching (*Session DTW*)
- Biological Applications of Plasmas I (*Session ET1*)
- Inductively Coupled Plasmas (*Session ET2*)
- Plasma Sheaths (*Session FT1*)
- Plasma Chemistry (*Session FT2*)
- Poster Session I (*Session GTP*)
 - Inductively Coupled Plasmas
 - Material Processing I
 - Instabilities in Reactive Discharges
 - Computational Methods for Plasmas
 - Plasma Dynamics
 - Ozone Production
 - Lighting Plasmas I

- Transport Coefficients
- Glows
- Capacitively Coupled Plasmas
- Diagnostics I
- Electron Collisions
- Diagnostics I (*Session HW1*)
- Nanostructures and Nanoparticles (*Session HW2*)
- Plenary Lecture: GEC Foundation Talk (*Session JW*)
- GEC Business Meeting (*Session KW*)
- Atomic Ionization (*Session LW1*)
- Innovative Applications of Discharges (*Session LW2*)
- Lighting I (*Session MW1*)
- Material Processing I (*Session MW2*)
- Poster Session II (*Session NWP*)
 - Diagnostics II
 - Collisional Ionization
 - Lighting Plasmas II
 - High Pressure Discharges
 - Plasma Sheaths
 - Plasma Propulsion
 - Nanotechnology
 - Negative Ion Plasmas
 - Magnetically-Enhanced Plasmas
- Rydberg Plasmas and Highly Excited Atoms (*Session PR1*)
- Glows (*Session PR2*)
- Electron Scattering (*Session QR1*)
- Environmental Applications (*Session QR2*)
- Workshop: Thermal Plasmas (*Session RRW*)
- Poster Session III (*Session SRP*)
 - Modeling of Glows
 - Diagnostics III
 - Electron Scattering from Atoms
 - Recombination
 - Biological Applications of Plasmas
 - High Pressure Plasma Chemistry and Environmental Applications
 - Laser Kinetics
 - Dusty Plasmas
 - Plasma-Surface Interactions
 - Material Processing II

-Innovative Applications of Plasmas

-Post-deadline Abstracts

- High Pressure Discharges and Arcs (*Session TR1*)
- Fluorocarbon Etch Mechanisms (*Session TR2*)
- Reception and Banquet (*Session UR*)
- Biological Applications of Plasmas (*Session VF1*)
- Magnetically-Enhanced Plasmas (*Session VF2*)
- Diagnostics II (*Session WF1*)
- Lighting II (*Session WF2*)
- Scattering from Molecular Targets (*Session XF1*)
- Material Processing II (*Session XF2*)

PRESENTATION FORMATS

Papers that have been accepted for presentation are listed in the technical program. Invited papers are allotted 25 minutes, with 5 additional minutes for questions and discussion. Oral contributed presentations are allotted 12 minutes, with 3 additional minutes for questions. Poster sessions will be provided with 48" by 96" posterboards. Presenters may mount their posters anytime earlier in the day upon which their presentation is scheduled. Poster materials must be removed at the close of the poster session.

GEC STUDENT AWARD FOR EXCELLENCE

In order to recognize the outstanding contribution students make to the GEC and to encourage further student participation, the GEC will continue to award a prize for the best paper presentation by a student. A subcommittee of the GEC Executive Committee will choose the award winner. Students competing for the \$500 award, in the order of their appearance in the program, are:

Kathleen De Bleecker, University of Antwerp, "Numerical Investigation of Growth Mechanisms of Cluster in a Silane Capacitively Coupled RF Discharge", Tuesday, October 21, 9:00.

Zviad Tsakadze, Nanyang Technological University, "PECVD of Self-Assembled Ordered Carbon Nanotip Arrays in High Density Inductively Coupled Plasmas", Tuesday, October 21, 11:00.

Hyun Chul Kim, Pohang University of Science and Technology, "Effective Frequency Concept for Dual Radio-Frequency Discharges", Tuesday, October 21, 11:30.

Paul Boyle, Dublin City University, "Analytical Model of a Dual Frequency Capacitive Sheath", Tuesday, October 21, 16:15.

Nicolas Bulcourt, École Polytechnique, "UV Absorption Spectrum of the radical CF₂ in an Ar/C₄F₈/O₂ Dual Frequency Capacitive Discharge", Wednesday, October 22, 8:00.

Dragana Maric, University of Belgrade, "Study of pd and j/p^2 Scaling in Abnormal Glow Discharges in Argon", Thursday, October 23, 8:00.

REGISTRATION

The registration desk will be located in the Cathedral Hill Hotel. Registration will be available Monday evening, October 20, to Friday morning, October 24, 2003. The on-site conference registration fee is \$310 for regular registrations and \$190 for students and retirees.

BANQUET AND RECEPTION

An opening reception will be held on the evening of Monday, October 20, 2003, in the Cathedral Hill Hotel, starting at 19:00, located in the Mezzanine Lobby.

The conference banquet will be held in the Pavilion Room of the Cathedral Hill Hotel on Thursday evening, October 23, starting with a reception in the Mezzanine Lobby at 18:00. Banquet tickets are \$40 and are available upon registration. Conference participants are encouraged to attend the reception and the banquet.

E-MAIL AND OTHER BUSINESS SERVICES

Free e-mail access will be available to conference participants in the Cathedral Hill Hotel near the registration desk. Other business services (fax, photocopy services, etc.) will be available from the hotel business center.

AUDIO-VISUAL EQUIPMENT

Each conference room will be equipped with an overhead projector and an LCD projector. If additional equipment is required, please contact the conference secretary.

DINING OPTIONS

A list with dining options in the vicinity of the Cathedral Hill Hotel is included in the registration packet provided to each conference participant.

GUEST PROGRAM

Downtown San Francisco offers a wide variety of attraction for guests. The Cathedral Hill Hotel is within walking distance to many tourist sites, such as Japantown and Nob Hill. San Francisco is known for its excellent mass transportation, including Muni (bus and trams), and BART (Bay Area Rapid Transit). A short bus or cab ride is all it takes to see the Golden Gate Bridge, Fisherman's Wharf, and Alcatraz.

CALL FOR NOMINATIONS FOR GEC GENERAL AND EXECUTIVE COMMITTEES

The GEC Executive Committee (ExComm) is the governing body of the GEC. It is the responsibility of the ExComm to oversee all aspects of the conference. This includes selection of meeting sites, budgetary decisions, selection of special topics and invited speakers, accepting and rejecting abstracts, and arranging of the program. The General Committee and the ExComm meet during the GEC, and the ExComm meets again during the summer to plan the program of the next GEC. There are numerous communications between members of the ExComm (usually e-mail) during the year to insure the successful completion of their duties. We have been fortunate over the years to have a dedicated group of volunteers who have been willing to take on these very necessary roles.

The by-laws of the Gaseous Electronics Conference describe the process whereby members of the ExComm are elected. At the GEC Business Meeting (to be held on Wednesday, October 22, at 11:15 in the International

Ballroom of the Cathedral Hill Hotel), nominations are accepted for members of the GEC General Committee (GenComm).

The GenComm consists of the ExComm and 6 at-large members elected at the Business Meeting. The eligible voting membership of the GEC (defined as those attending the Business Meeting) elects 6 at-large members. The GenComm then meets to fulfill its only duty: to elect new members of the ExComm.

The ExComm membership consists of the Chair, Treasurer, Past-Secretary, Secretary, Secretary-elect, past or incoming Chair, and 4 at-large members. The Chair is a 4 year term (1 year incoming, 2 years Chair, and 1 year past-Chair), the Secretary is a 3 year term (1 year incoming, 1 year Secretary, 1 year past-Secretary), and all other ExComm members serve 2 years. The Secretary is the person who manages the local arrangements for the meeting and is usually "recruited" and appointed to the ExComm.

The ExComm welcomes nominations, including self-nomination, for both the GenComm and the ExComm. Becoming a GenComm and/or ExComm member provides a unique opportunity to see both how the GEC is run and to influence its future direction by helping to define the programs and choosing future sites.

Please submit your nominations to the GEC Chair or any member of the ExComm. The ExComm also welcomes inquiries on hosting future GECs.

GEC 2003 EXECUTIVE COMMITTEE

Lepsha Vušković, Chair

Old Dominion University

Tim Sommerer, Past Chair

GE Research

Helen Hwang, Secretary

NASA Ames Research Center

Uwe Kortshagen, Past-Secretary

University of Minnesota

Bill Graham, Secretary-Elect

Queen's University Belfast

Don Madison, Treasurer

University of Missouri-Rolla

Jean-Paul Booth

École Polytechnique

Bish Ganguly

Air Force Research Laboratory

Akihiro Kono

Nagoya University

Tom Rescigno

Lawrence Berkeley National Laboratory

Ann Orel

University of California, Davis

Jong W. Shon

Lam Research Corporation

CONFERENCE SECRETARY

Dr. Helen Hwang

NASA Ames Research Center

Mail Stop 230-3

Moffett Field, CA 94035 USA

Phone: (650) 604-1368

Email: gec@dm1.arc.nasa.gov

PLEASE NOTE

The APS has made every effort to provide accurate and complete information in this *Bulletin*. However, changes or corrections may occasionally be necessary and may be made without notice after the date of publication. To ensure that you receive the most up-to-date information, please check the meeting Corrigenda distributed with this *Bulletin*.

Epitome of the 56th Gaseous Electronics Conference of the American Physical Society

19:00 MONDAY EVENING
20 OCTOBER 2003

AM **Reception and Registration**
Mezzanine Lobby, Cathedral Hill
Hotel

8:00 TUESDAY MORNING
21 OCTOBER 2003

BT1 **Dusty Plasmas**
California Ballroom, Cathedral Hill
Hotel

BT2 **Atmospheric Pressure Glow
Discharges**
International Ballroom, Cathedral
Hill Hotel

10:00 TUESDAY MORNING
21 OCTOBER 2003

CT1 **Carbon Nanotube Growth**
Meyyappan, Zhou
California Ballroom, Cathedral Hill
Hotel

CT2 **Capacitively Coupled Plasmas**
International Ballroom, Cathedral
Hill Hotel

11:45 TUESDAY MORNING
21 OCTOBER 2003

DTW **Special Session: Trends in
Plasma Etching**
International Ballroom, Cathedral
Hill Hotel

13:15 TUESDAY AFTERNOON
21 OCTOBER 2003

ET1 **Biological Applications of
Plasmas I**
Stoffels, Stalder, Petrović
California Ballroom, Cathedral Hill
Hotel

ET2 **Inductively Coupled Plasmas**
International Ballroom, Cathedral
Hill Hotel

15:30 TUESDAY AFTERNOON
21 OCTOBER 2003

FT1 **Plasma Sheaths**
California Ballroom, Cathedral Hill
Hotel

FT2 **Plasma Chemistry**
International Ballroom, Cathedral
Hill Hotel

19:15 TUESDAY EVENING
21 OCTOBER 2003

GTP **Poster Session I**
El Dorado, Cathedral Hill Hotel

8:00 WEDNESDAY MORNING
22 OCTOBER 2003

HW1 **Diagnostics I**
California Ballroom, Cathedral Hill
Hotel

HW2 **Nanostructures and
Nanoparticles**
Shiratani
International Ballroom, Cathedral
Hill Hotel

10:00 WEDNESDAY MORNING
22 OCTOBER 2003

JW **GEC Foundation Talk**
Coburn
International Ballroom, Cathedral
Hill Hotel

11:15 WEDNESDAY MORNING
22 OCTOBER 2003

KW **Business Meeting**
International Ballroom, Cathedral
Hill Hotel

13:15 WEDNESDAY AFTERNOON
22 OCTOBER 2003

LW1 **Atomic Ionization**
Schulz
California Ballroom, Cathedral Hill
Hotel

LW2 **Innovative Applications of
Discharges**
International Ballroom, Cathedral
Hill Hotel

15:30 WEDNESDAY AFTERNOON
22 OCTOBER 2003

MW1 **Lighting I**
Kroesen
California Ballroom, Cathedral Hill
Hotel

MW2 **Material Processing I**
Gottscho, Cunge
International Ballroom, Cathedral
Hill Hotel

19:15 WEDNESDAY EVENING
22 OCTOBER 2003

NWP **Poster Session II**
El Dorado, Cathedral Hill Hotel

8:00 THURSDAY MORNING
23 OCTOBER 2003

PR1 **Rydberg Plasmas and Highly
Excited Atoms**
Vrinceanu, Gould
California Ballroom, Cathedral Hill
Hotel

PR2 **Glows**
International Ballroom, Cathedral
Hill Hotel

10:00 THURSDAY MORNING
23 OCTOBER 2003

QR1 **Electron Scattering**
Buckman
California Ballroom, Cathedral Hill
Hotel

QR2 **Environmental Applications**
Rousseau
International Ballroom, Cathedral
Hill Hotel

11:30 THURSDAY MORNING
23 OCTOBER 2003

RRW **Thermal Plasma Workshop**
International Ballroom, Cathedral
Hill Hotel

13:30 THURSDAY AFTERNOON
23 OCTOBER 2003

SRP **Poster Session III**
El Dorado, Cathedral Hill Hotel

15:30 THURSDAY AFTERNOON
23 OCTOBER 2003

TR1 **High Pressure Discharges and
Arcs**
Tachibana, Miles
California Ballroom, Cathedral Hill
Hotel

TR2 **Fluorocarbon Etch Mechanisms**
International Ballroom, Cathedral
Hill Hotel

18:00 THURSDAY EVENING
23 OCTOBER 2003

UR **Reception and Banquet**
Mezzanine/Pavilion, Cathedral Hill
Hotel

8:00 FRIDAY MORNING
24 OCTOBER 2003

VF1 **Biological Applications of
Plasmas II**
Lohmann, Pimblott
California Ballroom, Cathedral Hill
Hotel

VF2 **Magnetically-Enhanced Plasmas**
International Ballroom, Cathedral
Hill Hotel

10:00 FRIDAY MORNING
24 OCTOBER 2003

WF1 **Diagnostics II**
California Ballroom, Cathedral Hill
Hotel

WF2 **Lighting II**
Uhrlandt, Bartschat
International Ballroom, Cathedral
Hill Hotel

13:15 FRIDAY AFTERNOON
24 OCTOBER 2003

XF1 **Scattering from Molecular
Targets**
Miller
California Ballroom, Cathedral Hill
Hotel

XF2 **Material Processing II**
Chang, Bradley
International Ballroom, Cathedral
Hill Hotel

MAIN TEXT

SESSION BT1: DUSTY PLASMAS

Tuesday morning, 21 October 2003

California Ballroom, Cathedral Hill Hotel at 8:00

Gerrit Kroesen, Eindhoven University, presiding

8:00

BT1 1 Transverse optical mode in a one-dimensional dusty plasma lattice

JOHN GOREE, BIN LIU, KHARE AVINASH, *The Department of Physics and Astronomy, The University of Iowa, Iowa City, IA 52242* A dusty plasma is an ionized gas containing small particles of solid matter. The particles can arrange in an ordered structure, which is a crystalline form of strongly-coupled plasma. This structure sustains several vibrational modes. We formed the structure into a 1-D chain. We observed an oscillation transverse to the chain, which we term the transverse optical mode. In this mode, particle displacement is restored by a parabolic potential due to a groove in lower electrode. The dispersion relation was measured, verifying that the optical wave has negative dispersion, with oppositely directed group and phase velocities. A theoretical dispersion relation is presented and compared to the experiment and a molecular dynamics simulation. We found that gas damping has a large effect on the dispersion relation. Without damping, the wave is only allowed in a frequency band between two cutoff frequencies. With damping, the wave can propagate a short distance for frequencies outside this band. Work supported by NASA and DOE.

8:15

BT1 2 Nonlinear mixing of compressional waves in a 2D dusty plasma crystal*

V. NOSENKO, K. AVINASH, J. GOREE, B. LIU, *Dept. of Physics & Astronomy, The University of Iowa* A dusty plasma is an ionized gas containing micron-size particles of solid matter. These particles acquire a large negative electric charge, and due to mutual repulsion and the plasma's weaker radial electric fields, they arrange themselves in a regular pattern with crystalline or liquid-like order. In our experiment, polymer microspheres were suspended in the sheath of a gas discharge plasma. They settled in a 2D triangular crystalline lattice with hexagonal symmetry. The particles can be imaged directly, and their positions and velocities calculated. Two sinusoidal compressional waves with different frequencies were launched in the plasma crystal by pushing the particles with modulated Ar⁺ laser beams. Waves at the sum and difference frequencies and harmonics were observed propagating in the lattice. Phonons interacted nonlinearly only above an excitation-power threshold. We compare our results to a theory based on a 1D Yukawa chain model, and to a 2D MD simulation using Yukawa interparticle potential, and find a good agreement.

*Work supported by NASA and DOE.

8:30

BT1 3 Low-pressure diffusion equilibrium of negative-ion dusty plasmas

K. OSTRIKOV, I. B. DENYSENKO, S. XU, *Plasma Sources and Applications Center, NIE, Nanyang Technological University, 637616 Singapore* S. V. VLADIMIROV, *School of Physics, The University of Sydney, 2006 NSW Australia* H. SUGAI, *Department of Electrical Engineering, Nagoya University, Nagoya 464-8603, Japan* M. Y. YU, *Faculty of Physics and Astronomy, Ruhr-University, 44780 Bochum, Germany* A self-consistent fluid theory of one-dimensional complex electronegative plasmas in a parallel-plate low-pressure discharge is presented. The low-pressure diffusion equilibrium is maintained through the self-organized sources and sinks of electrons and positive/negative ions in nanoparticle-containing plasmas. It is shown that the colloidal particle subsystem strongly affects the stationary state of the discharge by dynamically modifying the electron temperature and the particle creation/loss processes. The model includes ionization, ambipolar diffusion, electron/ion collection by the colloidal particles, electron attachment, positive-negative ion recombination, and relevant elastic and inelastic collisions. The spatial profiles of electron and positive/negative ion number densities, electron temperature, and colloidal particle charge in electronegative silane discharges are computed for variable particle size, input power, neutral gas pressure and rates of negative ion creation/loss.

8:45

BT1 4 Production and reactions of silicon atoms in hot wire deposition of amorphous silicon

WENGANG ZHENG, JILA, *University of Colorado and NIST* ALAN GALLAGHER, JILA, *University of Colorado and NIST* Decomposing silane and hydrogen molecules on a hot tungsten filament is an alternative method of depositing hydrogenated microcrystal and amorphous Si for thin-film semiconductor devices. This "hot-wire" method can have significant advantages, such as high film deposition rates. The deposition chemistry involves Si and H atoms released from the filament, followed by their reactions with the vapor and surfaces. To establish these deposition pathways, we measure radicals at the substrate with a home built, threshold ionization mass spectrometer. The design and operation of this mass spectrometer for radical detection, and the behavior of Si atom production and reactions, will be presented. This work is supported by the National Renewable Energy Laboratory, Golden, CO 80401

9:00

BT1 5 Numerical investigation of growth mechanisms of clusters in a silane capacitively coupled radio frequency discharge

KATHLEEN DE BLEECKER, ANNEMIE BOGAERTS, *Dr. WIM GOEDHEER, Dr. RENAAT GIJBELS, Prof. Dr. UNIVERSITY OF ANTWERP, BELGIUM TEAM, FOM INSTITUTE FOR PLASMAPHYSICS "RIJNHUIZEN"*, THE NETHERLANDS TEAM A one-dimensional fluid model was developed to simulate the formation of dust particles in a low-pressure cc rf silane (SiH₄) discharge. The 1D fluid model describes the discharge by a combination of particle, momentum and energy density balances of the ions, electrons and neutrals. The balance equations are coupled to the Poisson equation for the calculation of the electric field and this makes the model fully self-consistent. In particular, the coupling between particle growth and changes of plasma properties is incorporated. A set of 65 species (neutrals, radicals, ions and electrons) and a total of 73 reactions (electron impact reactions with silanes, neutral-neutral and ion-neutral reactions) are described in the model. Most of the reactions and rate

constants are taken from Bhandarkar et al.¹ The model includes the formation of silicon hydrides (Si_nH_m) containing up to twelve silicon atoms. Typical results of the model include the densities and fluxes of the various species, as well as the importance of various chemical reactions on the growth mechanism of the nano-clusters. Anion-induced chain reactions are considered to be the main pathway leading to cluster formation.

¹U. V. Bhandarkar, M. T. Swihart, S. L. Girshick and U. R. Kortshagen, *J. Phys. D: Appl. Phys.* 33, 2731(2000)

9:15

BT1 6 Nano particle diagnostics in a silane plasma J. REMY, M. SOROKIN, G.M.W. KROESEN, W.W. STOFFELS, *Eindhoven University of Technology, Department of Physics, PO Box 513, 5600 MB Eindhoven, The Netherlands* Amorphous silicon solar cells are cheap to produce but lack high efficiency and lifetime. Embedding plasma produced nano material into the intrinsic layers increases lifetime as well as efficiency, without increasing production costs. Nano particle formation in a silane discharge is studied using various diagnostic techniques. Electrical diagnostics measuring voltage and current are combined with optical techniques yielding chemical information. Infrared absorption techniques reveal the densities of various active species during the first stages of particle formation. Experimental results can be linked to plasma and particle nucleation models.

SESSION BT2: ATMOSPHERIC PRESSURE GLOW DISCHARGES

Tuesday morning, 21 October 2003

International Ballroom, Cathedral Hill Hotel at 8:00

James Williamson, Innovative Scientific Solutions, Inc., presiding

8:00

BT1 1 Spatio-Temporally Resolved Spectroscopic Measurements of an Atmospheric Pressure Glow Discharge in Helium CURTIS ANDERSON, MIN HUR, JOACHIM HEBERLEIN, UWE KORTSHAGEN, *University of Minnesota, Mechanical Engineering* The production and decay mechanisms of the excited species in an atmospheric pressure glow discharge in Helium with slight Nitrogen impurities have been investigated by using spectral light emission from He^* ($4s^3S - 2p^3P$: $\lambda = 706$ nm), $N_2(C^3\Pi_u - B^3\Pi_g$: $\lambda = 337$ nm), and $N_2^+((0,0)B^2\Sigma_u^+ - X^2\Sigma_g^+$: $\lambda = 391$ nm). A voltage of 2 kV at 20 kHz was applied between two electrodes covered with .635 mm thick Al_2O_3 plates. Using a gated intensified CCD camera synchronized with the electrical discharge signal, both the radial and axial evolution of these lines were studied. The formation of the cathode layer was observed in the center region immediately following gas breakdown, with its thickness decreasing in time. This layer was found to propagate radially outwards between consecutive half-cycles. The maximum density of high-energy electrons was found at 1 μs prior to the current maximum, decreasing rapidly beyond this time. The greatest N_2^+ emission occurs at current maximum owing to Penning ionization. It is longer lived than He^* emission. This research is supported by the Department of Energy under grant DE-FG02-00ER54583

8:15

BT2 2 Numerical study of the barrier discharge in Helium at atmospheric pressure PENG ZHANG, CURTIS ANDERSON, MIN HUR, JOACHIM HEBERLEIN, UWE KORTSHAGEN, *University of Minnesota, Mechanical Engineering* We have developed a two-dimensional fluid model for an atmospheric pressure glow (APG) discharge in helium with nitrogen impurities. The model is used to study the breakdown evolution in the APG. The results show that the breakdown first appears at the center of the gap, followed by the axial and radial propagation of the ionization wave. The radial propagation extends beyond the electrode region due to edge effects. The current density shows a delay of the current maximum from center to the periphery of the electrode. The surface charge on the dielectrics is nonuniform with a maximum at the center. The radial profiles of the current density and the profile evolution of excitation rates qualitatively agree with experimental results. The effects of impurities and Penning ionization are also discussed. This work is supported by the Department of Energy under grant DE-FG02-00ER54583 and by the University of Minnesota Supercomputing Institute.

8:30

BT2 3 Parametric dependence and control of pulsed phenomena in helium dielectric barrier atmospheric-pressure glow discharges JICHUL SHIN, *The University of Texas at Austin* LAXMINARAYAN L. RAJA, *The University of Texas at Austin* There is rapidly growing interest in atmospheric-pressure glow (APG) discharges since the first report of such discharges over 10 years ago. Especially, dielectric-barrier controlled APG discharges (DB-APG) are of special interest owing to the large number of possible applications. A number of interesting features of these discharges are currently subject of debate in the literature. For example, the role of metastables in pulse formation and cause for multiple pulses are not clearly understood. In this talk we report new experimental studies that seek to explain several of these observed DB-APG discharge peculiarities. Contrary to literature reports of order 1 kHz lower limit for helium DB-APG phenomena, we report discharge phenomena at arbitrarily low frequencies below the 1 kHz limit, albeit under very weak discharge conditions. The number of pulses formed each half cycle is found increase rapidly with decreasing frequency but pulse widths are found to remain relatively invariant to discharge operational conditions. We conclude that pulse phenomena in DB-APG discharges is controlled by classical Paschen breakdown processes followed immediately by extinction behaviour. External voltage increase rates and the overall duration of external voltage increase are found to determine pulse intensity and the number of pulses per cycle of the discharge. Based on these insights, we report the possibility of significant control over discharge pulse intensity and repetition rate using other waveforms such as square-wave pulses.

8:45

BT2 4 Modelling of a Dielectric Barrier Glow Discharge at Atmospheric Pressure in Nitrogen and Helium MYRIAM MADANI, VITO ANNEMIE BOGAERTS, *University of Antwerp (UA)* DIRK VANGENEUGDEN, VITO RENAAT GIJBELS, *University of Antwerp (UA)* PLASMA SIMULATIONS GROUP (UA) TEAM, PLT (VITO) TEAM In the last decade there has been a growing interest in the Dielectric Barrier Glow Discharge at atmospheric pressure. Its main advantage is the possibility to avoid the technological and economical drawbacks involved with a vacuum system, necessary in low-pressure plasma processes. Possible applications are deposition of coatings and reactive sur-

face treatments (e.g. cleaning, sterilization, activation, etc.). To optimize the above-mentioned applications of this kind of discharge, it is essential to have a good understanding of the plasma parameters and the processes occurring in the reactor. Some of these characteristics can be obtained experimentally, but other parameters, such as particle densities, are difficult to measure. Therefore, our objective is to obtain a better knowledge of the atmospheric pressure Dielectric Barrier Glow Discharge by means of a combination of modeling and experimental research. In the presentation we will give a short description of a 2 dimensional fluid model developed for the dielectric barrier discharge in helium and nitrogen. Furthermore we will show results such as particle density distributions and electrical characteristics such as potential and electric field distributions and time variations of discharge currents.

9:00

BT2 5 CORRELATED ELECTRICAL AND OPTICAL MEASUREMENTS IN AN ATMOSPHERIC PRESSURE GLOW DISCHARGE

GAGIK NERSISYAN, *Queens University Belfast, Belfast BT7 INN, Northern Ireland* PHILIP STEEN, *Queens University Belfast, Belfast BT7 INN, Northern Ireland* TOM MORROW, *Queens University Belfast, Belfast BT7 INN, Northern Ireland* WILLIAM GRAHAM, *Queens University Belfast, Belfast BT7 INN, Northern Ireland* Atmospheric pressure glow discharges (APGD) generated in both helium and in air in the presence of flowing helium have been studied. They are created between two planar metallic electrodes covered by glass plates by applying a sinusoidal electrical field with frequency range from 1 to 50 kHz and the strength up to 5kV/cm. Time variations of electrical parameters such as discharge current, gap and memory voltages and fast images have been used to establish the main elementary processes, initiating and sustaining the APGD, and to control the discharge mode. Time resolved spectroscopy of different species, involved in discharge processes, elucidates the role of long-living helium metastables and molecular helium ions in the establishment of a uniform glow mode. The decay time of excited molecular nitrogen ions populated directly by helium metastables is about 300ns. There is a correlation between the electrical and

optical characteristics of the APGD, showing that the generation of a uniform glow mode coincides with a high density of accumulated surface charge on the dielectric plates. We are currently using LIF technique to determine the helium metastable density.

9:15

BT2 6 Generation Mechanism of the Atmospheric Glow in a DBD Configuration

EUGEN ALDEA, *Eindhoven University of Technology, Dept of Applied Physics, Eindhoven, The Netherlands* COR SCHRAUWEN, *TNO-TPD, Division Models and Processes, Eindhoven, The Netherlands* RICHARD VAN DE SANDEN, *Eindhoven University of Technology, Dept of Applied Physics, Eindhoven, The Netherlands* In this contribution we analyze the basic conditions needed for uniform glow plasma generation. A simple analysis of the glow generation indicates that it is extremely improbable that the metastables or ions can have a significant contribution to glow generation via a pre-ionization mechanism. The low diffusion rate of ions and metastables excludes any mechanism of streamers or electron avalanches superposition. The preionization mechanism based on ions or metastables cannot also explain why the standard breakdown mechanism of atmospheric plasma streamer breakdown does not occur and he can not explain either how the glow to arc transition a notorious instability of atmospheric plasmas is avoided. Besides these theoretical arguments no evidence was found in the experimental current-voltage characteristics, plasma emission or breakdown voltage suggesting a significant pre-ionization or even the presence of a large amount of metastables. We conclude that the major problem in generation of atmospheric glow plasma is glow to arc transition. In this respect metastables are rather the problem for a stable plasma generation because their presence enhance the probability of stepwise ionization and glow to arc transition. The experimental data suggests that the surface of the dielectrics plays a major role in uniform and stable atmospheric glow plasma generation. The surface effect is probably due to a high secondary emission at the surface. Beside the surface material an electronic controlled negative feedback which prevents glow to arc transition was prove to be also essential for the glow generation.

SESSION CT1: CARBON NANOTUBE GROWTH

Tuesday morning, 21 October 2003; California Ballroom, Cathedral Hill Hotel at 10:00

Uwe Kortshagen, University of Minnesota, presiding

Invited Papers

10:00

CT1 1 Low temperature plasmas in carbon nanotube growth and functionalization.

M. MEYYAPPAN, *NASA Ames Research Center*

This talk will first briefly introduce carbon nanotubes and their applications. Then two areas, where cold plasmas are effective, will be discussed. PECVD has been widely used in producing CNTs. The plasma-grown CNTs appear to be lot more vertically oriented than thermal CVD-grown samples, perhaps due to the electric field. Growth results from an inductive plasma and a DC-hot filament system along with some plasma diagnostics will be discussed. Challenges and future opportunities will be outlined. For a variety of applications, it is important to be able to attach chemical groups to the sidewalls of CNTs. While traditionally wet chemistry is used for this purpose, low temperature plasmas are effective to achieve functionalization. Results for chemical functionalization using a microwave cavity will be presented.

10:30

CT1 2 Carbon nanotubes as robust electron field emitters in gaseous and vacuum environments.OTTO ZHOU, *University of North Carolina*

This abstract not available.

Contributed Papers

11:00

CT1 3 PECVD of self-assembled ordered carbon nanotip arrays in high density inductively coupled plasmas Z. TSAKADZE, S. XU, J. LONG, K. OSTRIKOV, *Plasma Sources and Applications Center, NIE, Nanyang Technological University, 637616 Singapore* R. STORER, *Flinders University, GPO Box 2100, Adelaide 5001 SA, Australia* Large area, highly uniform and high-density self-assembly ordered arrays of various carbon nanostructures (CNs) have been grown in high density, low frequency inductively coupled plasma source. The methane-hydrogen-argon gas mixture has been used for plasma discharge. Both vertically aligned nanotips and highly ordered pyramid-like structures are formed on lightly doped silicon (100) substrates, pre-coated with thin (30-40 nm) layered Ni / Fe / Mn catalysts in a DC-bias controlled floating temperature regime. The scanning electron micrographs show that there is a minimum negative DC bias (in the 50-60 V range) that enables the growth of small carbon nanotips. The minimum temperature for the nanotip growth is approximately 270°C. The x-ray diffractometry shows that the carbon nanostructures are well graphitized. Raman spectroscopy displays a clear position and well-defined shape of the peaks, indicating a well-structured graphitic phase in the films with the elevated sp^2 content. A high degree of positional and directional ordering of the CNs is achieved at remarkably low growth temperatures and pressures without any preliminary heating or pre-patterning of the samples. It is postulated that the self-assembly of the CNs is controlled by the competition of the reactive chemical etching and plasma-enhanced chemical vapor deposition processes. The nanostructures in question target the electron field emission applications.

11:15

CT1 4 Stability of atmospheric pressure glow discharge and application to carbon nanotube deposition TOMOHIRO NOZAKI, *Tokyo Institute of Technology, University of Minnesota* KEN OKAZAKI, *Tokyo Institute of Technology* UWE KORTSHAGEN, JOACHIM HEBERLEIN, *University of Minnesota* This paper describes carbon nanotube deposition using helium-based glow barrier discharge. Two important issues will be discussed: The stability of glow discharge and aligned growth of nanotube. Silicone substrate having 20 nm nickel film was secured on metallic bottom electrode where the temperature was elevated by 600C. In addition to CH₄ or C₂H₂, the process gas also include hydrogen (~10 vol% in order to etch out excess carbon deposited on Ni particle. Highly contaminated helium tends to form filamentary discharges, and then severely deteriorates deposited materials. It also limits operating conditions such as gap separation, voltage amplitude, and so on. The stability issue will be extensively discussed in terms of emission spectroscopy which also makes clear chemical processes. Nanotubes vertically grow in the presence of directional electric field, and this is a big challenge in barrier discharges because dielectric barrier forces to use AC voltage to maintain stable plasma conditions. Alignment of nanotube also

depends on carbon sources. C₂H₂ generally provides curly nanotubes, whereas rather straight nanotubes likely grow with methane. Control growth of nanotube will be discussed based on voltage waveform (Sin/Pulse) and carbon source.

11:30

CT1 5 Gas-surface kinetics modeling for carbon nanotube deposition D. B. HASH, T. R. GOVINDAN, M. MEYYAPPAN, *NASA Ames Research Center* DEEPAK BOSE, *Eloret Corporation* The role of the interaction between the gas and transition metal catalyzed substrates in the chemical vapor deposition (CVD) of carbon nanotubes (CNT) is of considerable interest. To be able to use computational tools to predict the growth of CNTs and thus optimize process parameters and catalyst recipes, this interaction must be modeled. To this end, a computational fluid dynamics model of a dc plasma enhanced CVD reactor is extended to include a surface chemistry model. The fluid model solves a set of partial differential equations for gas phase species mass, gas temperature, plasma temperature and plasma potential. For the surface, chemical kinetic rate expressions are used for the chemisorption and subsequent dehydrogenation of gas phase hydrocarbons as well as carbon diffusion through the catalyst. The expressions for the conservation of mass at the surface form a set of ordinary differential equations that are time-integrated and coupled to the gas model to provide CNT growth rates.

SESSION CT2: CAPACITIVELY COUPLED PLASMAS

Tuesday morning, 21 October 2003

International Ballroom, Cathedral Hill Hotel at 10:00

Alex Vasenkov, *University of Illinois at Urbana-Champaign*, presiding

10:00

CT2 1 Generation of uniform, large area VHF capacitive plasma using phase-modulation and two-frequency technique HIDEO YAMAKOSHI, KOJI SATAKE, HIROSHI MASHIMA, YOSHIKI TAKEUCHI, MASAYOSHI MURATA, TATSUFUMI AOI, *Mitsubishi Heavy Industries, Ltd., Japan* TARO UCHIYAMA, *Keio Univ., Japan* In this paper, two techniques are proposed to generate uniform VHF plasma. In both techniques, two VHF voltages, with different phases, are supplied to an electrode such that an envelope representing the spatial distribution of the VHF voltage on the electrode in a split second moves time by time. Phase-modulation technique utilizes a phase-shifter. A VHF signal from an oscillator is divided into two branches. Then, the shifter placed between a divider and an amplifier varies the phase of one branch. The electrode is a ladder-shape, formed by assembling a plurality of parallel longitudinal rods and two parallel lateral rods into form of lattice. Each branch is connected to the electrode through each set of feeding points placed on each lateral rod. Plasma uniformity within ~10% was demonstrated at 60 MHz for the substrate size of 1.4 m ~1.1 m, using nitrogen gas of

10 Pa. Two-frequency technique utilizes a beat generated by their frequency difference. Two VHF powers whose frequencies are 60.0 and 60.3 MHz, respectively are supplied to the electrode through the feeding points. Plasma uniformity of 15% and deposition rate of 0.7 nm/s 20% was obtained with power of 4 kW, pressure of 8 Pa and SiH₄ flow rate of 3 SLM.

10:15

CT2 2 Non-uniformities in large-area high-frequency capacitive discharges AMELIE PERRET, PASCAL CHABERT, JACQUES JOLLY, JEAN-PAUL BOOTH, JEAN GUILLON, *Laboratoire de Physique et Technologie des Plasmas, UMR 7648, Ecole Polytechnique, 91128 Palaiseau, France* Low pressure capacitive RF discharges are routinely used in the Flat Panel Industry to process large-area glass substrates ($> 1 \text{ m}^2$). In order to reach higher process throughputs, the substrate size is being continually increased while the use of Very High Frequency (up to 100 MHz) promises high density sources with low energy ion bombardment. However, strong non-uniformity of plasma production is expected if the excitation wavelength becomes comparable to the reactor size (standing wave effect) and/or if the plasma skin depth becomes comparable to the plate separation (skin effect)¹. Ion flux uniformity measurements performed in a large-area square capacitive discharge have shown a strong standing wave effect, in good agreement with theory at 60 MHz and above². A retarding field energy analyser has been constructed and will be used for ion energy uniformity measurements in argon. The influence of the composition on plasma uniformity is also studied.
¹Lieberman et al, *Plasma Sources Sci. Technol.* 11 (2002)
²Perret et al. *Appl Phys Lett*, accepted 2003

10:30

CT2 3 The role of secondary electron emission and electron heating in RF plasmas ALEC GOODYEAR, PAULO LIMA, NICHOLAS BRAITHWAITE, *The Open University, Oxford Research Unit* The bounding surfaces of a plasma reactor provide a potential source of potent electrons when under bombardment from plasma species. Necessary conditions for secondary electrons to be effective is that they are emitted from surfaces at potentials significantly lower than that of the bulk plasma and in sufficient quantity. The relative effectiveness of these secondaries in comparison with direct radio-frequency heating of the plasma bulk electrons depends on the emission surface material and on a range of plasma parameters such as pressure, power, drive frequency, and feed gas. An embedded perturbation surface has been engineered into the ground electrode of a capacitively coupled GEC reactor to investigate these effects. A combination of DC and RF voltages have been applied to the test surface and the plasma perturbation observed with temporally and spatially resolved optical emission spectroscopy. Direct observation has been made of optical emission associated with secondary electron emission and that associated with RF heating for low to medium pressure RF plasmas (50-500 mTorr) at 13.56 MHz. The frequency dependence of the relative contributions to heating have also been investigated.

10:45

CT2 4 One-dimensional fluid simulations of very low-pressure, high-frequency, capacitively coupled plasma discharges GUANGYE CHEN, *The University of Texas at Austin* LAXMI-NARAYAN L. RAJA, *The University of Texas at Austin* Fluid modeling approaches have traditionally encountered several shortcomings when used for simulation of capacitively coupled

plasma discharges under very low-pressure and high-frequency conditions. For example, fluid models fail to accurately predict important features such as the electron heating and the electron temperature profiles in the discharge. Recent interest in such discharges (e.g. dual frequency plasma reactors) has rekindled interest in modeling of such systems. While particle approaches such as PIC are quite accurate in this regime, the large computational burden precludes their use in the routine modeling of these systems. We explore extensions of the classical fluid modeling technique that improve accuracy of the method for the low-pressure, high-frequency regime. A one-dimensional model is for our studies. All assumptions that relate to transport closure in the governing equations for the electrons are systematically relaxed. The electron momentum equation is used in lieu of the drift-diffusion approximation. The electron diffusive heat flux term in the electron energy equation is evaluated using an integral collisionless formulation that accounts for non-local effects resulting from electron free-streaming in the discharge. Both these extensions to the traditional fluid treatment of electron kinetics are found to significantly improve accuracy of the fluid model. The typical underprediction of electron heating near the sheath-plasma interface is overcome and improved predictions for non-uniform electron temperature profiles are obtained.

11:00

CT2 5 2-D simulations of capacitively coupled RF plasmas: influence of process parameters TATIANA NOVIKOVA, *LPICM, Ecole Polytechnique, 91128 Palaiseau Cedex, France* BILLEL KALACHE, *LIMHP, Université Paris-Nord, 93430, Villetaneuse, France* PAVEL BULKIN, *LPICM, Ecole Polytechnique, 91128 Palaiseau Cedex, France* KHALED HASSOUNI, *LIMHP, Université Paris-Nord, 93430, Villetaneuse, France* PERE ROCA I CABARROCAS, *LPICM, Ecole Polytechnique, 91128 Palaiseau Cedex, France* Modeling of hydrogen and silane plasmas is necessary for optimization of microcrystalline silicon growth. The ratio of atomic hydrogen to SiH_x radicals has been identified as the critical parameter for this process. Numerical simulations of the discharge may give the insights on the set of process parameters which optimize this ratio. We extend our 1-D fluid model of hydrogen discharge [1] to 2-D model in cylindrical geometry. Species considered are electrons (including secondary), positive and negative ions. Transport and cross-sections data were calculated with EEDF obtained from two-term expansion of the Boltzmann equation. The results show that variations of pressure and RF-frequency have strong influence on the discharge parameters: self-bias voltage, sheath width, ratio between power transferred to ions and to electrons, concentration of atomic hydrogen, radial variations of the fluxes. Some preliminary results on silane-hydrogen mixtures will be presented. [1] T. Novikova et al. *J. Appl. Phys.* 93, 3198 (2003).

11:15

CT2 6 Acceleration to periodic steady-state for multi-dimensional radio-frequency plasma discharge simulations EDWARD HAMMOND, PARVIZ MOIN, *Stanford University* Simulation of radio-frequency plasma discharges can be extremely time-consuming due to the slow evolution to the periodic steady-state. Many modellers employ an ad hoc acceleration technique where species that change more slowly in time are advanced separately from those that evolve more rapidly, and rates of change for the species densities from period to period are extrapolated to speed convergence [Sommerer and Kushner, *J. Appl. Phys.*, 71, 1654 (1992)]. Analytical methods for determining the periodic

steady state have been limited to one dimension [Lin and Adomaitis, *J. Comp. Phys.*, 171, 731 (2001)]. This work will describe a multi-dimensional technique for acceleration to the periodic steady state and will present applications of this technique in one and two dimensions. The number of radio-frequency periods required to reach steady-state can be reduced by up to two orders of magnitude. Also, the technique will be used to perform simulations at a variety of conditions to validate a model for an argon discharge with experimental data gathered in the GEC Reference Cell geometry.

11:30

CT2 7 Effective Frequency Concept for Dual Radio-Frequency Discharges HYUNCHUL KIM, JAEKOO LEE, *Dept. of Electronic and Electrical Engineering, Pohang University of Science and Technology, Pohang, Korea* JONGWON SHON, *Lam Research Corporation, Fremont, CA, USA* Capacitively coupled radio-frequency (rf) discharges have been extensively studied for the last years because of their widespread applications, especially in plasma processing. For further improvements of their performance, dual frequency (DF) capacitively coupled discharges (CCP) have attracted much attention. We introduce a new concept of effective frequency to enhance our understanding of DF CCP by considering them as conventional single frequency CCPs of simpler and well-known systems. Of its wide potential applications, this concept is particularly useful in explaining several physical issues associated with dual rf discharges such as the independent control of the ion flux and the ion bombardment energy, the power dissipation mode transition, and the ion bombardment energy distribution function. For these issues, the effective frequency is quantitatively defined by analyzing a homogeneous plasma model for dual rf discharges and ion dynamics in collisionless dual rf sheaths. Our results are also compared with our particle-in-cell simulation results.

SESSION DTW: SPECIAL SESSION: TRENDS IN PLASMA ETCHING

Tuesday morning, 21 October 2003

International Ballroom, Cathedral Hill Hotel at 11:45

Brett Cruden, Eloret Corporation, presiding

11:45

DTW 1 Semiconductor Industry Plasma Processing Needs RICHARD WISE, *IBM Microelectronics* SIDDHARTHA PANDA, *IBM Microelectronics* WENDY YAN, *IBM Microelectronics* SEMICONDUCTOR RESEARCH AND DEVELOPMENT CENTER TEAM The plasma requirements of dry etch equipment used for advanced semiconductor process development and low cost semiconductor manufacturing are reviewed. Introduction of ArF (193nm) photolithography has resulted in increased demands on resist selectivity, increased sensitivity to plasma induced or exacerbated line edge roughness, and the introduction of novel hard and soft mask schemes. State of the art plasma processing chambers must be able to deliver low DC bias due to line edge roughness requirements with adequate ion/radical density to prevent loss of critical dimension control in deep features. These same systems may be required to operate in a high

DC bias, low plasma density regime to achieve adequate etch rate on different films, and in many cases the system must be able to switch between low and high DC bias modes. The acceptable plasma density is limited by that necessary to provide adequate production of passivation agents necessary to achieve selectivity to ArF photoresists. Further limits on plasma density may be needed due to device and etch profile sensitivity to differential charging. The allowable DC bias may be limited to avoid damage to shallow implanted regions and thin gate. Decreases in gate length have increased sensitivity to non-anisotropic profiles, which in turn requires a minimum of DC bias to provide anisotropy. Particle sensitivity has resulted in a migration toward integrated plasma processing, putting additional demands on the stability and flexibility of the plasma equipment. State of the art plasma tooling must be capable of operating over a wide range of plasma densities, delivering both high and low DC bias, and provide RF stability over a wide range of wafer/chamber impedances. The increased uniformity requirements of 300 mm tools requires the anode and cathode potential be uniformly distributed over the entire surface, and that the plasma generation be as uniform as possible. Extended wet clean cycles have driven the need for integrated cleans, which also must be capable of removing deposited films uniformly over the chamber surface.

12:00

DTW 2 Recent Trends in Silicon Etching: Controlled Flexibility THORSTEN LILL, MEIHUA SHEN, SHASHANK DESHMUKH, DAVID MUI, PATRICK LEAHEY, JOHN HOLLAND, ALEX PATERSON, PODLESNIK DRAGAN, *Applied Materials* Recent developments like the move to 300 mm wafers, the introduction of 193 nm resists with low plasma etch resistance, the rapid movement towards sub 100 nm structures, and the requirement to mix several processes in one chamber have triggered an exciting new wave of innovation in plasma etching. Interestingly, the most significant areas of innovation in the area of conductor etching do not necessarily pertain to the basic source technology, but to improved flexibility and control. Tunable sources which allow to control the ion and neutral flux densities across the wafer as well as a flexible temperature management of the wafer surface have been developed and new features are added to meet the ever increasing requirements of future technology nodes. At the same time, smaller structures such as advanced gate or shallow trench structures on logic or very high aspect ratio trenches for dRAM devices lead to an increasing number of process steps to obtain the desired "perfect" profile. These two trends lead to an "explosion" of process parameters per etch recipe and to decreasing step times thus requiring hardware/process solutions that allow for larger flexibility to open the process window. At the same time ever tighter repeatability requirements call for better control of all parameters. For advanced gate etching, wafer-to-wafer control of the critical dimension (CD) of 1 nm 3 sigma are being requested in 300 mm mass production. The overall CD budget for the gate etcher at the 90 nm node is 5 nm 3 sigma which includes proximity and doping as well as across the wafer effects. In this paper, we will present approaches to resolve the arising conflict between flexibility and process control. This will include the areas of process chemistry, chamber design, chamber wall effects, advanced control features, the understanding of advanced photoresists as well as on-board metrology. The paper will focus on the basic mechanisms as well the implementation of these new approaches in IC mass production.

12:15

DTW 3 Trends in Dielectric Etch for Microelectronics Processing ERIC A. HUDSON, *Lam Research Corp.* Dielectric etch technology faces many challenges to meet the requirements for leading-edge microelectronics processing. The move to sub 100-nm device design rules increases the aspect ratios of certain features, imposes tighter restrictions on etched features critical dimensions, and increases the density of closely packed arrays of features. Changes in photolithography are driving transitions to new photoresist materials and novel multilayer resist methods. The increasing use of copper metallization and low-k interlayer dielec-

tric materials has introduced dual-damascene integration methods, with specialized dielectric etch applications. A common need is the selective removal of multiple layers which have very different compositions, while maintaining close control of the etched features profiles. To increase productivity, there is a growing trend toward in-situ processing, which allows several films to be successively etched during a single pass through the process module. Dielectric etch systems mainly utilize capacitively coupled etch reactors, operating with medium-density plasmas and low gas residence time. Commercial technology development increasingly relies upon plasma diagnostics and modeling to reduce development cycle time and maximize performance.

SESSION ET1: BIOLOGICAL APPLICATIONS OF PLASMAS I

Tuesday afternoon, 21 October 2003; California Ballroom, Cathedral Hill Hotel at 13:15

Bill Graham, Queens University of Belfast, presiding

Invited Papers

13:15

ET1 1 Plasma needle: Treatment of living cells and tissues.

EVA STOFFELS,* *Eindhoven University of Technology, The Netherlands*

Non-thermal plasmas are capable of refined treatment of heat sensitive surfaces. Recently, many non-thermal sources working under atmospheric pressure have been constructed. Their main applications are various surface treatments: cleaning, etching, changing the wettability/adhesion, and bacterial decontamination. A new research at the Eindhoven University of Technology focuses on in vivo treatment by means of a novel non-thermal plasma source (the plasma needle). At present, a fundamental study has been undertaken to identify all possible responses of living objects exposed to the plasma. Plasma treatment does not lead to cell death (necrosis), which is a cause of inflammation. On the contrary, we observe various sophisticated reactions of mammalian cells, e.g. cell detachment (loss of cell contact) and programmed cell death (apoptosis). Moreover, under certain conditions the plasma is capable of killing bacteria, while eukaryotic cells remain unharmed. These findings may result in development of new techniques, like bacterial sterilization of infected (living) tissues or removal of cells without inflammatory response, and on a longer time scale to new methods in the health care. Possible applications include treatment of skin ailments, aiding wound healing and sterilization of dental cavities.

*In collaboration with Ingrid Kieft and Raymond Sladek, Eindhoven University of Technology, The Netherlands.

13:45

ET1 2 Plasma Characteristics of Electrosurgical Discharges.*

KENNETH R. STALDER, *Stalder Technologies and Research, Redwood City, CA*

Surgical devices utilizing electrical discharges of ever increasing sophistication have been used for decades for numerous procedures. Cushing and Bovie in 1928, for example, developed high-frequency spark generators to cauterize blood vessels and remove unwanted tissue by a thermal ablation processes. Modern Bovie's (named after their inventor) use a high-frequency discharge from an electrode to nearby tissue to thermally ablate tissue. Spectroscopic analysis shows that these discharges are hot and are well represented by a thermal equilibrium model, and temperatures near 2000 K are easily achieved. New electrosurgical devices utilizing repetitive electrical discharges in a conducting saline environment have recently been developed. Electron emission from an active electrode during certain portions of the voltage waveform causes the formation of a vapor layer surrounding the electrode and the subsequent ionization and dissociation of species in this region. Electron temperatures of approximately 4 eV are achieved during the plasma phase. Water molecules are dissociated into reactive fragments, and the salt species are also excited and ionized in this nonequilibrium plasma. It is thought that the reactive species interact with nearby tissue, causing localized tissue removal (ablation) which surgeons can exploit during surgical procedures. Flowing saline surrounding the plasma region cools untargeted tissue and removes the reaction products. This presentation will focus on experimental results of the plasma conditions and discuss our current efforts to understand the complex reactions of the various plasma species with tissue structures such as collagen. A short clip showing tissue removal will also be shown.

*Research supported by ArthroCare Corporation.

Contributed Papers**14:15**

ET1 3 Argon Micro-Cell Plasma with Applications in Bio-Medical Technology JAN VAN DIJK, *Department of Electronics and Electrical Engineering, Keio University, Japan* YASUHIRO HORIUCHI, *Department of Electronics and Electrical Engineering, Keio University, Japan* TOSHIAKI MAKABE, *Department of Electronics and Electrical Engineering, Keio University, Japan* In bio-medical technology, plasmas have recently been acknowledged as a viable instrument for performing micro-surgery. This in-vivo application obviously demands strict compatibility with the human tissue which is to be treated. That in turn imposes strict requirements on the pressure (1 atmosphere) and gas temperature

(37 C) in which the plasma operates. In addition, the plasma source must be compact and reliable, while the plasma species should not poison the body fluids with which they are in contact. In this contribution we will discuss the plasma-physical and electrical properties of an RF-operated argon micro-cell plasma (MCP) configuration which is believed to be able to meet these design restrictions. Results of a numerical study with the help of the two-dimensional Relaxation ConTinuum (RCT) model [1-2] will be presented. We shall focus on the spatial variation of the feed gas temperature for various plasma operating conditions. Special attention will be paid to the volumetric and surface heating mechanisms. [1] T. Makabe, N. Nakano and Y. Yamaguchi, *Phys. Rev. A* (45), 2520 (1992) [2] T. Makabe, "Advances in Low Temperature RF Plasmas" Elsevier, (2002)

Invited Papers**14:30**

ET1 4 Application of non-equilibrium plasmas in treatment of wool fibers and seeds.
ZORAN PETROVIC,* *Institute of Physics Belgrade, Serbia and Montenegro*

While large effort is under way to achieve stable, large area, non-equilibrium plasma reactors operating at atmospheric pressure we should still consider application of low pressure reactors, which provide well defined, easily controlled reactive plasmas. Therefore, the application of low pressure rf plasmas for the treatment of wool and seed was investigated. The studies were aimed at establishing optimal procedure to achieve better wettability, dyeability and printability of wool. Plasma treatment led to a modification of wool fiber topography and formation of new polar functional groups inducing the increase of wool hydrophylicity. Plasma activation of fiber surface was also used to achieve better binding of biopolymer chitosan to wool in order to increase the content of favorable functional groups and thus improving sorption properties of recycled wool fibers for heavy metal ions and acid dyes. In another study, the increase of germination percentage of seeds induced by plasmas was investigated. We have selected dry (unimbibed) Empress tree seeds (*itPaulownia tomentosa* Steud.). Empress tree seed has been studied extensively and its mechanism of germination is well documented. Germination of these seeds is triggered by light in a limited range of wavelengths. Interaction between activated plasma particles and seed, inside the plasma reactor, leads to changes in its surface topography, modifies the surface layer and increases the active surface area. Consequently, some bioactive nitrogenous compounds could be bound to the activated surface layer causing the increment of germination percentage.

*N. Puač, Institute of Physics; M.Radetić, D.Jocić, P.Jovančić, Faculty of Technology and Metallurgy, Belgrade; D.Grubišić, Z. Giba and S.Živković, Institute for Biological Research, Belgrade.

SESSION ET2: INDUCTIVELY COUPLED PLASMAS

Tuesday afternoon, 21 October 2003

International Ballroom, Cathedral Hill Hotel at 13:15

Deepak Bose, Eloret Corporation, presiding

13:15

ET2 1 Generation of high-density, uniform plasmas by internal RF current sheets: key concepts and experimental verification Z. TSAKADZE, K. OSTRIKOV, S. XU, *Plasma Sources and Applications Center, NIE, Nanyang Technological University, 637616 Singapore* E. TSAKADZE, *RISOE National Laboratory, PO Box 49, DK-4000 Roskilde, Denmark* The results on experimental investigation of the low-frequency (0.46 MHz) inductively coupled plasmas sustained by the internal oscillating RF current (IOC) are presented. The plasma is generated in the inductively coupled plasma source (ICP) with a specially designed configuration of the internal RF coil. Various diagnostic tools, such as the magnetic probes, optical emission spectroscopy and the Langmuir

probe, have been used to investigate the electromagnetic, optical and global properties of the argon plasma. Their dependence on the applied RF power and gas filling pressure has also been studied. It is found that the uniformity of the electromagnetic field inside the studied plasma chamber is significantly improved compared with that in the conventional ICP source with external flat coil configuration. A reasonable agreement between the experimental data and previously computed electromagnetic field topography inside the chamber is reported. The Langmuir probe measurements reveal that the spatial profiles of the electron density, the effective electron temperature, plasma potential and electron energy distribution/probability functions are featuring a high degree of the radial and axial uniformity and a weak azimuthal dependence, which is consistent with the theoretical predictions. As the input RF power rises, however, the azimuthal dependence of the global plasma parameters vanishes. Finally, the obtained results demonstrate that by introducing the internal oscillated RF currents one can noticeably improve the uniformity of the plasma density, electromagnetic field topography and power deposition into the plasma.

13:30

ET2 2 Thomson Scattering Measurements in an Inductively Coupled Plasma GARY CRAIG, PHILIP STEEN, TOM MORROW, BILL GRAHAM, *Queen's University of Belfast, BT7 1NN, N. Ireland, UK* Electron energy distribution functions (EEDF's) are central to the understanding of the physics and chemistry of low temperature plasmas. Here we use Thomson Scattering of the second harmonic of a Nd:YAG laser (532 nm) and an ICCD detector to determine the eedfs in Argon, Nitrogen and Oxygen plasmas. The plasmas are operated at pressures ranging from 25 mT to 250 mT. In Argon the eedfs at low pressure and power are bi-Maxwellian. At higher pressures and powers a Maxwellian distribution is obtained. In oxygen and nitrogen plasmas, however, under these conditions the eedfs are bi-Maxwellian. At powers greater than 50 W measurements become problematic due to the plasma heating effects, with temperatures as high 1200 K being observed at 300 W. In molecular plasmas, changes in the Raman spectra due to heating also become very significant and so, problematic. Solutions such as pulsing the plasma system and using calculated Rayleigh and Raman profiles are being examined.

13:45

ET2 3 Measurement of cold electrons in a pulsed inductively coupled plasma MICHAEL HEBERT, UWE KORTSHAGEN, *Mechanical Engineering, University of Minnesota* DIRK UHRLANDT, *Institut für Niedertemperatur-Plasmaphysik, Greifswald 17489, Germany* During the afterglow of a low pressure pulsed plasma, energetic electrons are rapidly lost to the walls while low energy electrons remain trapped within the ambipolar potential well, resulting in the fast cooling of the electron ensemble. In time, a collapse of the ambipolar potential occurs which depletes the electron energy distribution function in the high-energy range. Late in the afterglow, elastic electron-atom collisions are the only electron heating mechanism remaining. For a gas with poor thermal contact between gas atoms and electrons, diffusive cooling can cool electrons to temperatures around the gas temperature, and, in principle, even below that. We report direct measurements of cold electrons in the late afterglow that have been performed using a cylindrical Langmuir probe. The Laframboise model¹ has been employed to determine the electron temperatures. This work is supported by DOE under grant No. ER-54554. ¹ J. Laframboise, Theory of cylindrical and spherical Langmuir probes in a collisionless plasma at rest, in: *Rarefied Gas Dynamics: P. 4th Int. Symp. Toronto/Canada 1964*, vol.2, 22-43.

14:00

ET2 4 ICPs Enhanced with Ferromagnetic Cores VALERY GODYAK, *Osram Sylvania* Analysis of of inductively coupled plasma (ICP) system that includes the plasma itself and a set of supporting means (an induction coil, a matching network, a feed line and an rf generator) suggests many advantages in using ferromagnetic cores in inductive plasma sources. Introduction of a ferromagnetic core dramatically improves ICP characteristics, much like it does in a conventional transformer. A ferromagnetic core increases coupling between the induction coil and plasma resulting in increased power transfer efficiency and reduction of many undesirable effects intrinsic to a conventional ICP. Utilization of ferromagnetic cores allows for a significant reduction of ICP operating frequency, thus simplification and overall reduction of ICP system cost. Different kinds of commercial ICPs enhanced with ferrite cores that have found applications in lighting and in plasma processing of materials are considered in this presentation.

14:15

ET2 5 Plasma and Electrical Characteristics of an ICP in Magnetic Field VALERY GODYAK, *Osram Sylvania* ROBERT PIEJAK, *Osram Sylvania* BENJAMIN ALEXANDROVICH, *Osram Sylvania* EEDFs, plasma parameters and currents in an induction coil of a cylindrical ICP with a flat coil, immersed in a weak homogeneous magnetic field, have been measured at the driving frequency 28.6 MHz. The measurements were performed at the condition of controlled discharge power dissipated in plasma, taking into account rf power losses dissipated in supporting hardware. The following range of ICP external parameters was covered in this experiment: argon pressure, 1-100 mTorr; magnetic field, 0-25 G; discharge power, 25-200 W. The measurement at moderate discharge power showed an unexpectedly weak dependence of the EEDF shape and electron temperature on the magnetic field when the EEDF, in the elastic energy range, is close to a Maxwellian distribution. In this regime, a negligibly small cyclotron resonance effect could be observed even at lowest argon pressure, when the electron collision frequency was much less than the electron cyclotron frequency. Increasing the magnetic field from zero to that corresponding to the cyclotron resonance (10 G) resulted in a doubling of the plasma density. Only at small discharge power, when the EEDF was essentially non-Maxwellian, did we observe a weak cyclotron resonance effect in modification of the EEDF and a rise in the effective electron temperature and plasma density, similar to that found previously in Ref. 1. We found a significant drop in the rf coil current and voltage with increasing magnetic field. The relative change in the coil voltage and current being much stronger than the change in the plasma parameters leads to a dramatic (up to an order of magnitude) reduction in the coil loss, thus improving the power transfer efficiency. We show that the insensitivity of plasma parameters to the magnetic field at high plasma density when the EEDF is close to a Maxwellian distribution is a consequence of ionization and electron energy balance in the ICP. [1] ChinWook Chung et al, *Phys. Rev. Lett.* 88, 095002-1 (2002)

14:30

ET2 6 Comparison of spatially-resolved experimental and calculated electron distribution functions and other plasma parameters in inductively coupled argon plasma V. KOLOBOV, R. ARSLANBEKOV, N. ZHOU, *CFD Research Corp.* V. GODYAK, *Osram Sylvania* Spatially resolved measurements of the electron energy probability function (EEDF) have been performed in inductively coupled argon plasma a wide range of operating conditions (gas pressures $p=0.3-300$ mT, driving frequency 0.45-13.56 MHz, power absorbed in plasmas 5-200 W). Self-consistent hybrid simulations of the system have been performed using a spatially inhomogeneous electron Boltzmann solver (based on two-term spherical harmonics expansion) and continuum (fluid) model for ion and neutral transport. The comparison of experimental and simulation results allows us to gain insight into importance of different physical processes (plasma chemistry, ion inertia effect, gas heating, temporal variation of the EEDF, Lorentz force effect, etc) under different operating conditions.

14:45

ET2 7 Angular Dependence of Electron Velocity Distributions in Low-pressure Inductively Coupled Plasmas* ALEX VASENKOV, *Dept. of Electrical and Computer Engr., University of Illinois, Urbana, IL 61801* MARK J. KUSHNER, *Dept. of Electrical and Computer Engr., University of Illinois, Urbana, IL*

61801 The nearly noncollisional electron transport typical of low-pressure (< 10 s mTorr) and low-frequency (< 10 s MHz) inductively coupled plasmas (ICPs) has the potential to produce highly anisotropic angularly dependent electron velocity distributions (AEVDs). The properties of AEVDs in axially symmetric ICPs sustained in Ar and Ar/C₄F₈ mixtures were investigated using a Monte Carlo simulation (MCS) embedded in a two-dimensional plasma equipment model. The coefficients for a Legendre polynomial expansion of the angular dependence of the AEVDs are directly computed during advancement of the trajectories of pseudo-electrons in the MCS. These coefficients are used to reconstruct the AEVDs. Significant anisotropy of the AEVDs occurs in the azimuthal-radial (θr) plane for a wide range of pressures and frequencies due to both linear (proportional to E_θ) and nonlinear forces (proportional to B_r), with the nonlinear forces dominating at lower frequencies. Angular anisotropy of the AEVDs in the radial-axial (rz) plane is attributed to acceleration by non-linear Lorentz forces resulting from the rf magnetic field. The anisotropy is particularly significant when the skin layer is anomalous.

*Work was supported by the National Science Foundation (CTS99-74962), Semiconductor Research Corp. and CFD Research Corp.

SESSION FT1: PLASMA SHEATHS

Tuesday afternoon, 21 October 2003

California Ballroom, Cathedral Hill Hotel at 15:30

Uwe Czarnetzki, University of Bochum, presiding

15:30

FT1 1 Overview of our recent experiments and thoughts about plasma presheaths NOAH HERSHKOWITZ, EUNSUK KO, XU WANG, *University of Wisconsin - Madison, Engineering Physics Dept.* GREG SERVERN, *University of San Diego - San Diego, Physics Dept.* Recent experiments in weakly collisional multipole plasmas with two positive ion species show the presence of ion-ion two stream instabilities in presheaths near boundary plates. This shows that the two ion species interact with each other. Direct measurements with LIF demonstrate that Ar ions in an Ar-He plasma exit the plasma and the plasma/sheath boundary with a velocity greater than the Bohm velocity. Measurements of phase and group velocity of ion acoustic waves launched into the presheath as well as Mach probe data provide additional drift velocity related data. The role of ionization and collisions (especially charge exchange collisions) in presheaths in multi-dipole plasmas is explored. *Work Supported by US DOE grant DE-FG02-97ER 54437

15:45

FT1 2 Generalising Planar, Cylindrical and Spherical Diodes for Non-Zero Potential Gradient ORSON SUTHERLAND, ADRIAN ANKIEWICZ, ROD BOSWELL, *Plasma Research Laboratory, RSPHysSE, Australian National University* The primary tools of analysis in the study of ion extraction from plasmas are the Child-Langmuir and Langmuir-Blodgett laws. These relations describe the flow of charged particles in planar, cylindrical and spherical diodes based on the assumption of zero initial ion velocity and zero electric field at the entry to the diode. However,

in the case of extraction from a plasma, though the assumption of zero initial velocity is justifiably maintained, the hypothesis of zero electric field is flawed. This is because the plasma sheath which joins the bulk plasma to the beam has an intrinsic electric field of non-zero gradient at the sheath/beam boundary or meniscus. Typically this gradient is on the order of the MV/m. In this work, we present generalisations to the Child-Langmuir and Langmuir-Blodgett laws to incorporate a non-zero electric field gradient at the meniscus and discuss implications for ion beam extraction.

16:00

FT1 3 Plasma-Sheath Model with Diffuse Electron Boundary

NATALIA STERNBERG, *Clarke University* VALERY GODYAK, *Osram Sylvania* The plasma-sheath model with diffuse electron boundary was first considered by Bohm in order to construct a discrete plasma-sheath model. To account for the transition region where the electron density drops from $n_e \approx n_i$ to $n_e \ll n_i$ (here, n_e is the electron density and n_i is the ion density), Bohm assumed in the sheath model a continuous ion flux while keeping the electrons in the Poisson equation. He also assumed the zero-field boundary condition at the patching point of the plasma and the sheath solutions. Although Bohm's model became the classical sheath model, it is not a consistent model of the sheath, but rather a model that includes the sheath and an infinitely large intermediate region where $n_e \approx n_i$. Because of the zero-field boundary condition, one cannot patch the sheath solution directly with the asymptotic plasma solution, used today to model the plasma region. This led to the belief that the only way to approximate the full solution of the plasma-wall problem is to use matched asymptotic expansions, which require modeling of the transition region and mastering of complicated mathematical techniques. In this presentation, we show that by eliminating the requirement of the zero-field boundary condition in the classical sheath model, it is possible to patch the plasma and the sheath solutions directly. We develop a simple technique for choosing the patching point, which yields a good approximation of the full solution by the patched solution.

16:15

FT1 4 Analytical Model of a Dual Frequency Capacitive Sheath

P. C. BOYLE, *Dublin City University, Ireland* J. RO-BICHE, *Dublin City University, Ireland* M. M. TURNER, *Dublin City University, Ireland* A. R. ELLINGBOE, *Dublin City University, Ireland* An analytical sheath model for a capacitively coupled radio-frequency plasma discharge operated with two frequencies is presented under the assumptions of a time-independent, collisionless ion motion. Expressions are obtained for the time average electric potential within the sheath, nonlinear motion of the electron sheath boundary and nonlinear instantaneous sheath voltage. The model is valid under the condition that the low frequency (lf) electric field amplitude E_{lf} in the sheath is much higher than the high frequency (hf) electric field amplitude E_{hf} . This condition is fulfilled under typical operational conditions for dual frequency capacitive discharges in microelectronics processing applications. We show that the hf electric field modifies the sheath structure significantly because of the electron response to E_{hf} . This model has been compared to particle-in-cell plasma simulations, finding good quantitative agreement. We will discuss the dependence of the maximum sheath width and the dc sheath voltage drop on the hf/lf current ratio and on the hf/lf frequency ratio.

16:30

FT1 5 Collisional sheath dynamics in the intermediate rf frequency regime NONG XIANG, *Institute for Fusion Studies, University of Texas* FRANK L. WAELBROECK, *Institute for Fusion Studies, University of Texas* A sheath model is proposed for the case when the rf frequency ω is comparable to or larger than the ion plasma frequency of the bulk plasma ω_{pi} , and the ion collision in the sheath is significant, namely, the ion collision frequency $\gamma_i \geq \max(\omega, \omega_{pi})$ or the ion mean-free-path is much shorter than the thickness of the sheath. In this case, the ion velocity is governed by the localized ion momentum equation that can be solved easily. We find that the ion velocity in the sheath varies with time and the resulting ion energy distribution is bimodal even though the rf frequency is much larger than the ion plasma frequency in the sheath. The results of the model are compared with the numerical solutions of the fluid equations. Both are in very good agreement.

16:45

FT1 6 Structure of electric field in sheath and presheath regions of a low-pressure ICP Ar plasma measured by laser-induced fluorescence-dip spectroscopy K. SASAKI, K. TAKIZAWA, A. KONO, *Department of Electronics, Nagoya University, Japan* Electric field in sheath and presheath regions plays essential roles in plasma processing of materials. We have developed laser-induced fluorescence-dip spectroscopy of Ar for the measurement of electric field in various processing plasmas. This is a very sensitive method, and a detection limit of 6 V/cm was achieved by observing the Stark spectrum of an Ar high Rydberg state with a principal quantum number of 40. In the present work, we measured the distribution of electric field in sheath and presheath regions of a low-pressure ICP Ar plasma. A biased electrode was inserted in the plasma, and the electric field in front of the electrode was measured. When the voltage between the electrode and the plasma was 70 V, we observed steep decay of the electric field from 700 V/cm to 20 V/cm within a distance of 1.5 mm from the electrode. The steep decay was followed by a long tail component with electric field less than 10 V/cm. The experimental result was compared with the distribution of electric field evaluated by a simple fluid model. As a result, the electric field observed in the sheath region agreed well with the theoretical result.

17:00

FT1 7 Analytical and numerical study of the cathode sheath formation in a high-pressure discharge for XeCl laser BE-LASRI AHMED, *Laboratoire de Physique des Plasmas, Matériaux Conducteurs et leurs Applications U.S.T.O Faculté des Sciences, Département de Physique U.S.T.O El M'NAOUAR B.P. 1505 Oran Algeria* The purpose of this paper is to study the evolution of the cathode sheath for an initially preionized high-pressure discharge for XeCl Lasers. A simplified analytical model, and longitudinal one-dimensional numerical model are developed. The results show that under normal conditions of operation, the cathode electric field can reach values as high as 106 V/cm. These elevated values are largely responsible of the development of the instabilities in this region of the discharge. A transition from capacitive to resistive behavior of the sheath occurs rapidly because of the large multiplication of cathode-emitted electrons in the sheath electric field. Results are presented for different values of

the secondary electron emission coefficient. It is shown that the electrical and chemical behavior of the plasma can be strongly affected by the presence of the sheath. Key words: Cathode Sheath, Discharge, Excimer laser, Modeling, Secondary emission.

17:15

FT1 8 A different way of looking at the Plasma-Sheath Boundary Region RAOUL FRANKLIN, *Oxford Research Unit, The Open University, Oxford, England* The plasma-sheath boundary region has been the subject of study for eighty years, but there are aspects that are still not well understood. At low pressures it is clear that the structure is - plasma-transition layer-thin electron sheath -(thick)ion sheath, and at high pressures it is plasma-collisional sheath, without the need to introduce further structure. As the plasma becomes collisional, there is a question as to how long it is appropriate to speak in terms of the Bohm criterion. Furthermore if the sheath is many ion mean free paths long, the ions may be brought back into collisional equilibrium with the electric field, even though their speed exceeds the ion sound speed of the plasma from which they derive. We examine computationally this intermediate pressure region in terms of how to describe the ion motion, showing how the two limits go over from the one to the other. Most practical gas discharge plasmas are in such a transitional pressure region.

SESSION FT2: PLASMA CHEMISTRY

Tuesday afternoon, 21 October 2003

International Ballroom, Cathedral Hill Hotel at 15:30

Jurgen Roepke, Institute for Base Temperature of Plasma Physics-Greifswald, presiding

15:30

FT2 1 On Plasma Chemistry in H₂-Ar-N₂-Microwave Discharges with Admixtures of Methane or Methanol F. HEMPEL, D. LOFFHAGEN, L. MECHOLD,* J. RÖPCKE, *Institut für Niedertemperatur-Plasmaphysik, Greifswald, Germany* P.B. DAVIES, *Department of Chemistry, University of Cambridge, UK* Tuneable infrared diode laser absorption spectroscopy has been used to detect the methyl radical and nine stable molecules, CH₄, CH₃OH, C₂H₂, C₂H₄, C₂H₆, NH₃, HCN, CH₂O and C₂N₂, in H₂-Ar-N₂ microwave plasmas containing up to 7% of methane or methanol. The degree of dissociation of the hydrocarbon precursor molecules varied between 20 and 97%. The methyl radical concentration was found to be in the range from 10¹² to 10¹³ molecules cm⁻³. By analysing the temporal development of the molecular concentrations under static conditions it was found that HCN and NH₃ are the final products of plasma chemical conversion. The fragmentation rates of methane and methanol and the respective conversion rates to HCN, NH₃, CH₄, C₂H₂, C₂H₄ and C₂H₆ have been determined for different H₂ to N₂ ratios. A model of the chemical reactions in H₂-N₂-Ar-CH₄ plasmas has been developed and the main reaction pathways of important neutral species are discussed.

*present address: Laser Components, Olching, Germany

15:45

FT2 2 Hydrogen Generation in a Microhollow Cathode Discharge in an Atmospheric-Pressure Ammonia-Argon Mixture

HONGWEI QUI, *Stevens Institute of Technology* K. MARTUS, *William Paterson University* W. LEE, *Stevens Institute of Technology* K. BECKER, *Stevens Institute of Technology* A micro hydrofuel reformer for H₂ generation has been developed using a single microhollow cathode discharge (MHCD) with a mixture of ammonia (NH₃) and argon (Ar) as the operating gas. The MHCD was constructed from two pieces of thin metal separated by a mica spacer with a single hole, roughly 0.1 mm in diameter, through the three layers. The efficiency of the MHCD reactor for H₂ generation from NH₃ was analyzed by monitoring the products formed in the discharge in a mass spectrometer. Using a gas mixture of a few percent NH₃ in Ar at one atmosphere, the single-hole MHCD reactor achieved an ammonia conversion of 20%. The effects of NH₃ partial pressure and discharge power on the hydrogen production were investigated. We also explored the possibility of using a plasma reactor consisting of a 2-dimensional array of MHCDs operated in parallel. Work supported by the NSF, the William Paterson University ART Program, and the NJCST.

16:00

FT2 3 Numerical Simulation of Dielectric Barrier Discharge of Atmospheric Air

NING ZHOU, *nz@cfdr.com, CFD Research Corp* R. ARSLANBEKOV, *CFD Research Corp* V. KOLOBOV, *CFD Research Corp* Uniform glow dielectric barrier discharges (DBDs) at atmospheric pressures have rekindled the interest in both industries and academia recently. We have numerically studied the plasma dynamics in DBDs of atmospheric air (Nitrogen/Oxygen mixture), using the commercial code CFD-ACE + PLASMA, which employs a hybrid numerical model of fluid equations for heavy particles and electron kinetic (Boltzmann) equation. The detailed gas phase chemistry (over 200-step) of N₂ and O₂ was compiled to include three body reactions, molecular ions and volume recombination processes, which are important at high pressures. The numerical simulation covers a wide range of driving frequencies (10 - 100 kHz) and applied voltages (1 - 10 kV). The product of pressure and gap length (typically mm), pL is about 100 Torr cm, and the breakdown corresponds to the right-hand branch of the Paschen curve. One-dimensional results will be presented with available comparison data. The issues involved in multi-dimensional modeling (eg, filamentation) will also be discussed.

16:15

FT2 4 Characterization of an Aluminum Laser-Induced Plasma at Low Fluence in Ambient Air with Time and Spatial Resolution

OLIVIER BARTHÉLEMY, JOËLLE MARGOT, *Groupe de physique des plasmas, Université de Montréal* MOHAMED CHAKER, *INRS-Énergie, Matériaux et Télécommunications* MOHAMAD SABSABI, *Industrial Materials Institute NRC* TUDOR W. JOHNSTON, STEPHANE LAVILLE, BORIS LE DROGOF, FRANCOIS VIDAL, *INRS-Énergie, Matériaux et Télécommunications* Plasmas produced by interaction of a laser with a solid target under moderate fluence conditions (typically 10 J/cm²) are of great interest for various applications, including synthesis of thin films and nanomaterials, and laser-induced plasma spectroscopy. Despite this interest, there are relatively little systematic investigation of the characteristics of such plasmas. In this work, we examine a plasma produced from aluminum under at-

mospheric environment. Using spectroscopic diagnostics, we examine the time and space dependence of temperature and electron density of the plasma. The influence of the laser pulse wavelength (from 266 to 1064 nm) and duration (from 80 fs to 8 ns) on these parameters is also investigated. We show that the plasma is spatially uniform and that plasma expansion occurs isotropically over a typical distance of 1 mm.

16:30

FT2 5 Combustion Enhancement Using a Silent Discharge Plasma Reactor*

LOUIS ROSOCHA, DAVID PLATTS, DON COATES, SY STANGE, *Los Alamos National Laboratory* Electric fields affect flame propagation speed, stability, and combustion chemistry. External electrodes, arc discharges, and plasma jets have been used to combust gas mixtures outside their flammability limits. Experiments with silent electrical discharges (SEDs) and propagating flames have shown that flame propagation velocity is actually decreased (combustion retarded) when an SED is applied directly to the flame region, but velocity is increased (combustion promoted) when applied to the unburned gas mixture upstream of a flame. More recent work has proposed electric arc/microwave-driven plasma-generating fuel nozzles to produce dissociated fuel or ionized fuel for aircraft gas turbine engine combustor mixers. In contrast to prior works, we have used a silent discharge plasma (SDP) reactor to break up large fuel molecules into smaller molecules and create free radicals/active species in a gas stream before the fuel is mixed with an oxidizer and combusted. A cylindrical SDP reactor was used to "activate" propane before mixing it with air and igniting the combustible gas mixture. With the plasma, the physical appearance of the flame changes and substantial changes in mass spectrometer fragmentation peaks for fuel and combustion products are observed (i.e., combustion is enhanced). Results of changes in the degree of combustion will be discussed in terms of variations in the plasma specific energy.

*Work supported by US Department of Energy.

16:45

FT2 6 Power and Air Chemistry Simulations for Plasma Continuously Generated by an Electron Beam with a Sustaining Electric Field

ROBERT VIDMAR, *University of Nevada, Reno* KENNETH STALDER, *Stalder Technologies and Research* Plasmas generated by a high-energy electron beam in air at pressures corresponding to sea level to 91.4 km (300 kft) altitude perturb the local chemical equilibrium. Recent studies have shown that externally-imposed electric fields can slow the deionization rate substantially due to many factors, including enhanced detachment of electrons from O₂⁻ ions by oxygen singlet delta. The dominant positive ion following an electron-beam ionization pulse first start as O₂⁺, but then rapidly reacts to form numerous other ions such as NO⁺. Slow electrons produced by the high-energy electron beam rapidly attach to oxygen, but then subsequently react to form numerous other negative ion species and ultimately form NO₃⁻ in the late afterglow. If water vapor is present in natural amounts, as high as 1 then hydrated complexes form. Energy contained in vibrationally excited N₂ and O₂ consumes much of the power in the discharge. Air chemistry simulations are discussed with results on the addition of NO_x reactions, various imposed E-field scenarios, and power estimates for sustaining electron densities ranging from 1E10 to 1E13 cm⁻³. This material is based on research sponsored by the Air Force Research Laboratory, under agreement number F49620-01-1-0414.

17:00

FT2 7 Simulation of $O_2(^1\Delta)$ yields in mixtures of O_2 and inert gases in low pressure plasmas* D. SHANE STAFFORD, *Dept. of Chemical and Biomolecular Engineering, University of Illinois* MARK J. KUSHNER, *Dept. of Electrical and Computer Engineering, University of Illinois* Current trends in pumping chemical oxygen-iodine lasers (COIL) involve producing the $O_2(^1\Delta)$ energy donor in electric discharges, thereby circumventing the hazards and complexity of conventional $O_2(^1\Delta)$ production via liquid chemistries. In this work we have investigated the scaling of $O_2(^1\Delta)$ yield with energy deposition in mixtures of O_2 with He and Ar in rf discharges at pressures of a few to 10 Torr using a global plasma kinetics model. The global model was modified to address steady-state plug flow with one-dimensional gas hydrodynamics. We found that $O_2(^1\Delta)$ yield increases linearly with energy deposition per molecule of O_2 up to a few eV per molecule, with yields peaking around 40 percent near 10 eV. We also found that further increases in energy deposition serve only to increase gas dissociation and heating, thereby reducing the $O_2(^1\Delta)$ yield. We will also discuss secondary effects from other parameters such as gas mixture and pressure, including results from a one-dimensional hydrodynamics model.

*Work supported by AFOSR and NSF.

17:15

FT2 8 EXPERIMENTAL AND THEORETICAL STUDIES ON SINGLET DELTA OXYGEN PRODUCTION IN ELECTRON-BEAM SUSTAINED DISCHARGE ANATOLY NAPARTOVICH,* *RSC TRINITY, Troitsk, Moscow Region, Russia* IGOR KOCHETOV, *RSC TRINITY, Troitsk, Moscow Region, Russia* MIKHAIL FROLOV, ANDREY IONIN, YURI KLIMACHEV, ANDREY KOTKOV, YURI PODMARKOV, LEONID SELEZNEV, DMITRY SINITSYN, NIKOLAY VAGIN, NIKOLAY YURYSHEV, *Lebedev Physics Institute, Moscow, Russia* GORDON HAGER, *AFRL, Kirtland AFB, NM 87117-5776, USA* TRINITY COLLABORATION, LEBEDEV COLLABORATION, AFRL COLLABORATION Electric properties and spectroscopy of an e-beam sustained discharge (EBS) in oxygen containing mixtures at gas pressure up to 100 Torr were experimentally studied. The discharge in pure oxygen and its mixtures with noble gases was shown to exist only at low input energy. When adding small amount of CO or H_2 , specific input energy grew substantially. Spectroscopic measurements of singlet delta and singlet sigma dynamics in the EBS were performed. Detailed kinetic model of EBS plasma for conditions of the experiments was developed taking into account gas-dynamic expansion. Theoretically synthesized molecular spectra show good agreement with measurements. Kinetic modeling verified by the experiments shows a good promise of the discharge technique for singlet delta production. It is predicted that the close control of gas temperature for experimental conditions will allow for breaking threshold in oxygen-iodine laser.

*Corresponding

SESSION GTP: POSTER SESSION I

Tuesday evening, 21 October 2003

El Dorado, Cathedral Hill Hotel at 19:15

I. Langmuir, GE Research Laboratory, presiding

GTP 1 INDUCTIVELY COUPLED PLASMAS

GTP 2 Global Model of Time-Modulated Electronegative Discharges for Neutral Radical and Electron Temperature Control SUNGJIN KIM, M.A. LIEBERMAN, A.J. LICHTENBERG, *University of California, Berkeley* Control and reduction of neutral radical flux/ion flux ratio and electron temperature T_e is required for next generation etching in the microelectronics industry. We investigate time-modulated power for these purposes using a volume-averaged (global) oxygen discharge model. We consider pressures of 10-50 mTorr and plasma densities of 10^{10} - 10^{11} cm^{-3} . In this regime, the discharge is found to be weakly electronegative. The modulation period and the duty ratio (on-time/period) are varied to determine the optimum conditions for reduction of $FR = O\text{-atom flux/ion flux}$ and T_e . Two chambers with different height/diameter ratios ($< < 1$, and unity) are examined to determine the influence of the surface-area/volume ratio. At a fixed duty ratio, both FR and T_e are found to have minimum values as the pulse period is varied, with the minimum value decreasing as the duty ratio decreases. Significant reductions in FR and T_e are found. Support provided by Lam Research, NSF Grant ECS-0139956, California industries, and UC-SMART Contract SM99-10051.

GTP 3 Self-Consistent Simulations of Inductively Coupled Discharges at Very Low Pressures Using a FFT Method for Calculating the Non-local Electron Conductivity for the General Case of a Non-Uniform Plasma OLEG POLOMAROV, *University of Toledo* CONSTANTINE THEODOSIOU, *University of Toledo* IGOR KAGANOVICH, *Princeton University* A self-consistent system of equations for the kinetic description of non-local, non-uniform, nearly collisionless plasmas of low-pressure discharges is presented. The system consists of a non-local conductivity operator, and a kinetic equation for the electron distribution function (EEDF) averaged over fast electron bounce motions. A Fast Fourier Transform (FFT) method was applied to speed up the numerical simulations. The importance of accounting for the non-uniform plasma density profile in computing the current density profile and the EEDF is demonstrated. Effects of plasma non-uniformity on electron heating in rf electric field have also been studied. An enhancement of the electron heating due to the bounce resonance between the electron bounce motion and the rf electric field has been observed. Additional information on the subject is posted in http://www.pppl.gov/pub_report/2003/PPPL-3814-abs.html and in <http://arxiv.org/abs/physics/0211009>

GTP 4 Numerical Study of SF₆ Plasma Characteristics at Different Operating Conditions NING ZHOU, *nz@cfdrc.com, CFD Research Corp* V. KOLOBOV, *CFD Research Corp* R. ARSLANBEKOV, *CFD Research* Inductively coupled plasmas (ICP) using SF₆ and its mixtures are of great interest to semiconductor material processing. It is well known that the SF₆ plasma is characterized as highly electronegative due to the large cross-section for electron attachment. However recent work (S Rauf et al., JAP, V.92, 6998(2002)) reveals electropositive SF₆ plasma under certain conditions. The proposed study will focus on the underlying physics of the SF₆ plasma transition from electronegative to electropositive, in low pressure ICP regime. In particular, the influential parameters such as pressure, ICP power and SF₆ fraction in mixture will be examined. In the numerical models (a hybrid code, CFD-ACE+PLASMA, with multi-dimensional fluid equations for heavy particles and kinetic equation for electron), non-Maxwellian electron kinetics, particularly in low density regime will be investigated using homogenous and inhomogenous (non-local) Boltzmann solver. The SF₆ reaction chemistry and the cross-section data will be carefully examined to properly encompass both electro-negative and electro-positive regions. The numerical results will be compared with available experiment/modeling data.

GTP 5 Low-frequency inductively coupled plasmas: plasma parameters and potential industrial applications K. OSTRIKOV, S. XU, *Plasma Sources and Applications Center, NIE, Nanyang Technological University, 637616 Singapore* Low-temperature RF plasmas have recently emerged as efficient chemically active environment for various applications ranging from microstructuring of semiconductor wafers to synthesis of advanced materials with unique properties. The underlying physics and applications of the low-frequency (460 kHz) inductively coupled plasma (LF ICP) source are discussed. The plasma source has successfully been used for various applications, including low-temperature plasma-enhanced chemical vapor deposition of vertically aligned carbon nanotubes and self-assembly ordered nanopillar arrays for field emission applications, plasma enhanced DC sputtering deposition of ternary AlCN thin films, fabrication of micro/optical electronically important Si/SiC quantum dots with controllable bandgaps, surface hardening and modification of metallic alloys (plasma nitriding), as well as plasma-based synthesis of other advanced materials (TiN, SiC, CN, etc.). The deposition rates and main properties of the grown materials can be efficiently controlled by the plasma parameters and discharge operating regimes. The techniques for tailoring the species composition using the electron energy distribution functions (EEDF) are also discussed. The results suggest that the LF ICPs are efficient in fabrication of templates with embedded nanoparticles, control of the substrate temperature, deposition of nano-films with controllable deposition rates, and generation of nanocluster clouds.

GTP 6 A Variable Frequency Tuning Scheme for Inductive Plasma Sources KAVEH NIAZI, *Intel Corporation* ZHAN CHEN, *Intel Corporation* OLEH KARPENKO, *Intel Corporation* A common approach for the efficient coupling of RF power to an inductive plasma source consists of a matching network with variable capacitive components that adjust in response to the varying load conditions of the plasma source. The use of variable capacitances in industrial applications such as semiconductor equipment is non-trivial, however. The high voltage ratings often required for semiconductor equipment result in capacitors that are expensive and quite bulky. In addition the motors that are used to adjust the

capacitances often have a slower response time than desired. An alternate approach, the use of fixed capacitors and a variable frequency source signal to reduce the reflection coefficient, to an acceptable level, addresses both these concerns and is discussed in this paper. By using a circuit model for the plasma source and matching network, it is possible to predict an optimal frequency and corresponding reflection coefficient for a given plasma load condition. In this paper numerical predictions of the reflection coefficient for the variable frequency matching scheme are presented for common inductive plasma source impedance parameters. In addition if the limits on the allowed VSWR and the plasma source impedance are specified, the numerical model presented provides a simple scheme for specifying the required frequency range and fixed capacitance values for the matching network.

GTP 7 Characterisation of an inductively coupled oxygen discharge PHILIP STEEN, CORMAC CORR,* SERGI GOMEZ,† GARY CRAIG, BILL GRAHAM, *Queens University of Belfast, BT7 INN, UK* Oxygen is a weakly negative molecular gas and as such a number of different species, O₂, O, O⁺, O₂⁺, O⁻ may be present in the discharge. In order to get a handle on the important processes occurring in inductively coupled oxygen discharges it is important to know something about the relevant densities of the above species and how they interact with each other and with changing plasma input parameters such as power and pressure. To this end we report measurements made in a low-pressure 13.56 MHz inductively coupled GEC cell operating in oxygen. In particular atomic oxygen temperature and density measurements made using two photon LIF, with measured temperatures ranging from approximately 400 K in the low power capacitive mode to near 2000 K in the higher power inductive mode and measured densities from 1x10¹² cm⁻³ in capacitive to 2x10¹⁴ cm⁻³ when inductive. Electron energy distributions measured using Langmuir probes and Thomson Scattering, giving electron densities from 5x10⁸ cm⁻³ when in capacitive mode to 5x10¹⁰ cm⁻³ when in inductive mode. Negative ion density measurements were also made using a photo-detachment technique giving O⁻ densities of 2x10⁹ cm⁻³ in capacitive mode to approximately 6x10⁹ cm⁻³ in inductive mode. During the course of some of this work an instability was also observed in the form of periodic modulations in the light output, floating potential, electron and positive and negative ion densities and this will also be discussed.

*Currently at Ecole Polytechnique, 91128 Palaiseau France

†Currently at UC Santa Barbara, USA

GTP 8 Real-time Monitoring of Drifting Ion Flux and Ion Energy in a High-Density, Inductively Coupled Plasma MARK SOBOLEWSKI, *National Institute of Standards and Technology* Measurements of the radio-frequency (rf) voltage and current applied to a plasma reactor, interpreted by plasma sheath models, provide an ability to monitor the total ion flux and ion energy distribution at surfaces inside the reactor. Such measurements are useful for monitoring drift in manufacturing or laboratory reactors when direct measurements of ion flux or energy are impossible or impractical. In this study rf measurements were used to monitor drift in Ar and Ar/CF₄ discharges in an inductively coupled, high-density plasma reactor. One source of drift in such reactors is the deposition of a conductive surface layer on the dielectric window beneath the inductive source. As this layer grows, a greater fraction of the source power excites currents in the layer, rather than

in the plasma, resulting in less efficient operation and a reduction in plasma density and ion flux. These changes in turn affect the coupling of rf bias power into the discharge, producing changes in delivered rf bias power or voltage, sheath voltages, and ion energy distributions. Using rf measurements, the resulting changes in ion flux and energy were monitored in real time, as the surface layer was deposited and removed.

GTP 9 On the electron heating mechanism in low pressure high density inductively coupled plasma (ICP) K.-I. YOU, *Korea Basic Science Institute* W. K. KIM, *Dept. of Electrical and Computer Engineering, HanYang University* CHINWOOK CHUNG, *Dept. of Electrical and Computer Engineering, HanYang University* The electron heating mechanism in a low-pressure inductively coupled plasma (ICP) is investigated. Two types of resonant coupling between electrons and radio frequency electric fields are possible in low pressure ICP[1]. The electron bounce resonance corresponding to the first resonant coupling is a dominant electron heating mechanism in a finite size ICP[2]. We find out that the electron bounce resonance has a dependence on electron density when we calculate energy diffusion coefficients against electron density. This dependence on the electron density seems to be related to electron motion in the skin layer. The change in the electron bounce resonance is analyzed and discussed in this paper.

GTP 10 MATERIAL PROCESSING I

GTP 11 Reactive RF plasma growth of highly transparent (002) AlN films CHANDRU MIRPURI, S. Y. HUANG, J. D. LONG, K. OSTRIKOV, S. XU, *Advanced Materials and Nanostructures Laboratory, NIE, Nanyang Technological University, 637616 Singapore* Radio frequency (RF) magnetron sputtering plasma assisted CVD has been employed for synthesizing highly orientated transparent aluminum nitride (AlN) films. Crystalline (002) AlN films have been grown on (111) Si substrates at a typical substrate temperature of 350C. The structural and bonding states are found to be sensitive to the deposition conditions including sputtering pressure, RF power, substrate temperature, and nitrogen gas inlet. X-ray diffraction patterns reveal the formation of highly c-oriented AlN films at a sputtering pressure of 0.8 Pa. Field emission scanning electron microscopy images indicate that the AlN films are highly uniform over large substrate areas and exhibit a zone 1 columnar structure of a typical length of 100-500 nm with the aspect ratio of about 25. It is found that the columnar structure is embedded in a few nm thick amorphous layer and singly oriented in the (002) direction. X-ray photoelectron and energy dispersive x-ray spectroscopy analysis suggest that AlN films deposited at RF power of 400 W feature a chemically pure and near stoichiometric AlN. The bonding states of the AlN films are predominantly the E2 (high) and E1(TO) phonon modes as depicted by Raman and Fourier transform infrared spectroscopy. Hydrogenated AlN films feature a high optical transmittance of 85% in the visible region of the spectrum, suggesting potential applications for optical coatings and as a buffer layer for high quality GaN growth.

GTP 12 A VHF-UHF Etch System with High Density, Low Electron Temperature and Radially Adjustable Uniformity JOHN H. KELLER, *K2 Keller Consulting, LLC* Inductive plasmas were successful in silicon etching and metal etching, due to their high plasma density and good uniformity. However, inductive or Inductively Coupled Plasmas, ICP, were less successful in oxide etching. This presumably is because these plasmas have a reduced percentage of hot tail electrons compared to Capacitively Coupled Plasmas, CCP. In addition, in ICP there is an aspect ratio damage effect due to the higher temperature of the bulk electrons. VHF-UHF (60-500 MHz)-CCP can have high plasmas density, since Ni is proportional to F_2 . Thus high-density plasmas with hot tail electrons can be produced. A CCP system, which has high density, a low RF plasma potential, with low temperature electrons near the wafer, and adjustable radial uniformity will be discussed. In addition a magnetic filter may be used to further reduce the electron temperature near the wafer.

GTP 13 Etching with Electron Beam-Generated Ion-Ion Plasmas S.G. WALTON, D. LEONHARDT, C. MURATORE,* D.D. BLACKWELL,† R.F. FERNSLER, *Plasma Physics Division, Naval Research Laboratory, Washington, DC 20375* Positive ion-negative ion (ion-ion) plasmas are thought to prevent device damage and isotropic etch profiles associated with surface charging, because of their ability to deliver anisotropic fluxes of both positive and negative ions to the substrate surface. Ion-ion plasma formation in halogen-based gases requires low electron temperatures and is therefore commonly observed in the afterglow of pulsed plasmas, thereby limiting the duration and magnitude of the negative ion flux. Electron beamgenerated plasmas, because of their inherently low electron temperatures (< 1.0 eV), are capable of producing ion-ion plasmas during all plasma phases and thus have the potential for processing in the absence of electrons. In this work we present the results of experiments aimed at determining the feasibility of an ion-ion etching process. Pulsed, electron beam-generated plasmas produced in Ar/SF₆ mixtures are used to etch Si substrates. Positive and negative ions are delivered to the substrates using a low frequency (< 100 kHz) electrode bias. Etch rates will be presented as a function of various input parameters and compared to etch rates using conventional (electron-ion) electron beamgenerated plasmas. This work supported by the Office of Naval Research.

*ASEE/NRL Postdoctoral Research Fellow

†SFA Inc., Largo, MD 20774

GTP 14 Deposition of High Quality Poly- and Microcrystalline Silicon Films by a Surface-Wave Excited Plasma HIROTAKA TOYODA, SATORU SOMIYA, HIDEO SUGAI, *Department of Electrical Engineering, Nagoya University* Nowadays, attentions has been given to deposition of microcrystalline silicon (μ c-Si) or polycrystalline silicon (poly-Si) films using high density plasma (HDP) sources. Among various HDPs, surface-wave excited plasma (SWP) is attractive because it has low electron temperature and low plasma potential that are preferred to fabricate electronic devices with reduced ion damage. In this paper, we report poly-Si and μ c-Si film deposition using a planer type H₂/SiH₄ SWP. Microwave power (2.45GHz, 2kW) is coupled to the H₂/SiH₄ plasma ($< 5 \times 10^{11}$ cm⁻³) through slot antennas that are installed on a dielectric window. Using this HDP source, μ c-Si films (grain size < 10 nm) are deposited at a deposition rate as high as 50 nm/s. In the case of SWP sources, strong interaction

of high-density plasma with dielectric surface (microwave window) sometimes induces impurity desorption. To reduce the impurity incorporation into the deposited film, various kinds of modified antenna structure or window materials are investigated.

GTP 15 Study of corrosion protection of aluminum by siliconoxide-polymer coatings deposited by a dielectric barrier discharge under atmospheric pressure J.F. BEHNKE, A. SONNENFELD, O. IVANOVA, R. HIPPLER, *University of Greifswald, Institute of Physics, Germany* T. X. H. TO, G. V. PHAM, K. O. VU, T. D. NGUYEN, *Institute for Tropical Technology, 18 Hoang Quoc Viet, Hanoi, Vietnam* Aluminum surfaces were treated with the plasma of a dielectric barrier discharge under atmospheric pressure in air and in nitrogen. Tetraethoxysilan (TEOS) was used as the precursor for the deposition of a thin SiO_x polymer film with an anticorrosive and an adhesive characteristics. The substrate temperature was varied from 25 C to 50 C. The coated aluminum surface was provided with a painting of primer. The corrosion performance of the layers was evaluated by adhesion measurements, by salt spraying test and by electrochemical impedance spectroscopy. The corrosion resistance of the layers depends on the substrate temperature. The results of the impedance measurements show that a surface treatment with a substrate temperature of 50 C supplies the best corrosion protection. The same results were found by using the salt spraying test.

GTP 16 INSTABILITIES IN REACTIVE DISCHARGES

GTP 17 Fusion Reactor Control DIRK PLUMMER, *DIRK ARNOLD PLUMMER, PE* The plasma kinetic temperature and density changes, each per an injected fuel density rate increment, control the energy supplied by a thermonuclear fusion reactor in a power production cycle. This could include simultaneously coupled control objectives for plasma current, horizontal and vertical position, shape and burn control. The minimum number of measurements required, use of indirect (not plasma parameters) system measurements, and distributed control procedures for burn control are to be verifiable in a time dependent systems code. The International Thermonuclear Experimental Reactor (ITER) has the need to feedback control both the fusion output power and the driven plasma current, while avoiding damage to diverter plates. The system engineering of fusion reactors must be performed to assure their development expeditiously and effectively by considering reliability, availability, maintainability, environmental impact, health and safety, and cost.

GTP 18 Non-local instability of low temperature plasma discharges D. MACKEY, *Dublin City University, Ireland* L. PLANTIE, *Dublin City University, Ireland* M. M. TURNER, *Dublin City University, Ireland* Gas discharges exhibit a number of well-known instabilities that give rise to periodic modulation of the plasma density and temperature in space and sometimes time, such as the classical striations often seen in direct current discharges. The mechanism of classical striations is related to the steady drift of electrons along the electric field, and consequently this phe-

nomenon cannot occur in a sufficiently high-frequency discharge. However, high-frequency discharges are known to be affected by related processes, such as instabilities associated with multi-step ionization or other ionization mechanisms that are nonlinear functions of the plasma density. In this paper, we discuss another mechanism of instability of high-frequency discharges, which is related to the non-local interaction of the plasma electrons with the electrostatic potential. This instability can produce a spatial modulation of the plasma density and temperature in the absence of the nonlinear mechanisms mentioned above. We show that this non-local instability can be observed in particle-in-cell simulations and in a hydrodynamic model. Analysis of the hydrodynamic model shows that the instability may affect low pressure, high aspect ratio discharges such as those coming into use for a number of processing applications.

GTP 19 COMPUTATIONAL METHODS FOR PLASMAS

GTP 20 Analysis of the role of metastables in the GEC reference cell in argon by means of 1-D PIC simulations LAURA LAURO-TARONI, ALEC GOODYEAR, RAOUL FRANKLIN, NICHOLAS BRAITHWAITE, *The Open University, Oxford Research Unit* 2-D fluid simulations in [1] indicate that metastables greatly enhance the plasma density, but this is in contrast with [2], whose simulations don't include metastables but show agreement with experimental data. A simple evaluation suggests that at the degree of ionization of the regimes analysed ($< 10^{-5}$) neither metastable pooling nor step-wise ionization is a competitive source of ions compared to direct ionization from neutrals. We have performed simulations with a 1-D PIC/MCC code [3] at 100, 250, 1000 mtorr and driving voltages of 100, 200, 400 V, with and without secondary emission and metastables. The excited states are modelled as two lumped states at 11.6 and 13.1 eV [4] and the radiative decay with a simple decay time [3]. Even without secondaries, the metastable profiles show a fair agreement with experiment [5]. Adding secondaries at 100 and 250 mtorr enhances plasma density, while the metastables are hardly affected. The EEDF varies with power (i.e. applied voltage) and pressure, being unaffected by the inclusion of secondaries or metastables in these regimes. The EEDF is Maxwellian at low pressure/ low voltage (100 mtorr, 100 V), but it becomes Druyvesteyn-like with increasing pressure and power (1 torr, 400 V). [1] D.Lyberopoulos and D. Economou, *J. Res. Natl. Stand. Technol.*, 100, 473 (1995) [2] J.P. Boeuf and L.C. Pitchford, *Phys. Rev. E*, 51 (1995) 1376 [3] M.M.Turner, priv. comm. [4] M.Kushner, priv. comm. [5] B.Mc-Millin and M.Zachariah, *J.Appl.Phys.*, 77 (1995) 5538

GTP 21 Solution of multi-term time-dependent Boltzmann equation in moment representation and its application to numerical treatment of plasmas YURIY SOSOV, *University of Toledo* CONSTANTINE THEODOSIOU, *University of Toledo* The multi-term time-dependent Boltzmann equation for 2.5D-velocity geometry is solved numerically by application of a Hilbert-transform to the system of differential equations for the coefficients of the Legendre polynomial expansion of the distribution function to obtain a system of differential equations for the

moments of the distribution function in the velocity space (moment representation). The expansion coefficients of the distribution function are then obtained through an inverse Hilbert transform from the moment representation. Direct calculation of the moments of the distribution function, instead of the distribution function itself, allows construction of finite difference schemes that numerically conserve particle density and appropriately transform mechanical momentum and energy, as well as higher moments of the distribution function in the velocity space. We will present a study of numerical/difference schemes to calculate transport and collision terms in the moment representation as they apply to plasma simulations. Furthermore, we derive boundary conditions for the expansion coefficients of the distribution function at $v = 0$ based on continuity arguments and suggest various boundary conditions at $v =$ practical infinity.

GTP 22 Some thoughts toward more reliable solution techniques for the Boltzmann equation EDWARD RICHLEY

Techniques for determining electron distribution functions in discharges have evolved along various and widely differing paths. Each has its advantages, and all have disadvantages. Often overlooked is the time-dependent continuum approach. With the distinct advantage of representing the dynamics of the discharge in a quantitative manner, this is potentially a very reliable approach for obtaining a solution. It draws on well-established computational methods developed over many years in the study of reactive flow, and can be applied to the energy-dependent Boltzmann equation. The process of discretization introduces inevitable errors, some of which are quite subtle and due to the interaction of time-dependent quantities. Often, the choice of what to discretize is as important as the method used for solution. This talk will focus on the development of representations which lend themselves to numerical solution by time-dependent finite-difference methods, and which mitigate the deleterious effects of some numerical artifacts which would otherwise arise.

GTP 23 PLASMA DYNAMICS

GTP 24 Aerodynamic Boundary Layer Control Using EHD Effects of a One Atmosphere Uniform Glow Discharge Plasma (OAUGDP)* J. REECE ROTH, RAJA CHANDRA MOHAN

MADHAN, MANISH YADAV, JOZEF RAHEL, *University of Tennessee Plasma Sciences Laboratory, Department of Electrical and Computer Engineering, Knoxville, TN* STEPHEN P. WILKINSON, *Flow Physics and Control Branch, NASA Langley Research Center, Hampton, VA* SUBSONIC PLASMA AERODYNAMICS TEAM We have demonstrated the use of Lorentzian momentum transfer from the One Atmosphere Uniform Glow Discharge Plasma (OAUGDP) to exert electrohydrodynamic (EHD) body forces on aerodynamic flows using two physical processes [1]. One process is the use of paraelectric (the electrostatic analog of paramagnetism) flow acceleration by a surface OAUGDP generated by asymmetric plasma actuators. The second physical process is peristaltic flow acceleration, in which a OAUGDP is generated on phased plasma actuator strips to effect flow acceleration of atmospheric air over a flat plate. This phased excitation pro-

duces a traveling electrostatic wave analogous to the moving lights on a theatre marquee, which accelerates the ions and neutral gas to velocities of interest for some aerodynamic applications, such as flow re-attachment for internal and external aerodynamics [3]. We have conducted boundary layer flow measurements with a Pitot-static probe to measure the Lorentzian momentum-induced flow using peristaltic flow acceleration, and an additive combination of peristaltic and paraelectric effects that have produced velocities in excess of 5 meters per second at a height of 0.8 mm above the surface containing the electrodes. [1] Roth, J. R., R. C. M. Madhan; H. Sin, and S. P. Wilkinson (2003), Flow Re-Attachment and Acceleration by Paraelectric and Peristaltic Electrohydrodynamic (EHD) Effects, AIAA Paper 2003-0531, 41st AIAA Aerospace Sciences Meeting, January 6-9, Reno NV, 2003.

*This work was supported in part by AFOSR Contract AF F49620-01-1-0425 (Roth), Dr. John Schmisser, Program Manager

GTP 25 Three-dimensional Flow Acceleration Using Plasma Aerodynamic Actuators JOZEF RAHEL, J. REECE ROTH, XIN

DAI, *University of Tennessee Plasma Sciences Laboratory, Department of Electrical and Computer Engineering, Knoxville, TN* Several types of non-equilibrium atmospheric pressure discharges are capable of inducing gas flow acceleration, e.g. DC corona discharge, One Atmosphere Uniform Glow Discharge Plasma (OAUGDP) or surface barrier discharge (SBD). Typical experimental values of gas flow velocities lie within the range of 2-10 m/sec. After analysis of the complete electrohydrodynamic (EHD) body forces it was concluded that in all mentioned discharge types the gas flow is induced dominantly by the interaction of the Coulomb force and the net charge generated by the discharge. The limitation on further increase of induced gas flow speed is given by the sparking voltage in the case of corona discharge, or by viscous friction losses in the case of dielectric actuators, where gas acceleration is performed in the close vicinity of a dielectric wall. To overcome this shortcoming for dielectric actuators, an attempt to extract the gas flow from the vicinity of the wall was made. Several axial-symmetric electrode configurations were tested: a double helix spiral on the walls of a hollow cylindrical tube; star-like and flower-like configurations on the planar dielectric plate, and their three dimensional projections; and finally axial-parallel electrode system on the walls of a hollow cylindrical tube. The resulting gas flow velocity was measured with a Pitot-static probe. In all electrode configurations the gas flow was successfully extracted from the vicinity of wall, and can be further manipulated. A possible application is the construction of an ozone blower that does not contain movable mechanical parts.

GTP 26 Acoustic shock wave induced strong double layers formation in the positive column PETER BLETZINGER, ISSI,

Dayton, OH BISWA GANGULY, *Air Force Research Laboratory, WPAFB, OH* ALAN GARSCADDEN, *Air Force Research Laboratory, WPAFB, OH* The influence of shock waves on plasmas has been of high interest for some years. We have shown that there is an interaction between the nonequilibrium plasmas and weak acoustic shock waves which results in the formation of a strong double layer at the shock front [1]. This interaction is enhanced by both plasma E/N and shock wave Mach number increases. We have characterized the double layer strength by optical emission, microwave interferometric electron density and by floating or capacitive probe measurements of the voltage jump at

different Mach numbers, gas pressures, and (E/N) s in a N_2 positive column discharge. The measured double layer voltage jump at the shock front increases from 24 V at Mach 1.8 to 48 V at Mach 2.2, and is in both cases far greater than the $2kT_e$ voltage jump expected for weak double layers. Optical emission shows similar increase with Mach number and when the pressure is decreased from 3 to 1.5 Torr with a corresponding E/N increase by about 50 percent. Similar trends are also observed in the local electron density jump. All these effects show a strong dependency on the polarity of the discharge versus the shock wave propagation direction. These dependencies on polarity, Mach number and E/N are also evident in the global discharge voltage and current responses of the positive column. These double layer results are consistent with the modifications of the shock wave velocity and shock wave broadening observed in a positive column. I. P. Bletzing, B. Ganguly and A. Garscadden, *Phys.Rev. E* 67, 047401 (2003).

GTP 27 OZONE PRODUCTION

GTP 28 Experimental and theoretical study of atmospheric pressure oxygen discharge with dielectric barriers TAKASHI KIMURA, YOSUKE HATTORI, AKINORI ODA, *Nagoya Institute of Technology, Japan* Atmospheric pressure oxygen discharge with dielectric barriers, which is one of successful attempts to obtain high O_3 production, was studied experimentally and theoretically. The discharge was produced between the parallel plate electrodes whose surfaces were covered with Pyrex glass with 0.5 mm thickness in the discharge gap (d) range from 0.3 mm to 2.0 mm using sinusoidal voltage source with the frequency of 1 kHz. The amplitude of applied voltage was about 6 kV. The radii of upper and lower electrodes made of stainless steel were 100 mm ϕ and 220 mm ϕ respectively. Typical O_3 concentration and the production rate for $d = 1.5$ mm were about 3900 ppm and 190 g/kWh, where the total flow rate was 4 l/min and the dissipated power was 9 W. The O_3 concentration and the production rate did not depend on d strongly in d range from 0.7 to 1.5 mm. The discharge current measured at any d included one long pulse (the width of about 100 μ s) and many short pulses. These experimental results were compared with the simulation results of one dimensional fluid model. The results of the simulation predicted that the discharges generated under our experimental conditions were transient glow discharges. This work is partially supported by Grant-in-Aid from the Japan Society for the Promotion of Science.

GTP 29 Modelling of Current Density Redistribution in Hollow Needle to Plate Electrical Discharge Designed for Ozone Generation* VITEZSLAV KRIHA, *Dept. of Physics, FEE CTU, Technická 2, Prague, Czech Republic* Non-thermal plasma of atmospheric pressure electrical discharges in flowing air can be used to generation of ozone. We have been observed two modes of discharge burning in a hollow needle to plane electrodes configuration studied in the ozone generation experiments: A low current

diffuse mode is characterized by increasing of the ozone production with the discharge current; a high current filamentary mode is disadvantageous for the ozone generation (the ozone production decreases when the discharge current increases). A possible interpretation of this effect is following: The filamentary mode discharge current density is redistributed and high current densities in filaments cores lead to degradation of the ozone generation. Local fields in the discharge can be modified by charged metallic and/or dielectric components (passive modulators) in the discharge space. An interactive numerical model has been developed for this purpose. This model is based on Ferguson's polynomial objects for both the discharge chamber scene modelling and the discharge fields analyzing. This approach allows intuitive modifications of modulators shapes and positions in 3D scene followed by quantitative comparison of the current density distribution with previous configurations.

*This work has been supported by Grant Agency of the Czech Republic under contract No. 202/02/P139.

GTP 30 Effect of trigger electrodes configuration of a double discharge ozonizer on ozone generation characteristics MITSUAKI SHIMOSAKI, *Saga University* NOBUYA HAYASHI, *Saga University* SATOSHI IHARA, *Saga University* SABUROH SATOH, *Saga University* CHOBEI YAMABE, *Saga University* The double discharge method has been developed to generate ozone efficiently. In order to realize a high performance ozonizer, ozone generation characteristics such as ozone concentration, ozone yield and gas ozone generation per unit time are required to be clarified. In the double discharge type ozonizer, the trigger discharge electrode plays an important role on the ozone generation. However the detailed mechanism of the trigger discharge has not been studied. In this paper, the effect on ozone concentration and ozone yield was investigated, when the number of the trigger electrodes was varied. Also, the characteristics of the trigger discharge was studied in detail. The ozone yield increased with the trigger discharge power, when the trigger discharge power was up to approximately 0.04 W, and the ozone yield decrease with the discharge power from 0.04 W. The maximum ozone yield was 115 g/kWh, when the numbers of trigger electrodes were 4.

GTP 31 Ozone Production by Atmospheric Pulsed Discharge Using a Partly Covered Electrode SHUNICHI KANEDA, NOBUYA HAYASHI, SATOSHI IHARA, SABUROH SATOH, CHOBEI YAMABE, *Saga University* Atmospheric pulsed discharge has been used for efficient ozone production. In this research, the double discharge method was employed to obtain a atmospheric pulsed discharge. This method consists of two discharges, i.e., a pre-discharge and main discharge. However this configuration has problem that the discharge power and volume are limited by occurrence of arc discharge. In order to revise the problem, the brand new double discharge type ozonizer was proposed. The ozonizer has an anode partly covered with the dielectric, which increases the discharge volume. Basic parameters such as discharge voltage and current waveforms, and ozone concentration were investigated to characterize the discharge. As the result, the discharge power and volume was increased, and the ozone concentration and generation yield were enhanced.

GTP 32 Ozone Synthesis in DC Driven Micro Hollow Cathode Discharge ATSUSHI YAMATAKE, KOICHI YASUOKA, SHOZO ISHII, *Tokyo Institute of Technology* The ozone generation in a high pressure micro-discharge driven by DC voltage source was studied. High pressure gas of oxygen, air or a mixture

of oxygen and nitrogen passed through an electrode-hole of a few hundred micrometers within several micro-seconds. The maximum ozone concentration of $13.7\text{g}/\text{Nm}^3$ was obtained at the efficiency of $204\text{g}/\text{kWh}$ in pure oxygen. The measured distribution of the ozone molecules showed that the oxygen molecules were dissociated within the micro-plasma and ozone molecules were generated in the downstream of the discharge space. The ozone concentration drastically decreased with increasing the specific energy or the ratio of nitrogen to oxygen. Only 25ppm of ozone was detected with air. That is because the electron temperature within the micro-plasma was high enough to synthesize NO_x that dissociated ozone molecules catalytically. In conclusion, the spatial and temporal control of the ozone synthesis can be possible by using the micro-hollow cathode discharges.

GTP 33 LIGHTING PLASMAS I

GTP 34 Simulation of plasma parameters in He-Xe gas mixtures and comparison with experiment YURIY SOSOV, CONSTANTINE THEODOSIOU, *University of Toledo* Breakdown (Paschen) and current-voltage(I-V) curves for discharge in He/Xe mixtures are calculated for a simple 1D-space geometry. The necessary for the calculation values of secondary emission coefficients, gamma, for excited and ionized atoms of He and Xe were obtained through the best fit of the breakdown curves acquired in the simulation to the experimental discharge curves for pure He and Xe [Postel and Cappelli, *Appl. Phys. Lett.* **76**, 544]. The values of gammas are within the range of similar experimental data available in the literature [Y. Raizer, *itGas Discharge Physics* (Springer-Verlag, 1991) p. 74]. Using these secondary emission coefficients and assuming their applicability to gas mixtures Paschen and I-V curves are calculated and compared with the experimental ones. Our results indicate that higher values of the discharge voltage, compared to those obtained through the Townsend's equation, $\gamma(e^{ad} - 1) = 1$, could be explained by the reactions that effectively transfer positive charge from He ions and ionized molecules to neutral Xe atoms (i.e. $rmXe + rmHe^+ \rightarrow rmXe^+ + rmHe$ and $rmHe_2^+ + rmXe \rightarrow rmXe^+ + 2rmHe$). Values of the charge transfer reaction constants are estimated through a best fit of the simulations to the experimental curves.

GTP 35 Observations in a TmI^3 -TII-Hg metal-halide lamp and the influence of TmI^3 * J. J. CURRY, C. J. SANSONETTI, *NIST*, H. G. ADLER, *Osram Sylvania*, M. KANING, B. SCHALK, L. HITZSCHKE, *Osram GmbH, Munich, Germany* S. D. SHASTRI, *Advanced Photon Source, Argonne National Laboratory*, Observing fluorescence induced by x-rays from the Advanced Photon Source, we have measured spatially-resolved absolute densities of Hg, Tm, I, and Tl in two TmI^3 -TII-Hg metal-halide lamps that are nominally identical except for differing amounts of TmI^3 . One lamp contains 0.4 mg of TmI^3 , while the other lamp contains 2.2 mg. Both are jacketed, 240 W fused quartz lamps containing 16 mg of Hg, 0.3 mg of TII, and 0.5 mg of Ar buffer gas each in addition to the TmI^3 . The lamps were operated vertically with an

inductive ballast. In the low- Tm arc, the core was off-center, so two orthogonal scans perpendicular to the arc axis were used to obtain more information about the three-dimensional distributions. The spatially-resolved measurements are time-averaged, but time-resolved densities, in select locations, have also been obtained.

*Work supported in part by the U.S. Dept. of Energy under contract number W-31-109-ENG-38.

GTP 36 EXCIMER EMISSION FROM CATHODE BOUNDARY LAYER DISCHARGES M.M. MOSELHY, J. ANSARI, K.H. SCHOENBACH, *Old Dominion University*, The excimer emission from direct current glow discharges between a planar cathode and a ring shaped anode of 0.75 mm diameter, separated by only $250\ \mu\text{m}$, was studied in high-pressure xenon and argon. The thickness of the cathode boundary layer (CBL) plasma, approximately $150\ \mu\text{m}$, with a discharge sustaining voltage of approximately 200 V, indicates that the discharge is restricted to the cathode fall and the negative glow. For currents on the order of 1 mA, the discharge in xenon changes from an abnormal glow into a mode showing selforganization of the plasma. At this transition, maximum excimer emission (at 172 nm) with internal efficiencies of 3 to 5% is observed. The maximum radiant emittance is $4\ \text{W}/\text{cm}^2$ for atmospheric pressure operation. In the case of argon, selforganization of the plasma was not seen, however the emission of the excimer radiation (128 nm) again shows a maximum, in this case at the transition from abnormal to normal glow, with efficiencies of 2%. The maximum radiant emittance is $1.6\ \text{W}/\text{cm}^2$ for argon at 600 Torr. The positive slope of the current-voltage characteristics at maximum excimer emission indicates the possibility to generate large area flat excimer sources. Work supported by NSF (CTS-0078618 and INT-0001438).

GTP 37 VUV Emissions from a High-Pressure Cylindrical Dielectric Barrier Discharge N. MASOUD, *Stevens Institute of Technology* K. MARTUS, *William Paterson University* K. BECKER, *Stevens Institute of Technology* High-pressure Dielectric Barrier Discharges (DBDs) produce non-equilibrium plasmas that can be used in a variety of applications. The emissions from a high-pressure cylindrical DBD in a mixture of Ne and H_2 is proposed as a light source for 121.6nm radiation. Neon resonance lines and excimer emissions, as well as, Hydrogen Lyman-alpha emission lines have been analyzed from a cylindrical DBD plasma in this work. The discharge source consists of a 1/4" dielectric tube with two outer electrodes and the discharge is sustained by RF power at 13.56MHz. Results of measurements of the relative intensity of the resonance lines and excimer emission for pure Neon and Neon-Hydrogen admixtures as a function of Hydrogen concentration, discharge pressure, gas flow rate, and RF power will be presented and discussed. Results of the time dependence of the emissions after the RF power supply was turned will also be presented. Work supported by the NSF and through the William Paterson University ART Program

GTP 38 High-pressure dielectric barrier discharge Xenon lamps generating short pulses of high-peak-power VUV radiation (172nm) with high pulse-to-pulse reproducibility ROBERT CARMAN, BARRY WARD, RICHARD MILDREN, DEBORAH KANE, *Physics Dept, Macquarie University, North Ryde, Sydney, NSW 2109, Australia* Dielectric barrier discharges (DBDs) are used to efficiently generate radiation in the ultraviolet and vacuum-ultraviolet spectral regions (88nm-350nm) by form-

ing rare-gas and rare-gas halide excimers in a transient plasma. Usually, DBD lamps generate the light output quasi-continuously or in bursts with a high degree of stochastic or random variability in the instantaneous UV/VUV intensity. However, regular pulses of high-peak-power UV/VUV, with high pulse-to-pulse reproducibility, are of interest for applications in biology, surface treatment and cleaning, and time-resolved fluorescence spectroscopy. Such pulses can be generated from spatially homogeneous plasmas in a Xe DBD when the discharge is driven by uni-polar voltage pulses of short duration (100ns)¹. In the present study, we will report Xe DBD lamp performance and VUV output pulse characteristics for gas pressures up to 2.5bar and excitation conditions tailored for high-peak-power output. The experimental results will be compared to theoretical results from a detailed 1-D computer model of the spatio-temporal evolution of the plasma kinetics and Xe species population densities. ¹R.P.Mildren and R.J.Carman, *J.Phys.D*, 34, L1-L6, (2001)

GTP 39 A nonlocal radiation transport and 1-D Boltzmann model for low pressure Hg-Ar discharges

J. APRUZESE, *Naval Research Laboratory, Washington, DC* J. GIULIANI, *Naval Research Laboratory, Washington, DC* G. PETROV, *Berkeley Scholars, Inc., Springfield, VA* A 1-D, steady state model for a low-pressure Ar-Hg plasma has been recently developed and used to study a positive column discharge with properties similar to the conventional mercury fluorescent lamp [1]. The model consists of the Boltzmann equation for the EEDF including the spatial gradient term self-consistently coupled to a collisional-radiative equilibrium description of 5 Ar and 11 Hg species, as well as the gas thermal balance equation and an equation for the ambipolar potential. The effect of radiation trapping on the resonant level populations was initially treated with effective lifetimes following the conventional Holstein theory. The description of the averaged plasma properties was found to be satisfactory, but some model predictions were not in accordance with radially resolved measurements. The model was then substantially improved by incorporating a 1-D radiation transport model. The latter includes the isotope structure of 254 and 185 nm lines, the effects of foreign gas collisional broadening, partial frequency redistribution of the emission profile of 185 nm line, Voigt profiles for all other lines, and nonlocal photopumping. The radiation transport model is self-consistently coupled with the kinetic part of the model through species population dynamics. [1] G. M. Petrov and J. Giuliani, *J. Appl. Phys.* vol. 94 (2003)

GTP 40 Comparison of a 1-D radiation/Boltzmann model with fluorescent lamp data

G. PETROV, *Berkeley Scholars, Inc., Springfield, VA* J. GIULIANI, *Naval Research Laboratory, Washington, DC* A spatially dependent, steady state collisional-radiative model for a low-pressure Ar-Hg plasma is developed to study the conventional mercury fluorescent lamp. The model consists of the 1-D electron Boltzmann equation for the EEDF, self-consistently coupled to a 1-D radiation transport model, a collisional-radiative equilibrium model, the gas thermal balance equation and an equation for the ambipolar potential. The collisional-radiative model incorporates 5 Ar and 11 Hg species. Details of the model will be presented in an associated poster. The radially dependent EEDF, escape factors and coupling coeffi-

cients, electron density and mean energy, electron impact excitation and ionisation rates, electron particle and power balance terms, UV and visible radiation, particle and energy fluxes are investigated. We find substantially improved agreement between our new model and existing radially resolved data. Future exploration of the Ar-Hg column discharge will address the radial plasma properties of electrodeless discharges.

GTP 41 Diagnostic Study and Self-Consistent Modelling of a Low-Pressure He-Xe Discharge for Lighting Purpose

RENE BUSSIAHN, SERGUEI GORTCHAKOV, HARTMUT LANGE, DIRK UHRLANDT, *Institut für Niedertemperatur-Plasmaphysik, Greifswald, Germany* A glow discharge in a mixture of helium and 2% xenon in a cylindrical tube is considered, which can be used for the design of mercury-free low-pressure VUV radiation sources and fluorescent lamps. Optimal operation conditions with respect to the efficiency and the output power of the 147 nm resonance radiation of xenon atoms are evaluated by experimental investigations assisted by a self-consistent analysis of the dc positive column plasma. The column plasma is investigated in the range of the total pressure p_0 from 133 to 470 Pa at discharge currents I_z from 5 to 200 mA using tubes with the radii $r_w=0.5, 0.875$ and 1.12 cm. Tunable diode laser absorption spectroscopy has been applied to determine the absolute densities of the Xe ($1s_5$), Xe($1s_4$), Xe($1s_3$) and Xe($1s_2$) states and their radial profiles. The axial electric field has been measured by means of two Langmuir probes. Theoretical investigations of the dc column plasma use a self-consistent hybrid model which comprises a treatment of the non-local electron kinetics and the radial space charge confinement as well as a detailed balance description of all important excited states. The accuracy of the model is evaluated by detailed comparisons of model results and measurements for several discharge parameter conditions. In addition, the model is used for the study of the radiation efficiency and output power in extended parameter ranges of the dc glow discharge.

GTP 42 TRANSPORT COEFFICIENTS

GTP 43 Xe⁺ and Ne⁺ mobilities in Xe/Ne/He mixtures

E.-S. ET-TOUHAMI, L.C. PITCHFORD, *CPAT, U. Paul Sabatier and CNRS, Toulouse, France* A.V. PHELPS, *JILA, U. of Colorado and NIST* We have previously reported Xe⁺ mobilities in Xe/Ne mixtures¹ calculated using Monte Carlo simulation and used them to test mixture rules² by Blanc and by Mason and Hahn. Here we extend the calculations to Xe⁺ and Ne⁺ mobilities in mixtures of Xe, Ne, and He. As previously for Xe/Ne mixtures, we find that ion mobilities predicted by the Mason and Hahn mixture rule are accurate in all mixtures to within 20% of Monte Carlo calculations for E/N greater than 200 Td. In contrast, the ion mobilities determined from Blanc's law and other mixture rules tested are not sufficiently accurate at high E/N or are numerically too complicated to use. The Wannier³ formula, relating average ion energy, ion drift velocities, and masses of the ion and target atoms, yields

energies within 10% of Monte Carlo values for Xe^+ and Ne^+ in pure Xe, Ne, or He for E/N up to 1500 Td. The extension of the Wannier formula to ternary mixtures yields average ion energies agreeing well with Monte Carlo results.

¹J. de Urquijo et al, *Bull. Am. Phys. Soc* **45**, 28 (2000).

²E. A. Mason and H. Hahn, *Phys. Rev. A* **5**, 438 (1972).

³G. H. Wannier, *Phys. Rev.* **83**, 281 (1951).

GTP 44 SPATIAL PROFILES OF EXCITATION IN HELIUM ZELJKA NIKITIVIĆ, *Institute of Physics, University of Belgrade* GORDANA MALOVIĆ, *Institute of Physics, University of Belgrade* ALEKSANDRA STRINIĆ, *Institute of Physics, University of Belgrade* PETROVIĆ ZORAN, *Institute of Physics, University of Belgrade* In this paper we present electron ionization and excitation (and emission) coefficients for several lines of helium. We use drift tube technique for measuring absolute emission intensities in low-current self-sustained Townsend type discharges. In the experiment current was limited to less than $2\mu A$ to maintain uniform field conditions. The data were obtained from moderate E/N of 100 Td, where electrons are in equilibrium up to a relatively high E/N value of 3.3 kTd. It was not possible to achieve stable operation at higher E/N because of a sharp increase of breakdown voltage characteristic of helium. Apart from obtaining absolute emission and furthermore excitation data due to electron excitation that may be used to normalize the cross sections, at higher E/N effects of heavy particle excitation were also observed. We have performed measurements for 15 transitions of helium.

GTP 45 On the modification of the spatiotemporal electron relaxation process by electron-electron collisions DETLEF LOFFHAGEN, ROLF WINKLER, *Institut für Niedertemperatur-Plasmaphysik, 17489 Greifswald, Germany* Recently the spatiotemporal relaxation of electrons in weakly ionized inert gas plasmas and the inherent relaxation mechanisms have been studied. The nonequilibrium behavior of the electrons in the column-anode plasma of a glow discharge, maintained by an electric field and a continuous electron influx at the cathode side of the plasma, was determined by solving the spatially one-dimensional, time-dependent electron Boltzmann equation. Besides the electric field action and the cathode-sided electron influx, the impact of elastic and inelastic collisions of electrons with the neutral gas particles was taken into account. But, the influence of the Coulomb interaction between electrons has been neglected so far. By implementing the nonlinear electron-electron interaction into the space- and time-dependent electron kinetic equation, now it became possible to analyse the additional effect of the collisions between electrons on the spatiotemporal relaxation process. The analysis reveals that the electron-electron collisions significantly damp the excitation and development of spatial structures and remarkably reduce the non-local character of the behavior of the electron component during the entire temporal evolution and in steady state already at relatively low ionization degrees of the plasma.

GTP 46 Factors of the Synergy Effect of Insulating Gas Mixtures* TAKUYA ISHIGAKI, YUUKI HIROCHI, HIROTAKE SUGAWARA, YOSUKE SAKAI, *Hokkaido University, Japan* The critical values of the reduced electric field $(E/N)_{lim}$ of SF_6/N_2 are higher than the partial pressure weighted values given by linear interpolation between those of pure SF_6 and N_2 . Furthermore, $(E/N)_{lim}$ of SF_6/C_4F_8 partly exceeds even that of SF_6 .

These properties are called synergy effect. We have analyzed the synergy effect from a viewpoint of collaboration between electron collision and attachment, and the following characteristics of SF_6 , C_4F_8 and N_2 have been indicated as primary factors of the synergy effect: (a) a large attachment cross section of SF_6 laying in a low electronic excitation region, (b) a steep rise at the onset energy of an electronic excitation cross section of C_4F_8 , and (c) the presence of the peaks of the elastic collision and vibrational excitation cross sections of N_2 . Factor (a) plays the primary role for electron capture, and it is assisted by factors (b) and (c) in SF_6/C_4F_8 and in SF_6/N_2 , respectively. Factor (b) feeds electrons into the low-energy region in which factor (a) works efficiently. Factor (c) impedes the energy gain of low-energy electrons and prolongs the electron residence time in the low-energy region, that promotes the electron attachment. We will discuss electron behavior in SF_6/C_4F_8 , SF_6/N_2 and model gases, focusing on the factors.

*Work supported by MEXT of Japan under Grant-in-Aid 14750200

GTP 47 GLOWS

GTP 48 Investigation of field and plasma parameters near the slot antenna of a 915 MHz surface wave discharge* S. NAKAO, E. STAMATE, H. SUGAI, *Nagoya University, Department of Electrical Engineering* High-power planar surface wave discharges operating at pressures lower than hundreds of mTorr can be used to produce large diameter and high density plasmas. In spite of their intensive use for microelectronic technologies there are still unsolved problems concerning the production and heating mechanism, power dissipation and the role and origin of energetic electrons. Since most of these processes are localized in the vicinity of the dielectric plate this region needs a careful investigation. In this work we report spatial distribution of electric field and plasma parameters in the vicinity of a rectangular slot antenna $L=165$ mm, $l=11$ mm, arranged in the top of a cubic chamber of 400 mm in characteristic dimension and perpendicular to the direction of the microwave power injection. A spherical Langmuir probe (1.4 mm in diameter, made of Ag) was used to detect the plasma parameters and to peak up the electric field signal, $/E/$. At the same time, a metallic thermocouple (MTC) made of Pt+ Pt13 thermocouple (DTC) were used to measure the local temperature resulted by plasma heating—for MTC—and plasma plus microwave electric field heating—for DTC. All three probes could be simultaneously moved in 3D space in the vicinity of the slot. Both $/E/$ and the effective temperature, T_{eff} , increased significantly when reaching the slot location but their magnitude was not constant along it. The good correlation between $/E/$ and T_{eff} fluctuations confirms that the energetic electrons are associated with strong local electric fields.

*This work has been performed under the 21st Century COE Program by the Ministry of Education, Culture, Sports, Science and Technology in Japan.

GTP 49 Characterization of a large-area microwave plasma in N₂-O₂ ELENA TATAROVA, FRANCISCO M. DIAS, VASCO GUERRA, CARLOS M. FERREIRA, *Centro de Física dos Plasmas, Instituto Superior Técnico, 1049-001 Lisboa, Portugal* In this work we present an investigation of a large-scale, slot antenna excited surface wave plasma source operating at $\omega/2\pi = 2.45$ GHz and $p = 0.5 - 2$ Torr in N₂-O₂ mixtures. The surface waves propagate radially and azimuthally along the interface between the plasma and a quartz dielectric plate located at the top wall of a large diameter cylindrical metal camera. Since the electric field intensity decreases exponentially from the interface, the reactor can be separated in two parts. The first one is the active discharge zone close to the interface and the second one is the remote electric field-free plasma. The spatial distribution of several emitted lines, such as the first negative and second positive systems of nitrogen and the NO γ -bands, is obtained for the active discharge zone. The 3-D distribution of the electric field is calculated from the solution to the Maxwell's and the dispersion equations, and a kinetic model is developed to calculate the concentrations of the different heavy particles of interest. From the comparison of measured and calculated quantities, the mechanisms of production and loss of the various species are discussed.

GTP 50 Wave Driven N₂-O₂ Discharges as Sources of Active Species J. HENRIQUES, *CPAT, Université Paul Sabatier, 118 rte de Narbonne, 31062 Toulouse, France* E. TATAROVA, *Centro de Física dos Plasmas, Instituto Superior Técnico, 1049-001 Lisboa, Portugal* C.M. FERREIRA, *Centro de Física dos Plasmas, Instituto Superior Técnico, 1049-001 Lisboa, Portugal* A. RICARD, *CPAT, Université Paul Sabatier, 118 rte de Narbonne, 31062 Toulouse, France* Microwave N₂-O₂ discharges driven by traveling surface waves attract attention as sources of active species, in particular for cold plasma sterilization of surgical material and other medical devices. The objective of this study is to investigate the concentration of various active species, such as O(3P) and N(4S) atoms, N₂⁺ ions, and N₂(A) and NO(A) molecules, as a function of the spatial position and the mixture composition in an azimuthally symmetric surface wave driven discharge operating at 2.45 GHz. The plasma column is created in N₂-xO₂ mixtures ($x < 10\%$ at the pressure $p = 5$ Torr, in a quartz glass tube with inner radius $a = 0.25$ cm and with flow rates in the range $Q = 300 - 1000$ sccm. Emission spectroscopy is used to measure the N₂(1+, 2+, 1-) and NO(γ , β) band intensities along the discharge column length. NO titration is used to determine the densities of N and O atoms in the post-discharge, close to the end of the discharge. A theoretical model is developed which accounts in a self-consistent way for the electron and heavy particle kinetics, gas thermal balance and wave electrodynamics. This model provides a satisfactory interpretation of the experimental data.

GTP 51 Influence of electron collisions with N₂(A³ Σ_u^+) metastables in the nitrogen afterglow VASCO GUERRA, *Centro de Física dos Plasmas, Instituto Superior Técnico, 1049-001 Lisboa, Portugal* PAULO A. SÁ, *Departamento de Física, Fac. Eng., Universidade do Porto, 4200-465 Porto, Portugal* JORGE LOUREIRO, *Centro de Física dos Plasmas, Instituto Superior Técnico, 1049-001 Lisboa, Portugal* In this work we present a study of the influence of electron collisions with metastable molecules N₂(A³ Σ_u^+) during the afterglow of a nitrogen microwave discharge operating at $\omega/2\pi = 433$ MHz and $p = 3.3$ Torr, in a tube with radius $R = 1.9$ cm. In particular, we discuss *i*) the effect

of superelastic collisions $e + N_2(A) \rightarrow e + N_2(X)$ in the electron energy distribution function (EEDF) and consequently in the electron impact excitation rate coefficients; and *ii*) the importance of the stepwise excitation processes $e + N_2(A) \rightarrow e + N_2(B, C)$ in the heavy-particle kinetics. This is an important issue since the concentrations of both N₂(A) metastables and electrons initially decrease in the afterglow, but then raise and pass through pronounced maxima, whose origin is in collisions involving very high vibration levels of ground-state molecules ($v \geq 38$) and N(⁴S) atoms. [1] V. Guerra, P. A. Sá and J. Loureiro, accepted for publication in *Plasma Sources Sci. and Technol.*

GTP 52 Dependence of Gas Temperature of Oxygen Plasma on Discharge Conditions KOICHI NAOI, TAKESHI SAKAMOTO, HARUAKI MATSUURA, HIROSHI AKATSUKA, *Research Laboratory for Nuclear Reactors, Tokyo Institute of Technology* In order to examine the effect of discharge condition of oxygen plasma on its gas temperature, we examined change in the rotational temperature of a microwave discharge oxygen plasma by optical emission spectroscopy measurement (OES). The rotational temperature is an essential parameter since it can be interpreted as an approximate value of the gas temperature of the plasma. To simulate the oxygen plasma for an application to industrial processing, we used a microwave discharge oxygen plasma in a cylindrical quartz tube (i.d. 30 mm) with its discharge pressure 0.20 - 2.00 Torr. Since the emission intensity of band spectra originated from electronically excited states of oxygen molecule (e.g. atmospheric absorption band) was too weak to analyze, we observed the spectrum of OH band system $A[<]ex2\Sigma^+ \rightarrow X^2\Pi$. In order to obtain the rotational temperature from the observed spectra, we calculated the intensity of the OH band system above for the change in the vibrational quantum number $\Delta v = 0$, for a number of given rotational and vibrational temperatures beforehand. After that, we determined the temperatures by comparison of the measured spectra with the calculated one. It was found that the rotational temperature was almost independent of the discharge pressure or of the position in the discharge tube, and ranged 0.13 - 0.14 eV. The effect of the admixture of noble gases into the oxygen plasma is now being investigated.

GTP 53 Pattern Formation in Cathode Boundary Layer Microdischarges K.H. SCHOENBACH, M.M. MOSELHY, *Physical Electronics Research Institute, Old Dominion University, Norfolk, VA 23529, USA* Direct current glow discharges in xenon between a planar, 100 μ m thick cathode and a ring shaped anode, separated by 250 μ m, were found to be stable up to atmospheric pressure. Photographs in the visible and VUV (172 nm) range of the spectrum show the transition from a homogeneous to a structured plasma. The plasma patterns, regularly arranged filaments that are most pronounced at lower pressures (100 Torr), show discrete changes when the current is decreased by fractions of mA. This selforganization of the plasma requires the presence of a second stable branch in addition to the abnormal cathode fall in the voltage-current density characteristic of the cathode boundary layer (CBL) discharges. A model of the cathode fall by von Engel and Steenbeck [1], which was modified to take thermal conduction as a loss process into account, in addition to radiation, indicates the presence of stable plasma filaments at current densities in the

range from 10 to 100 A/cm², before transition into an arc. [1] A. von Engel and M. Steenbeck, *Elektrische Gasentladungen, ihre Physik und Technik*, Vol. 2, p. 121. Work supported by NSF (CTS-0078618 and INT-0001438).

GTP 54 CAPACITIVELY COUPLED PLASMAS

GTP 55 Power dissipation characteristics of the dual-frequency capacitively coupled plasma BUIL JEON, HONG-YOUNG CHANG, *Dept. of Physics, Korea Advanced Institute of Science and Technology* Power dissipation characteristics of the dual-frequency capacitively coupled plasma were measured. Low (2MHz) frequency and high (27MHz) frequency power source were used to generate plasma. 27MHz RF power was used to enhance plasma density and 2MHz power was used to enhance ion acceleration energy to the electrode. We could see the role of high-frequency and low-frequency power in dual-frequency CCP by measuring the power dissipation characteristics. High-frequency power is mostly dissipated by electrons in the bulk plasma and low-frequency power is mostly dissipated by ions in the sheath region. Using both high and low frequency power, we could control power dissipation by ions or by electrons. This means that we can control plasma density and ion acceleration energy to the electrode simultaneously.

GTP 56 Langmuir Probe Studies In A Dual Frequency Etch Reactor DOUGLAS KEIL, *Lam Research Corporation* ERIC A. HUDSON, *Lam Research Corporation* WAN-LIN CHEN, *Lam Research Corporation* REZA SADJADI, *Lam Research Corporation* LAM RESEARCH CORPORATION Advances in ultra large-scale integration (ULSI) have typically depended upon the ability to etch smaller feature sizes. Timely design of reactors capable of meeting these needs requires a deeper understanding of the underlying physics of the plasmas used. In this work, a double Langmuir probe is used to measure plasma ion saturation current and electron temperature in a dual RF frequency capacitively coupled dielectric etch system. The high-energy end of the electron energy distribution function dominates the measured electron temperature (i.e. a tail weighted T_e). An estimate of plasma density is derived from the measured ion saturation current using Bohm type arguments. T_e and density are reported as pressure and RF power is varied for a Bottom Anti-Reflective Coating (BARC) etch recipe. The results obtained are compared with corresponding etch rate variations. The problems encountered in such measurements are reviewed as well as their solutions. Although the BARC etch process is a fluorocarbon-based process, it is shown that deposition-related measurement problems are actually minimal for the particular gas chemistry used. Furthermore, the practical advantages and disadvantages of using single Langmuir probes vs. double probes under these conditions are also discussed.

GTP 57 Global Model for Asymmetric, Diode-Type Dual Frequency Capacitive Discharge JISOO KIM, M.A. LIEBERMAN, A.J. LICHTENBERG, *University of California, Berkeley* Dual frequency capacitive reactors can have desirable properties for dielectric etch: low cost, robust uniformity over large areas, and control of dissociation. In the ideal case, the high frequency power controls the plasma density (ion flux) and the low frequency voltage controls the ion bombarding energy. Typical operating conditions are: discharge radius 15-30 cm, length 1-3 cm, pressure 30-200 mTorr, high frequency 27.1-160 MHz, low frequency 2-13.6 MHz, and powers of 500-3000 W for both high and low frequencies. The decoupling of the high and low frequencies is an important feature of dual frequency capacitive discharges. In this work, we describe a global (volume-averaged) model having different top and bottom plate areas that incorporates particle balance, and ohmic and stochastic heating for high and low frequencies. The model is used to obtain the decoupling of high and low frequencies and to investigate limitations to ideal decoupling. Support provided by Lam Research, NSF Grant ECS-0139956, California industries, and UC-SMART Contract SM99-10051.

GTP 58 Particle-In-Cell Simulations of Asymmetric Dual Frequency Capacitive Discharge Physics ALAN WU, A.J. LICHTENBERG, M.A. LIEBERMAN, J.P. VERBONCOEUR, *University of California, Berkeley* Dual frequency capacitive discharges are finding increasing use for etching in the microelectronics industry. In the ideal case, the high frequency power (typically 27.1-160 MHz) controls the plasma density and the low frequency power (typically 2-13.56 MHz) controls the ion energy. The electron power deposition and the dynamics of dual frequency rf sheaths are not well understood. We report on particle-in-cell computer simulations of an asymmetric dual frequency argon discharge. The simulations are performed in 1D (radial) geometry using the bounded electrostatic code XPDP1. Operating parameters are 27.1/2 MHz high/low frequencies, 10/13 cm inner/outer radii, 3-200 mTorr pressures, and 10^9 - 10^{11} cm⁻³ densities. We determine the power deposition and sheath dynamics for the high frequency power alone, and with various added low frequency powers. We compare the simulation results to simple global models of dual frequency discharges. Support provided by Lam Research, NSF Grant ECS-0139956, California industries, and UC-SMART Contract SM99-10051.

GTP 59 Kinetic simulations of capacitively coupled plasmas with external circuit ROBERT ARSLANBEKOV, VLADIMIR KOLOBOV, NING ZHOU, *CFD Research Corp.* Low-pressure capacitively coupled plasmas (CCPs) are widely used for various applications. The simulation models of CCP are mainly based on either fluid description of electrons or Particle-in-Cell with Monte Carlo (PIC-MC) models. The fluid models are not adequate for low-pressure CCPs since the electron distribution function is strongly non-Maxwellian. The PIC-MC models are numerically expensive and suffer from various drawbacks such as numerical heating. To model CCPs kinetically we use the recently developed multi-dimensional Boltzmann solver which is self-consistently coupled with the Poisson solver and other modules such as Chemistry Module. The Boltzmann solver incorporates various advanced numerical techniques such as the use of total energy ϵ with

instantaneous potential $\phi(t, \mathbf{r})$. The electron kinetic equation contains a term with $\partial\phi/\partial t$ describing "drift" along the total-energy axis by virtue of time varying ϕ and it turned out to be important in this formulation. The developed model is fully 3D and can be applied to low-pressure as well as high-pressure CCPs. We apply this model for simulations of low-pressure CCPs in argon and helium in 1D and 2D. The external circuit is modeled by the SPICE code. We obtain various scaling laws such as voltage-current characteristics and compare results with other simulations and available experimental data.

GTP 60 Methods to Achieve Uniformity in High Frequency Sources DANIEL HOFFMAN, *Applied Materials* Capacitive sources have shown utility in dielectric etchers. Based on plasma density efficiency, the choice of frequency for this type of source tends toward the VHF (Very High Frequency) range where the source creates plasma nearly volumetrically and wastes little or no power in the creation of undesired sheaths. Counter balancing the drive toward higher frequency is possible non-uniformity due to spatial voltage sag associated with the finite phase velocity of the radiating structure. Traditionally, the fundamental mode standing wave can predict large non-uniformities. However, there are two standing wave solutions: in polar coordinates- the J₀ and the J₁ solutions. If the right amount of J₁ solution can be added to the standing wave, good uniformity can be achieved. This paper discusses how boundary conditions and use of the cathode as a receiver can assist improving the uniformity beyond the intrinsic free-wave limits.

GTP 61 Effect of Driving Frequency on the EEDF of Capacitively-Coupled Argon Plasmas* KENICHI NANBU, *Institute of Fluid Science* HIDETO TAKEKIDA, *Institute of Fluid Science* HOSOKAWA YOSHIYUKI, *Kobelco System* One of the most severe validations of the codes for analyzing low temperature plasma is whether use of a code makes it possible to reproduce EEPF (electron energy probability function) obtained from measurements. Abdol-Fattah and Sugai examined experimentally the effect of driving frequency (13-50MHz) on the EEPF of capacitively-coupled argon plasma. They did a special device so as to make the self-bias voltage negligibly small. The electrode distance 66mm, the pressure is 100mTorr, and the peak-to-peak voltage is 80V. We examined the effect using code based on the particle modeling developed by us. It was shown that the agreement between the simulation and experiment is good for 13, 27, and 37MHz. However, an appreciable difference between the two appears for 44 and 50MHz. *Acknowledgement: The authors express their thanks to Prof. H.Sugai for presenting them the result of measurements before publication.

*Comparison of Simulation and Experiment

GTP 62 Measurement and modeling of voltage and plasma distribution of VHF-driven capacitively-coupled ladder-shaped electrode KOJI SATAKE, HIDEO YAMAKOSHI, MATSUHEI NODA, *Mitsubishi Heavy Industries, Ltd., Japan* Voltage and plasma density distributions along electrode-rods of ladder-shaped electrodes were measured and theoretical models were pro-

posed. Measurements were performed in test chambers, which were transparent for plasma emission observation and had probing points for voltage distribution measurements. Argon or nitrogen gas at 100 mTorr is used and the rod diameter and the rod to earth electrode spacing were 6 mm and 29 mm, respectively. The length of the rod was 1 m in the case of 1D, and the size of the electrode was 50 x 40 cm and the rod-to-rod spacing was 26 mm in the case of 2D. Measured ion saturation current distributions, which were coincident with the appearance of the plasma emission, was almost proportional to the voltage distribution. The proportional ratio of the current and the voltage increases with excitation frequency. Theoretical models of lossy transmission-line (for 1D) or transmission-network (for 2D) which consist of electrode's skin resistance and inductance, sheath capacitance and plasma impedance showed very good agreement with the measurements. Standing wave was a dominant cause of the distribution in 60-150 MHz range while a voltage drop dominated in over 150 MHz in the case of rod length of 1 m. Wavelength of the propagation wave in this case was about half of that in free space.

GTP 63 The mode transition for power dissipation induced by driving frequency in capacitively coupled plasma SHINJAE YOU, *Kaist* HYUNCHUL KIM, *Postech* JAEKU LEE, *Postech* HONGYOUNG CHANG, *Kaist* KAIST TEAM, *POSTECH TEAM* We measured electrical characteristics of capacitively coupled plasma at low pressure (20 mTorr) with different driving frequencies. From these measurements, we observed a significant change in discharge power characteristics during frequency increase. While increasing the frequency, a square dependence of power characteristics changes to a linear dependence. This observed result reveals that a power dissipation mode transition from ion-dominated dissipation mode to electron-dominated dissipation mode takes place during driving frequency increase. Both results obtained from a simple sheath model and a PIC simulation are in a good agreement with the experimental data.

GTP 64 DIAGNOSTICS I

GTP 65 Distributions of absolute C₂ and C₃ densities in low-pressure, high-density C₄F₈ plasmas measured by broadband absorption spectroscopy combined with laser-induced fluorescence M. ARAMAKI, M. KOBAYASHI, K. SASAKI, *Department of Electronics, Nagoya University, Nagoya 464-8603, Japan* Deposition of neutral radicals plays important roles for the selective etching of SiO₂ using fluorocarbon. To date, many works have been carried out for the diagnostics of CF_x radicals in fluorocarbon plasmas. In the present work, we measured distributions of absolute C₂ and C₃ radical densities in low-pressure, high-density C₄F₈ plasmas excited by helicon-wave discharges. The absolute densities of C₂ and C₃ were evaluated by broadband absorption spectroscopy using a Xe. The spatial distribution of relative C₂ and C₃ densities were measured by laser-induced fluorescence. The distributions of the absolute densities were determined by

combining the two measurements. For the accurate determination of the absolute densities, we measured the rotational temperature of C_2 by laser-induced fluorescence. Plasmas were produced at rf powers of 0.6~1.4 kW and C_4F_8 pressures of 2~10 mTorr. The C_2 radical density was on the order of 10^{11} cm^{-3} at the center of the plasma column. It increased with the distance from the center, and was higher than $1 \times 10^{12} \text{ cm}^{-3}$ at a distance of 8 cm from the center of the plasma column. Spatial distribution of the C_3 radical density was also hollow, and its absolute density was one-order of magnitude lower than the C_2 radical density.

GTP 66 The measurement of ion drift velocity by Mach probes in unmagnetized plasmas EUNSUK KO, XU WANG, NOAH HERSHKOWITZ, *Dept. Engineering Physics, University of Wisconsin - Madison* Ion flow velocities in unmagnetized plasmas are measured by Mach probes, and compared to a recent simulation by Hutchinson [1]. The measurements are performed using two Mach probes, one is a spherical Mach probe and the other is planar. The spherical Mach probe consists of a conducting sphere that has two conducting probe tips, insulated from the sphere and mounted at $\theta = 0^\circ$ and 180° with respect to the flow direction. The planar Mach probe consists of two single sided planar Langmuir probes back to back with an insulator between them. The experiments are performed in a double-plasma device for $v_f > 1.0c_s$ and along a presheath in a multi-dipole DC plasma for $v_f < 1.0c_s$ with Argon pressure ranging from 0.1 to 3mTorr. The upstream and downstream probe tips and the surface of the sphere were simultaneously biased at the same potential to minimize the probe edge effects, and to better resemble the simulation. *Work Supported by US DOE grant DE-FG02-97ER 54437 [1] I. H. Hutchinson, *Plasma Phys. Control. Fusion*, 44 1953 (2002)

GTP 67 Emission spectroscopy of pulse electrical discharge in water solution* MILAN SIMEK, MARTIN CLUPEK, VACLAV BABICKY, PAVEL SUNKÁ, *Institute of Plasma Physics, Za Slovankou 3, 18221 Prague 8, Czech Republic* DEPARTMENT OF PULSE PLASMA SYSTEMS TEAM Optical emission induced by pulse discharge in water was investigated in a reactor with the needle-plate electrode geometry. The ISA JobinYvon and Chromex spectrometric systems monitored the optical emission through quartz optics and color glass filters. High time resolution was obtained by synchronizing the data acquisition systems with the high-voltage circuitry for the discharge. Time-resolved spectra of the discharge were recorded. Results can be summarized as follows. 1) Most of the emission features in the 250-1050 nm spectral range can be assigned to HI, OI and OH radicals. 2) Time-resolved experiments reveal that almost the whole emission produced by HI and OI species is related to the first microsecond of the high-voltage pulse. On the other hand, characteristic emission at the OH band was clearly identified only at the later times when amplitude and width of HI and OI lines decreased substantially.

*Supported by the Grant Agency of the Czech Republic under contract No.202/02/1026.

GTP 68 Effect of Kr Gas Dilution on O Atom Density in Inductively Coupled Kr/O₂ Plasma MASARU HORI, *Dept. of Quantum Eng., Nagoya University* SOICHI IKUMA, *Dept. of Quantum Eng., Nagoya University* TOSHIO GOTO, *Dept. of Quantum Eng., Nagoya University* Oxygen-based plasmas have been used for the low temperature oxidation of materials. It has been reported that the high quality SiO₂ film was formed at a low temperature by Kr dilution O₂ plasma. From the viewpoint of developing the low temperature oxidation processes used for the gate dielectric film in LCD devices, a quantitative study on the behavior of O atom in the Kr/O₂ mixture plasma is strongly required. In this study, we measured the absolute O atom and metastable Kr atom densities in an inductively coupled Kr/O₂ plasma using vacuum ultraviolet absorption spectroscopy technique. The transition lines used for absorption measurements were $^3S_0 - ^3P_2$, $^3S_0 - ^3P_1$ and $^3S_0 - ^3P_0$ at 130.2 nm for O atom and $^3D_3 - ^3P_2$ at 811.3 nm for metastable Kr atom. The absolute O atom density was almost constant on $4 \times 10^{13} \text{ cm}^{-3}$ although the Kr dilution ratio was increased from 0 to 99% at an rf power of 200W, a pressure of 107 Pa, and a total gas flow rate of 100 sccm. The effect of metastable Kr atom on the production of the O atom has been discussed.

GTP 69 Energy Distribution Measurement of Atoms and Ions Sputtered by a Magnetron Plasma* H. MATSUI, H. TOYODA, K. SHIBAGAKI, K. SASAKI, T. KATO, S. IWATA, S. TSUNASHIMA, H. SUGAI, *Nagoya University* In sputter deposition of thin films by magnetron discharge, it has been believed that their film characteristics are significantly influenced by energetic neutral and/or ionic species ejected from the target. In the present study, energy distributions of sputtered particles are measured by a quadrupole mass analyzer (QMA) installed with an energy filter. A magnetron plasma is maintained by DC power ($\sim 450 \text{ V}$, 0.2 A) applied to a permalloy target (Fe, Ni) at argon pressure lower than $\sim 10 \text{ mTorr}$. An extractor of the QMA is placed 10 cm away from the target. Signals at mass/charge ratio (m/e) from 52 to 58 are measured and their intensities are well-explained by taking account of isotope ratio, atomic composition of permalloy and ionization cross sections of Fe and Ni. At lower pressures, sputtered atoms having such high energies as $\sim 10 \text{ eV}$ are observed.

*This work has been performed under the 21st Century COE Program by the Ministry of Education, Culture, Sports, Science and Technology in Japan

GTP 70 ELECTRON COLLISIONS

GTP 71 A New Method for Measuring Absolute Cross Sections for Electron Impact Ionization of High Rydberg Atoms* K. NAGESHA, K.B. MACADAM, *Dept. of Physics and Astronomy, University of Kentucky, Lexington KY 40506-0055* Absolute electron impact ionization cross section (EIICS) measurements for highly excited states are normally impeded by

difficulties in determining accurate target density and electron-target overlap volume, especially when ground-state target density, excitation efficiency and projectile/target beam dimensions are not known accurately. With ground states of gas/vapor targets a calibration technique such as the relative flow method may be used. Such circumvention is not trivial with excited states. We have developed a new approach that is based instead on accurately controlling the sizes of laser beams and the detection window. This method is suitable for ions with initial kinetic energies in the thermal and subthermal range. We determine the ionization fraction independently of electron-beam dimensions and eliminate the need to determine absolute ion and Rydberg densities. We present EIICs for highly excited sodium Rydberg atoms below 2 eV electron energy, measured using this new method.

*This work was supported in part by NSF Grant No. PHY-9987954

GTP 72 Magnetic Resonance of short-lived negative ions*

EMIL TOADER, *University of Bucharest, Romania* KENNETH STALDER, *Stalder Technologies, Redwood City, CA* BILL GRAHAM, *Queen's University Belfast, Northern Ireland* Here we present the possibility of creating short-lived (labile or exotic) negative ions, from the scattering of free electrons and polarized molecules in a discharge. In the interaction the electrons do not lose energy. Their mechanism of formation, structure and stability are completely different from those corresponding to stable negative ions. A classical analysis, based on an effective potential with a centrifugal term and a polarized term, shows that low energy electrons can orbit for some time around a polarized molecule. A quantum mechanics model shows that such labile negative ions can be in states that are characterized by the molecular quantum mechanics numbers K (rotational) and J (total), and the electron quantum numbers l (orbital) and j (total). The molecule is in the magnetic field created by the rotating electron, and can change its magnetic moment, so the short-lived negative ion can make the transitions between the different rotational states. Each transition corresponds to a variation of the magnetic energy, so we can have a doublet transition both in emission and absorption, at radio-frequencies from 1 to 150 MHz in deuterium and oxygen. The dispersion curves are specific to each polarized molecule and the transition frequencies can be measured using resonant detection methods.

*Supported by the QUB IRCEP Distinguished Visiting Fellow Scheme

GTP 73 Quantal and Classical Radiative Cascade in Ultracold Rydberg Plasmas

M. RAYMOND FLANNERY, *Georgia Institute of Technology* DANIEL VRINCEANU, *ITAMP, Harvard University* Atoms in high (n, ℓ) states formed in cold Rydberg plasmas decay to the ground state in a succession of radiative transitions populating intermediate excited states. A classical treatment presents radiative cascade in a physically transparent way and reveals the "trajectory" in $n\ell$ space obeyed by the cascade, scaling rules and other aspects hidden within the quantal approach. Quantal-Classical correspondence in radiative decay is directly demonstrated. Classical transition probabilities are also presented

and are in excellent agreement with quantal transition probabilities, even for moderate quantum numbers. Research supported by AFOSR, Grant 49620-02-1-0338 and NSF Grant 01-00890.

GTP 74 Energy Exchange Processes in Optically Pumped Carbon Monoxide Plasmas

YURI UTKIN, IGOR ADAMOVICH, WILLIAM RICH, *Dept. of Mechanical Engineering, The Ohio State University* The vibrational mode of CO, flowing in an optical absorption cell, is excited by a c.w. CO laser. Very high vibrational levels of CO are populated by V-V energy exchange processes. The gas ionizes by an associative ionization mechanism, and a glow-type plasma with a low gas temperature is maintained in the cell. The concentration of free electrons in the cell can be varied over a large range, and electron energy distribution is determined from probe measurements. Energy is transferred from high vibrational levels of ground electronic state CO to the first excited singlet state of CO (X singlet sigma to A singlet pi) in electron-CO collisions. Subsequent Fourth Positive Band electronic radiation from the A state appears to be the major channel removing energy from the primary vibrational up-pumping process. This Fourth positive radiation is monitored by vacuum UV emission spectroscopy, and major energy transfer channels in this important class of non-thermal plasmas are inferred.

GTP 75 Vibrationally Excited N₂ in Our Thermosphere

LAURENCE CAMPBELL, *SoCPES, Flinders Uni, GPO Box 2100, Adelaide, SA 5001, Australia* DAVID CARTWRIGHT, *Theoretical Division, Los Alamos National Laboratory, New Mexico, NM 87545, USA* MICHAEL BRUNGER, PETER TEUBNER, *SoCPES, Flinders Uni, GPO Box 2100, Adelaide, SA 5001, Australia* Vibrationally excited N₂ is believed to be important in determining both the normal ionospheric electron density and the production of NO in disturbed polar atmospheres. Although a number of mechanisms have been proposed for producing an enhanced N₂ vibrational population, it appears that no analysis of N₂ has been reported which treats both the excited electronic states and vibrational levels of the ground-state self-consistently. Here we present results from just such a study, using our enhanced statistical equilibrium code [1]. In addition, electron energy transfer rates for direct vibrational excitation of N₂ are also reported. [1] D. C. Cartwright *et al.* J. Geophys. Res. 105 (2000), 20857.

GTP 76 Calculated Cross Sections for the Electron-Impact Detachment from Negative Ions Using the Deutsch-Mrk (DM) Formalism

H. DEUTSCH, *Universitaet Greifswald, Germany* P. SCHEIER, *Universitaet Innsbruck, Austria* K. BECKER, *Stevens Institute of Technology, USA* T. MAERK, *Universitaet Innsbruck, Austria* The Deutsch-Mrk (DM) formalism, which was originally developed for the calculation of electron impact ionization cross sections of neutral atoms, molecules, clusters, and positive ions, is extended here to the calculation of electron impact detachment cross sections from negative atomic ions. Our approach uses a fitting procedure based on the (few) available experimental data for H-, B-, C-, and F- to determine the set of additional empirical

parameters required for the application of the DM formalism for negative ion targets. Subsequently, those parameters were used to calculate the O- detachment cross section, for which two sets of experimental data are available for comparison and the Li- detach-

ment cross section, for which no experimental data are available. This work has been carried out within the Association EURATOM-AW. It was partially supported by the U.S. Department of Energy and by the FWF, NB, and AW, Wien, Austria.

SESSION HW1: DIAGNOSTICS I

Wednesday morning, 22 October 2003

California Ballroom, Cathedral Hill Hotel at 8:00

Alexander Bolshakov, NASA Ames Research Center,
presiding**8:00**

HW1 1 UV absorption spectrum of the radical CF_2 in an $Ar/C_4F_8/O_2$ dual frequency capacitive discharge NICOLAS BULCOURT, *Laboratoire de Physique et Technologie des Plasmas (LPTP), Ecole Polytechnique, France* JEAN-PAUL BOOTH, *Laboratoire de Physique et Technologie des Plasmas (LPTP), Ecole Polytechnique, France* ERIC HUDSON, *Lam Research Corp., Fremont, USA* JORGE LUQUE, *Lam Research Corp., Fremont, USA* DANIEL MOK, *Department of Applied Biology and Chemical Technology, The Hong Kong Polytechnic University, Hung Hom, Hong Kong* EDMOND LEE, *Department of Chemistry, University of Southampton, Highfield, Southampton SO17 1BJ, United Kingdom* JOHN DYKE, *Department of Chemistry, University of Southampton, Highfield, Southampton SO17 1BJ, United Kingdom* FOO-TIM CHAU, *Department of Applied Biology and Chemical Technology, The Hong Kong Polytechnic University, Hung Hom, Hong Kong* Broad band UV absorption spectroscopy of CF_2 was performed in an industrial $Ar/C_4F_8/O_2$ dual RF frequency (2 and 27 MHz) capacitive discharge (Lam Research Corp.). The objective was to obtain the radial profiles of the CF_2 density and temperature. To achieve this experimental and simulated spectra were compared. The spectra were simulated using Franck-Condon factors and rotational constants calculated theoretically using an improved potential energy function (PEF) of the A state and a published PEF for the ground state. CF_2 spectra for beam paths including and excluding the confined plasma volume were compared. Results showed that the gas temperature at the center of the reactor is high (roughly 550 K) and decreases towards the wall of the chamber. Radical production and gas heating mechanisms will be discussed.

8:15

HW1 2 Sub-Millimeter Absorption Measurements of Temperature and Density in Fluorocarbon Plasmas ERIC BENCK, KAREN SIEGRIST, DAVID PLUSQUELLIC, *National Institute of Standards and Technology* Sub-millimeter (300 GHz to 1 THz) absorption spectroscopy is being developed as a diagnostic for measuring radical densities and temperatures in processing plasmas for microelectronics. Most molecules, radicals, and ions have transitions suitable for detection at these frequencies and the necessary spectroscopic data is available in the literature for determining the absolute radical densities. Initial measurements are being conducted with a backward-wave-oscillator (BWO) source and a liquid-He-cooled bolometer detector. The narrow linewidth (< 10 kHz) of the BWO is ideally suited for measuring the translational temperatures of radicals through the Doppler broadening of the absorption lineshape. Previous temperature measurements in an inductively coupled Gaseous Electronics Conference (GEC) Reference Reactor found all the radicals to have temperatures close to room temperature. Other spatially resolved plasma diagnostics, such as laser-induced fluorescence, in similar inductive sources have found significantly higher rotational temperatures within the plasma. The difference in plasma temperature diagnos-

tic results is being investigated by measuring the radial density and temperature distributions. Initial results indicate that the low temperatures being measured with the BWO are probably due to the geometry of the GEC Reference cell which has a large volume of gas surrounding the plasma. This results in the line-integrated absorption signal of the BWO being dominated by the cooler, denser gas surrounding the plasma.

8:30

HW1 3 Measurement of spatio-temporal distribution of etch product in an Inductively Coupled Plasma by using CT-OES YASUFUMI MIYOSHI, MASARU MIYAUCHI, KOMUKAI YASUO, TOSHIAKI MAKABE, KEIO UNIVERSITY, YOKOHAMA, JAPAN Fluorocarbon plasma is a practical source for silicon dioxide etching in LSI manufacturing process. A number of species which include electrons, ions, and radicals are generated by reactions in gas phase and on surface in plasma processing. In SiO_2 etching with high rate, a large amount of volatile/nonvolatile etch products, such as SiF_x ($x=1-4$), are emitted to the gas phase from the surface, and occupy a finite percentage of the gas composition. Etch products and their derivatives participate in many physical and chemical processes as ionization and dissociation in gas phase and as re-adsorption on the surface. Their space- and time- behavior have a great influence on plasma etching. It will be significant to investigate the spatio-temporal structure of etch products and their daughter products, and discuss the influence to the plasma structure. In our recent study, we have measured spatio-temporal structure of SiF_x ($x=1,2,3$) in CF_4/Ar mixture driven by RF(13.56MHz)-ICP(Inductively Coupled Plasma), by using newly developed CT(Computerized Tomography)-OES(Optical Emission Spectroscopy) system. We discuss the profile of the etch products near the SiO_2 surface as a function of LF(500 kHz) bias source.

8:45

HW1 4 Diagnostics of Microwave Cavity Discharges Modified by Weak Shock Waves S. POPOVIC, P. KESSARATIKOON, L. VUSKOVIC, *Department of Physics, Old Dominion University, Norfolk, VA* Electrodeless discharges are convenient active plasma media for shock dispersion studies in weakly ionized gas since there are no solid objects in the path of the shock wave that may distort the shock structure. The dispersed shock does not exhibit the splitting effect observed in d.c. glow discharges. Attenuation of the shock amplitude in the central segment of the cavity cannot be completely understood in terms of the inhomogeneous pumping effect and differs quantitatively between TM (parallel) and TE (perpendicular) modes. The spatial distribution of electron density is a very important parameter that indicates efficiency of microwave absorption, power balance and the region of energy deposition. In this work we applied one of the most frequently used methods to measure electron density - Stark broadening of Hydrogen Balmer lines - together with several other techniques involving N_2 and N_2^+ emission bands. Cross-correlation spectroscopy was developed for determination of the local electric field. Thermal effects in the discharge were evaluated on the basis of measured radial distributions of the rotational and vibrational temperature.

9:00

HW1 5 Using RF measurements and simple, empirical plasma models to enhance the performance of dielectric etch systems

STEVEN SHANNON, DANIEL HOFFMAN, JANG-GYOO YANG, *Applied Materials* ALEX PATERSON, THEODOROS PANAGOPOULOS, JOHN HOLLAND, DOG BUCHBERGER, BRAD MAYS, ALLEN FOX, MIKE CHAFIN, TROY DETRICK, *Applied Materials* Control of RF power delivery is an essential part of the overall operation of a plasma processing chamber. By in large, the majority of commercial plasma chambers rely on the RF power as the main control parameter. Previous work by others has shown benefits of controlling plasma processing based on individual RF parameters such as total RF current or peak-to-peak voltage; however, these approaches are still largely based on heuristic arguments. Alternatively, the advent of commercially available accurate RF probes, RF measurements of a known reference point between the matchbox and cathode, combined with RF characterization of the process chamber and a simple plasma model can provide information about the plasma discharge and on-wafer conditions that can be used to develop a control scheme which can provide a more direct control of the plasma process. In this work, the integration of RF metrology into plasma processing systems was developed. This work included a methodology for characterizing a process chamber and development of models that could be easily analyzed in a real-time control algorithm. Validation of the model was made through comparison to other plasma diagnostics. Finally, implementation of this simple

RF/plasma model to provide consistent, high quality etch performance on Applied Materials dielectric etch tools will be presented.

9:15

HW1 6 CF and CF₂ kinetics in a pulsed ICP in CF₄

JEAN-PAUL BOOTH, *LPTP, Ecole Polytechnique, France* HANA ABADA, *LPTP, Ecole Polytechnique, France* PASCAL CHABERT, *LPTP, Ecole Polytechnique, France* NICOLAS BULCOURT, *LPTP, Ecole Polytechnique, France* DAVID GRAVES, *U.C. Berkeley* Laser Induced fluorescence (LIF) was used to determine axial profiles of CF and CF₂ density and gas temperature in an inductively-coupled plasma in CF₄ at 33 mTorr. The gas temperature reaches 800 K in the reactor centre, causing considerable gas rarefaction at constant pressure. This must be taken into account when calculating radical fluxes due to diffusion. The steady-state CF and CF₂ density profiles are hollow, showing that the net radical fluxes are away from the reactor surfaces (where they are produced) towards the reactor centre (where they are destroyed). In the post-discharge the gas cools in about a millisecond. The CF density drops rapidly due to gas-phase reactions, probably with molecular fluorine. The CF₂ density initially increases (by a factor of about 3) for the first millisecond, before decaying slowly. This increase is due to continued surface production of CF₂ in the afterglow, combined with the disappearance of the rapid gas-phase CF₂ loss process. Numerical simulations using the FEMLAB package were used to understand the diffusive and convective radical transport in the afterglow.

SESSION HW2: NANOSTRUCTURES AND NANOPARTICLES

Wednesday morning, 22 October 2003; International Ballroom, Cathedral Hill Hotel at 8:00

David Hash, NASA Ames Research Center, presiding

Invited Papers

8:00

HW2 1 Silicon nano-structure formation using plasma under micro-G and one G conditions.*

MASAHARU SHIRATANI,[†] *Kyushu University, Japan*

Although growth kinetics of silicon particles formed in plasmas under one G condition has been fairly well understood using silane high-frequency discharges during the last decade,¹ effects of gravity on the kinetics have not been clarified yet. This study aims to reveal effects of gravity on growth rate and structure of such particles below several hundred nm in size. For this purpose, we have compared the growth rate and structure of nano-particles formed under the microgravity (μ G) condition using a drop experiment facility with those done under the one G condition. Our experiments with an rf sputtering reactor fulfill the five requirements necessary for the drop experiments: 1) the experimental setup is small enough to be settled in the drop capsule, 2) the growth rate of particles is much higher than 3 nm/s, 3) the number density of particles is high enough to be observable with HRTEM, 4) collection efficiency of particles is high, 5) a method preparing a HRTEM sample for a relatively small number of particles is developed. There is a large structural difference between them: Si particles of metastable structure are formed under the μ G condition, while Si crystal particles of several kinds of shape are done under the one G condition. Moreover, the number density of particles for μ G is three orders of magnitude higher than that for one G, although their growth rate has little dependence on gravity. In order to get information on the mechanism bringing about such structural difference, we have taken video images of plasmas as well as measured emission spectrum, T_e and n_i . All of them obtained for μ G are almost the same as those for one G. Therefore, further study is necessary for identifying the mechanism.¹ Y. Watanabe, M. Shiratani and K. Koga: *Pure & Appl. Chem.* 74 (2002) 483.

*Work supported by JSF and JSPS.

[†]Work performed in collaboration with Mr. Tomohide Kakeya, Dr. Kazunori Koga, and Prof. Yukio Watanabe.

Contributed Papers

8:30

HW2 2 Synthesis of silicon nanoparticles using atmospheric-pressure microdischarges R. MOHAN SANKARAN, DEAN HOLUNGA, RICHARD C. FLAGAN,

KONSTANTINOS P. GIAPIS, *Caltech* We report on the gas-phase synthesis of silicon nanoparticles using a high-pressure plasma microreactor operated in the microhollow cathode mode. Microreactors allow for short residence times in the reaction zone (< 1 msec) that limit the particle growth process and prevent the formation of larger particles and agglomerates. In addition, charging of the particles in the plasma may reduce coagulation downstream. In our experiments, direct-current microdischarges are formed at atmospheric pressure between a capillary tube (i.d. = $178 \mu\text{m}$) that serves as the cathode and an anode tube of arbitrary size. Argon/silane gas mixtures are flown through the microdischarge and particle formation is monitored downstream using a radial differential mobility analyzer (DMA) which separates particles based on their electrical mobility. Results have shown that exceptionally narrow size distributions are produced with mean sizes varying between 3 and 10 nm (± 1 nm). Particle size can be controlled by changing the silane concentration and/or plasma parameters. The particle crystallinity and properties are assessed by transmission electron microscopy (TEM) and optical techniques.

8:45

HW2 3 Monte Carlo simulation of nanoparticle transport in a plasma SARAH WARTHESEN, STEVEN GIRSHICK, UWE KORTSHAGEN, *Department of Mechanical Engineering, University of Minnesota, Minneapolis, MN 55455* A Monte Carlo method was developed to simulate momentum and charge exchange collisions between nanoparticles and surrounding gas species in a low-pressure capacitive plasma, modeling the transport mechanisms of diffusion, gas drag, thermophoresis, and electrostatic force. The simulation finds application in the optimization of reactor parameters during plasma enhanced chemical vapor deposition of thin films, when particles formed in the gas phase may be transported to the film substrate and deposit in the growing film. A series of simulations were performed to explore the relative roles of the different processes for transport of neutral particles. Diffusion was found to dominate the transport of 1-nm-diameter particles. Thermophoresis becomes relatively more important as particle size increases, and can be used to control the deposition efficiency of particles above 3 nm in diameter. This work is supported by NSF through IGERT grant DGE-0114372 and the Minnesota Supercomputing Institute.

9:00

HW2 4 Nanoparticle film deposition using a hypersonically expanded plasma X. WANG, J. HAFIZ, R. MUKHERJEE, A. GIDWANI, T. RENAULT, J. HEBERLEIN, P. McMURRY, S. GIRSHICK, *Department of Mechanical Engineering, University of Minnesota, Minneapolis, USA* C. PERREY, W. MOOK, C. B. CARTER, W. GERBERICH, *Department of Chemical Engineering and Materials Science, University of Minnesota, Minneapolis, USA* Nanostructured Si-Ti-N films were synthesized using hypersonic plasma particle deposition. In-situ measurements of particle size and charge distributions were obtained using a sampling probe interfaced to a scanning mobility particle sizer (SMPS). Measured particle size was found to depend on pressure in the expansion chamber and on reactant flow rate, with higher pressures and higher reactant flow rates favoring larger particles. Bipolar charge distributions were measured, and the particle charge fraction was found to increase strongly as particle size increased. In addition part of the sampled aerosol was delivered to a small hypersonic impactor connected in parallel with the SMPS, for deposition onto TEM grids for off-line analysis. Microstructural characterization of the deposited nanoparticle films was performed using scanning and transmission electron microscopy, X-ray photoelectron spectroscopy and X-ray diffraction.

9:15

HW2 5 Hydrogenated Silicon Thin Films With Nanocrystalline Inclusions* S. THOMPSON, U. KORTSHAGEN, *Dept. of Mechanical Engineering, University of Minnesota, Minneapolis, MN 55455* C. R. PERREY, C. B. CARTER, *Dept. of Chemical Engineering and Materials Science, University of Minnesota, Minneapolis, MN 55455* T. J. BELICH, J. KAKALIOS, *School of Physics and Astronomy, University of Minnesota, Minneapolis, MN 55455* Hydrogenated silicon thin films with nanocrystalline inclusions (a/nc-Si:H) have received considerable attention due to reports of superior electronic properties and an enhanced resistance to light-induced defect formation. The films examined in this study were deposited using RF 13.56 MHz PECVD of hydrogen and helium diluted silane with pressures in the range of 100 to 2000 mTorr. High resolution transmission electron microscopy studies confirm the presence of nanocrystallites in the films. The sensitivity of RF voltage and current harmonics to particle formation in the plasma are explored with respect to plasma conditions. Optical absorption spectra, obtained by CPM, and conductivity measurements indicate a/nc-Si:H film properties similar to those of standard a-Si:H.

*This work is supported in parts by NSF IGERT grant DGE-0114372, NSF MRSEC DMR-0212302, NREL/AAD-9-18668-13, and the 3M Heltzer Endowed Chair.

SESSION JW: GEC FOUNDATION TALK

Wednesday morning, 22 October 2003; International Ballroom, Cathedral Hill Hotel at 10:00
David Graves, University of California, Berkeley, presiding

10:00

JW 1 The Evolution of Plasma Etching in Integrated Circuit Manufacturing.

JOHN W. COBURN, *Dept. of Chemical Engineering, University of California, Berkeley, CA 94720-1462*

Remarkable progress has been made in the implementation of plasma etching into integrated circuit manufacturing during the past 30 years. One perspective of some of the highlights responsible for this progress will be presented. The evolution of the etching equipment from the batch barrel systems of the 1960s to the high density single wafer plasma systems in use today will be reviewed. A few of the key advances in the processing chemistry will be summarized along with some

of the more important technical developments. More recent progress in understanding and controlling the effects of the reactor wall and other internal surfaces will also be presented. Today each wafer is exposed to a plasma etching environment between 10 and 20 times during its manufacture and without the highly anisotropic etching provided by this critical process, high density integrated circuit manufacturing would not be possible.

SESSION LW1: ATOMIC IONIZATION

Wednesday afternoon, 22 October 2003; California Ballroom, Cathedral Hill Hotel at 13:15

Yong-Ki Kim, National Institute of Standards and Technology, presiding

Invited Papers

13:15

LW1 1 Three-Dimensional Imaging of Ionization Processes.

MICHAEL SCHULZ,* *University of Missouri-Rolla*

Atomic collisions represent a particularly suitable testground to study the few-body problem. Since the Schrodinger equation is not analytically solvable for more than two mutually interacting particles, detailed experimental data on this topic are essential to guide theoretical modeling efforts. For single ionization of He by electron impact numerous kinematically complete experiment have been performed [1]. It was thought that a profound understanding of the basic features observed in the fully differential cross sections had emerged, at least at large projectile energies. However, this conclusion was based on experiments carried out for rather restricted electron emission geometries. Here, we present complete three-dimensional images of fully differential cross sections for single ionization by ion impact [2]. In the data we observe unexpected features which so far were not predicted by any published theoretical model. We propose a higher-order ionization mechanism involving the projectile-residual target ion interaction to explain these features. Work supported by NSF and DFG. [1] H. Ehrhardt et al., *Z. Phys D1*, p. 3 (1986) [2] M. Schulz et al., *Nature* 422, p. 48 (2003).

*Work performed in collaboration with A. Hasan, N. Maydanyuk, D.H. Madison, M. Foster, S. Jones, R. Moshhammer, D. Fischer, and J. Ullrich.

Contributed Papers

13:45

LW1 2 Low Energy Electron Impact Ionization of He—Experimental Doubly Differential Cross-sections

ERIC SCHOW, CHRISTINA MEDINA, JAMES GREGORY CHILDERS, MURTADHA A. KHAKOO, *California State University, Fullerton, CA, USA* Experimental doubly-differential cross-sections (DDCSs) for the electron impact ionization of He will be presented. The DDCSs are taken at incident electron energies ≤ 40 eV and for scattering angles from 10° to 130° . Determination of these DDCSs, using conventional crossed-beam electron spectroscopy, is made possible by the application of a recently developed moveable target source method¹. Comparison with available theoretical DDCSs will be made. Funded by the National Science Foundation.

¹M. Hughes et al. *Meas. Sci. Technol.* **14**, 841 (2003).

14:00

LW1 3 Atomic and Molecular Double Photoionization Calculations Using Exterior Complex Scaling*

C. W. McCURDY, LBNL D. A. HORNER, UC Berkeley T. N. RESCIGNO, LBNL Exterior complex scaling (ECS) is a technique that allows for the correct application of outgoing boundary conditions for scattering problems with multiple electrons in the continuum. It is demonstrated that B-splines can be used to implement exterior complex scaling of electronic coordinates in a variety of applications. Specifically, this implementation allows the entire, well-established

technology of B-splines in atomic and molecular physics to be applied to the problems of multiple photoionization in atoms and molecules. The combination of B-splines and ECS allows one to solve the first-order Schrödinger equation for the wave function that describes single photon absorption without detailed specification of asymptotic boundary conditions. Results will be presented for singly and triply differential cross sections for double photoionization of helium that establish the accuracy of this method. We will also present results on double photoionization of molecular hydrogen. These are the first fully ab initio results for double photoionization of a molecular target.

*This work was performed under the auspices of the US Department of Energy by the University of California Lawrence Berkeley National Laboratory. The work was supported by the US DOE Office of Basic Energy Science, Division of Chemical Sciences. Calculations were performed on the computers of the National Energy Research Scientific Computing Center.

14:15

LW1 4 Double ionization of helium by photon impact*

STEVE JONES, DON MADISON, *University of Missouri-Rolla* Absolute measurements of fully differential cross sections for photo double ionization of helium provide a sensitive test of reaction models. One of the most popular models for more than a decade now is the 3C approximation, which employs a product of three Coulomb waves for the final double-continuum state of the atom. 3C calcu-

lations are generally in good agreement with the measured angular distributions but not the absolute magnitudes. Previous 3C studies used Hylleraas or similar wave functions for the ground state of helium. Such wave functions are known to be inaccurate when any two particles come close together. Here we use a ground-state wave function due to Pluvillage. The 3C and Pluvillage wave functions are analogs—both treat all three two-body Coulomb interactions exactly, albeit independently, and satisfy the cusp conditions of Kato as any interparticle separation tends to zero. Thus we expect to see some improvement in the absolute magnitudes compared to previous 3C studies.

*Sponsored by NSF

14:30

LW1 5 Radiative Recombination in the Terrestrial Nightglow: $e + O^+ \rightarrow O^* + h\nu$ T. G. SLANGER, P. C. COSBY, B. D. SHARPEE, D. L. HUESTIS, *SRI International* Large aperture telescopes have been equipped with superbly calibrated high-resolution spectrographs with performance comparable with the best laboratory instrumentation. From analysis of spectra of the "empty sky" (really the Earth's atmosphere) we have made the first experimental determination of the relative strengths of 25 emission lines between 390 and 930 nm from Rydberg excited states following the reaction $e + O^+ \rightarrow O^* + h\nu$ in the terrestrial ionosphere. We observe ns, np, nd \rightarrow 3s, 3p orbital transitions, around the $O^+(^4S)$ core, for $n=3-11$ and for triplet and quintet overall spin. Two modern calculations of cross sections for radiative recombination are in use by atmospheric scientists [1] and astronomers [2]. In general, the observed relative intensities agree rather well with theory, especially for the quintet states. Modeling the triplets is complicated by optical trapping. Supported by the NSF and NASA. [1] V. Escalante and G. A. Victor, *Planet. Space Sci.* **40**, 1705 (1992). [2] D. Pequignot, P. Petitjean, and C. Boisson, *Astron. Astrophys.* **251**, 680 (1991).

14:45

LW1 6 Ionization in the Noble Gases via Positronium Formation* J.P. MARLER, *University of California, San Diego* J. P. SULLIVAN, C.M. SURKO, *University of California, San Diego* Positrons can be useful in the ionization of atoms in two main ways. At low energies, ionization mainly occurs through the process of positronium formation (i.e. the positron forms a temporary bound state with the ionized electron before annihilating.) At higher energies, direct ionization (i.e. an electron is stripped from the atom but all three remain free particles at the end of the interaction) becomes dominant. This talk will discuss recent experiments using a high-resolution, trap-based positron beam to study ionization in the noble gases by positron impact. The experiments exploit the properties of positron orbits in a magnetic field to measure absolute cross sections for both elastic and inelastic processes. [1,2] These measurements will be compared with theoretical predictions [3] and the results of previous experiments [4]. *This work is supported by NSF and ONR. [1] S. J. Gilbert et al., *Phys. Rev. Lett.* **82**, 5032 (1999) [2] J. P. Sullivan, et al., *Phys. Rev. A.* **66**, 042708 (2002) [3] M.T. McAlinden and H.R.J. Walters, *Hyperfine Interactions* **73**, 65-83 (1992) [4] G. Laricchia et al., *J. Phys B.* **35**, 1-16 (2002) *Present Address: Photon Factory, KEK, Tsukuba, Japan

SESSION LW2: INNOVATIVE APPLICATIONS OF DISCHARGES

Wednesday afternoon, 22 October 2003

International Ballroom, Cathedral Hill Hotel at 13:15

Tim Sommerer, GE Research Laboratory, presiding

13:15

LW2 1 Instabilities of electronegative inductive plasma discharges MICHEL TUSZEWSKI, ROBERT WHITE, *Los Alamos National Laboratory* Different types of electronegative plasma instabilities are observed in Inductively Coupled Plasmas (ICPs), depending on the source design. We describe the relaxation oscillations seen in three low-pressure inductive plasma discharges operated with argon and sulfur hexafluoride gas mixtures. Two distinct phenomena, downstream instabilities and source oscillations, occur in certain domains of gas pressure, radio frequency power, and electronegative gas chemistry. The downstream instabilities develop at some location well below the plasma source. They are consistent with ion two-stream instabilities, in ICPs with sufficiently long downstream regions. Source oscillations consist of large amplitude density variations within the ICP plasma. They are consistent with capacitive to inductive mode transitions, in ICPs with sufficiently large capacitive currents.

13:30

LW2 2 Analytic and Numerical Models for Electronegative Plasmas* M. LAMPE, W. M. MANHEIMER, S. P. SLINKER, R. F. FERNSLER, G. JOYCE, *Naval Research Laboratory* We present some simple analytic modeling which clarifies the physical and mathematical mechanisms underlying the singular features of electronegative plasmas that have been noted by previous investigators. With a minimum of mathematical complexity, we are able to show how the discharge stratifies into an electronegative core and an electropositive halo, with an abrupt transition between the two regions; how the location of the transition is determined; how the extreme flatness of the core density profile leads inevitably (in the zero-Ti limit) to an extremely sharp density fall-off at the edge of the core; why the core remains strongly electronegative even in the limit of small (but non-zero) electron attachment; and why the electronegativity of the core changes character when the ion-ion recombination rate exceeds the ionization rate. Using simulation as well as analytic theory, we also discuss the effect of ion temperature in broadening the core/halo transition, and the effects of two-stream instability between the inward-flowing negative ion and the outward-flowing positive ions.

*Supported by ONR

13:45

LW2 3 The Microhollow Cathode Discharge as ion source for mass spectrometry KERSTIN KUNZE, *Institute of Spectrochemistry and Applied Spectroscopy, Dortmund, Germany* MANUELA MICLEA, *Institute of Spectrochemistry and Applied Spectroscopy, Dortmund, Germany* JOACHIM FRANZKE, *Institute of Spectrochemistry and Applied Spectroscopy, Dortmund, Germany* KAY NIEMAX, *Institute of Spectrochemistry and Applied Spectroscopy, Dortmund, Germany* ISAS DORTMUND COLLABORATION Microhollow Cathode Discharges (MHCD) are atmospheric pressure, non-equilibrium discharges and well studied for the generation of excimer radiation. The investigated discharge consists of two platinum electrodes with a hole diameter of 100 μ m separated by a 200 μ m thick Al_2O_3 insulator. Diode laser atomic ab-

sorption spectroscopy reveals a gas temperature of 2000 K and 1000 K and electron density of $6 \times 10^{15}/\text{cm}^3$ and $2 \times 10^{14}/\text{cm}^3$ for Ar and He, respectively [1]. The ionization degree of 10^{-3} to 10^{-5} at atmospheric pressure makes the plasma suitable as a mass selective detector for analytical purposes. Hereby the discharge expands from atmospheric pressure on anode side to a low-pressure regime on cathode side. The MHCD does not only act as an ion source, but the small aperture serves also as sampler for the quadrupole mass spectrometer. Halogenated hydrocarbons in gas mixtures as well as liquid samples, pre-separated by a gas chromatograph, could be detected by the halogen mass in the low ppb range. [1] M. Miclea et al., Proc. XVI-th ESCAMPIG Conf., 14-18 July, Grenoble - France (2002)

14:00

LW2 4 Thermionic Cathodes Novel Way to Increase Electron Density in Atmospheric Air and Nitrogen DC Glow Discharges ZDENKO MACHALA, *Mechanical Engineering Department, Stanford University, CA, USA* CHRISTOPHE O. LAUX, *Ecole Centrale Paris, Chatenay-Malabry, France* CHARLES H. KRUGER, *Mechanical Engineering Department, Stanford University, CA, USA* We employ thermionic electron emission in DC air and nitrogen glow discharges at atmospheric pressure. Atmospheric air and nitrogen glow discharges have been studied in our laboratory over the past few years with an overall goal to produce nonequilibrium plasmas with high electron number densities (at least 10^{12} cm^{-3}) and relatively low gas temperatures (about 2000 K), as well as to meet the challenges of low power requirements and large plasma volumes. Although thermionic emission is often used in arcs, we operate glow discharges producing nonequilibrium plasma where electron temperature is elevated with respect to the gas temperature (T_g 2000-3000 K). We study LaCrO_3 and Mo as thermionic cathode materials, other materials are to be tested. The essential advantage of thermionic cathodes is that when heated they supply more electrons than ordinary metal cathodes (previously used Pt). As a result, an increase of the electron density by 1-2 orders of magnitude has been achieved (10^{13} - 10^{14} cm^{-3}), together with higher current densities (5-40 A/cm²), lower electric fields (200-800 V/cm) and lower power budget than in the discharges with ordinary cathodes. We surround the discharges with glass tubes, and use a swirl gas injection in order to stabilize them and to control their properties. We employ emission spectroscopy as diagnostics although many challenges have been encountered. Experimental data on DC discharges with thermionic cathodes reveal a falling region in our discharge E-j characteristics. DC glow discharges with thermionic cathodes represent a promising way for producing nonequilibrium superionized plasmas in air or nitrogen at atmospheric pressure. Research funded by Air Force Office of Scientific Research, Grant F49620-01-1-0389.

14:15

LW2 5 The Extraction of Ion Species from Electron Beam-Produced Ion-Ion Plasmas S.G. WALTON, D. LEONHARDT, R.F. FERNSLER, *Plasma Physics Division, Naval Research Laboratory, Washington, DC 20375* Negative ions are formed in plasmas by electron attachment to gas molecules and positive ion-negative ion (ion-ion) plasmas are produced when this attachment rate is so large that most electrons convert to negative ions before leaving the plasma. In halogen-based gases, attachment rates increase dramatically with decreasing electron temperature, maxi-

mizing at conditions usually found only during the afterglow of pulsed plasmas. Electron beam-generated plasmas, however, are found to have low electron temperatures (0.2-1.0 eV) and thus represent a novel approach to producing ion-ion plasmas continuously. We present the results of experiments aimed at forming modulated, electron beam-generated ion-ion plasmas produced in Ar/SF₆ mixtures. Temporally resolved ion flux and energy distributions are reported for positive and negative ions extracted during all phases of plasma production using a low frequency, low voltage electrode bias. Supporting Langmuir probe and microwave transmission measurements are also reported. The results will be discussed in terms of the requirements needed to produce ion-ion plasmas and extract fluxes of both positive and negative ions. This work supported by the Office of Naval Research.

14:30

LW2 6 A Novel Generation Method of Dielectric Barrier Discharge Using Piezoelectric Transformer KENJI TERANISHI, *Chiba Institute of Technology* SUSUMU SUZUKI, *Chiba Institute of Technology* HARUO ITOH, *Chiba Institute of Technology* Dielectric Barrier Discharge (DBD) is generated by a Piezoelectric Transformer (PT) in atmospheric pressure. The PT is placed parallel to a glass plate coated with evaporated aluminum on one side as the dielectric electrode. Then, applying a voltage to the PT, the DBD appears between the gap. An Indium Tin Oxide (ITO) glass plate is also used as the dielectric electrode to observe the micro-discharge patterns by a CCD camera in a direction perpendicular to the electrode surface. The area of micro-discharges, where induces higher surface potential than the breakdown potential between the gap, spreads wider with increasing the applied voltage to the primary part of the PT. The number density of micro-discharges at a certain place is almost proportional to the surface potential at the same place on the PT. Moreover, we proved that the DBD is capable of applying to a compact ozoniser. The maximum ozone concentration is 13.9 g/Nm³, and the maximum yield efficiency of 340.4 g/kWh is obtained. The obtained yield efficiency of 340.4 g/kWh is close to the theoretically maximum yield efficiency of 400 g/kWh reported by Kitayama et al.¹.¹ J. Kitayama and M. Kuzumoto : *J. Phys. D: Appl. Phys.*, Vol.30, pp.2453-2461 (1997)

14:45

LW2 7 Rotating power deposition in a capacitively-coupled plasma discharge EDWARD HAMMOND, PARVIZ MOIN, *Stanford University* Empirical data have shown that, by pulsing the power applied to radio-frequency discharges, etch selectivity can be improved and damage due to charge buildup can be mitigated [Samukawa and Mieno, *Plasma Sources Sci. Technol.*, 5, 132 (1996)]. Many experiments and simulations of pulsed power deposition have varied the application of power in time, and they have demonstrated that a reduction in electron temperature can reduce charge buildup and the associated damage to gate oxides [Hwang and Giapis, *J. Vac. Sci. Technol. B*, 15, 70 (1997)]. This work will describe three dimensional simulations of a novel power deposition concept in a capacitively-coupled discharge where the power is varied in both space and time with a rotating voltage amplitude envelope. The impact of different power deposition methods on the ion flux uniformity and the electron temperature at the powered electrode will be described and compared to a baseline case.

SESSION MW1: LIGHTING I

Wednesday afternoon, 22 October 2003; California Ballroom, Cathedral Hill Hotel at 15:30

David Smith, GE Research Laboratory, presiding

Invited Papers

15:30

MW1 1 Behavior of metal halide lamps under microgravity and hypergravity conditions.GERRIT KROESEN, *Eindhoven University of Technology*

Metal halide lamps or HID (High Intensity Discharge) lamps are gaining popularity because of their very high energy efficiency. The applicability of these lamps is limited by two physical phenomena: de-mixing and helical instabilities. These two phenomena are strongly linked. On the earth surface, gravity causes convection, which strongly affects the radial and axial density profiles of the various species in the lamp. This makes it virtually impossible to study the demixing and instability phenomena in a clear way. Therefore, we have launched an effort to study these lamps under microgravity conditions. As diagnostics, spatially resolved high-resolution emission spectroscopy and laser diode absorption spectroscopy is applied, as well as direct video-imaging. Results of the first experiments (during the 34th ESA parabolic flight campaign) will be presented. The aim is to continue the experiments on board the International Space Station.

Contributed Papers

16:00

MW1 2 Near Infrared Emission from Metal Halide Lamps with Rare Earth Salts

J. E. LAWLER, *Univ. of Wisconsin-Madison* A Fourier transform infrared (FTIR) spectrometer is being used to study gas phase near-IR emission from Metal Halide-High Intensity Discharge (MH-HID) lamps with doses containing rare earth salts. Spectral limits of resolution down to 0.125 cm⁻¹ are adequate to fully resolve pressure broadened features from MH-HID lamps in both spatially resolved and spatially averaged measurements. Near-IR emission spectra are dominated by atomic line emission, not molecular bands as first expected. A similar result was found for MH-HID lamps with Na/Sc salts [1]. Although the most reliable absolute measurements require the use of a gold-coated IR integrating sphere, the broad spectral coverage of the FTIR makes it possible to perform an internal absolute calibration of the near-IR emission by comparing the near-IR emission to the mid-IR "black body" emission of the fused silica arc tube. The emissivity of fused silica is near one from 1200 to 2400 cm⁻¹ and thus its emission in this range is well understood. Additional work with an IR integrating sphere is needed, but the total near-IR emission from lamps with rare earth salts seems to be lower than the 20-30% expected. [1] D. J. Smith, G. A. Bonvallet, and J. E. Lawler, *J. Phys. D: Appl. Phys.* in press.

16:15

MW1 3 Plasma Dynamics and Thermal Effects during Startup of Metal Halide Lamps*

ANANTH BHOJ, *Dept. Chemical and Biomolecular Engr., University of Illinois, Urbana, IL 61801* GANG LUO, *Dept. Mechanical and Industrial Engr., University of Illinois, Urbana, IL 61801* MARK J. KUSHNER, *Dept. Electrical and Computer Engr., University of Illinois, Urbana, IL 61801* The interaction of temperature gradients, convective flow fields and plasma dynamics is important to the breakdown and onset of the glow phase during the startup of metal halide lamps. At starting pressures of 10s to a few hundred Torr, small changes in E/N resulting from convection can produce rapid and significant perturbations to plasma properties. These processes were compu-

tationally investigated using a model lamp geometry for comparison to companion experiments. A 2-dimensional plasma hydrodynamics model using unstructured meshes was extended with an ambipolar module in order to carry calculations deep into the glow phase. The plasma model was interfaced to a 2-d fluid dynamics code which solves Navier-Stokes' equations using a second order finite volume method and returns neutral gas velocities and temperatures. Mixtures of Ar/Xe and Ar/Hg were investigated at pressures of 10s Torr. We found that during the early breakdown phase, energy deposition is low and thermal effects are small. As the plasma density and energy density increases, thermal gradients develop which produce velocity flow fields, first near the powered electrode and later in the bulk plasma.

*Work was supported by the National Science Foundation (CTS99-74962) and General Electric R&D Center.

16:30

MW1 4 Radiation Trapping in Electrodeless Lamps: Complex Geometries and Operating Conditions*

KAPIL RAJARAMAN, *Dept. of Physics, University of Illinois, Urbana, IL 61801* MARK J. KUSHNER, *Dept. of Electrical and Computer Engr., University of Illinois, Urbana, IL 61801* Electrodeless gas discharges are finding increasing applications as lighting sources, especially for Ar/Hg based fluorescent lamps. The particulars of resonance radiation trapping from Hg are important considerations in the design of these sources. For simple geometries, analytical formulas for the radiation trapping factors can be derived. For many lamp designs, however, the geometries are complex, and there are spatially non-uniform densities of the emitting and absorbing atoms. To address these complexities, a Monte Carlo model for resonance radiation transport has been developed which accounts for frequency resolved emission and absorption. This radiation transport model has been integrated into a 2-D self-consistent plasma equipment model which accounts for electromagnetics, electron energy transport, and heavy particle transport, and the solution of the Poisson's equation. The influence of the

lamp geometry has been studied by varying the size and shape of bulb, as well as the number and positions of the inductive coils. The coil frequency, coil power, cold-spot temperature and the initial pressure were varied to investigate their effects on the trapping factors.

*Work supported by the National Science Foundation (CTS99-74962)

16:45

MW1 5 High Intensity Electrodeless Lamps Excited by Circularly Polarized Microwave Discharges* JIN JOONG KIM, DONG HO WON, JUNG TAE KO, *Dept of Optical Engineering, Sejong University* JEONG WON KIM, *Taewon Lighting R&D Laboratory* We report on the demonstration of high intensity electrodeless lamps using rotating microwave discharges of molecular vapors at 100-400 kPa with no external magnetic fields, including sulfur and indium-monobromide. We place in a cylindrical waveguide a quartz ball of 3-cm-diam filled with 10 Torr of argon gas and a few mg of a molecular fill. The waveguide system generates circularly polarized microwaves and propagates the TE₁₁ mode as the dominant mode at 2.45 GHz. Unlike conventional high-pressure electrodeless discharge lamps, the bulb in our system is stationary and the microwaves rotate in a TE₁₁ mode in the waveguide at 2.45 GHz with an input power of up to 1.2 kW. When the vapor in the lamp breaks down by microwaves, the discharge zone is observed to rotate at a frequency of 3-10 Hz. We offer an explanation of the lethargic rotation of the plasma discharges based on local field argument and collision frequency. The rotating plasma discharges generate white light plasmoids of a luminance of up to 7E7 cd/m². The emission spectra are no different from those observed in conventional lamps. A movie will be shown to demonstrate the rotating plasma discharges.

*Work supported by a contract from the Korean Ministry of Commerce, Industry, and Energy

17:00

MW1 6 Frequency dependence in Xe Dielectric Barrier Discharges Excimer Lamp HARUAKI AKASHI, *Dept. Appl. Phys., National Defense Academy, Japan* AKINORI ODA, *Dept. Sys. Eng., Nagoya Institute of Technology, Japan* YOSUKE SAKAI, *Dept. Eng., Hokkaido University, Japan* Discharge development dependence on driving frequency in AC Xe Dielectric Barrier Discharge (DBD) Excimer Lamp was calculated using 1.5D fluid model. The driving frequency had been changed from 10KHz to

50MHz, and other conditions such as pressure(300Torr), amplitude(5KV), gap length(1cm) and dielectric barrier thickness(0.2cm) were fixed. At low frequency, discharge development in excimer lamp seems to be cathode directed streamer discharge. And peak electron density was obtained at vicinity of both dielectric barriers at the end of the streamer discharge. These peaks were appeared at cathode side in each half period. As the frequency increases(~ 2MHz), the discharge development becomes more like rf glow discharge. Near the both dielectric barriers, the peaks in electron density were also obtained, however, these peaks were not formed by streamers. These peaks were made by the rf glow discharge, and appeared at anode side in the case of high driving frequency. Positive ions were trapped inside the discharge space and two peaks were formed at the vicinity of the dielectric barriers. In the case of higher than 10MHz, electron density in the bulk area increased appreciably. As a result, light output efficiency increased with increasing driving frequency, and had its peak value at around 2MHz, then decreased gradually.

17:15

MW1 7 A Xenon dielectric barrier discharge lamp (172nm) with a fast-pulse voltage driver: Influence of the voltage waveform on plasma kinetic issues and light output ROBERT CARMAN, BARRY WARD, RICHARD MILDREN, DEBORAH KANE, *Physics Dept, Macquarie University, North Ryde, Sydney, NSW 2109, Australia* An important class of vacuum-ultraviolet (VUV) excimer lamps based on high pressure rare-gas and rare-gas halogen mixtures utilize the dielectric barrier discharge (DBD) to generate a transient, non-equilibrium plasma that yields high electrical to VUV conversion efficiency. Recent interest has focussed on the use of pulsed voltage excitation techniques (rather than conventional AC sinusoidal waveforms) to alter the physical appearance of the DBD micro-discharges from filamentary (AC) to semi-diffuse, conical or homogeneous (pulsed), whilst at the same time dramatically improving the lamp performance and VUV efficiency^{1,2}. We report results from a combined experimental/computer modelling study of a short-pulse excited co-axial DBD Xe lamp to investigate the influence of the pulsed voltage waveform on the discharge structure, lamp performance, VUV output, and electrical efficiency. The underlying plasma kinetics issues relating to lamp performance, including parasitic collisional processes that act to quench key xenon species population densities, are examined in detail. ¹ Vollkommer F and Hitzschke, US patent 5604410 (1997) ² R.P.Mildren and R.J.Carman, *J.Phys.D*, 34, L1-L6 (2001)

SESSION MW2: MATERIAL PROCESSING I

Wednesday afternoon, 22 October 2003; International Ballroom, Cathedral Hill Hotel at 15:30
Jong W. Shon, Lam Research Corporation, presiding

Invited Papers

15:30

MW2 1 Why we need more tuning knobs in plasma etching and what knobs work best.
RICHARD GOTTSCHO, *Lam Research Corporation*

Edge effects, wafer-scale loading, micro-scale loading, and nano-scale transport phenomena all conspire to demand more flexibility in both plasma reactor and plasma process design. In addition, economics are driving increased efficiency in the use of capital and in situ processing of complex stacks—one reactor is used for etching different kinds of films sequentially. As a result of these trends, there is no recourse but to add more tuning knobs to the reactor. The traditional knobs have been based largely on changing chemistry for a fixed mode of power coupling, fixed distribution of gas

injection, and a fixed wafer temperature. More recently, dynamic re-distribution of gas and plasma power coupling have been implemented. Most recently, dynamic control of wafer temperature and wafer temperature uniformity have been implemented to gain independent control of sticking and reaction coefficients on the sidewalls of nano-structures. In this talk, I will discuss these trends and draw on numerous examples as I highlight remaining areas that challenge those designing next generation reactors and processes.

16:00

MW2 2 Plasma-walls interaction and process drifts during silicon gate etching processes.

GILLES CUNGE, *CNRS-LTM*

Silicon gate etching is performed in high-density plasmas operating in HBr/Cl₂/O₂ chemistry. During the etching process, SiOCl layers are depositing on the Al₂O₃ chamber walls. The formation of this layer on the reactor walls modifies the surface loss probability and thus the concentrations of radicals involved in the etching process, leading to process instabilities. However, the chemical nature of these layers, their deposition mechanism and their influence on the plasma chemistry remains poorly understood. In the present paper, we will first present a new and very simple method to generate, on the wafer, exactly the same layers that are formed on the chamber walls. We will then use quasi in situ XPS measurements to have access to the chemical nature of the layers formed on the chamber walls, during plasma etching processes. We will show that the layer deposited on the walls during the etching of a blanket silicon wafer is a chlorine rich silicon oxide layer. By contrast, the presence of photoresist on the etched wafer results in the deposit of a chlorine rich carbon layer due to the presence of CCl_x etch product in the gas phase. In a second step, the precursor species responsible for the deposit is investigated. The absolute gas phase concentrations of SiCl_x (X=0-2), SiBr and SiF_x (X=1-2) and CCl_x etch product has been measured by broadband UV absorption spectroscopy. In parallel, the chemical nature of the ions bombarding the walls has been measured by mass spectrometry. These quantitative measurements give some insights on the respective roles of ions and neutral in the depositing process. Finally, the influence of the chemical nature of the layer coating the chamber walls on the plasma chemistry will be discussed. A particular emphasis will be given on the recombination rates of halogen atoms, which are highly sensitive to the walls chemistry.

Contributed Papers

16:30

MW2 3 Device Damage Reduction in Metal Etch Chambers by Pulsed Source Plasma

ALEX PATERSON, *Applied Materials, Inc* JOHN YAMARTINO, *Applied Materials, Inc* YASUSHI TAKAKURA, *Applied Materials, Inc* JOHN HOLLAND, *Applied Materials, Inc* MIKE BARNES, *Applied Materials, Inc* The reduction of charging damage by the electron shading effect has become crucial for good yield and reliability as semiconductor devices are continually scaled to smaller feature sizes, <0.25μm. The electron shading effect occurs in via etching and dense-line pattern etching, both of which are commonly repeated in multi-level interconnect processes. It is known that there is a positive correlation between electron shading device damage and the electron temperature, reducing the electron temperature will reduce the damage. One method of reducing the electron temperature of the plasma is to use pulsed source power and there are many examples in the literature where it has been shown to reduce the electron shading effect in a research environment. The challenge, from a supplier stand-point, is to reliably utilize this technique in wafer etch production without degrading other etching features. This paper describes work done at Applied Materials to bring the benefits of pulsed source power into a production capacity. The effect of source rf frequency, pulse frequency and bias frequency on plasma parameters and device wafer charging structures will be discussed.

16:45

MW2 4 Etching of a Deep Small Contact Hole for sub 80nm ULSIs: Enhancement of Aspect Ratio Dependent Etching and Selectivity to Masking Layers

SUNG-IL CHO, KYEONG-KOO CHI, CHANG-JIN KANG, WOO-SUNG HAN, JOO-TAE MOON, *Semiconductor R&D Center, Samsung Electronics Co. Ltd., San #24, Nongseo-Ri, Kiheung-Eup, Yongin-Si, Kyungki-Do, 449-900, Korea* In etching of deep small contact holes for ULSI devices of sub 80nm-design rule, we should overcome two major problems: the low selectivity to the ultra thin masking layers and the etch-stop due to aspect ratio dependent etching (ARDE). As a way to solve these problems, we studied the effect of CO. By an addition of CO to C₄F₆/O₂/Ar plasma in a magnetically enhanced reactive-ion-etcher (MERIE), the selectivity to 193nm photoresist increases to 6, by 20% higher than that without CO. The lag of etch rate due to ARDE at the aspect ratio of 12 was less than 10%. To analyze the effect of CO on the C₄F₆/O₂/Ar plasma, we investigated the chemical species in the gas phase as a function of CO flow rate with an optical emission spectroscopy (OES). The results of OES show that the density of F in the gas phase decreases with CO flow rate, but the densities of CO, O₂, and O increase. The addition of CO to the fluorine-contained plasma can effectively scavenge the fluorine radical. Therefore, we can increase the ratio of CF₂/F, so that the selectivity to the masking layer increases. Whereas, the polymer thickness inside the deep contact holes, analyzed by a field emission Auger electron spectroscopy (FE-AES), becomes thinner with the addition of CO, which, we consider, is due to the increase of O decomposed from CO. The radical, O, can reach the bottom of the deep contact holes because it has relatively low sticking coefficient, improving the etch-stop due to ARDE. Based on these finding, we could successfully etch contact holes of 80nm-diameter and aspect ratio 12.

17:00

MW2 5 Design and Development of a Novel Dual Gas Delivery System in a Plasma Reactor NICOLAS GANI, *Applied Materials* MEIHUA SHEN, *Applied Materials* YAN DU, *Applied Materials* WILFRED PAU, *Applied Materials* JOHN HOLLAND, *Applied Materials* THEODOROS PANAGOPOULUS, *Applied Materials* VALENTIN TODOROW, *Applied Materials* PATRICK LEAHEY, *Applied Materials* HOAN NGUYEN, *Applied Materials* As the IC technology rapidly approaches sub 0.10µm geometry, requirements for features critical dimensions (CD) and profile control in gate etch across the wafer become increasingly stringent. Profile and CD uniformity control are related not only to a uniform distribution of etch species (ionic and neutral species) but also more importantly to a uniform distribution of passivation sources (by-products related). While the etch species distribution across the wafer can be effectively controlled through center to edge plasma source power ratio, the etch-byproducts distribution is governed by gas flow dynamics through the balance of convection flux versus diffusion flux. It is therefore critical to design a gas delivery system in a plasma reactor that can offer the flexibility to control the by-products distribution over a wide process region for various applications. This paper presents the development of the tunable gas nozzle design for a decoupled plasma source reactor. Detailed experimental as well as simulations results will be discussed in order to reach an optimal configuration. The process performance for advanced sub 100nm gate etching application on the system will be also presented.

17:15

MW2 6 The first wafer effect in the gate etching of DRAM with high density plasma etcher Y.J. JUNG, *Samsung Electronics Company Limited* K.J. MIN, *Samsung Electronics Company Limited* C.J. KANG, *Samsung Electronics Company Limited* W.S. HAN, *Samsung Electronics Company Limited* J.T. MOON, *Samsung Electronics Company Limited* PROCESS DEVELOPMENT TEAM, OES analysis was performed to analyze the first wafer effect in the gate etching by high density plasma etcher. The first wafer in a lot shows smaller CD gain as well as shorter endpoint time compared to the rest of the wafers in the lot when the lot was etched after long idle status of the high density plasma etcher. This effect should be cleared for the manufacturing of sub-100nm device. In this study, high density plasma poly-Si etcher(DPS, AMAT) was used with Cl₂/SF₆ chemistry in main etch step followed by HBr/O₂ chemistry in OE step. Spectrum analysis was performed by using optical emission spectroscopy system(SMART-PAS, SEMISYSCO). Si₃N₄ layer was used as a hard mask for the gate etch. From the analysis of the spectra change between the wafers in the lot, it was observed that the intensity of Cl and Br were higher in the etch step of the first wafer compared to the rest of the wafers in the lot. The higher Cl and Br concentration in the first wafer was considered to be related to the condition of the chamber wall. That is, long idle time which results in evacuation of the polymer on wall surface, causes the difference of radical concentration for the first wafer. It was also observed that breakthrough step with CF₄ gas affects the Cl and Br intensity in the main etch and over etch step, which supports the effect of the wall condition on the Cl and Br concentration.

SESSION NWP: POSTER SESSION II

Wednesday evening, 22 October 2003

El Dorado, Cathedral Hill Hotel at 19:15

I. Langmuir, GE Research Laboratory, presiding

NWP 1 DIAGNOSTICS II

NWP 2 A Metastable Helium Beam by a Penning Discharge for Measurement of Electric Field in Plasmas K. TAKIYAMA, S. NAMBA, *Hiroshima University, Japan* D. ANDRUCZYK, B.W. JAMES, *The University of Sydney, Australia* T. OHGO, *Fukuoka University of Education, Japan* T. ODA, *Hiroshima Kokusai Gakuin University, Japan* We have developed a high-sensitive laser-induced fluorescence (LIF) technique for measuring electric fields in plasmas using the Stark effect of He atoms. For a plasma that does not contain He gas, however, this technique requires a He beam probe with a sufficient density of singlet He metastable atoms (2S). A design study of a pulsed 2S beam produced in a discharge of the He gas beam was made. A numerical calculation suggested the possibility of generating high-density 2S atoms with high efficiency using plasmas with high Te. The Penning discharge was adopted to excite the beam. The beam source consisting of a fast acting valve, a skimmer and the discharge section was designed and constructed. The Beam properties were measured with a fast ion gauge and spectroscopic methods. Emission spectra from the plasma column showed that Te was high enough to produce sufficient 2S atoms. This was also confirmed from LIF observation of 2S atoms.

NWP 3 Ion Energy Distributions at the Cathode of a DC Plasma ALAN REES, *Hidden Analytical* ALEX CAREW, *Hidden Analytical* IAN NEALE, *Hidden Analytical* CLAIRE GREENWOOD, *Hidden Analytical* YOLANDA GONZALVO, *Hidden Analytical* MARK BUCKLEY, *Hidden Analytical* The energy distributions for mass-identified, positive ions arriving at the cathode of a DC plasma have been measured using a Hiden EQP mass/energy analyser for both argon and nitrogen plasmas. The plasma was operated at a range of voltages between the driven, planar cathode and a grounded anode 4cm from the cathode and parallel to it. A central sampling orifice (100µm diameter) in the cathode formed the entrance to the analyser and connected the pressure regions of the plasma reactor and the analyser. The gas pressures in the reactor were in the range 10 to 100mTorr. For discharges in argon the most prominent ions arriving at the cathode were Ar⁺ ions with smaller currents of Ar⁺⁺ and impurity ions such as ArH⁺ and H₃O⁺, attributable to traces of water vapour in the unbaked reactor. The ions were generated primarily in the sheath region in front of the cathode and their energy distributions were modified by collisions with gas molecules in crossing the sheath to the cathode. In the case of the Ar⁺ ions, symmetrical charge exchange was the dominant collision process and led to pronounced thermalisation of the ions. For discharges in nitrogen, charge exchange was again significant for the N₂⁺ ions, but for

the N^+ ions this process was less effective. The experimental data are compared with earlier experimental work and discussed in terms of a well known theoretical model of the sheath region and the transmission characteristics of the analyser for ions over a wide energy range.

NWP 4 Distribution of Fe atom density in a dc magnetron sputtering plasma source measured by laser-induced fluorescence imaging spectroscopy K. SHIBAGAKI, N. NAFARIZAL, K. SASAKI, H. TOYODA, S. IWATA, T. KATO, S. TSUNASHIMA, H. SUGAI, *Nagoya University, Japan*

Magnetron sputtering discharge is widely used as an efficient method for thin film fabrication. In order to achieve the optimized fabrication, understanding of the kinetics in plasmas is essential. In the present work, we measured the density distribution of sputtered Fe atoms using laser-induced fluorescence imaging spectroscopy. A dc magnetron plasma source with a Fe target was used. An area of 20×2 mm in front of the target was irradiated by a tunable laser beam having a planar shape. The picture of laser-induced fluorescence on the laser beam was taken using an ICCD camera. In this way, we obtained the two-dimensional image of the Fe atom density. As a result, it has been found that the Fe atom density observed at a distance of several centimeters from the target is higher than that adjacent to the target, when the Ar gas pressure was relatively high. It is suggested from this result that some gas-phase production processes of Fe atoms are available in the plasma. This work has been performed under the 21st Century COE Program by the Ministry of Education, Culture, Sports, Science and Technology in Japan.

NWP 5 Development of the so-called third stage laser Thomson scattering diagnostics of plasmas KATSUNORI MURAOKA, *Interdisciplinary Graduate School of Engineering Sciences, Kyushu Univ., Japan* YUKIHIKO YAMAGATA, *Interdisciplinary Graduate School of Engineering Sciences, Kyushu Univ., Japan* TAISHI HISANO, *Interdisciplinary Graduate School of Engineering Sciences, Kyushu Univ., Japan* KIICHIRO UCHINO, *Interdisciplinary Graduate School of Engineering Sciences, Kyushu Univ., Japan* KOICHI MIYAZAKI, *Dept. of Electrical and Electronics Engineering, Kurume National College of Technology, Japan*

In the recent review article,¹⁾ we indicated that the incoherent laser Thomson scattering (LTS) diagnostics of plasmas for measurements of electron densities and temperatures (or more generally EEDFs) be classified as having evolved from the first stage where a whole Thomson spectrum be obtained during a single laser pulse from plasmas having electron density of above 10^{18} m^{-3} , through the second stage where data accumulation be prerequisite for ne below 10^{18} m^{-3} , and to the third stage where a strong suppression of stray light in addition to the data accumulation be necessary to measure at an extremely small size of less than $100 \mu\text{m}$ near to material surfaces. The third stage LTS was first demonstrated for a PDP (plasma display panel)-like discharge three years ago employing a triple grating polychromator. In order to further expand its applicable ranges, we are pursuing a more general approach by taking into account such factors as laser divergence, stray light suppression and other aspects. The present status is presented. 1) K. Muraoka, K. Uchino, Y. Yamagata, Y. Noguchi, M. Mansour, P. Suanpoot, S. Narishige, and M. Noguchi, *Plasma Sources Sci. Technol.* 11 (2002) A143.

NWP 6 Spectroscopy investigations of the excited particles in an rf plasma-aided laser ablation plume* YOSUKE SAKAI, NOBUKAZU SAKURA, MARIA-ANTOANETA BRATESCU, YOSHIYUKI SUDA, HIROTAKE SUGAWARA, *Hokkaido University, Sapporo 060-8628, Japan* The purpose of this work is to explain the relation between the composition of a laser ablation plume due to chemical reactions and the properties of the obtained CN film. The ablation plume composition and consequently the film properties were changed by an additional rf plasma. An ArF excimer laser ($\lambda = 193 \text{ nm}$, pulse duration: 20 ns, fluence: 4 J cm^{-2}) was focused on a crystal graphite target in vacuum and in N_2 gas with pressures of 0.1–10 Torr. The rf plasma power was about 60 W. The number density distributions of the excited species produced in the laser ablation plume (C, N, C_2 , N_2 , CN) were detected using the optical emission spectroscopy (OES) and the laser absorption spectroscopy (LAS). Rf plasma increases the excited CN radical and the excited N_2 molecule number densities and decreases the excited C_2 molecule number density. The explanation could be done in relation with C number density in rf plasma added to the laser ablation plume. Using OES and LAS methods the velocities of different excited species in the rf plasma-aided laser ablation plume were measured.

*This work was supported partly by Grant-in-Aid for Scientific Research (C) of Japan Society for the Promotion of Science.

NWP 7 Laser spectroscopy investigations of the collisional processes in Ar and CH_4 mixtures in a dielectric barrier discharge* YOSUKE SAKAI, YASUNAO YOSHIKAZI, MARIA-ANTOANETA BRATESCU, YOSHIYUKI SUDA, *Hokkaido University, Sapporo 060-8628, Japan*

We investigated different collisional processes in Ar and CH_4 mixtures in a Dielectric Barrier Discharge (DBD) used for diamond like carbon materials production. The DBD discharge was operated in a 20 mm electrode gap distance by an rf 200 kHz power source, which was modulated with a frequency of 2.5 kHz. The Ar pressure was changed from 4 to 80 Torr. The ratio between CH_4 partial pressure and the total pressure was varied from 0% to 50%. The rf power was changed from 30 W to 140 W. We investigated the excitation transfer from Ar(I_{S_5}) to CH($A^2\Delta$) using laser collisional induced fluorescence (LCIF) method. The excitation transfer from Ar(I_{S_5}) to CH($A^2\Delta$) process probed by laser pumping of Ar(I_{S_5}) at 772.589 nm was detected by the change of Ar and CH radical emission line intensities. A typical LCIF spectrum shows the emission lines at 431.4 nm, 738.4 nm, 750.4 nm and 763.5 nm. We studied the collisional mixing between Ar(I_{S_5} , I_{S_3}) and Ar(I_{S_4} , I_{S_2}) in DBD using an optical-optical double resonance (OODR) absorption spectroscopy. The collisional mixing in Ar(I_{S_5}) levels and the transfer of excitation from Ar(I_{S_5}) to CH($A^2\Delta$) were investigated for different DBD parameters.

*This work was supported partly by Grant-in-Aid for Scientific Research (C) of Japan Society for the Promotion of Science.

NWP 8 Filtered Raman/Thomson Scattering Measurements in E-Beam Sustained Non-Equilibrium Plasmas WONCHUL LEE, *Dept. of Chemistry, The Ohio State University* WALTER LEMPERT, *Depts. of Mechanical Engrg. and Chemistry, The Ohio State University*

In this paper we will present experimental results demonstrating the utility of a new spectrally filtered rotational Raman/Thomson scattering instrument for characterization of weakly ionized, non-equilibrium molecular plasmas. The instrument, which pairs a rubidium vapor filter with a narrow line-

width, pulsed titanium:sapphire laser, is shown to attenuate elastic (and/or molecular Rayleigh) scattering by more than seven orders of magnitude, while efficiently transmitting pure rotational Raman scattering (from heavy species) and/or Thomson scattering. Proof-of-concept spectra will be presented demonstrating sensitivity of $\sim 10^{12} \text{ cm}^{-3}$, 0.10 eV, and ~ 10 K for electron number density, electron temperature, and heavy species rotational/translational temperature, respectively. Spectra obtained as part of an on-going study of the influence of vibrational excitation on the rate of O₂-detachment in low (~ 300 K) temperature, atmospheric pressure, electron-beam sustained air plasmas will also be presented. Acceleration of the net detachment rate by \sim three orders of magnitude will be demonstrated when the air medium is vibrationally excited using a CO laser-based pumping process.

NWP 9 COLLISIONAL IONIZATION

NWP 10 Measurements of ionization and attachment coefficients in c-C₄F₈ and in 0.468% and 4.910% c-C₄F₈/Ar mixtures YAMAJI MASAHIRO, NAKAMURA YOSHIHARU, *Keio University, Japan* The density normalized ionization and attachment coefficients in c-C₄F₈ and in 0.468% and 4.910% c-C₄F₈/Ar mixtures have been measured by the steady-state Townsend method in the ranges of E/N over 250-10000Td in pure c-C₄F₈, 25-1000Td in 0.468% c-C₄F₈/Ar mixture, and 70-1000Td in 4.910% c-C₄F₈/Ar mixture. Each coefficient is derived from Townsend's equation by the curve fitting method. This is the first measurement in the c-C₄F₈/Ar mixture as far as we know. The α/N in the mixtures are nearly equal to that in pure Ar at high E/N range, and become lower as E/N decreases. The pressure dependences of α/N , η/N and $(\alpha - \eta)/N$ are observed in the 4.910% mixture and pure c-C₄F₈. Urquijo et al. also found similar tendency in $(\alpha - \eta)/N$ in pure c-C₄F₈, but their results are lower than our results. Tagashira et al. observed the tendency in all coefficients (α/N , η/N and $(\alpha - \eta)/N$), and their results are higher than our results.

NWP 11 Importance of higher order effects in single ionization of hydrogen and helium ZHANGJIN CHEN, *Laboratory for Atomic and Molecular Research, University of Missouri-Rolla, Rolla, MO 65401, USA* DON H. MADISON, *Laboratory for Atomic and Molecular Research, University of Missouri-Rolla, Rolla, MO 65401, USA* COLM T. WHELAN, *Department of Physics, Old Dominion University, Norfolk, VA 23529, USA* H. R. J. WALTERS, *Department of Applied Mathematics and Theoretical Physics, The Queens University of Belfast, Belfast BT7 INN, UK* For the processes of electron impact ionization, it has been found that the second order effects are crucial in explaining both the positions and magnitudes of the binary and recoil peaks in the triple differential cross sections (TDCS). However, theoretical calculations of second-order amplitudes typically resort to several simplifying approximations such as the closure approximation and using plane waves for the projectile to make the calculation tractable. Based on our previous work for atomic excitation, we have

developed a second-order distorted wave theory for atomic ionization which does not use closure but instead sums over all intermediate states. The method will be applied to the calculation of the TDCS for electron impact ionization of hydrogen and helium.

NWP 12 Post Collision Interaction Effects for Electron Impact Ionization of S and P Shell Electrons in Inert Gases A. PRIDEAUX, *University of Missouri-Rolla* D.H. MADISON, *University of Missouri-Rolla* The standard Distorted Wave Born Approximation (DWBA) for atomic ionization neglects the post-collision interaction (PCI) between the two outgoing electrons in the approximation for the final state wavefunction. This approximation is valid for high enough energy, but at lower energy this interaction becomes more important. We will report results of a DWBA approach which includes PCI effects to all orders of perturbation theory in the final state wavefunction. Theoretical and experimental fully differential cross sections will be compared for electron-impact single ionization of the 3s and 3p shells of Argon, and for the 4p shell of Krypton.

NWP 13 Ionization of silicon atoms by electron impact* YONG-KI KIM, *NIST* Ionization cross section for the silicon atom has been calculated using the binary-encounter-Bethe (BEB) model¹. The peak value of the experimental cross section by Freund et al.² is about 30% higher than the direct ionization cross section obtained from the BEB model. The ground-state atoms (3s²3p²3P) can easily be excited to the autoionizing level (3s3p³S) by dipole and spin allowed excitation. The cross section for this autoionizing process estimated using the BE-scaled Born cross section³ indicates that the process accounts for less than 1/2 of the difference between the experiment and theory. On the other hand, metastable atoms in the 3s²3p²1D level (0.78 eV above the ground level) can be excited to the 3s3p³1D and ¹P autoionizing levels (estimated to be 9.83 eV and 10.68 eV above the ground level) with large cross sections. The theoretical peak cross section for an equal mixture of the ground-state and metastable Si atoms agrees well with the experimental peak cross section.

*Work supported in part by the Office of Fusion Energy Sciences, USDOE

¹Y.-K. Kim and M. E. Rudd, *Phys. Rev. A* **50**, 3954 (1994).

²R. S. Freund et al., *Phys. Rev. A* **41**, 3575 (1990).

³Y.-K. Kim, *Phys. Rev. A* **64**, 032713 (2001).

NWP 14 Fundamental Physics Observed by Three-Dimensional Imaging of Single Ionized Electrons by Ion-Atom Collisions M. FOSTER, D. H. MADISON, S. JONES, M. SCHULZ, *University of Missouri-Rolla, Rolla, MO, USA* Three-dimensional fully-differential cross sections (FDCS) have provide insight into the mechanisms that contribute to interesting new physics (M. Schulz et al., *Nature* **422**, 48 (2003)). Experiments have observed unique ring-like structures for the traditional recoil lobe for single ionization of helium by a 100 MeV/amu C⁶⁺. The ring-shaped structure is not predicted by theory at this energy. However, recent new measurements have been made for 2 MeV/amu that also contained a similar shaped structure. Surprisingly, this structure is now predicted by the Continuum-Distorted-Wave-Eikonal-Initial-State model (CDW-EIS). The first-Born approximation (FBA) which should be valid for high energy approximations does not contain the ring like structure. The FBA is

cylindrically symmetric about the momentum, q , transferred to the target atom and could never predict a ring structure centered on the beam axis. The mechanisms that caused both the ring structures and the failure of the theory for higher energies will be discussed.

NWP 15 Ionization Cross Sections for Ion-Atom Collisions in High Energy Ion Beams

IGOR D. KAGANOVICH, EDWARD A. STARTSEV, RONALD C. DAVIDSON, *Plasma Physics Laboratory, Princeton University, Princeton, NJ 08543* Knowledge of ion-atom ionization cross sections is of great importance for many accelerator applications. When experimental data and theoretical calculations are not available, approximate formulas are frequently used. Based on experimental data and theoretical predictions, a new fit for ionization cross sections by fully stripped ions is proposed. The Born approximation and classical trajectory calculations are frequently used to estimate the cross sections. Neither approximation is expected to be valid over the entire range of projectile ions and target atoms. Aspects of both models must be included in order to address the shortcomings in the underlying assumptions. A large difference in cross section, up to a factor of six, calculated in quantum mechanics and classical mechanics, has been obtained for 3.2 GeV I^- and Cs^+ ions. Because at such high velocities the Born approximation is well validated, the classical trajectory approach fails to correctly predict the stripping cross section at high energies for electron orbitals with low ionization potential. Additional information on the subject will be posted in <http://www.ppl.gov/pub/report/2003/> and in <http://arxiv.org/abs/physics/>

NWP 16 Electron-Impact Ionization of WF_6 and Cl_2 *

RALF BASNER, *Institut für Niedertemperatur-Plasmaphysik, Greifswald, Germany* KURT BECKER, *Stevens Institute of Technology, Hoboken, USA* We report the results of experimental studies of the formation of positive ions by electron impact on WF_6 and Cl_2 from threshold to 900 eV. The measurements were carried out in a time-of-flight mass spectrometer with complete collection of fragment ions with kinetic energy. No evidence for the formation of the parent WF_6^+ ion was found. Dissociative ionization of WF_6 resulting in seven different singly and five different doubly charged fragment ions was found to be the dominant ionization process. The ion spectrum is dominated by the WF_5^+ fragment ion. All fragment ions are formed with excess kinetic energy. The total ionization cross section of WF_6 is $6.3 \times 10^{-16} \text{ cm}^2$ at 70 eV impact energy. In the case of Cl_2 we have measured the positive ion formation of Cl_2^+ , Cl_2^{++} , Cl^+ , and Cl^{++} . The parent Cl_2^+ ion has the largest partial ionization cross section. The singly and doubly charged fragment ions are formed with significant excess kinetic energy. Our preliminary studies show a total ionization cross section of Cl_2 of about $7.5 \times 10^{-16} \text{ cm}^2$ at 70 eV.

*Work supported in part by the US Department of Energy

NWP 17 Dissociative ionization and product distributions of low-lying ionization channels of benzene and pyridine by electron impact

CHRISTOPHER E. DATEO, *Eloret Corporation* WINIFRED M. HUO, *NASA Ames Research Center* GRAHAM FLETCHER, *Eloret Corporation* We report recent results of a continuing theoretical study of the dissociative ionization (DI) and product distributions of two organic molecules, benzene (C_6H_6) and pyridine (C_5H_5N), from their low-lying ionization channels. Our approach makes use of the fact that electronic motion is much faster than nuclear motion allowing DI to be treated as a two-step

process. The first step is the electron-impact ionization resulting in an ion with the same nuclear geometry as the neutral molecule. In the second step, the nuclei relax from the initial geometry and undergo unimolecular dissociation. For the ionization process we use the improved binary-encounter dipole (iBED) model [W.M. Huo, *Phys. Rev. A* 64, 042719-1 (2001)]. For the unimolecular dissociation, we use multiconfigurational self-consistent field (MCSCF) methods to determine the minimum energy pathways to the possible product channels. More accurate methods are then used to obtain better energetics of the paths which are used to determine unimolecular dissociation probabilities and product distributions. In the study of the minimum energy pathways, we optimize all bond angles and bond distances. For benzene this procedure requires variational optimization of 30 nuclear coordinates and for pyridine, 27 coordinates are optimized. For benzene, we find the first dissociative ionization channel produces $C_6H_5^+$ and H. This result differs from the photoionization measurements of benzene by Feng et al. [R. Feng, G. Cooper, C.E. Brion, *J. Electron Spectrosc. Relat. Phenom.* 123, 211 (2002)] who reported the production of H_2 from the lowest dissociative channel.

NWP 18 LIGHTING PLASMAS II

NWP 19 Radial Cathoporesis in Hg-Ar Fluorescent Lamp Discharges at High Power Density

Y. AIURA, G. A. BONVALLET, J. E. LAWLER, *Univ. of Wisconsin [1]* Radial cathoporesis is a process in which the lower ionization potential atoms (Hg) are preferentially ionized and expelled from a multi-component (Hg-Ar) discharge. This process is important at high power densities which occur in some types of fluorescent lamps (e.g. the electrodeless Endura/Icetron lamp developed at Osram Sylvania Inc.). Recent attempts to reconcile extensive absolute measurements on Icetron lamp discharges with self-consistent numerical models were only partially successful [2]. Radial cathoporesis as well as some other high power density phenomena need to be re-examined. We have set up an axial absorption experiment at 185 nm on the ground level Hg atoms in an operating Icetron lamp. The High Sensitivity Absorption Spectroscopy (HSAS) facility at the Synchrotron Radiation Center in Stoughton WI is used in this study. The HSAS facility provides an intense synchrotron radiation continuum, very high spectral resolving powers from a 3 m focal length vacuum echelle spectrometer, and superb S/N ratios from a CCD detector array. Preliminary results will be presented and discussed. [1] Supported by the NSF & USHIO Inc. Experimental lamp provided by OSRAM-SYLVANIA Inc. [2] J. J. Curry, G. G. Lister, J. E. Lawler, *J. Phys. D: Appl. Phys.* 35, 2945 (2002)

NWP 20 Temperature measurements using selected Tm and Dy lines in Metal Halide Lamps

Y. AIURA, J. E. LAWLER, *Univ. of Wisconsin-Madison* The 1 m Fourier transform spectrometer (FTS) at the National Solar Observatory on Kitt Peak was used to record UV to IR emission spectra of Metal Halide-High Intensity Discharge (MH-HID) lamps with doses containing rare earth salts. All intrinsic structure is fully resolved in these spectra. Many additive lines were found to have nearly perfect Lorentzian

profiles and to be surprisingly narrow ($\text{FWHM} < 1 \text{ cm}^{-1}$) [1]. Fitting these profiles to Lorentzian functions provides a sensitive test for radiation trapping and line blending [1]. We have used this fitting approach along with recently measured absolute transition probabilities [2,3] to select sets of lines in Tm I, Tm II, Dy I, and Dy II which are good for temperature determinations in MH-HID lamps. [1] H. Adler, L. Riley, & J. E. Lawler in Proceedings of the Ninth International Symposium on the Science and Technology of Light Sources LS:9 ed: R S Bergman (2001, Ithaca: Cornell University Press) p 129. [2] M. E. Wickliffe & J. E. Lawler, *J. Opt. Soc. Am. B* 14, 737 (1997) [3] M. E. Wickliffe, J. E. Lawler, & G. Nave, *J. Quant. Spectrosc. Radiat. Transfer* 66, 363 (2000).

NWP 21 Improved Fidelity X-ray Transmission Images of HID Lamps* G. A. BONVALLET, J. E. LAWLER, *Univ. of Wisconsin-Madison* The linearity of modern X-ray detection systems has made possible detailed Hg density/temperature maps in High Intensity Discharge (HID) lamps [1]. These maps provide critical data in the near wall region, and some information on the convective cell structure of HID lamps. In the current work an ultrabright microfocuss (source diameter < 40 microns) X-ray tube with a Mo anode was used to produce magnified transmission images with a phosphor image plate detection system. Special attention was given to calibration of the system using cells containing reference solutions of Hg in nitric acid. Possible losses in image fidelity due to the spread of X-ray energies from the microfocuss lab source, and due to forward scattering of X-rays were explored in detail using both reference solutions of Hg in nitric acid and numerical simulations. Results for pure Hg lamps and Metal-halide HID lamps will be presented. *Supported by the NSF. [1] J. J. Curry, M. Sakai, & J. E. Lawler, *J. Appl. Phys.* 84, 3066 (1998).

NWP 22 Broadening of the Na D lines in dependence on the Xe pressure in HID lamps* MANFRED KETTLITZ, OLGA KRYLOVA, MARTIN WENDT, HARTMUT SCHNEIDENBACH, *Institute for Low-Temperature Plasma Physics, F.-L.-Jahn-Str. 19, D-17489 Greifswald, Germany* The influence of the variation of the Xe pressure on the broadening of the Na D lines in HID short arc lamps is investigated. The discharge lamps have an inner diameter of 1.5 mm and an electrode gap of 6 mm. The lamps contain 6 mg NaI and between 1 and 20 bar Xe. Additionally, they are filled with TII and mixtures of rare earth iodides. They are horizontally operated with a 300 Hz rectangular voltage and the input power is varied in a range of 20 to 40 W which leads to different Na vapor pressures. The plasma temperatures are measured by emission spectroscopy via Bartels method with the Na 819 nm and the Tl 535 nm lines. In the arc center the temperature reaches values of about 4500 K. The Na D lines show a strong broadening and are self-reversed. Therefore, radiation transport calculations are done to compare the measured line profiles with calculated ones. The increase of the Xe pressure leads to a strong increase of the broadening of the red wing of the Na D lines.

*This work is supported in part by German Federal Ministry for Education and Research (BMBF).

NWP 23 On the electrode sheath voltage in high-pressure argon, xenon and mercury discharges* MANFRED KETTLITZ, MICHAEL SIEG, MARTIN WENDT, HARTMUT SCHNEIDENBACH, *Institute for Low-Temperature Plasma Physics, F.-L.-Jahn-Str. 19, D-17489 Greifswald, Germany* LARS DABRINGHAUSEN, OLIVER LANGENSCHIEDT, MARCO REDWITZ, *Ruhr-University of Bochum, Fundamentals of Electrical Engineering, Universitaetsstr. 150, D-44780 Bochum, Ger-*

many The electrode sheath voltage (ESV) and the electrical field strength are measured in high-pressure argon, xenon and mercury discharges. The experiments in Ar and Xe are performed in the model lamp developed in Bochum. The electrode holders can be moved in the tube by stepping motors so that the electrode distance can be varied during operation. For the experiments in Hg we used lamps with different electrode-gap lengths but with otherwise identical geometric and filling conditions for obtaining a similar arc plasma. The electrodes consist of pure tungsten and have diameters between 0.5 and 1 mm. The discharges are vertically operated with a sinusoidal 50 Hz current. There are two significant differences in the shape of the ESV of mercury discharges compared to the rare gases: 1. a very pronounced ignition peak earlier and much higher than in the rare gases and 2. a remarkable voltage minimum near zero in the first quarter of a half cycle. The pronounced ignition peak is due to the fact that a spot mode occurs at the electrode in the Hg discharge whereas the rare gases show a diffuse mode in this parameter range. For lower discharge currents a spot mode occurs also in rare gases and the ESV has in that case also a higher ignition peak as in the Hg discharge but no minimum. The field strengths are compared with theoretical values. The model considers radiation transport in an axially homogeneous arc column.

*This work is supported in part by German Federal Ministry for Education and Research (BMBF).

NWP 24 Microwave Discharge Characteristics of Plasma Lighting System BYEONG-JU PARK, JOON-SIK CHOI, YONG-SEOG JEON, HYUN-JUNG KIM, JI-YOUNG LEE, *LG Electronics Inc.* PLS (plasma lighting system) is an electrode-less light source to provide visible light of continuous spectrum with high power efficiency. The light source comprises a bulb containing a plasma-forming medium. When the bulb is placed in a microwave energy field, the field ionizes buffer gas within the bulb. A low-pressure plasma discharge forms within the bulb, heating the bulb wall, vaporizing materials such as sulfur within the bulb to generate light. The goal of our experiment is to find suitable lamp operating parameter and to achieve higher light-conversion efficiency. For this work we studied experimentally the microwave discharge characteristics of initial buffer gas, plasma geometry, bulb rotation effect, and emission spectrum features in the PLS.

NWP 25 Investigation of metal-halide high-pressure discharge lamps containing thallium iodide* ST. FRANKE, H. SCHNEIDENBACH, H. SCHÖPP, *INP Greifswald, F.-L.-Jahn-Str. 19, D-17489 Greifswald, Germany* Spatial temperature profiles of discharge lamps containing Hg, TmI₃ and TII are presented (cylindrical quartz vessel with 12.2 mm inner diameter, 18 mm electrode distance, 120 W power input, vertical operation). Temperatures are determined using the self-reversed Tl 535 nm line. The method of Bartels [1] is compared with the method described by Karabourniotis [2]. Applying Abel's inversion to optically thin Hg, Tl and Tm lines partial pressures are obtained. The axial homogeneity within the discharge vessel is examined and changes of the radial temperature profile with varying TII filling are investigated. The results are compared with model calculations, where the power balance is solved taking account of the radiation transport. The contributions of the radiating species to the light flux are discussed. At present much effort is taken to replace mercury in metal-halide lamps with more environment friendly materials. Leaving the well known subject reliability of temperature mea-

measurements with the Tl 535 nm line is proofed, because the Tl transition at 535 nm is an indispensable diagnostic line for the discharge plasmas in the scope of interest. [1] H. Bartels, *Z. Physik* **128** (1950) 546. [2] D. Karabourniotis, *J. Appl. Phys.* **57** (1985) 4861.

*In Collaboration with OSRAM Munich/Germany. Work supported by the German BMBF.

NWP 26 Study of high-pressure xenon discharges with metal-halide additives* MARTIN WENDT, HARTMUT SCHNEIDENBACH, MANFRED KETTLITZ, MICHAEL SIEG, *Institute for Low-Temperature Plasma Physics, F.-L.-Jahn-Str. 19, D-17489 Greifswald, Germany* REDWITZ MARCO, *Ruhr-University of Bochum, Fundamentals of Electrical Engineering, Universitaetsstr. 150, D-44780 Bochum, Germany* The plasma column of atmospheric pressure wall-stabilized discharges in xenon with metal-halide additives has been studied theoretically considering an axially homogeneous arc column. The energy balance with radiation transport has been solved numerically with the assumption of local thermodynamic equilibrium. The convection has been neglected and a pressure constant in time and space has been assumed. The transport properties have been calculated in higher-order Chapman-Cowling approximation with recently published electron-atom collision cross-sections for xenon. The resulting electrical characteristics, temperature profiles, radiation intensities and fluxes for Xe-discharges with and without admixtures of NaI, TlI and rare-earth iodides are discussed. The analysis is done for dc, ac and pulsed discharges in a current range between 1 and 20 amperes. Temperature profiles and radiation intensities are compared with measurements.

*This work is supported in part by the German Research Society (DFG)

NWP 27 Effects of Additional Pulsed Potential on Sustaining Discharge in an AC-type PDP Cell SHINTANI YOUICHI, TACHIBANA KUNIHIDE, *Department of Electric Science and Engineering, Kyoto University* The aim of our research is to understand the discharge mechanisms by using additional pulse on the third electrode in the sustain period to improve luminous efficiency of AC-type Plasma Display Panel (AC-PDP). For this purpose, we measured the spatiotemporal behaviors of Xe*(1s₅, 1s₄, 2p) atoms by using microscopic laser absorption spectroscopy and optical emission spectroscopy with a specially designed PDP cell equipped with transparent glass prisms as barrier ribs. When a pulse train was applied on the address electrode synchronously with the rise of the sustain pulse, the auxiliary discharge between the address electrode and one of the sustain electrode (preceding anode) started almost simultaneously with the main discharge between the two sustain electrodes, and the density of Xe*(1s₅) atoms distributed over the whole cell area. When the center of address pulse was set at the rising edge of sustain pulse, predischARGE occurred between the address electrode and one of sustain electrode, and the main discharge was weakened. In addition, we are testing other cell structures having auxiliary electrodes.

NWP 28 HIGH PRESSURE DISCHARGES

NWP 29 Ion flux energy and angle distributions to the cathode surfaces in PDPs J.Q. WANG, *IPED, Xi'an Jiaotong U., China* L.C. PITCHFORD, J.-P. BOEUF, *CPAT, U. Paul Sabatier and CNRS, Toulouse, France* Sputtering of the MgO coating on the dielectric surface in plasma display panel cells (PDPs), caused by impacting ions and fast neutrals, is a lifetime limiting factors in these devices. We present here a study of the influence of gas mixture and operating conditions on the ion flux energy and angle distributions in PDPs in coplanar electrode geometries and in Xe/Ne mixtures. The models used are a 2D electrical model (based on fluid equations) to determine the space and time dependent electric field and ionization source term, and then a Monte Carlo simulation of the ion trajectories. We find that the energy and angle distributions of the ion fluxes (integrated over the current pulse) depend on position along the surface and on the percentage of Xe in the mixture. Higher energy ions arrive with angles between 0 and about 30° at the surface nearest the anode, while those ions arriving at points further from the anode have lower energies and higher average angles of incidence. The extraction of the sputtering rate of the MgO from our distributions depends on assumptions about the sputtering yield of MgO as a function of energy and angle.

NWP 30 Gas Temperature Determination and Ar Metastable Density Measurement in a N₂-Ar Dielectric Barrier Discharge JAMES M. WILLIAMSON, *Innovative Scientific Solutions, Inc., Dayton, OH* PETER BLETZINGER, *Innovative Scientific Solutions, Inc., Dayton, OH* BISWA N. GANGULY, *Air Force Research Laboratory, WPAFB, OH* The bulk gas temperature in a 30% N₂/Ar short-pulsed (< 15nS, FWHM) dielectric barrier discharge was determined from the rotationally resolved plasma emission of N₂⁺ 1st negative and N₂ 2nd positive as well as the time-resolved diode-laser absorption of metastable Ar. The line-integrated metastable Ar population density was also measured by diode-laser absorption. The gas temperature, derived from the N₂⁺ and N₂ emission spectra, was determined from contour analysis of individual vibrational bands in the 1st negative and 2nd positive systems while the Doppler width of metastable Ar from the absorption spectrum was used to determine the temperature under the same discharge cell conditions. The determined temperatures did not vary, within experimental uncertainty, as a function of discharge repetition rate in the range 500 Hz to 30 kHz; the temperature of the 2nd positive emission was higher than the 1st negative while the temperature from the Ar metastable Doppler width was the same or slightly lower than the 1st negative temperature. Although the temperature remained constant, the time-resolved, line-integrated metastable Ar density decreased, per pulse, with increasing discharge repetition rate. The effect of pressure scaling on both the metastable Ar density and gas temperature will be presented.

NWP 31 Electrical and Optical Characteristics of RF Driven Hollow Slot Microplasmas in Open Air at Atmospheric Pressure* ZENGQI YU, AZER YALIN, OVIDIU STAN, KATSUMI HOSHIMIYA, R. ABDUR, VIJAY SURLA, GEORGE COLLINS, *Colorado State University* The hollow slot discharge has been operated in open air at atmospheric pressure with pd values of ~10Torr-cm and E/N values of ~70 Td. It can sustain a

plasma with rare gases or without in the open air. We have scaled the hollow slot length from quarter of inch to over a foot, and run it at RF frequencies of 4 MHz and 13.56 MHz. We measured the RF electrical characteristics of the plasma at the 13.56 MHz. Stable discharges, with sinusoidal currents, are obtained up to power densities of $> 180 \text{ kW/cm}^3$, before non-sinusoidal currents and RF glow-to-arc transitions occur. We observed the optical spectra in the VUV region from the hollow slot atmosphere plasma with several different gases and their mixtures, including dry air, room air, argon, helium, nitrogen, and mixtures of these gases with oxygen and hydrogen. Atomic lines of Oxygen, Hydrogen and Nitrogen can be altered by the choice of gas concentration and discharge conditions. Potential applications of these sources are under investigation.

*This work is supported by NSF grant #ECS - 0097061

NWP 32 COLD MICRO-PLASMA JETS IN ATMOSPHERIC PRESSURE AIR A.H. MOHAMED, S. SUDDALA, K.H. SCHOENBACH, *Physical Electronics Research Institute, Old Dominion University Norfolk, VA 23529, USA* Direct current microhollow cathode discharges (MHCDs) have been operated in air, nitrogen and oxygen at pressures of one atmosphere. The electrodes are $250 \mu\text{m}$ thick molybdenum foils, separated by an alumina insulator of the same thickness. A cylindrical hole with a diameter in the $100 \mu\text{m}$ range is drilled through all layers. By flowing gases at high pressure through this hole, plasma jets with radial dimensions on the same order as the microhole dimensions, and with lengths of up to one centimeter are generated. The gas temperature in these jets was measured by means of a microthermocouple. The lowest temperatures of close to room temperature were measured when the flow changed from laminar to turbulent. The results of spectral emission and absorption studies indicate high concentrations of byproducts, such as ozone, when the discharge is operated in air or oxygen. This work is supported by the U.S Air Force Office of Scientific Research (AFOSR).

NWP 33 Gas Temperatures of a High-Pressure MicroHollow Cathode Discharge Inferred from Rotational Band Emission Spectroscopy PETER KURUNCZI,* *Stevens Institute of Technology* KURT BECKER, *Stevens Institute of Technology* The gas kinetic temperature of a high-pressure microhollow cathode discharge (400 Torr neon) has been determined using emission spectroscopy of the 2nd Positive and 1st Negative systems of molecular nitrogen. Through collisions, the rotational population distribution within a given rotational band can equilibrate to the gas kinetic temperature, so that the rotational temperature will reflect the gas temperature [1]. Interestingly, two different rotational temperatures have been measured, approximately 400 degrees K from the 2nd Positive system and 900 degrees K from the 1st Negative system. By taking into consideration the rotational relaxation time of molecular nitrogen in neon, and the lifetimes and quenching rates of the excited rotational levels [2], it has been determined that the lower temperature of 400 degrees K from the 2nd Positive System reflects the true gas temperature. While the higher temperature of 900 K results from the 1st Negative System suffering from rotational heating and insufficient time to equili-

brate to the gas kinetic temperature due to collisional quenching of its upper levels. 1. J.E. Lawler 1998 *J. Phys D: Apply Phys.* 31 1556 2. N.K. Bibinov, A.A. Fateev, K. Wiesemann, *Plasma Sources Sci. Tech.* 10 (2201) 579-588

*Currently a postdoc at the University of Houston, Chem Eng Dept

NWP 34 Experimental and theoretical study of a helium atmospheric pressure barrier discharge at 100 kHz R. FOEST, M. SCHMIDT, *Institut of Low-Temperature Plasma Physics, Greifswald, Germany* V.S. MAIOROV, YU.B. GOLUBOVSKII, *University of St. Petersburg, Physical Faculty, St. Petersburg, Russia* J.F. BEHNKE, *University of Greifswald, Institute of Physics, Greifswald, Germany* A homogeneous barrier discharge is obtained in helium at 100 kHz and atmospheric pressure. Measurements of the electrical characteristics of a discharge show that positive and negative current peaks are asymmetric. At higher amplitudes of the external voltage, multiple peaks of discharge current can be observed. The discharge homogeneity is not violated, when a small (0.1%) admixture of HMDSO is added to the gas. The results are compared with the one-dimensional fluid simulations. The experimental electrical characteristics agree well with the calculations in the assumption of the presence of a certain admixture. Moreover, it is necessary to assume that the excimers He_2^* are efficiently destroyed without the corresponding production of ions.

NWP 35 Initiation of the homogeneous glow barrier discharge in nitrogen YU. B. GOLUBOVSKII, V. A. MAIOROV, *University of St. Petersburg, Physical Faculty, St. Petersburg, Russia* J. BEHNKE, J.F. BEHNKE, *University of Greifswald, Institute of Physics, Greifswald, Germany* The evolution of a single-electron avalanche in a parallel-plane barrier discharge in nitrogen is studied with the help of a two-dimensional fluid model. When the photoemission is the main source of secondary electrons, the electron avalanche forms a wide front of secondary electron avalanches starting from the cathode. At not very high overvoltages, when the primary avalanche does not turn into a streamer, a quasi-homogeneous discharge covering a whole electrode surface may be initiated. After the extinction of a primary avalanche, the discharge turns into the Townsend phase, which is followed by the space-charge phase and finally by the afterglow. The duration of current peak is larger than that in the one-dimensional model, which is caused by the non-instantaneous expansion of the discharge front outward the initial region. The proposed mechanism may be responsible for the ignition of the homogeneous glow discharge in nitrogen observed at low frequencies.

NWP 36 Atmospheric pressure afterglow plasma* SHIRSHAK DHALI, *Southern Illinois University* RAYAN YELLINA, *Southern Illinois University* BIJAN PASHAIE, *Southeast Missouri State University* A radio frequency driven atmospheric pressure plasma source is discussed. The plasma produces an afterglow, which can be used for plasma chemical reactions under ambient conditions. The light intensity measurement shows that the discharge is continuous in time unlike low frequency dielectric-barrier discharges, which are intermittent in nature. The discharge, under ambient conditions, can be generated in Argon, Helium and Nitrogen. Trace amounts of H_2 or O_2 in Ar or He produce disso-

ciated H and O respectively. We will report the results of voltage and power measurements. Unlike low frequency dielectric-barrier discharges, at RF frequency (13.65 MHz) the power depends on the square of the RF peak voltage. We estimate the electron densities to be about $10e7 \text{ cm}^{-3}$ in the RF plasma.

*Funded by NSF

NWP 37 Characteristic analysis of hydroxyl radical generated by atmospheric pressure discharge JAI HYUK CHOI, *Department of Metallurgical Engineering, Yonsei University, 134 Shinchon-dong, Seodaemun-Ku, Seoul 120-749, Korea* HONG KOO BAIK, *Department of Metallurgical Engineering, Yonsei University, 134 Shinchon-dong, Seodaemun-Ku, Seoul 120-749, Korea* SE-JONG LEE, *Department of Material science and Engineering, Kyungsoong University, Korea* KI MOON SONG, *Department of New Material Science Applied Physics, Korea* In atmospheric pressure discharge process, some active species like ozone and hydroxyl radical, are generated from reaction among electron, nitrogen, oxygen and water vapor etc. Among these species, hydroxyl radical has a strong sterilization effect because of its high reduction potential (2.56V). For better understanding about generation of hydroxyl radicals by atmospheric pressure discharge, OES analyses were carried out at atmospheric pressure in corona discharge and two DBD types (volume DBD and coplanar DBD). We compared with the relative intensity of active species from OES data. And we also calculated the intensity ratio of the first negative system of N_2^+ (391.4nm) to the second positive system of N_2 (337.1nm) to know which type of plasma generate the electrons with higher energy. And with this emission spectra, we analyzed the gas temperature by our simulation code. And from these results, we could conclude the relationship between the intensity of electron energy, gas temperature and generation of hydroxyl radical in each type of the atmospheric pressure discharge.

NWP 38 Air Chemistry, Reactions, Simulations, and Power Estimates for Plasma Continuously Generated by an Electron Beam with a Sustaining Electric Field ROBERT VIDMAR, *University of Nevada, Reno* KENNETH STALDER, *Stalder Technologies and Research* An air-chemistry code specifically adapted to model plasma generation in air with up to 2km (300 kft) is discussed in the context of electron beam ionization and electric field sustainment for electron densities from $1E10$ to $1E13 \text{ cm}^{-3}$. In addition to delta-function electron-beam generation, various scenarios of continuous and pulsed generation are quantified. The addition of NO_x negative ions has improved the air chemistry simulations and late time negative-ion concentrations. The importance of NO_3^- as well as oxygen singlet delta and the vibrational states of O_2 and N_2 as a function of time after excitation is quantified as well as the power required to sustain the plasma. This material is based on research sponsored by the Air Force Research Laboratory, under agreement number F49620-01-1-0414.

NWP 39 Non-thermal Air Plasma at Atmospheric Pressure* XINPEI LU, *Old Dominion University, Norfolk, VA 23529* FRANK LEIPOLD, *Old Dominion University, Norfolk, VA 23529* O. MINAYEVA, *Old Dominion University, Norfolk, VA 23529* MOUNIR LAROUCI, *Old Dominion University, Norfolk, VA 23529* An AC-driven, non-thermal, atmospheric pressure air plasma is generated within the gap separating a disk-shaped metal electrode and a water electrode. The plasma species are identified by emission spectroscopy. The ignition phase and the steady-state

are studied by a high-speed CCD camera. It is found that the plasma always initiates at the surface of the water electrode. The plasma exhibits different structures depending on the polarity of the water electrode: when the water electrode plays the role of cathode, a relatively wide but visibly dim plasma column is generated. When the water electrode is anode, the plasma column narrows but increases its light emission. The maximum rotational and vibrational temperature of molecular nitrogen are 1800K and 2600K respectively. The electron density in the plasma was measured utilizing the conductivity. It is found to be $3 \times 10^{13} \text{ cm}^{-3}$ in the center of the discharge during the peak current of $I_{\text{peak}} = 40 \text{ mA}$. It is also found that the OH (A-X) emission intensity stays at high value during the discharge period.

*This work was supported by AFOSR grant F49620-00-1-0168 and F49620-03-1-0325

NWP 40 PLASMA SHEATHS

NWP 41 Asymptotic Matching and Patching of Plasma and Sheath Solutions NATALIA STERNBERG, *Clark University* VALERY GODYAK, *Osram Sylvania* Two approaches are found in the literature to join the plasma and sheath solutions. One, called patching, dates back to Langmuir and Bohm, and is applied to construct a discrete plasma-sheath model with a sharp interface and at least a continuous transition in the physical quantities. The second approach is the one of matched asymptotic expansions, which has its primary goal to approximate the full solution by the plasma and the sheath solutions, and requires the introduction of an intermediate region. Over the years, the interpretation of the results obtained by patching (where $\lambda_D \neq 0$), and by asymptotic matching (where $\lambda_D = 0$) were blended together and gave rise to a new interpretation of the sheath. The sheath became the region which stretches from the point where the ion velocity reaches the ion-sound speed up to the wall and consists of two parts: the ion-electron sheath (where $n_e \approx n_i$) and the "ion sheath" (where $n_e \ll n_i$). Here, n_e is the electron density and n_i is the ion density. In this presentation, we will discuss the differences between patching and asymptotic matching, and show that this new notion of the sheath contradicts not only the common perception of the sheath, but also both, patching and asymptotic matching techniques. We will show that the ion-electron sheath is contained in the intermediate region, and the sheath is in fact the ion sheath. We will also show that whether patching or asymptotic matching is used, the solution gives a consistent result only for the ion sheath.

NWP 42 Method of matched asymptotic expansions vs. intuitive approaches: Calculation of space-charge sheaths and arc cathode spots* M. S. BENILOV, *Departamento de Física, Universidade da Madeira, Largo do Municipio, 9000 Funchal, Portugal* A comparison is performed of results predicted by the method of matched asymptotic expansions and intuitive approaches in four problems of the theory of plasma-wall interaction: a collisionless steady-state sheath, a matrix sheath, a collisionless RF sheath, and arc cathode spots. In the first three problems, asymptotic results are compared with those given by the Child-Langmuir model and by different variants of patching, and

with the exact solution. In the fourth problem, a model is suggested of steady-state solitary spots with a step-function dependence of the density of the energy flux from the plasma on the temperature of the cathode surface. An asymptotic solution is compared with that obtained with the use of Steenbeck's principle of minimum power and with the exact solution. In all the four problems, the method of matched asymptotic expansions provides a considerably higher accuracy.

*The work was performed within activities of the project No. 2411/99 of FCT and of the project NumLiTe and action COST-529 of the EC

NWP 43 Planar and cylindrical solutions to the kinetic plasma-sheath problem with cold ions* ZOLTAN STERNOVSKY, *Department of Physics, University of Colorado, Boulder CO 80309-0390* SCOTT ROBERTSON, *Department of Physics, University of Colorado, Boulder CO 80309-0390* Self-consistent potential profiles for the collisionless plasma-sheath problem in the kinetic approach are presented. A distributed plasma source is assumed that creates ions at rest. The set-up of the problem is based on the work by Self [S. A. Self, *Phys. Fluids* 6, 1762 (1963)]. The equations are solved numerically in both planar and cylindrical geometry from the plasma midplane to the wall. The approach here is to use a power series approximation near the midplane where the potential is small compared to the electron temperature. The solution is then extended to the wall by integrating Poisson's equation. The planar results are nearly identical to those of Self. In the cylindrical case, the current to the wall is shown to be approximately $0.38 n_0 q cs$ which is significantly smaller than the Bohm current of $0.61 n_0 q cs$, where n_0 is the central plasma density, q is the elementary charge, and cs is the ion sound speed. Comparison is given with solutions in the fluid approach of the plasma-sheath problem.

*Research supported by the Office of Fusion Energy Science of the Department of Energy

NWP 44 The Measurement of Ion Drift Velocities in Presheaths in Ar and He-Ar Plasmas XU WANG, EUNSUK KO, NOAH HERSHKOWITZ, *University of Wisconsin - Madison* The presheath is a region of weak electric field that accelerates ions into the sheath at the plasma boundary. Presheath measurements were carried out near a plate 15cm in diameter mounted in a multi-dipole DC plasma with pure Ar and He-Ar gas mixtures ($P_{total} > = 1.0\text{mTorr}$, $n_e > = 1E9\text{cm}^{-3}$, $T_e < = 2\text{eV}$). By using the dispersion relation in the presheath for single and multi-ion species plasmas and phase velocity measurements that were performed by launching ion acoustic waves with both a continuous sinusoidal wave and a pulse, and detected by a cylindrical probe with a boxcar averager, ion drift velocity profiles were obtained in pure Ar plasma with different neutral pressures and the relationship between Ar and He ion drift velocities was determined in He-Ar plasma respectively. Using Ar ion drift velocities from LIF data [1], the He ion drift velocities were determined. Measurements by launching a continuous sinusoidal wave and a pulse are compared. *Work supported by US DOE grant DE-FG02-97ER54437 [1] G. D. Severn, Xu Wang, Eunsuk Ko and N. Hershkovitz, *Phys. Rev. Lett.* 90, 145001 (2003).

NWP 45 Effects of electron dynamics on rf sheaths NONG XIANG, *Institute for Fusion Studies, University of Texas at Austin* A common approach to study of rf sheaths is to separate the description of the sheaths from that of the bulk plasma. In order to solve the resulting set of equations, an appropriate boundary con-

dition for the sheath model has to be specified at the sheath-plasma boundary. We will show that in the high rf frequency regime where $\omega \gg \omega_{pi}$ (Here ω is the rf frequency and ω_{pi} is the ion plasma frequency), for a collisionless sheath, the entrance ion current into the sheath depends on the electron dynamics in the bulk plasma. If the driven current is high enough so that $J_{rf}/J_i \geq \sqrt{m_i/m_e}$ (Here J_{rf} is the rf driven current, J_i is the ion current, m_i and m_e are ion and electron mass respectively), the electron inertia will play an important role in determining the boundary conditions for the sheaths.

NWP 46 Electric Fields in Plasma Flows to Insulating Walls LAWSON HARRIS, 2796 Johnson Road, Scotia, NY 12302 In the analysis of plasma flows to insulating walls, it often is desired to represent the plasma flow as the sum of two regions, a broad flow of essentially neutral plasma extending from the center of the discharge to the vicinity of the wall, and a narrow space-charge sheath very near the wall. The need then arises to properly match the properties of the neutral region and the sheath at their common boundary. In the established analysis(1) for this problem, the electric field in the neutral-plasma region is calculated by differentiating the Boltzmann equilibrium distribution of electron density vs. electric potential. With the usual approximations made to permit analytic solutions, the result of that calculation is an infinite electric field when the ion flow velocity reaches the Bohm velocity, a condition of particular interest in the matching process. Proposals have been made to avoid the difficulty of a matching boundary at an infinite electric field by interposing an intermediate patch region(2) or by placing the boundary where the flow velocity does not equal the Bohm velocity(3), but none has yet been generally accepted. To overcome this problem, a different calculation of electric field is proposed here, one based on an approximate integration of the Poisson equation. The result is an electric field that remains finite at all flow conditions and permits a simple matching of a neutral-plasma region to a space-charge sheath. (1)R. N. Franklin, *Plasma Phenomena in Gas Discharges*, Clarendon Press, Oxford, 1976. (2)R. N. Franklin and J. R. Ockendon, *J. Plasma Phys.* 4, 371-385, 1970. (3)Valery Godyak and Natalia Sternberg, *IEEE Trans. Plasma Science* 31, 303, 2003.

NWP 47 Ar ions fall out faster than Bohm in a multiple ion plasma. Why?* GREG SEVERN, *Dept. of Physics, University of San Diego, San Diego, CA 92110* NOAH HERSHKOWITZ, *Dept. of Engineering Physics and Center for Plasma-Aided Manufacturing, University of Wisconsin-Madison, Madison, WI 53706* XU WANG, *Dept. of Engineering Physics and Center for Plasma-Aided Manufacturing, University of Wisconsin-Madison, Madison, WI 53706* EUNSUK KO, *Dept. of Engineering Physics and Center for Plasma-Aided Manufacturing, University of Wisconsin-Madison, Madison, WI 53706* SHEATH TEAM† Most plasmas of industrial importance comprise multiple ion species and electrons. Recent theoretical work has furnished both fluid and kinetic formulations of the generalized Bohm criterion (GBC) which permit a continuum of solutions, both faster and slower than an individual ion species Bohm speed, for the speed at which individual ion species reach the sheath edge. We have recently demonstrated that in a He-Ar plasma discharge, the Ar ions reach the sheath edge traveling nearly twice the Ar Bohm speed ($\approx 1.8\sqrt{kT_e/M_{Ar}}$), as determined by LIF and emissive probe diagnostics. What do the measured ion velocity distribution functions suggest concerning individual and inter-ion interactions? Where do our results lie

along the continua of solutions, and why, and what is gained by experimentally exploring the solution space set up by the GBC? These things are discussed as they bear on the answer to the question.

*Work supported by DOE grant no.DE-FG02-97ER54437 and NSF grant no. PHY9722658

†G.D. Severn, N.Hershkowitz, X. Wang, and E. Ko, Phys. Rev. Lett. **80** 145001 (2003)

NWP 48 Experimental Study of the Anode Sheath in Hall Thrusters LEONID DORF,* YEVGENY RAITSES, NATHANIEL FISCH, *Princeton Plasma Physics Laboratory* Near-anode processes in Hall Thrusters and crossed field devices in general have apparently eluded significant experimental scrutiny. Our recent measurements in the near-anode region of a Hall thruster have revealed interesting phenomena: the anode sheath changes from negative to positive at the same operating conditions of the thruster after thruster has been operating for a long time. The thruster operation becomes more stable when the anode sheath is positive. The change of the anode regime may be associated with a dielectric coating, which appears on the anode surface. The possibility of thruster operation with a positive sheath was also predicted theoretically. The effect of the anode surface area on the anode sheath and stability of thruster operation were studied experimentally using biased and emissive probes. The results of this study are presented. This work was partially supported by the US DOE under contract No. DE-AC02-76CH03073.

*Graduate Student

NWP 49 Ion Energy Distribution Functions in a Confined Capacitively Coupled Dual Frequency Discharge in Ar and H₂: Measurements and Simulations* D. M. O'CONNELL, *Dublin City University, Ireland* P. C. BOYLE, *Dublin City University, Ireland* M. M. TURNER, *Dublin City University, Ireland* A. R. ELLINGBOE, *Dublin City University, Ireland* Measurements and simulations of the ion energy distribution function (IEDF) at the grounded electrode of a confined, capacitively coupled, radio-frequency, plasma operated at two frequencies are presented. Experimentally, the discharge consists of two parallel plates of equal area. One electrode is driven simultaneously at two frequencies, 27.12 MHz and 1.94 MHz. The other electrode is grounded. A cylindrical quartz tube surrounding both electrodes confines the plasma, resulting in large sheath voltages (>100V) on both the powered and grounded electrodes. A differentially pumped hidden mass spectrometer, incorporating an energy analyzer, is installed at the grounded electrode. A 10 μm orifice at the center of the electrode allows mass resolved energy analysis of particles impinging on the electrode. In contrast to single frequency reactors, dual frequency reactors have the ability to independently control the ion flux and the ion impact energy onto the electrodes. The high frequency voltage can be used to control the plasma density, thus the ion flux onto the electrodes. The second lower frequency voltage allows the sheath voltage to be controlled, thus controlling the impact energy of the ions onto the electrode. The shape of the IEDF is predominantly influenced by the low frequency voltage. We present measurements and simulations for discharges in argon, where there is essentially only one positively charged ion species,

and for hydrogen, where there are three, H⁺, H₂⁺ and H₃⁺. The case of hydrogen is by far the most challenging, both experimentally and computationally. We will present and critically discuss experimental data and computational results obtained with a particle in cell simulation with Monte Carlo collisions.

*Research supported by European Union funding under EURATOM DCU Contract ERB 5004 CT960011

NWP 50 PLASMA PROPULSION

NWP 51 A New Type Microplasma Thruster Using Surface Wave Discharges Excited by Microwaves YOSHINORI TAKAO, KOUICHI ONO, KAZUO TAKAHASHI, YUICHI SETSUHARA, *Department of Aeronautics and Astronautics, Graduate School of Engineering, Kyoto University, Kyoto, Japan* Reducing the scale of propulsion systems is of critical importance on the development of very small and high performance spacecrafts, so-called "nanosatellites". This paper presents numerical and experimental investigations of an Ar microplasma excited by azimuthally symmetric surface waves and its application to ultra small thrusters on nanosatellites. The plasma/fluid numerical simulation have shown that in a dielectric tube 1mm in radius, the electron density is as high as $1.0 \times 10^{14} \text{ cm}^{-3}$ for a plasma absorbing power of 0.1 W at atmospheric pressures, assuming that the plasma is in thermal equilibrium. The thrust and specific impulse of microplasma thrusters with a micro nozzle have been estimated to be 3 mN and 400 sec, respectively, which are enough for nanospacecrafts less than 1kg. These numerical results are compared with microplasma discharges in Ar excited by 2.45-GHz microwaves in a quartz tube.

NWP 52 Experimental Study on Flow Characteristics of Stationary Arc Jet through a Magnetic Nozzle TOSHIKI KANUMA, MITSUO MATSUZAKI, HARUAKI MATSUURA, HIROSHI AKATSUKA, *Research Laboratory for Nuclear Reactors, Tokyo Institute of Technology* We measured basic plasma parameters of a supersonic helium arc jet accelerated through a magnetic nozzle. The arc jet was generated by a normal arc discharge under atmospheric pressure, and ejected into a rarefied gas wind tunnel (7.0×10^{-4} Torr) with a uniform longitudinal magnetic field (0.16 T). Then, it flowed through a uniform magnetic channel, and after that, expanded out of the end of the magnetic coils. The longitudinal velocity of the plasma jet was measured by Mach probes. At the point of maximum gradient of the magnetic field, the Mach number had its maximum value 4.8. The electron temperature T_e decreased to 0.1 eV as it flowed to the downstream region. After passing through the maximum point of the Mach number, the increase in the electron temperature was observed ($T_e = 0.5 \text{ eV}$), where the plasma became dark. The increase in the electron temperature results from the shockwave at the peak of the Mach number. Consequently, the increase in T_e results in the low-

ering of the intensity of the visible radiation from the plasma, since radiation from the plasma was mainly due to the excited states of atoms due to the recombination, and in addition, the rate of the recombination was enhanced as the electron temperature became lower.

NWP 53 Effects of channel wall material and geometry on plasma flow in Hall thrusters* YEVGENY RAITSES, *Princeton Plasma Physics Laboratory* MICHAEL KEIDAR, *University of Michigan, Ann Arbor* NATHANIEL FISCH, *Princeton Plasma Physics Laboratory* Plasma-wall interaction plays an important role in operation of Hall thrusters. Secondary electron emission from ceramic walls of the thruster channel can strongly affect the electron temperature, electron mobility and, as a result, the whole structure of the acceleration and ionization regions. In addition, a characteristic frequency of electron wall collisions depends on the channel width. In this work we study these effects by comparing integral discharge characteristics and plasma parameters for different thruster configurations

*This work was supported by grant from the US Department of Energy under Contract No. DE-AC02-76-CHO3073

NWP 54 NANOTECHNOLOGY

NWP 55 Ion and neutral fluxes in Ar+H₂+CH₄ RF plasmas for PECVD of self-assembled ordered carbon nanotip arrays I. B. DENYSENKO, J. D. LONG, P. RUTKEVYCH, Z. L. TSAKADZE, S. XU, K. OSTRIKOV, *Plasma Sources and Applications Center, NIE, Nanyang Technological University, 637616 Singapore* This work presents the results of the numerical modeling of the low-frequency (460 kHz) inductively coupled plasmas (ICPs) of an Ar+H₂+CH₄ gas mixture used in the PECVD of self-assembled ordered carbon nanotip (CNTP) arrays. A global model of the discharge has been developed and applied for the analysis of the effect of variation of the plasma parameters, such as the absorbed RF power, partial pressures of Ar, H₂, and CH₄ on the CNTP growth process. The electron energy, densities of the neutral and charged species and their fluxes on the catalyzed nanostructured surface are calculated. The computed neutral densities and the CH₄ conversion factor for different gas inlet flow rates and RF input powers have been compared with the quadrupole mass spectrometric measurements. The obtained results are in a remarkable agreement with the experimental data. The numerical data show that the main neutral species in the plasma under the favorable CNTP growth conditions are Ar, H, H₂, CH, CH₄, CH₃, CH₂, C₂H₂, C₂H₄ and C₂H₅ whereas the abundant ion species are Ar⁺, H⁺, H₂⁺, CH₄⁺, CH₃⁺, C₂H₂⁺, C₂H₄⁺, and C₂H₅⁺. The fluxes of the neutral particles on the growth surface have been compared with the fluxes of ions. It is found that, in the CNTP self-assembly process, the incoming fluxes of the carbon-bearing ions (CH₃⁺, CH₄⁺, CH₅⁺, C₂H₂⁺, C₂H₄⁺, and C₂H₅⁺) are comparable with or exceed the fluxes of the relevant neutral species. Thus, the positive ions are believed to play a major role in the nano-assembly process in question.

NWP 56 Investigation of Meltblown Microfiber and Electrospun Nanofiber Fabrics Treated with a One Atmosphere Uniform Glow Discharge Plasma (OAUGDP)* WEIWEI CHEN, *Department of Electrical and Computer Engineering, University of Tennessee* J. REECE ROTH, *Department of Electrical and Computer Engineering, University of Tennessee* PETER P.-Y. TSAI, *Textiles and Nonwovens Development Center (TANDEC), University of Tennessee* Nanofiber webs are made by the electrospinning (ES) process [1], which uses the repulsive electrostatic force to spin fibers from a polymer solution or melt at room temperature and low energy input. We have developed apparatus at the UT Textiles and Nonwovens Development Center (TANDEC) to produce fabrics with fiber diameters of tens of nanometers. This paper will report data on the distribution function of nanofiber diameters that were taken from digitized SEM images of the electrospun materials. It is also found in the tensile tests that the strength of the electrospun nanofiber fabrics is up to ten times that of the coarser meltblown material. The one atmosphere uniform glow discharge plasma (OAUGDP) developed at the UT Plasma Sciences Laboratory generates a normal glow electrical discharge at one atmosphere. This plasma has been used to treat meltblown and electrospun fabrics, with a resulting increase in surface energy [1]. We recently found that the surface energy of meltblown Nylon could be increased to 70 dynes/cm by five seconds of OAUGDP exposure, and was durable at this level for six months. Our results also show that Nylon and PU nanofiber fabrics can be exposed to the OAUGDP for treatment without significant damage for up to 10 seconds [1], a duration sufficient to produce important effects, including durable wettability. We will describe our progress in improving the properties of nanofiber fabrics using a variety of latest developments in OAUGDP reactor technology, including a new porous electrode that injects gases other than air to generate different active species for plasma treatment. [1] Tsai P. P.-Y., Chen W., Li X. and Roth J.R.: "Improving the Properties of Protective Clothing by Exposing Nanofiber Webs to a One Atmospheric Uniform Glow Discharge Plasma (OAUGDP)," National Science Foundation (NSF) Grantees Workshop and Conference, Birmingham, Alabama, Jan. 6-9, 2003.

*This research is supported by NSF grant DMI-0210554 of the Nanoscale Science and Engineering Initiative, NSF 01-157, Dr. Janet M. Twomey, program manager.

NWP 57 Intraction of ultra short pulse with methane in the production of hydrogen and carbon nanotube at atmospheric pressure KANETOSHI SHIBATA, *Kanto Polytechnic College, 632-1 Mitake Yokokura, Oyama, Tochigi 323-0813, Japan* LEKHA NATH MISHRA, *Energy and Environmental Science, Graduate School of Engineering, Utsunomiya University, 7-1-2 Yoto, Tochigi 321-8585, Japan* HIROAKI ITO, *Energy and Environmental Science, Graduate School of Engineering, Utsunomiya University, 7-1-2 Yoto, Tochigi 321-8585, Japan* NOBORU YUGAMI, *Energy and Environmental Science, Graduate School of Engineering, Utsunomiya University, 7-1-2 Yoto, Tochigi 321-8585, Japan* YASUSHI NISHIDA, *Energy and Environmental Science, Graduate School of Engineering, Utsunomiya University, 7-1-2 Yoto, Tochigi 321-8585, Japan* ENERGY AND ENVIRONMENTAL TEAM Experiments are performed to generate the hydrogen and carbon nanotubes from the decomposition of methane using ultra short pulses under the atmospheric pressure. The results of discharge of methane obtained by the Mass Spectrometer are presented. Specially, the spectrum of hydrogen is presented under the different conditions.

Carbon nanotube is observed by Scanning Electron Microscopy (SEM) and Transmission Electron Microscopy (TEM). The results of morphology of the carbon nanotubes are also presented. The results from this experiment could be useful for the industry in future.

NWP 58 Study of the anodic arc discharge for carbon nanotube production ERIK WALDORFF, MICHAEL KEIDAR, ANTHONY WASS, PERETZ FRIEDMANN, *University of Michigan*

Carbon nanotubes (CNTs) are unique nanostructures with remarkable electronic and mechanical properties. CNTs are currently considered to be a promising candidate as a next generation material having various applications. To-date, a variety of CNT fabrication methods have been developed, among them is an arc discharge method. Arc discharge is a relatively simple method having high rate of CNT production. In this method single-wall and multi-wall nanotubes are produced from an ionized carbon plasma with joule heating from the discharge used to generate the plasma. The University of Michigan carbon nanotube production facility in the Aerospace Engineering Department utilizes the anodic arc discharge. In this type of discharge, the Carbon plasma is supplied mainly by the anode ablation. In addition a buffer gas (Helium) with a pressure range of 100-1000 torr is introduced into the discharge chamber. The experimental anode ablation rate is about 2-4 m³/s and generally increases with the background gas pressure in the considered pressure range. A model of the anodic arc discharge is developed. The main component of this model is the anode ablation kinetics that takes into account the non-free nature of ablation due to the presence of a high-density discharge plasma. Different characteristic sub-regions near the surface, namely, space-charge sheath, Knudsen layer, presheath and a hydrodynamic layer are considered. The ablation rate is determined by the flow velocity at the edge of the Knudsen layer. Coupling solution of the non-equilibrium, Knudsen layer, with hydrodynamic layer and discharge column provides self-consistent solution for the ablation rate and plasma parameter distribution.

NWP 59 Production of Hydrogen and Carbon Nanotube by direct decomposition of methane using pulsed corona discharge under the atmospheric pressure LEKHA NATH MISHRA, *Energy and Environmental Science, Graduate School of Engineering, Utsunomiya University, 7-1-2 Yoto, Tochigi 321-8585, Japan* KANETOSHI SHIBATA, *Kanto Polytechnic College, 612-1 Mitake Yokokura, Oyama, Tochigi 323-0813, Japan* HIROAKI ITO, *Energy and Environmental Science, Graduate School of Engineering, Utsunomiya University, 7-1-2 Yoto, Tochigi 321-8585, Japan* NOBORU YUGAMI, *Energy and Environmental Science, Graduate School of Engineering, Utsunomiya University, 7-1-2 Yoto, Tochigi 321-8585, Japan* ENERGY AND ENVIRONMENTAL TEAM

In future, hydrogen is supposed to play an important role in the worldwide energy supply. It allows a more efficient utilization of fossil fuels and the reduction of noxious emissions, e.g. by fuel cells or the use of hydrogen enriched fuels in the combustion engines or gas turbines. Plasma methods are expected to allow low temperature and fuel flexible on-site hydrogen generation. Experiments are performed to develop a pulsed corona discharge system for the production of hydrogen and carbon nanotubes by direct methane decomposition under the atmospheric pressure. The corona discharge is energized by 10-20 μs wide voltage pulses

($\leq 7kV$) at a repetition rate of 0-5000 pulses per second. The spectrum of the gas is carried out by Mass Spectrometer. Experimentally, it is shown that the production of hydrogen gas depends on the pulsed width, input voltage, frequency, current and discharge time. The spectrum noted by the Mass Spectrometer is also presented. The structural geometry of the carbon nanotube is observed by Transmission Electron Microscope (TEM) and Scanning Electron Microscopy (SEM). The soot for this purpose is collected from the cathode. Different lengths noted for different soot collected from different parts with the help of TEM are also presented. The present experimental technique could be applicable for the future energy source using hydrogen and the nanoelectronics.

NWP 60 NEGATIVE ION PLASMAS

NWP 61 Production of the hydrogen negative ion by the magnetized sheet plasma KENTARO KUMITA, *Department of Physics, School of Science, Tokai University* HIRONORI OGAWA, *Department of Physics, School of Science, Tokai University* AKIRA TONEGAWA, *Department of Physics, School of Science, Tokai University* MASATAKA ONO, *Tokai University* KAZUTAKA KAWAMURA, *Tokai University* TOKAI UNIVERSITY PLASMA GROUP TEAM

In order to produce hydrogen negative ions H⁻, we have proposed a newly designed system of a magnetized sheet plasma crossed with a vertical gas-flow and an electron-emitter. When the secondary hydrogen gas is fed to the hydrogen sheet plasma through the gas injector, H⁻ rapidly increases on an upper side in the circumference of the plasma. Also, H⁻ is controlled by changing the applied voltage and the emission current of the electron-emitter made of tungsten filaments. The H⁻ production process is the dissociative electron attachment with cold electrons in the circumference of the plasma to the vibrationally excited hydrogen molecules, which results from the deexcitation of electronic excited hydrogen molecules with hot electrons in the mid-plane region. The characteristics of the H⁻ production depend on the cross section of the electron attachment to the vibrationally excited hydrogen molecules.

NWP 62 Generation of negative ions in a magnetic multipole plasma source with combined inductive and capacitive high frequency excitation TH. MOSBACH, H.-M. KATSCH, H.-F. DÖBELE, *Institut für Exp. Physik, Universität Essen*

Negative hydrogen and deuterium ions extracted from plasma sources have the potential for high-current charged and neutral particle beams for accelerator systems. Negative ions in the MeV energy range are of particular relevance for neutral beam plasma heating in fusion devices. Magnetic multipole plasma sources with filaments have been found to have a high content of negative ions. Plasma ion sources for long-term operation with fusion devices require, however, electrodeless excitation for various reasons. Inductively excited plasma sources generate ions but due to the absence of a high-energetic electronic component in the EEDF those sources do not operate at optimum. A combined inductive and capacitive high frequency excitation can be used to obtain both a high plasma density and high-energy electrons. Our aim is to control the electron energy distribution function of the plasma in such a way that

the rovibronic states of the hydrogen and deuterium molecules in the electronic ground state are over-thermally populated. Dissociative attachment of low-energy electrons to rovibronic highly excited molecules leads to the desired negative ions. We present first results on the detection of vibrationally excited electronic ground-state molecules by laser induced fluorescence with VUV radiation. This work is supported by the Deutsche Forschungsgemeinschaft DFG.

NWP 63 Negative Oxygen Ion Formation in a Pulsed Inductively RF Excited Argon-Oxygen Discharge and the Influence of Highly Excited Oxygen Molecules H.-M. KATSCH, C. MANTHEY, H.-F. DÖBELE, *Institut für Exp. Physik, Universität Essen*

The temporal behavior of negative oxygen ions oxygen / argon mixtures was investigated in the afterglow of a pulsed inductively excited modified GEC reactor. The objective of this investigation is an improved understanding of the production reactions of the negative ions and the loss processes of negative ions during the plasma decay phase. Collisions of O-minus ions with O atoms and metastable oxygen molecules lead to considerable electron production in the afterglow. This late supply of electrons entails a delayed formation of a so-called ion-ion plasma. Discharges with admixtures of argon (up to 8:2 argon : oxygen) are also strongly electronegative. An increase of the absolute O-minus density is observed with increasing argon fraction. At low pressures and high contents of argon it is necessary to consider an additional production reaction channel for the negative ions in order to explain the measured increase of the negative ion density. Appearance potential mass spectroscopy measurements show an increase of highly excited oxygen molecules with increasing argon fraction. It is, therefore, likely that additional negative ions are generated by dissociative attachment of highly excited metastable oxygen molecules [1]. [1] D. Hayashi and K. Kadota, *J. Appl. Phys.* 83 (1998) 697 This project is funded by the Bundesminister für Bildung und Forschung BMBF (FKZ 13N8052).

NWP 64 MAGNETICALLY-ENHANCED PLASMAS

NWP 65 Helium mixing effects on argon ion metastables in magnetically enhanced ICP* SANGHYUN JUN, *Department of Physics, Korea Advanced Institute of Science and Technology*

HONG YOUNG CHANG, *Department of Physics, Korea Advanced Institute of Science and Technology* The VDF (Velocity Distribution Function)s of argon ion metastables could be measured by diode LIF (Laser Induced Fluorescence) technique in magnetically enhanced ICP. We could take ion temperature, density and velocity from the VDFs. Total pressure remains in 10mTorr with varying the argon-helium mixing ratio. Power is 600W, and magnetic field 200Gauss. We investigate the argon ion characteristics theoretically as well as experimentally, comparing with plasma parameters by a electrical probe. Helium mixing have a little effect on the temperature and the velocity, but increases the density.

*sponsored by Korea Basic Science Institute (KBSI)

NWP 66 Measurement of plasma potential distribution in a pulsed bi-polar magnetron discharge A. VETUSHKA, S. KARKARI, J.W. BRADLEY, *Department of Physics, UMIST, Sackville Street, Manchester, M60 1QD, UK* Use of asymmetric bi-polar DC magnetron pulsing provides good process stability, arc free operation and leads to higher plasma densities, electron temperature in the vicinity of the substrate. A significant fraction of the high-energy ions can be created due to the substantial difference between the plasma potential and the floating substrate potential. Therefore, in order to control the properties of the growing film, it is necessary to know the plasma potential distribution throughout the plasma. The temporal evolution of the plasma potential in the magnetized discharge has been measured using an emissive probe. The potential of strongly emitting probe can respond to the fast changes in plasma potential, maintaining only a small sheath potential drop between the surface and plasma, allowing plasma potential to be readily determined directly at an oscilloscope. It has been shown that rapidly changing discharge voltage leads to the similar rapid changes in plasma potential. The results show large axial and radial variations in the plasma potential, and it has been observed that whole plasma is lifted to a potential above the most positive surface in the discharge. The spatial variations in plasma potential give rise to transient electric field in the discharge, which in combination with magnetic field lead to time-dependent EB drifts. 2D map of plasma potential distribution will be presented.

NWP 67 INFLUENCE OF THE EDF ANISOTROPY ON THE PROPERTIES OF CYLINDRICAL MAGNETRON DISCHARGE I.A. POROKHOVA, YU.B. GOLUBOVSKII, *St. Petersburg State University, Russia*

J. BEHNKE, J.F. BEHNKE, *University of Greifswald, Institute of Physics, Germany* An axially homogeneous weakly ionized plasma in cylindrical magnetron discharge is considered with the uniform magnetic field being applied axially and inhomogeneous electric field having only radial component. Representation of the phase-space distribution function in terms of spherical tensors has been successfully applied recently to describe swarm experiments in electric and magnetic fields. Further revision of the spherical tensor representation in the context of general non-hydrodynamic situation and special attention to an axisymmetric cylindrical plasma in electric fields is generalized in the present study on the axially homogeneous cylindrical magnetron discharge. An infinite hierarchy of the integro-differential equations for the expansion coefficients of the phase space distribution function is derived. The obtained hierarchy of equations is further simplified by transition into new variables of total energy and radius. The resulting system is solved numerically and the anisotropic functions and macroscopic properties are obtained.

NWP 68 Langmuir probe study of potential fluctuations in the dc cylindrical magnetron discharge P. KUDRNA, O. BILYK, A. MAREK, M. TICHY, *Department of Electronics and Vacuum Physics, Charles University Prague, Czech Republic*

E. MARTINES, *Consorzio RFX, Padova, Italy* M. HOLIK, J.F. BEHNKE, *University of Greifswald, Institute of Physics, Germany* The cylindrical magnetron in the post discharge configuration consists of cylindrical cathode mounted coaxially of the anode. The homogeneous magnetic field created by coils is applied parallel to the axis of the system. We present the measurements on two systems with

different length to radius ratio. The first system has the length of the discharge volume of 300 mm, the second 120 mm. The anode diameter is 60 mm for both systems. The potential fluctuations were measured by the floating Langmuir probe by means of the digital oscilloscope. The power density spectra were calculated in the range of magnetic fields 10 to 40 mT, pressures 1.5 to 7 Pa and discharge currents 100 and 200 mA. The wave number vs. frequency histogram derived from the fluctuations measured simultaneously from two Langmuir probes separated by 1.6 mm distance were evaluated and showed the negligible phase shift between the fluctuations at the positions of the probes.

NWP 69 Spatial changes of plasma parameters in the dc cylindrical magnetron discharge M. HOLIK, J.F. BEHNKE, *University of Greifswald, Institute of Physics, Germany* P. KUDRNA, O. BILYK, A. MAREK, M. TICHY, *Department of Electronics and Vacuum Physics, Charles University Prague, Czech Republic* In the cylindrical magnetron the symmetry and homogeneity of the magnetic field simplifies both the theoretical and experimental investigations. We present the measurements of spatial changes of electron density, plasma potential and mean electron energy on two systems with different length to radius ratio. The radial changes of plasma parameters have been measured by radially movable probes. The estimate of axial changes has been determined by measuring with three probes at three different axial positions. The magnetic field affect significantly radial as well as axial distribution of electron density within the discharge vessel. At low magnetic field of 10 mT the discharge is axially homogeneous, at higher magnetic field of 40 mT the two maxima positioned symmetrically with respect to the centre of magnetron appear. The measured profiles of the plasma potential and electron mean energy show the increase of the radial electric field with increase of the magnetic field strength.

NWP 70 Particle and energy balance in a Helicon plasma* AMNON FRUCHTMAN, *Holon Academic Institute of Technology, Holon 58102, Israel* GENNADY MAKRINICH, *Holon Academic Institute of Technology, Holon 58102, Israel* The dependencies of the plasma density on the magnetic field intensity and on the wave power in a helicon plasma source are studied. The ion saturation current into a flat Langmuir probe is measured for various magnetic field intensities and wave powers. A model for the plasma equilibrium, together with considerations of particle and energy balance, is used for calculating the electron temperature and the plasma density. The proposition that the measured increase in the plasma density with the increase of the magnetic field intensity is a result of an improving confinement, is examined. For the parameters of our experiment, this proposition implies that the electron collisionality is anomalously high. A different explanation is suggested; the density increase that follows an increase of

the magnetic field intensity results from an improved wave-plasma coupling via the helicon interaction, causing a larger fraction of the total wave power to be deposited inside the helicon source.

*Partially supported by the Israel Science Foundation

NWP 71 The influence of immersed RF antennas in high density, low pressure plasma sources ANE AANESLAND, (1) CHRISTINE CHARLES, (2) AASHILD FREDRIKSEN, (1) *Dep. Physics, University of Troms, Norway* ROD BOSWELL, (2) *PRL, Research School of Physical Sciences and Engineering, ANU, Canberra, Australia* In many plasma processing systems, the substrate is powered by an RF frequency, very often 13.56 MHz, and either grounded or dc isolated by a blocking capacitor. In the first case a dc current can flow from the plasma through the substrate to ground, while in the latter case a large self-bias can develop with current flowing only during the charge-up stage of the capacitor. To more fully investigate the interaction, we have used two different high density, low pressure plasma sources often used in plasma processing. i) a helicon source where a second antenna is inserted through the source end plate. The Helicon and immersed antenna have the same frequency of 13.56 MHz, so the RF generators are controlled by a phase shift. ii) a 2.45 GHz ECR source where a "one loop" antenna, with frequency 13.56 MHz, is inserted downstream from the source about 5 cm from the resonance zone. Both antennas are made of copper and in direct contact with the plasma, and are either grounded or dc isolated. Differences and similarities in results between the Helicon and ECR reactors, modified by the immersed antennas, will be outlined.

NWP 72 Cylindrical Hall current plasma thruster YEVGENY RAITSES, *Princeton Plasma Physics Laboratory* ARTEM SMIRNOV, *Princeton Plasma Physics Laboratory* NATHANIEL FISCH, *Princeton Plasma Physics Laboratory* The cylindrical Hall thruster is crossed field discharge device, which has a ceramic channel featuring both coaxial and cylindrical regions. The applied magnetic field is mainly radial in the coaxial region in order to sustain effective ionization of the working gas by magnetized electrons and to establish the axial electric field accelerating the ions. In the cylindrical region, the magnetic field can be changed from a solenoidal type to the cusp shape. By varying the magnetic field distribution, a significant voltage potential drop can be established in the cylindrical region with the larger volume to surface. Results of plasma measurements for two cylindrical laboratory thrusters with 2.6 cm and 9 cm diameter channels operated with xenon gas in the discharge voltage range of 50-300 V are presented. It was found that both these thrusters have unusually high ionization efficiency, which does not appear to be quantitatively explained by a reduction of plasma wall losses or by an enhanced electron temperature in the cylindrical region. Interestingly that the ion flux and stability of the thruster discharge are strongly altered by the magnetic field distribution in this region.

SESSION PR1: RYDBERG PLASMAS AND HIGHLY EXCITED ATOMS

Thursday morning, 23 October 2003; California Ballroom, Cathedral Hill Hotel at 8:00

Bill McConkey, University of Windsor, presiding

Invited Papers

8:00

PR1 1 Electron impact ionization of Rydberg atom.DANIEL VRINCEANU, *ITAMP, Harvard-Smithsonian Center for Astrophysics*

Collision between electron and Rydberg atom is important in ultracold plasmas, frozen Rydberg gases and formation of antihydrogen in a Penning trap. In superelastic scattering the electron gains the energy released by quenching the Rydberg atom. This is the most likely mechanism proposed to explain the heating of electrons observed in recent ultracold plasma experiments. Impact ionization and three-body capture are the two basic processes and the balance between the corresponding rates is essential in recombination in a cold plasma. Quantal calculations, initial angular momentum dependencies, scaling laws and correspondences to classical trajectory Monte Carlo simulations are presented and discussed.

8:30

PR1 2 Ultracold Rydberg Gases and Plasmas.*PHILLIP GOULD, *Department of Physics, University of Connecticut*

Ultracold Rb atoms, prepared by laser cooling techniques, are excited with pulsed UV light to near their ionization threshold. Depending on the photon energy, this results in either an ultracold gas of highly-excited Rydberg atoms or an ultracold plasma. We have observed these two phenomena together. Starting with a cold dense Rydberg gas, collisional ionization proceeds slowly until a threshold is reached, at which point superelastic electron collisions cause the ionization to "avalanche"[1], rapidly converting most of the atoms into a plasma. Surprisingly, if we wait long enough, the plasma partially reverts back to bound Rydberg atoms, presumably by the process of three-body recombination[2]. Measurements of the Rydberg state distribution at various times during this evolution should help us better understand this fascinating behavior. Due to their large polarizability, ultracold Rydberg atoms at high density can interact quite strongly. Besides possibly leading to ionization, these interactions cause line broadening and are responsible for molecular resonances which we have observed in the spectrum. These resonances result from avoided crossings of potential curves involving pairs of highly-excited atoms. These strong interactions can also cause conditional suppression of resonant Rydberg excitation, with potential applications in quantum computing. [1] M.P. Robinson, B. Laburthe Tolra, M.W. Noel, T.F. Gallagher, and P. Pillet, *Phys. Rev. Lett.* 85, 4466 (2000). [2] T.C. Killian, M.J. Lim, S. Kulin, R. Dumke, S.D. Bergeson, and S.L. Rolston, *Phys. Rev. Lett.* 86, 3579 (2001).

*Work done in collaboration with S. Farooqi, D. Tong, S. Krishnan, J. Stanojevic, Y.P. Zhang, A. Estrin, J. Ensher, C. Cheng, E. Eyster, and R. Ct, and supported by NSF.

Contributed Papers

9:00

PR1 3 Absolute Cross Sections for Electron Impact Ionization of Sodium Rydberg Atoms Below 2 eV* K. NAGESHA, K.B. MACADAM, *Dept. of Physics and Astronomy, University of Kentucky, Lexington KY 40506-0055*

We have measured absolute electron-impact ionization cross sections (EIICs) for highly excited sodium Rydberg atoms in *ns* and *nd* states, $n = 35$ to 51, below 2 eV electron energy. Experimental EIICs peak near 0 eV and lie in a range $7 \times 10^{-10} \text{ cm}^2$ for 35d to $4 \times 10^{-9} \text{ cm}^2$ for 50d. Energy dependence of EIICs is consistent with the binary encounter results of Vriens and Smeets [Ref: L. Vriens and A.H.M. Smeets, *Phys. Rev. A* 22, 940 (1980)]. The n dependence follows a power law with exponent 3.74 ± 0.28 at a fixed electron energy 0.2 eV and 5.46 ± 0.28 at a fixed electron-reduced-velocity 4.0. Measured cross sections are about 15 to 25 times larger than available theoretical values for $n = 35$ to 51. The discrepancy may indicate the role of large polarizabilities of high

Rydberg states hitherto disregarded in ionization formulations. Despite the lack of previous experimental verification, these formulations have been widely used for modelling of ionized media of laboratory, upper atmosphere, astrophysical and technological interest involving excited states.

*The authors thank M.J. Cavagnero and G.J. Ferland for helpful discussions. This work was supported in part by NSF Grant No. PHY-9987954

9:15

PR1 4 Long-range ultracold Rydberg molecules M. RAYMOND FLANNERY, *Georgia Institute of Technology* VALENTINE OSTROVSKY, *St. Petersburg State University* DANIEL VRINCEANU, *ITAMP-Harvard University* N. PRUDOV, *Russian Federal Nuclear Center*

The dipole-dipole interaction between two Rydberg atoms has a non-zero contribution in first-order perturbation theory, due to the large number of non-core-penetrating states which retain the angular-momentum degeneracy characteristic of atomic hydrogen. The combination of dipole-dipole attraction ($\sim R^{-3}$) and quadrupole-quadrupole repulsion ($\sim R^{-5}$) produces a set of electronic potential curves, which may support many vibrational states at large internuclear distances R

and which are relatively stable against predissociation, autoionization and radiative decay. The strongest binding in each Rydberg-Rydberg manifold corresponds to both electrons being in the most stretched Stark dipole states aligned in the same direction along the internuclear axis. Such diatoms possess significant net dipole moments and can therefore form larger clusters. *Directed-valence Rydberg orbitals* so introduced are basic to Rydberg-Rydberg interactions. Research supported by AFOSR, Grant 49620-02-1-0338 and NSF Grant 01-00890.

SESSION PR2: GLOWS

Thursday morning, 23 October 2003

International Ballroom, Cathedral Hill Hotel at 8:00

Mark Kiehlbauch, Lam Research Corporation, presiding

8:00

PR2 1 Study of pd and jp^2 scaling in abnormal glow discharges in argon DRAGANA MARIC, *Institute of Physics, University of Belgrade, Serbia and Montenegro* PETER HARTMANN, *Research Institute for Solid State Physics and Optics, Hungary* ZOLTAN DONKO, *Research Institute for Solid State Physics and Optics, Hungary* ZORAN PETROVIC, *Institute of Physics, University of Belgrade, Serbia and Montenegro* An abnormal glow discharge has been investigated experimentally and by one-dimensional heavy-particle hybrid model. Our measurements of Volt-Ampere characteristics and spatial profiles of emission covered a wide range of discharge conditions, at pressure \times electrode separation between 45 Pa cm and 150 Pa cm and at electrode gaps from 1.1 to 3.1 cm. We have found that both pd and jp^2 scaling are upheld above 75 Pa cm, while it breaks down at the lowest pressures covered here. The model was verified through the comparison of the measured and computed spatial profiles of light emission, which were in good agreement within investigated range of conditions.

8:15

PR2 2 Simulating Neutral Flow Effects in Pulsed Plasmas DAVID GRAVES, *University of California at Berkeley* MARK NIERODE, *University of California at Berkeley* Periodically pulsed plasmas offer several potential advantages in surface processing applications, and have been utilized for both thin film etching and deposition. In addition, similar effects occur during plasma ignition and extinction from a nominal steady state operation. One effect that has received relatively little attention is neutral flow induced by changes in gas temperature and molecular weight during plasma ignition or extinction. Gas mass density is proportional to mean molecular weight and inversely proportional to neutral temperature. Under some conditions, neutral gas mass density can change by factors of order 10 with plasma on/off transitions. Mass density changes on this order over several milliseconds can drive significant gas flows within chambers, and this can have important processing implications. In this talk, results from a simulation based on the FEMLAB code are described for non-isothermal, compressible neutral gas flows induced in plasma chambers due to this effect. Applications to pulsed plasmas for kinetic studies and for processing are highlighted.

8:30

PR2 3 Landau damping and anomalous skin effect in low-pressure gas discharges: self-consistent treatment of collisionless heating IGOR D. KAGANOVICH, *Plasma Physics Laboratory, Princeton University, Princeton, NJ 08543* OLEG POLOMAROV, *Department of Physics and Astronomy, University of Toledo, Toledo, Ohio 43606-3390* In low-pressure discharges, where the electron mean free path is larger or comparable with the discharge length, the electron dynamics is essentially nonlocal. Moreover, the electron energy distribution function (EEDF) deviates considerably from a Maxwellian. Therefore, an accurate kinetic description of the low-pressure discharges requires knowledge of the nonlocal conductivity operator and calculation of the nonMaxwellian EEDF. A self-consistent system of equations for the kinetic description of nonlocal, nonuniform, nearly collisionless plasmas of low-pressure discharges is derived. The importance of accounting for the nonuniform plasma density profile for computing the current density profile and the EEDF is demonstrated. It was shown that the bounce resonance between the electron motion in the potential well and the external rf electric field is greatly enhanced in inhomogeneous plasma.

8:45

PR2 4 On electron heating and thermalisation processes in surface wave plasma* E. STAMATE, S. NAKAO, M. ARAMAKI, A. KONO, H. SUGAI, *Nagoya University, Department of Electrical Engineering* The recent aim in ULSI technology of achieving low-damage processing and scaling down below 100 nm by reducing the operation pressure and electron temperature while keeping the plasma density larger than 10^{17} m^{-3} , requires further investigation of surface wave plasma (SWP), that should clarify the production and heating mechanisms, power dissipation, the role and origin of energetic electrons. So far, several theoretic mechanisms were proposed to explain the energy transfer at collision frequency less than the electromagnetic wave frequency, including resonant absorption at cutoff layer, Landau damping and transit-time heating. However, the experimental coverage is insufficient to draw any conclusion. In the present report we are investigating the heating mechanism by comparatively measuring the plasma parameters and the electric field distribution in the vicinity of the dielectric plate of two SWP discharges operating at 2.45 GHz and 915 MHz, respectively. Langmuir probes, metallic and dielectric thermal probes and Thomson scattering are used as diagnostics techniques. For instance, the electron energy probability function (EEDF) measured at $d=7$ mm with respect to the dielectric plate (10 mTorr, Ar, 250 W and 2.45 GHz) shows a very energetic tail with a beam like group of energetic electrons, while, only 10 mm away, the EEDF approaches a Maxwellian distribution. This behavior can only be explained by a collisionless mechanism.

*This work has been performed under the 21st Century COE Program by the Ministry of Education, Culture, Sports, Science and Technology in Japan.

9:00

PR2 5 Time Resolved Measurements of a Pulsed DC Hollow Cathode Discharge CRISTIAN PADURARU, *Stevens Institute of Technology* KURT H. BECKER, *Stevens Institute of Technology* ABE BELKIND, *Stevens Institute of Technology* JOSE LOPEZ, *Stevens Institute of Technology* YOLANDA A. GONZALEVO, *Hidden Analytical, UK* Plasma in a pulsed DC powered hollow cathode glow discharge was studied by time-resolved Langmuir probe and optical emission measurements. A rectangu-

lar hollow cathode was made from Al. Measurements were done using 100 kHz pulsing frequency and 80% duty cycle. The cathode was run in the regime of gas flow sputtering at about 6.5 Pa pressure in the chamber. Langmuir probe measurements were carried out in the remote plasma at 7 cm above the center of the hollow cathode opening. Optical emission from the Al and Ar ions was measured using photomultipliers and narrow band optical filters. Temporal evolution of electron temperature, plasma density, and density of sputtered material were analyzed in the remote plasma. The data are compared with time resolved measurements of a pulsed DC magnetron. This work is supported by the ATP award from NIST 70 NANBOH3031 by 10/01/00.

9:15

PR2 6 Investigation of the disturbing impact of a floating probe on a neon discharge plasma S. ARNDT, F. SIGENEGGER, *Institut für Niedertemperatur-Plasmaphysik, Greifswald* R. KOZAKOV, H. TESTRICH, C. WILKE, *Institut für Physik, University of Greifswald, Germany* The response of a neon column

plasma at 90 Pa on a disturbance caused by a floating Langmuir probe has been investigated experimentally and theoretically. A Langmuir probe was inserted in radial direction into the discharge several cm before the anode. The spatial evolution of the densities of the excited atoms in the $1s_3$ and $1p_8$ states was determined by optical methods. Depending on the insertion depth of the probe variations of up to 50% with respect to the undisturbed densities of the excited atoms in the positive column have been observed. The response of the plasma is theoretically described by a self-consistent model of the column and anode region. It includes the coupled solution of the Poisson's equation for the electric field and the hydrodynamic equations for electrons, ions and excited atoms. The spatial evolution of the transport and rate coefficients of the electrons and their collisions with the atoms are determined by the space-dependent electron Boltzmann equation. The glass carrier of the probe represents an additional surface for the recombination of electrons and ions. Its impact is modelled by a narrow enlargement of the ambipolar loss frequency which compensates for the ionization in the undisturbed column.

SESSION QR1: ELECTRON SCATTERING

Thursday morning, 23 October 2003; California Ballroom, Cathedral Hill Hotel at 10:00
Don Madison, University of Missouri-Rolla, presiding

Invited Papers

10:00

QR1 1 Collisions with Laser-Cooled, Metastable Helium Atoms.

STEPHEN J. BUCKMAN,* *RSPHysSE, Australian National University, Canberra, Australia*

Laser manipulation techniques have been used to create a bright beam of metastable He(2^3S) atoms which is used, amongst other things, as a source of cold atoms for loading a 3-D magneto-optical trap of He(2^3S). The trapped atoms provide an ideal vehicle for collision studies including atom-atom and electron-atom collisions, both with and without resonant, or near-resonant laser fields present. This talk will review the motivation for such studies and discuss the techniques which we use to create a cold (300 mK), dense (10^8 atoms/cc) cloud of trapped, excited He atoms. Experimental results for total electron scattering cross sections from He(2^3S) at energies between 5 and 100 eV will be presented, as will results of scattering from He(2^3P) atoms, formed in the trap by optical pumping of the 2^3S atoms at 1083 nm.

*This work was carried out by Linda Uhlmann, Robert Dall, Andrew Truscott and Ken Baldwin they kindly allow me to talk about it.

Contributed Papers

10:30

QR1 2 Electron-Impact excitation into the $4p^55p$ levels of Kr out of the metastable levels*

R. O. JUNG, TOM STONE, JOHN B. BOFFARD, L. W. ANDERSON, CHUN C. LIN, *University of Wisconsin-Madison* Cross sections for electron-impact excitation into the $4p^55p$ levels of Kr out of the two metastable levels, $1s_3$ ($4p^55s$, $J=0$) and $1s_5$ ($4p^55s$, $J=2$), have been measured by detecting the emission from the $4p^55p$ levels. We used two different kinds of metastable atom targets, one produced by a hollow cathode discharge and one by resonant charge-exchange collisions of Kr^+ ions with Cs atoms. Although the targets contain both kinds of metastable atoms, we are able to eliminate either the $1s_3$ or $1s_5$ metastables by laser quenching using absorption at 810.4 nm ($1s_5 \rightarrow 2p_8$) or 805.9 nm ($1s_3 \rightarrow 2p_4$) respectively. The variations of cross sections over the different levels of the $4p^55p$

configuration differ even qualitatively from the corresponding situation for excitation of metastable Ar. Explanations are given based on the difference in the coupling among the orbital and spin angular momenta of the $4p^5$ core and of the $5p$ excited electron.

*Supported by the National Science Foundation.

10:45

QR1 3 Electron-Cesium collisions using a Magneto-Optical Trap

JOHN MACASKILL, *University of Windsor, Canada* COR-MAC McGRATH, *University of Windsor, Canada* WLADYS-LAW KEDZIERSKI, *University of Windsor, Canada* JUSTIN TEEUWEN, *University of Windsor, Canada* WILLIAM MCCONKEY, *University of Windsor, Canada* IGOR BRAY, *Murdoch University, Australia* Cross sections for electron impact on Cesium have been measured using an entirely new experimental arrangement from that used in our previous studies^[1]. These cross sections are measured using the trap-loss technique of Schappe et al.^[2]. To summarize, a broad and intense electron beam of

constant current density is arranged to completely envelop a target of cold Cesium atoms formed using a Magneto-Optical Trap. The fluorescence decays of the MOT, in the presence and absence of the electron beam give a loss rate of atoms from the trap, that is in turn, related to a cross section. Experimental data, covering an extended energy range from our previous studies, are presented for the total and ionization cross sections for the Cesium $6^2S_{1/2}$ ground state and the $6^2P_{3/2}$ excited state. The data for the total cross sections are compared with CCC calculations of Bray, while data for the ionization cross sections are compared with a set of modified Born approximation calculations provided by Bartlett and Stelbovics^[3]. [1] *J. Elect. Spect. And Rel. Phen.*, 123, 173 (2002). [2] *Europhys. Lett.*, 29, 439 (1995). [3] Private Communication (2002). We are pleased to acknowledge the financial support of CIPI, CFI, and NSERC (CAN), and ARC (AUS).

11:00

QR1 4 Selective Production of Nitrogen Metastable Excited Molecules by Impulse-Field Electron Acceleration Method HIROTAKA SUGAWARA, YOSUKE SAKAI, *Hokkaido University, Japan* By applying a short intense impulse electric field to low-temperature electrons, they are accelerated in a practically collisionless condition when the impulse duration is shorter than the electron mean free time. The energy obtained by the electrons is controllable by the impulse intensity and duration, thus we can feed the electrons into a specific energy range in which the collisions of interest occur efficiently. In this talk, we will present a theoretical basis of the impulse-field electron acceleration (IFEA), and will discuss its application to selective production of $N_2(A^3\Sigma_u^+)$ metastable excited molecules. The selectivity was quantified as the efficiency η_i of the electron energy utilized for excitation of $N_2(A^3\Sigma_u^+)$, and the efficiency was compared with

those of electrons in other modes: η_e defined for electron swarms in DC equilibrium, and η_b for monoenergetic electron beams. η_b is regarded as the upper limit of η_i , and the maximum value of η_b estimated is about 80%. η_i values up to 20–30% have been achieved by IFEA simulations, and these values are higher than η_e which is at most 10%. The calculation results show that η_i is high at low electron temperatures and short impulse durations at which the electron energy distribution is concentrated.

11:15

QR1 5 Low-energy electron collisions with quasi-two electron atoms* KLAUS BARTSCHAT, *Drake University* IGOR BRAY, *Murdoch University* DMITRY FURSA, *Flinders University* We have recently investigated elastic electron scattering from quasi-two electron targets such as Mg, Zn, and Hg. Accurate total and momentum-transfer cross sections for these processes are of interest both for modelling transport processes in various lighting applications [1] and for the fundamental understanding of collision processes in magneto-optical traps and Bose-Einstein condensates [2]. To our big surprise, we found that a convergent description of these collisions within the close-coupling formalism is by no means trivial, since the theoretical results for the scattering lengths and the low-energy p-wave shape resonances, studied experimentally a long time ago [3], depend in a very sensitive way on the details of the numerical model. [1] G.G. Lister, in *Low Temperature Plasma Physics* (eds. R. Hippler, S. Pfau, M. Schmidt and K.H. Schoenbach), Wiley (New York, 2002) [2] K. Bartschat and H.R. Sadeghpour, *J. Phys. B.* **36** (2003) L9 [3] P.D. Burrow, J.A. Michejda and J. Comer, *J. Phys. B.* **9** (1976) 3225

*Work supported by the United States National Science Foundation and the Australian Research Council.

SESSION QR2: ENVIRONMENTAL APPLICATIONS

Thursday morning, 23 October 2003; International Ballroom, Cathedral Hill Hotel at 10:00
Sebastien Raoux, Applied Materials, presiding

Invited Papers

10:00

QR2 1 Abatement of atmospheric pollutants by plasma-catalysis association.

ANTOINE ROUSSEAU,* *GdR CATAPLASME, LPGP, bat 210 Univ. Paris-Sud / CNRS, 91405 Orsay, France*

Due to environmental regulations regarding air quality, including the indoor environment, extensive research is carried out in order to reduce emission of atmospheric pollutants such as Volatile Organic Compounds (VOC). Some conventional techniques exist for gas treatment. However, for many applications, particularly in the removal of very dilute concentrations of air pollutants, the non thermal plasma approach is likely to be the more appropriate because of its energy selectivity and its capability for the simultaneous removal of various pollutants. Recently, it has been shown that a combination of a non thermal plasma with catalysis leads to very promising results for the destruction of VOC at a very low energy cost. In order to understand the mechanisms of the plasma-catalysis synergy it is necessary to clarify the specific role of the flux on the catalytic surface of the UV photons, of the charged particle and of the radicals respectively. Unfortunately, most of the atmospheric plasmas used in the depollution field are unstationnary and strongly non homogeneous, which makes the plasma-catalysis interaction difficult to analyse, both experimentally and theoretically. Thus, our approach is to compare the plasma chemistry in an low pressure glow discharge and in a typical atmospheric non thermal plasma, both in contact with a catalytic surface. VOC oxydation products (CO + CO₂), as well as undesirable NO_x produced by the plasma itself (NO + NO₂), are measured by laser infrared absorption spectroscopy. It is shown that a catalysis may be activated by non equilibrium plasma near room temperature. These particular type of plasma-surface interaction is a stimulating new research field for plasma physicists.

*Gatiliva L., Ionikh Y., Mechtchanov A., Pasquiers S., Roepcke J.

Contributed Papers

10:30

QR2 2 In-situ observation of NO and NO₂ in streamer corona discharge by two-dimensional laser-induced fluorescence spectroscopy M. ARAMAKI, H. KURAKANE, K. SASAKI, *Department of Electronics, Nagoya University, Nagoya 464-8603 Japan* It is known that most of nitrogenous oxides which are released from factories, cars, and so on are mainly composed NO and NO₂. Hence, it is especially important to examine dissociation processes of NO and NO₂ in the research of the NO_x removal using high-pressure non-equilibrium plasmas. In-situ observations of NO and NO₂ in the plasma reactor are effective to investigate the reaction kinetics of NO_x. In the present work, we measured temporal variations of the density distributions of NO and NO₂ in streamer corona discharges between needle and planar electrodes by two-dimensional laser induced fluorescence spectroscopy. The two-dimensional images of the density distributions of NO and NO₂ were taken using an ICCD camera. The discharge atmosphere was air including NO₂ (1500~ 2000 ppm) at a pressure of 200 Torr. The NO₂ density decreased locally in the region below the needle electrode at 10 ms after the discharge. At the same time, we observed the appearance of NO in the region corresponding to the decay of NO₂. The significant production of NO was not observed when the discharge atmosphere was composed of N₂ and NO₂. Therefore, from these experimental results, it is suggested that NO is produced by a reaction $\text{NO}_2 + \text{O} \rightarrow \text{NO} + \text{O}_2$.

10:45

QR2 3 Aftertreatments of environmentally hazardous materials by combinations of barrier discharges with densification by adsorption/trapping YUKIHIKO YAMAGATA, *Interdisciplinary Graduate School of Engineering Sciences, Kyushu Univ., Japan* TAKASHI EBIHARA, *Interdisciplinary Graduate School of Engineering Sciences, Kyushu Univ., Japan* SHIRO KUBA, *Interdisciplinary Graduate School of Engineering Sciences, Kyushu Univ., Japan* KATSUNORI MURAOKA, *Interdisciplinary Graduate School of Engineering Sciences, Kyushu Univ., Japan* Emission of environmentally hazardous materials, such as volatile organic compounds (VOC), diesel particulate matters (DPM) and nitric oxides (NO_x), has been becoming more and more strictly regulated from health concern. Although thermodynamically non-equilibrium gas discharges have attracted much attention for the aftertreatment of these materials, the electrical efficiency is expected to be low because these materials are exhausted in very small concentrations. In this situation, we proposed a new scheme of removing these materials using a thermodynamically non-equilibrium gas discharge. The most salient feature of the aftertreatment is the combination of barrier discharges with densification by adsorption/desorption using honeycomb-structured adsorbents, such as zeolites. The latter structure ensures high gas flow rate, while the former is most appropriate for generating non-equilibrium plasmas on large-area surfaces. This feature has been fully exploited in the VOC, DPM and NO_x aftertreatments. The VOC was efficiently decomposed using a developed reactor, and a research towards commercialization is under way. The DPM and NO_x exhausted from a diesel engine were decomposed simultaneously by the barrier discharge. The experimental results of the treatments of VOC, DPM and NO_x based on this concept are described.

11:00

QR2 4 Use of an Atmospheric-Pressure Plasma to Treat the Exhaust of a 160 Hp Diesel Engine D. DIETZ, S. WIEMAN, T. CHOU, T.L. SU, O. MOGZINA, D. VACCARI, C. CHRISTODOULATOS, G. KORFIATIS, K. BECKER, *Stevens Institute of Technology* E. HOUSTON, P.J. RICATTO, R. CROWE, *PlasmaSol Corp.* We used a patented capillary plasma electrode (CPE) discharge in the exhaust of a 160 Hp Diesel engine to remove the gaseous contaminants in the hot exhaust gas (mainly unburned hydrocarbons, HCs). We found reductions in the total HCs of up to 70% and compound-specific reductions of more than 90% for complex aromatics. We also investigated the effect of the HC reduction in the gas phase on the condensed water and observed reductions of more than 50% of the total HC concentrations in the liquid phase. The possible impact of these findings for water harvesting applications will be discussed. Work supported by DARPA/DSO.

11:15

QR2 5 On synergetic effects at destroying of toluene and TCE by DC glow discharge and streamer corona at atmospheric pressure YURI AKISHEV, VLADIMIR KARALNIK, IGOR KOCHETOV, ANTON MONICH, ANATOLY NAPARTOVICH, NIKOLAY TRUSHKIN, * *State Research Center of Russian Federation Troitsk Institute for Innovation and Fusion Research (SRC RF TRINITI)* Results on toluene decomposition obtained from both experiments with DC glow discharge in gas flow and numerical calculations are compared in this report. In the case of a binary mixture of toluene and TCE (trichloroethylene), experiment shows synergetic effect, i.e. an addition of TCE in mixture increases the decomposition of toluene. Our numerical modeling showed this effect can be attributed to influence of ion-molecule reactions involving toluene and TCE molecules, which result in formation of heavy ions with better stability and lower mobility. The comparison of decomposition efficiencies between DC glow discharge and DC positive streamer corona is presented as well. In last case, the tested admixtures were toluene and TCE as well. Non-thermal plasma in humid airflow with dosed pollutants was created in a rectangular channel of 15 cm in width and 30 cm in length. The height of channel was 1.35 and 3.5 cm in the case of glow discharge and positive corona respectively. Gas flow velocity was 15-20 and 2.5 m/s in glow discharge and positive corona respectively. Humidity of airflow was varied up to 18% (volume concentration of water vapor). The electrode system consisted of 28 the paired elements (pin-to-crater) [1, 2] disposed evenly from each other. The pins served either as cathodes in the case of DC glow discharge or as anodes in the case of DC positive corona. Each pin had several emitting points. High-voltage power supply up to 30 kV was used to sustain both of the discharges mentioned above. Concentrations of toluene and TCE were varied from 15 to 500 ppm and measured with a gas chromatograph. 1. Yu. S. Akishev, M. E. Grushin, I. V. Kochetov, A. P. Napartovich, M. V. Pankin, and N. I. Trushkin, *Plasma Physics Reports*, 26, No. 2, 2000, pp. 157-163. 2. Yu. S. Akishev, A. A. Deryugin, V. B. Karalnik, I. V. Kochetov, A. P. Napartovich, and N. I. Trushkin, *Fiz. Plazmy* 20, 571 (1994) [*Plasma Physics Reports*, 20, 511 (1994)].

*TRINITI, Troitsk, Moscow region, 142190, Russian Federation

SESSION SRP: POSTER SESSION III
 Thursday afternoon, 23 October 2003
 El Dorado, Cathedral Hill Hotel at 13:30
 I. Langmuir, GE Research Laboratory, presiding

SRP 1 MODELING OF GLOWS

SRP 2 Parametric studies of argon glow discharges BELASRI AHMED, *Laboratoire de Physique des Plasmas, Matériaux conducteurs et leurs Applications* YANALLAH KHELIFA, *Laboratoire de Physique des Plasmas, Matériaux conducteurs et leurs Applications* The basis of this work is one-dimensional fluid model of electrical properties of a argon glow discharge with planar electrodes. The results from this model are the spatial profiles of electric field, the charged particle densities, and ionization source term. The range of current densities considered is between 0.1 and 0.6 mA/cm². To calculate the gas temperature, we solve the one dimensional heat transport equation. The gas temperature profile is reintroduced into the electrical model. In the fluid model, the electrons and ions are described by their continuity and momentum transfer equations in the drift diffusion approximation, and these equations are solved together with Poissons equation for the electric field.

SRP 3 Two-dimensional simulations of the transition from Townsend to glow discharge and subnormal oscillations ROBERT ARSLANBEKOV, VLADIMIR KOLOBOV, *CFD Research Corp.* The transition from Townsend to glow discharge is studied via two-dimensional simulations of discharges with moderate pd values corresponding to the right branch of the Paschen curve (p is the gas pressure and d the electrode spacing). The discharge model is coupled to the external circuit simulator SPICE enabling simulations of subnormal oscillations during the discharge transition from the Townsend to normal mode. This transition is accompanied by the radial constriction of the discharge and formation of a normal cathode spot. The electron thermal flux backscattered to the cathode is observed to be important in the Townsend regime, which contributes significantly to discharge instability by virtue of the secondary emission coefficient γ becoming an increasing function of E/N . The simulations are carried out for different gas pressures and different parameters of the external circuit. It is shown that the capacitance of the external circuit plays a crucial role in establishing subnormal oscillations. The predicted results are in agreement with experimental observations and previously published semi-analytical models.

SRP 4 Influence of Hypersonic Flow on RF Discharge Characteristics* NATHANIEL LOCKWOOD, *Air Force Institute of Technology* WILLIAM BAILEY, *Air Force Institute of Technology* The pioneering approach of Boeuf and Pitchford¹ is adopted and extended in a two dimensional numerical fluid model of an rf discharge in a hypersonic neutral gas flow. The electron transport is treated using the continuity, momentum and energy equations. The negative and positive ion densities are described by

continuity and momentum equations. The neutral gas flow field, including the velocity, density and temperature distributions, is independently specified. A self-consistent solution of these moment equations, coupled with Poissons equation, is achieved using a Newton-Raphson technique and successive line over relaxation. The effects of flow velocity, rf voltage and gas density on plasma properties and discharge characteristic are examined and discussed for a frequency of 13.56 MHz. Transverse and longitudinal discharge geometries are considered and the plasma conductivity, kinetic rates, electric field and current density are mapped. Electropositive and electronegative features of the discharge are explored by contrasting the behavior in Argon and Oxygen.

*Sponsored by Air Force Research Laboratory, Air Vehicles Directorate

¹A. Fiala, L. C. Pitchford, J. Boeuf., *Phys. Rev. E* 49, 5607 (1994)

SRP 5 Extension of the linear-field, source-function model of the abnormal cathode fall to obstructed discharges A. V. PHELPS, *JILA, U. of Colorado and NIST* L.C. PITCHFORD, *CPAT, U. Paul Sabatier, Toulouse* We extend a simplified model¹ of the abnormal cathode fall to parallel-plane, obstructed discharges in argon. An assumed linear variation of the electric field near the cathode relates the space-charge limited current density to the cathode fall voltage V_c and pressure times cathode fall thickness pd_c . The reciprocal electron yield per ion at the cathode equals the ions produced per electron emitted, i.e., the integrated "source function." At intermediate pd_c the source function and electron attenuation distance λ are scaled from Monte Carlo results. We use the local-field source function at large pd_c and a free-fall model at small pd_c . We include electron reflection and ion loss at the anode and the reduction of ion production for electrode separations d for which $d_c < d < 3\lambda$. The predictions agree well with experiment² for a very wide range of parameters, i.e., $0.001 < pd < 0.08$ Torr cm, $0.2 < j/p^2d^2 < 7000$ mA/cm² Torr², and $0.3 < V_c < 14$ kV, using electron yields expected for their sputtered and annealed Cu cathode and using an anode electron reflection probability of 0.45.

¹A. V. Phelps and L. C. Pitchford, *Bull. Am. Phys. Soc.* 47, 43 (2002).

²B. N. Klyarfel'd, L. G. Guseva, and A. S. Pokrovskaya-Soboleva, *Sov. Phys.-Tech. Phys.* 11, 520 (1966)

SRP 6 Model of a low pressure nitrogen glow discharge with graphite electrodes* CARLOS M. FERREIRA, *Department of Physics and Centro de Física de Plasmas, Instituto Superior Técnico, Lisboa, Portugal* BORIS F. GORDIETS, *Lebedev Physical Institute of the Russian Academy of Sciences, Moscow, Russia* MARIO J. PINHEIRO, *Department of Physics and Centro de Física de Plasmas, Instituto Superior Técnico, Lisboa, Portugal* We present a model describing the main trends of the principal processes occurring in nitrogen DC glow discharge plasma with two parallel graphite electrodes. At the cathode, it occurs the process of sputtering of C atom due to bombardment by energetic positive ions accelerated in the cathode fall region. However, experiments show that the source of C and CN can be also at anode. That is why we have assumed that the surface process for produc-

tion of C atoms is the process of collision with graphite surface by $N_2(a')$ molecules. CN molecules can be produced on graphite electrodes due to chemical adsorption of gas phase N atoms. These particles together with N atoms are deposited on discharge tube surface. Using experimental data, the best agreement with experiment is obtained.

*Acknowledgments: We thank Zoltán Donkó and Kinga Kutasi for providing us with experimental data

SRP 7 DC Discharge Studies Using PIC-MCC JEFF HAMMEL, *Electrical Engineering department, UC Berkeley* JOHN VERBONCOEUR, *Nuclear Engineering department, UC Berkeley* DC discharges are used in plasma materials processing for sputtering deposition, ion implantation, and other processes. The objective of this study is to model an unmagnetized DC discharge using the particle in cell with Monte Carlo collisions (PIC-MCC) method and compare the steady-state results with analytic models. Specifically, this model includes kinetic and nonequilibrium effects in 1D and 2D azimuthally discharges dominated by cathode fall, Faraday dark space, and negative glow regions, using He and Ar feed gases in parameter regimes relevant to materials processing. Simulation results include density striations propagating in the positive column, as well as a hot and cold electron populations in the negative glow. Cross-validation of PIC-MCC simulation and analytic models illustrates the shortcoming of the of the theoretical results and leads to the development of better analytic models with improved physics and more efficient computational models. Possible reasons for differences between the PIC and theoretical models are discussed.

SRP 8 Large-amplitude oscillations in a Townsend discharge in low-current limit VLADIMIR KHUDIK, ALEX SHVYDKY, *Plasma Dynamics Corp., MI* We have developed a regular analytical approach to study oscillations in a Townsend discharge when the distortion of the electric field in the discharge gap due to the spatial charge is small. In presented theory the secondary electron emission coefficient can take any value between zero and one. We have found that the large-amplitude oscillations of the particle current in the discharge gap are accompanied by small-amplitude oscillations of the gap voltage. Surprisingly, for certain impedances of the external electrical circuit, this highly dissipative system is governed by the Hamiltonian equations (so that the amplitude of the oscillations slowly changes in time). Direct Monte Carlo/particle-in-cell simulations confirm the theoretical results.

SRP 9 Ionizing potential wave in the discharge between two charged planes controlled by the secondary electron emission ALEX SHVYDKY, VLADIMIR KHUDIK, *Plasma Dynamics Corp., MI* We study analytically the discharge between two charged planes when the initial voltage between them is much higher than the breakdown voltage. We show that the discharge has a form of the ionizing potential wave that originates at the anode and propagates toward the cathode with a constant velocity proportional to the ion velocity, and the voltage across the discharge gap decreases linearly with time. The results of the theory are compared with those obtained from a 1D Monte Carlo/particle-in-cell simulation for different parameters of the discharge (such as the secondary electron emission coefficient, the initial voltage between the planes, and the length of the discharge gap). Also discussed are effects due to the photoemission from the cathode.

SRP 10 DIAGNOSTICS III

SRP 11 Ion collection by cylindrical probes in weakly collisional plasmas: theory and experiment* ZOLTAN STERNOVSKY, *Department of Physics, University of Colorado, Boulder CO 80309-0390* SCOTT ROBERTSON, *Department of Physics, University of Colorado, Boulder CO 80309-0390* MARTIN LAMPE, *Plasma Physics Division, Naval Research Laboratory, Washington, D.C. 20375-5346* A theoretical approach has recently been described [Z. Sternovsky, S. Robertson and M. Lampe, *Phys. Plasmas* 10, 300 (2003)] for including the effect of ion collisions in the orbit motion limited theory for cylindrical Langmuir probes. In plasmas with a single ion species, ion-neutral charge exchange collisions are dominant and their first order effect is to increase the magnitude of the collected ion current. Measurements in Ar and Ne gas discharges at plasma densities $<10e9$ cm⁻³ show that the theory is accurate only for probes with radii less than approximately half the Debye length. For larger probes, absorption of ions at the probe surface reduces the ion density locally causing the sheath to expand. This increases the volume from which the charge exchange ions are collected and further increases the ion current. Poor agreement between measurements and theory is also found, when the probe is placed close to the ionization source.

*Research supported by the Department of Energy, the Office of Naval Research and NASA.

SRP 12 TIME-RESOLVED MEASUREMENTS OF ELECTRON NUMBER DENSITY AND COLLISION FREQUENCY USING MICROWAVE ATTENUATION AND PHASE SHIFT MOSTOFA HOWLADER, *Department of Electrical and Computer Engineering, Univ. of Tennessee, Knoxville* YUNQIANG YANG, *Department of Electrical and Computer Engineering, Univ. of Tennessee, Knoxville* J. REECE ROTH, *Department of Electrical and Computer Engineering, Univ. of Tennessee, Knoxville* PLASMA SCIENCES LAB, DEPARTMENT OF ECE, UNIV. OF TENNESSEE, KNOXVILLE TEAM Microwave interferometry is a well-established non-perturbing plasma diagnostic technique. Compared with other diagnostic techniques, it is more robust and reliable in experimental applications. We describe an extended microwave interferometry technique to characterize the time-resolved electron number density and collision frequency of a fluorescent light tube plasma. This technique is based on a modern vector network analyzer and measures the attenuation and phase shift of a microwave signal when propagating through the plasma. These measured quantities are related to the real and imaginary parts of the plasma index of refraction, which is characterized by the electron number density and collision frequency. From this relationship between the measured quantities and plasma parameters, one can numerically derive the electron number density and collision frequency. By time-resolved measurements, we can obtain information about the variation of the electron number density and collision frequency during one 60-Hz plasma cycle. We expect to report the measurement of the electron number density and collision frequency of an atmospheric pressure plasma, which is generated in a parallel plate plasma reactor.

SRP 13 Optical and Electrical Measurements in Methane/Argon/Nitrogen Pulsed Discharges MICHAEL BROWN, ROBERT FORLINES, *Innovative Scientific Solutions, Inc. Dayton, OH* BISWA GANGULY, *Air Force Research Laboratory, WPAFB, OH* PLASMA DIAGNOSTICS COLLABORATION Optical emission, laser-induced fluorescence (LIF), and V-I measurements are made in pulsed discharges of methane/argon/nitrogen mixtures using a variable-electrode-gap pyrex tube and total pressures of 20-100 Torr. An overvoltage condition is reached in 20 ns with peaks ranging from 2-7 kV. The electrical measurements indicate that the mixture-dependent E/n can exceed 100 Td during the steady-state period. Optical emission of H(n=3) (656 nm) and CH(A-X) (431 nm) rise rapidly during the overvoltage and then remain relatively constant during the steady regime indicating a balance between direct-electron-impact production and destruction. The temporal decay of the CH* emission after the voltage and current fall is faster than that predicted by known quenching rates; this strongly suggests the importance of neutral chemistry in the destruction of CH fragments. While the discharge appears to be dominated by streamers, PD scaling data suggests avalanche ionization growth controlled discharge behavior as well. The H-atom emission is strongest near both electrodes and its Doppler width is greatest near the cathode. In contrast, the CH* emission is uniformly distributed between the electrodes and the rotational temperature of both CH* emission and LIF of the A-X system is independent of axial position as well. Corrected photomultiplier signals of CH* emission indicate a CH dissociation fraction of $1e-4$. Results quantifying CH number density on discharge operating conditions will be presented.

SRP 14 High-Efficiency Thomson Scattering Measurement System and Its Application to Spatially Resolved EEDF Measurement of Surface-Wave Excited Plasma A. KONO, J. KOBAYASHI, M. ARAMAKI, E. STAMATE, H. SUGAI, *Nagoya University* A high-efficiency Thomson scattering measurement system was constructed, which consists of a triple-grating spectrograph (TGS) and an ICCD camera. TGS has a f number of 3.6 and is equipped with a spatial notch filter (1 nm width, $\sim 10^{-9}$ rejection) for suppressing Rayleigh light. The plasma is irradiated with a frequency doubled Nd:YAG laser (532 nm, 300 mJ, 30 pps) and the photocathode of the ICCD camera is optimized for visible light detection. Thomson signal level in the present system is expected to be a factor of ~ 20 higher than our previous system (Rev. Sci. Instrum. 71, 2716 (2000)). The plasma chamber has a diameter of 40 cm and an axial (horizontal) length of 30 cm. The chamber is movable in a horizontal plane, while the (vertical) laser beam axis is fixed; the laser beam can approach as close as 1 mm to the end quartz plate, through which a surface wave plasma is excited. Thus two-dimensional EEDF measurements in the region of strong surface wave excitation can be performed. Preliminary measurements indicate a promising performance of the measurement system. (The work supported by the 21st Century COE Program from the Ministry of Education, Culture, Sports, Science and Technology in Japan)

SRP 15 Measurements of Rotational Temperatures in Atmospheric-Pressure Capillary Plasma Electrode (CPE) Discharge MARGARET FIGUS, *Stevens Institute of Technology* NINA ABRAMZON, *California State Polytechnic University Pomona*, and *Stevens Institute of Technology* KURT BECKER, *Stevens Institute of Technology* We report the results of rotational temperature measurements in atmospheric-pressure capillary plasma electrode (CPE) discharges in ambient air using the unre-

solved N2 second positive band. Assuming that the emitting N2 molecules can be described by a Maxwell-Boltzmann distribution characterized by a single rotational temperature, this temperature is determined from a fit of the measured emission spectrum to a calculated spectrum. If the emitting species are in equilibrium with the bulk gas in the plasma, then this temperature can be interpreted as the gas kinetic temperature in the plasma. We determined rotational temperatures for three different plasma regions: inside the capillary by analyzing radiation emitted along the axis of the capillary, between the capillaries, and perpendicular to the axis of the capillary. Each region has a different plasma density and, therefore, a different gas temperature with the plasma inside the capillary being the hottest. We also measured the rotational temperatures in each region as a function of the plasma power. As expected, the rotational temperatures increase with increasing discharge power. Work supported by the NSF and by ARO through a DURIP award.

SRP 16 The Hairpin Resonator: A New Look at an Old Technique ROBERT PIEJAK, VALERY GODYAK, RICHARD GARNER, BENJAMIN ALEXANDROVICH, *Osram Sylvania R. L. Stenzel*(1) first introduced a microwave resonator probe (referred to here as a hairpin probe) to measure local electron density in a low-pressure plasma discharge. Judging from literature citations, this technique appears to be rarely used. In order to compare electron density measurements of a Langmuir probe and microwave interferometer measurements, a hairpin probe was designed and built. Stenzel's original design was modified to increase coupling to the hairpin structure, to reduce cross coupling to the pick-up probe and to minimize plasma perturbation. In addition, a sheath correction was determined based on the fluid equations for collisionless ions in a cylindrical electron-free sheath, coupled with a determination of the capacitance between hairpin wires. Instead of using the microwave setup described by Stenzel(1) (sweep oscillator, TWT amplified, detector, Boxcar integrator X-Y recorder) an off the shelf spectrum analyzer with a tracking generator was used to monitor resonant frequency of the hairpin. The result of these changes is a relatively simple diagnostic tool that can be used to determine the electron density in a low-pressure plasma discharge. This system is believed to be accurate and has been found to be highly reproducible from day to day. Measurements are relatively easy to interpret. The hairpin probe can be used in rf and dc low-pressure discharges and in chemically active discharges where probe surface contamination is significant. It is also useable in weakly magnetized plasmas. In this work we discuss probe construction, design and usage. In addition, a series of measurements comparing the results of the hairpin probe, Langmuir probe and microwave interferometer results are also presented. The hairpin probe is a valuable plasma diagnostic technique that has been overlooked for too long. (1) R. L. Stenzel, Rev. Sci. Instrum., Vol. 47, No. 5, p. 503, (1976)

SRP 17 A DC Electrical Discharge as a Tool for Measuring Relative Concentration of Gases (i.e. Argon) in Double-Pane Windows ALEKSANDR SERGEYEV, *Physics Department, Michigan Technological University* JACEK BORYSOW, *Physics Department, Michigan Technological University* A DC electrical discharge at atmospheric pressure was used to obtain information about the presence of gaseous species (i.e. argon) inside a laboratory model of a double pane window. The discharge operated between two cylindrical copper electrodes tapered at their ends and separated by a gap of approximately 2.0 mm. The negative

high voltage power supply worked in a current source mode with a limit set to 1 mA. The typical voltage drop during this continuous discharge between the electrodes was in the range of 1000 V. No visible oscillations were observed throughout the entire region between the electrodes. The estimated electron density n_e was in the range of $5 \times 10^{10} \text{ cm}^{-3}$ at 1.0 mA current. The relative concentration of ground state argon-to-nitrogen was inferred from integrated emission lines of second positive system of nitrogen $C^3\Pi_u(v') \rightarrow B^3\Pi_g(v'')$, $v'' - v' = 2$ (for $v' = 0, 1, 2, 3, 4$) in the spectral range between 330 and 420 nm and argon line from the $3p^5 4p$ electronic state at 750.4 nm

SRP 18 ELECTRON SCATTERING FROM ATOMS

SRP 19 Differential Electron Impact Excitation of Argon P. VANDEVENTER, J.G. CHILDERS, M. A. KHAKOO, *California State University, Fullerton, CA, USA* C. J. FONTES, *Los Alamos National Laboratory, NM, USA* K. BARTSCHAT, *Drake University, Des Moines, IA, USA* D.H. MADISON, *University of Missouri, Rolla, MO, USA* S. SAXENA, R. SRIVASTAVA, *IIT Roorkee, India* A.D. STAUFFER, *York University, Toronto, Canada* New experimental and theoretical differential cross-sections (DCSs) and differential cross-section ratios for the electron impact excitation of the $3p^5 4s$ configuration of Argon will be presented. The experimental DCSs and DCS ratios are measured at the impact energies of 14eV, 15eV, 17.5eV, 20eV, 30eV, 50eV and 100eV for scattering angles in the range of 5° to 130° . Comparisons will be made with the new theoretical DCSs and DCS ratios for Argon derived from the R-Matrix method, the Distorted-Wave Born Approximation, the Unitarized First-Order Many-Body and the Relativistic Born Approximation.

SRP 20 Improved DCS Ratios r for the Differential Electron Impact Excitation of Argon CHRISTINA MEDINA, ERIC SCHOW, JAMES GREGORY CHILDERS, MURTADHA A. KHAKOO, *California State University, Fullerton, CA, USA* In an effort to determine the presence of second-order effects in electron scattering, we will present improved preliminary r -values¹ for Argon at low incident electron energies. Our data are concentrated at small scattering angles $\leq 40^\circ$ and incident energies ≤ 30 eV. The results are compared to available theoretical r -values from the R-Matrix method², the Distorted-Wave Born Approximation³, the Relativistic Distorted-Wave Approximation⁴ and the Unitarized First-Order Many-Body Theory⁵. Funded by the National Science Foundation.

¹M. A. Khakoo et al. *J. Phys. B.* **27**, 3159 (1994).

²K. Bartschat, Private Communication.

³D. H. Madison, Private Communication.

⁴A. D. Stauffer, Private Communication.

⁵C. J. Fontes, Private Communication.

SRP 21 Distorted-Wave vs. Close-Coupling Calculations for Electron-Impact Excitation to the $3p^5 3d$ Levels of Ar I* ARATI DASGUPTA, *Naval Research Laboratory* KLAUS BARTSCHAT, *Drake University* ALEXIE GRUM-GRZHIMAILO, *Moscow State University* DON MADISON, *University of Missouri-Rolla* NAVAL RESEARCH LABORATORY COLLABORATION, DRAKE UNIVERSITY COLLABORATION, MOSCOW STATE UNIVERSITY COLLABORATION UNIVERSITY OF MISSOURI-ROLLA COLLABORATION We present theoretical results from non-perturbative R-matrix (close-coupling) and perturbative distorted-wave calculations for electron-impact excitation from the ground state to the 12 fine-structure levels of the $3p^5 3d$ configuration in Ar I. For some transitions the results are found to be extremely sensitive to the theoretical model for both the collision process and the target structure. A critical evaluation of the results obtained in the different theoretical models for incident energies from threshold up to 200 eV will be presented. The results will be compared with other available predictions as well as the experimental data of Chilton and Lin [*Phys. Rev. A* **60**, 3712 (1999)].

*Work supported, in part, by the ONR, the NSF, and NATO

SRP 22 Comprehensive calculations for elastic electron scattering from Zn, Cd, and Hg atoms MEHRDAD ADIBZADEH, CONSTANTINE THEODOSIOU, *University of Toledo* NICHOLAS HARMON, *College of Wooster* We present theoretical results for differential, total, and momentum transfer cross sections for the elastic scattering of electrons by Zn, Cd, and Hg atoms and the subsequent determination of the Sherman functions, for energies below 1 keV. We used a fully relativistic approach with explicit inclusion of electron exchange and core-polarization effects. Good agreement is found with the limited available experimental data. Our work was motivated by our successful results for inert gases and alkaline earth atoms. Based upon our thus developed approach and acquired experience, we provide a comprehensive set of *recommended* cross sections and Sherman functions for elastic electron scattering from these atoms. We hope that our work will motivate more future experimental and theoretical research.

SRP 23 RECOMBINATION

SRP 24 Electron-Ion Recombination and Electronic Decay of Molecular Nitrogen Excited by Multi-Photon Laser Ionization* STEVEN ADAMS, CHARLES DEJOSEPH, ROBERT LEE, *Air Force Research Laboratory* JAMES WILLIAMSON, *Innovative Scientific Solutions Inc* The recombination of molecular nitrogen ions and electrons has been studied in a volume of pure N_2 (10-760 Torr) excited by a focused UV laser pulse. The tunable laser pulse induces multi-photon ionization through a resonant intermediate state resulting either in a 2+3 photon transition ($N_2(X^1\Sigma_g^+) \rightarrow N_2(a^1\Pi_g) \rightarrow N_2^+(B^2\Sigma_u^+)$) or a 3+2 photon transition ($N_2(X^1\Sigma_g^+) \rightarrow N_2(b^1\Pi_u) \rightarrow N_2^+(B^2\Sigma_u^+)$) as several resonant laser wavelengths are found in the 275-285 nm range. The primary $N_2^+(B^2\Sigma_u^+) \rightarrow N_2^+(X^2\Sigma_g^+)$ fluorescence is observed during laser absorption, and decays within a few nanoseconds after the laser pulse. Spectrally and temporally resolved secondary fluo-

rescence has been observed extending up to 1 μ s after photoionization and has been attributed to the N_2^* products of electron-ion recombination. The influence of pressure and laser flux on the time dependence of this secondary fluorescence are consistent with rapid N_4^+ formation by the three body process $N_2^+ + N_2 + N_2 \rightarrow N_4^+ + N_2$ followed by the somewhat slower $e + N_4^+$ recombination forming $N_2^* + N_2$. Experimental data are compared with a simple coupled rate equation model which includes several key species, such as $N_2^+(B^2\Sigma_u^+)$, $N_2^+(X^2\Sigma_g^+)$, N_4^+ , and $N_2(C^3\Pi_u)$. The model is also used to study the metastable N_2^* states formed as a result of resonant laser absorption and examine their possible influence on the observed secondary fluorescence.

*This work supported by the Air Force Office of Scientific Research

SRP 25 Observation of molecular assisted recombination in the magnetized sheet plasma AKIRA TONEGAWA, *Department of Physics, School of Science, Tokai University* HIRONORI OGAWA, *Department of Physics, School of Science, Tokai University* HIROYUKI YAZAWA, *Department of Physics, School of Science, Tokai University* MASATAKA ONO, *Tokai University* KAZUTAKA KAWAMURA, *Tokai University* TOKAI UNIVERSITY PLASMA GROUP TEAM Molecular assisted recombination (MAR) with vibrational hydrogen molecular has been observed to enhance the reduction of ion particle flux in a high density magnetized sheet plasma device (TPDSHEET-IV). There are two main paths for MAR: (1) $H_2(v) + e \Rightarrow H + H$ (dissociated attachment) followed by $H + H + e \Rightarrow H + H$ (mutual neutralization), and (2) $H_2(v) + A + e \Rightarrow (AH)^+ + H$ (ion conversion) followed by $(AH)^+ + e \Rightarrow A + H$ (dissociative recombination), where $A^+(A)$ is a hydrogen or an impurity ion (atom) existing in the plasma. The value of H^+ , H_2^+ and H_3^+ are observed in the mid-plane region with hot electron ($T_e = 10-15$ eV) by a mass-analyzer. On the other hand, negative ions of hydrogen atom H^- is localized in the circumference of existing cold electrons ($T_e = 3-5$ eV) by a probe assisted laser photodetachment method. A small amount of secondary hydrogen gas puffing into a hydrogen plasma decreased gradually the density of H_2^+ , H_3^+ and increased rapidly H^- in the plasma, while the conventional radiation and three-body recombination (EIR) processes were disappeared. These results can be well explained by taking the MAR in the plasma into account.

SRP 26 BIOLOGICAL APPLICATIONS OF PLASMAS

SRP 27 Deactivating bacteria with RF Driven Hollow Slot Microplasmas in Open Air at Atmospheric Pressure* ZENGQI YU, AMY PRUDEN, ASHISH SHARMA, GEORGE COLLINS, *Colorado State University* A hollow slot discharge operating in open air at atmospheric pressure has demonstrated its ability to deactivate bacterial growth on nearby surfaces exposed to the RF driven plasma. The cold plasma exits from a hollow slot with a width of 0.2 mm and variable length of 1-35 cm. An internal electrode was powered by 13.56 MHz radio-frequency power at a voltage below 200 V. External electrically grounded slots face the

work piece. The plasma plume extends millimeters to centimeter beyond the hollow slot toward the work piece to be irradiated. Argon-Oxygen gas mixtures, at 33 liters per minute flow, were passed through the electrodes and the downstream plasma was employed for the process, with treatment exposure time varied from 0.06 to 0.18 seconds. Bacterial cultures were fixed to 0.22 micron cellulose filter membranes and passed under the plasma at a controlled rate at a distance of about 5-10 millimeters from the grounded slot electrode. Preliminary studies on the effectiveness of the plasma for sterilization were carried out on *E. coli*. Cultures were grown overnight on the membranes after exposure and the resulting colony forming units (cfu) were determined in treated and untreated groups. In the plasma treated group, a 98.2% kill rate was observed with the lowest exposure time, and increased to 99.8% when the exposure time was tripled. These studies clearly demonstrate the ability of the RF-driven hollow slot atmospheric plasma to inhibit bacterial growth on surfaces.

*This work is supported by NSF grant #ECS - 0097061

SRP 28 Improved hemocompatibility of the inner surface of capillary PE tubing by microplasma surface modification J.L. SHOHET, J.L. LAUER, C. PRATOOMTONG, R.M. ALBRECHT, R.D. BATHKE, S. ESNAULT, J.S. MALTER, *U. of Wisconsin-Madison* S.B. SHOHET, *U. of California, SF* U.H. VON ANDRIAN, *Harvard Med. School* A hollow-cathode microplasma modified the luminal surface of small diameter (0.28 and 0.8 mm) up to 1 meter long polyethylene (PE) tubing. PE glycol was grafted to the luminal surface using O_2 plasma followed by Ar plasma. Feedstock gases and reaction products drift along the tubing which may cause nonuniform treatment. Emitted light from the plasma was fed into a monochromator at various positions to assess uniformity. Effectiveness was evaluated using capillary-rise, which is related to contact angle. Uniformity of the atomic surface composition along the length of the inner surface of the PE tubing was analyzed by XPS and transmission FTIR. To test hemocompatibility, a flow loop circulated heparinized human blood for various times at 37 C. Plasma-treated and untreated tubing were then examined with a scanning SEM to assess the morphology of adhering platelets. By modifying plasma parameters, uniformity along the tubing and proximity to the peristaltic pump can be optimized.

SRP 29 Electrical Aspects of Argon Micro-Cell Plasma with Applications in Bio-Medical Technology YASUHIRO HORIUCHI, *Department of Electronics and Electrical Engineering, Keio University, Japan* JAN VAN DIJK, *Department of Electronics and Electrical Engineering, Keio University, Japan* TOSHIAKI MAKABE, *Department of Electronics and Electrical Engineering, Keio University, Japan* Argon micro-cell plasma (MCP) is believed to be a viable tool for performing micro-surgery. The non-thermal nature of the discharge allows an effective treatment of pathological tissue without causing thermal damage to its surroundings. This bio-medical application imposes a number of design challenges on the plasma configuration which we will address by computer-aided source design. In this contribution we present a numerical study with the Relaxation Continuum model (RCT) [1-2] of the characteristics of an atmospheric argon MCP which is maintained by an RF source. The focus will be on the influence of the geometry and the externally applied RF amplitude and frequency on the plasma properties. In particular, attention will be paid to the effect of pulsed-mode operation on the gas temperature. In addition, the influence of the frequency and the field in the

wall sheath on the losses of the plasma species to the cell walls by drift-diffusion processes will be considered. [1] K. Okazaki, T. Makabe and Y. Yamaguchi, *Appl. Phys. Lett.* (54), 1742 (1989) [2] T. Makabe, "Advances in Low Temperature RF Plasmas" Elsevier, (2002)

SRP 30 HIGH PRESSURE PLASMA CHEMISTRY AND ENVIRONMENTAL APPLICATIONS

SRP 31 Formation of pentafluorosulfanylbenzene, $C_6H_5SF_5$, in a low temperature plasma of gases S_2F_{10} and C_6H_6 ADOLF JESIH, MAJA REMSKAR, TOMAZ SKAPIN, BOGDAN KRALJ, DUSAN ZIGON, *Jozef Stefan Institute, Jamova 39, 1111 Ljubljana, Slovenia* Sulfur fluorides SF_6 , SF_5Cl and CF_3SF_5 react with benzenes in a low temperature plasma to give mainly fluorinated benzenes, sulfides, disulfides, biphenyl and a minor quantities of pentafluorosulfanylbenzene, $C_6H_5SF_5$.¹ Aimed at the higher yields of pentafluorosulfanylbenzene, the most clean source of SF_5 radicals, S_2F_{10} , was used to react with benzenes in an inductively coupled radio-frequency discharge. The reaction products were trapped at 77 K and subsequently analysed by GC-MS and GC-FTIR spectroscopy. The quantities of pentafluorosulfanylbenzene in reaction products, where S_2F_{10} was used as one of the reactants were several times larger than in reaction products where SF_6 , SF_5Cl and CF_3SF_5 were used as the source of the SF_5 radicals, but reaction products were again numerous and not easily separable. The same reaction mixtures of sulfur fluorides and benzenes under plasma conditions deposit polymers, the properties and compositions of which will be discussed. [1] P. Klampfer, T. Skapin, B. Kralj, D. Zigon, A. Jesih, *Acta Chim. Slov.*, **50** (2003) 29.

SRP 32 HCL Depletion in High Pressure plasma for Excimer Lasers BELASRI AHMED, *Laboratoire de Physique des Plasmas, Matériaux Conducteurs et leurs Applications* HARRACHE ZOHEIR, *Laboratoire de Physique des Plasmas, Matériaux Conducteurs et leurs Applications* A Photon emission phenomena, with energies about electron Volts, has been experimentally observed in excimer molecules. This category of diatomic molecules gave rise to important researches and developments in lasers technology. The aim of this work is to study, through numerical modeling, the XeCl kinetics and the mechanisms affecting plasma uniformity in a discharge sustained excimer laser. In the model, the plasma is represented by a resistance inversely proportional to the electron density. Time variations of the electron density are obtained by solving the transport equations coupled to heavy species and external circuit. A detailed description of XeCl molecule and of the associated kinetics have been taken into account, together with the effect of the gas mixture composition on power deposition and the spatial uniformity of the plasma. The model predictions have been compared with the experimental results.

SRP 33 New Determination of the Methyl Radical Line Strength using a Pulsed Microwave Discharge G.D. STANCU, J. RÖPCKE, *Institut für Niedertemperatur-Plasmaphysik, Greifswald, Germany* P.B. DAVIES, *Department of Chemistry, University of Cambridge, UK* The accuracy of calculated methyl concentrations (and hence the validity of plasma chemical modelling based on methyl radical reactions) is directly related to the precision of methyl line parameters. In spite of the importance of the line strength it has only been measured for two line of methyl in the infrared and with an uncertainty of 30%^{1,2}. This contribution will describe spectroscopic studies of pulsed Ar microwave plasmas ($f=2.45$ GHz) containing (i) H_2 with C_2H_2 or CH_4 or (ii) di-*tert*-butyl peroxide. By combining a planar microwave reactor with an optical multi pass cell the detection sensitivity for transient plasma species by infrared tunable diode laser absorption spectroscopy (TDLAS) has been considerably improved. Based on time resolved TDLAS measurements, using the literature kinetic data on the CH_3 self recombination rate constant, the concentration and lifetime of CH_3 has been measured directly leading to accurately determined line strengths of several absorption lines of CH_3 around $16 \mu m$.

¹Wormhoudt et al. 1989 *Chem. Phys. Lett.* **156**, 47

²Yamada et al. 1983 *J. Chem. Phys.* **78**, 669

SRP 34 N-heptane decomposition in multi-needle to plate electrical discharge STANISLAV PEKAREK, *Czech Technical University in Prague, Czech Republic* MILAN POSPISIL, *Institute of Chemical Technology, Prague, Czech Republic* GROUP OF ELECTRICAL DISCHARGES TEAM Plasma based technologies are becoming more and more important for destruction of volatile organic compounds in air streams. The most frequent electrical discharges tested for VOC decomposition are corona and dielectric barrier discharge. We proposed [1] multi-hollow needles to plate atmospheric pressure discharge enhanced by the flow of the mixture of air with VOC through the needles. In this case all reactive mixture will pass through the active zone of the discharge. The high-speed gas flow near the exit of the needle will also efficiently cool the electrodes. Hence the higher values of the discharge current can be obtained without the danger of the discharge transition to the spark. The chemical reactions leading to the VOC decomposition can therefore be enhanced [2]. We performed an experimental study of the n-heptane decomposition efficiency on its concentration in air in the input of the discharge. We choose n-heptane, an important part of organic solvents and part of automotive fuels, as a representative of saturated alkanes. We found that with decreasing n-heptane concentration the decomposition efficiency increases. Acknowledgement: This work was supported by the research program No: J04/98:212300016 "Pollution control and monitoring of the Environment" of the Czech Technical University in Prague. References [1] S. Pekrek, V. Kha, M. Pospil - *J. Physics D, Appl. Physics*, **34**, 117 (2001). [2] O. Goosens, T. Callebaut, Y. Akishev, C. Leys *IEEE Trans. Plasma Sc.* **30**, 176 (2002).

SRP 35 Treatment of Perfluorocarbon Using Nonthermal Plasma Produced by Barrier Discharge NOBUYA HAYASHI, *Saga University* SATOSHI IHARA, *Saga University* SABUROH SATOH, *Saga University* CHOBEI YAMABE, *Saga University* Characteristics of fluorocarbon decomposition using a non-thermal plasma produced by the barrier discharge was investigated. The effective condition of the fluorocarbon treatment was determined by controlling the several parameters such as applied voltage, in-

put power and gas flow rate. The barrier discharge electrode utilized in this experiment was covered with several types of dielectrics in order to control electron density and electron energy of the produced plasma. The gas used was CF₄ (100ppm) diluted by Ar and air and the flow rate was 0.1 l/min. FTIR spectra of exhausted gas indicate that the maximum decomposition rate of 98dielectric with thickness of 0.3 mm (284 pF) at the input power of 4 W. Instantaneous byproducts in the discharge region and final byproducts of CF₄ decomposition were determined by the light emission spectroscopy and the FTIR, respectively.

SRP 36 The Advanced Oxidation Process (UV-Ozonation Type) Assisted By Excimer Lamp TOMOKAZU IKEMATSU, *Saga University* NOBUYA HAYASHI, *Saga University* SATOSHI IHARA, *Saga University* SABUROH SATOH, *Saga University* CHOBEI YAMABE, *Saga University* The advanced oxidation processes utilizing the excimer lamp was developed for water purification. The UV light with the wavelength of 222nm that destructs the hydrogen peroxide to hydroxyl radical realizes the AOPs. In this paper, the KrCl excimer lamp with the wavelength of 222 nm was adopted for UV-ozonation type AOP, in order to treat the water with organic acid (humic acid). The lamp was made of quartz glasses with a coaxial cylindrical shape. The grounded copper electrode was rolled on the outer side of the glass tube. The excimer gas flows in the gap of the glass tube between outer and inner electrodes. The UV light from the discharge was irradiated to ozonated water that flows inside the glass tube. The enhancement of reduction rate of the organic compound dissolved in water was achieved using UV excimer lamp with the wavelength of 222 nm. When the excimer gas pressure was 200 Torr, maximum discharge power was obtained and light emission intensity at 222 nm was highest. The reduction rate of the UV light irradiation (9 kV, 200 Torr) was larger than that of ozonation only, and the reduction rate was improved from 40

SRP 37 LASER KINETICS

SRP 38 Orestes Kinetics Model for the Electra KrF Laser* J.L. GIULIANI, P. KEPPLER, R.H. LEHMBERG, M.C. MYERS, J.D. SETHIAN, *Naval Research Laboratory* G. PETROV, *Berkeley Research Scholars, Inc.* M. WOLFORD, *Science Applications International Corp.* F. HEGELER, *Commonwealth Technology, Inc.* Orestes is a first principles simulation code for the electron deposition, plasma chemistry, laser transport, and amplified spontaneous emission (ASE) in an e-beam pumped KrF laser. Orestes has been benchmarked against results from Nike at NRL and the Keio laser facility. The modeling tasks are to support ongoing oscillator experiments on the Electra laser (500 J), to predict performance of Electra as an amplifier, and to develop scaling relations for larger systems such as envisioned for an inertial fusion energy power plant. In Orestes the energy deposition of the primary beam electrons is assumed to be spatially uniform, but the excitation and ionization of the Ar/Kr/F₂ target gas by the secondary electrons is determined from the energy distribution function as calculated by a Boltzmann code. The subsequent plasma kinetics of 23 species subject to over 100 reactions is followed

with 1-D spatial resolution along the lasing axis. In addition, the vibrational relaxation among excited electronic states of the KrF molecule are included in the kinetics since lasing at 248 nm can occur from several vibrational lines of the B state. Transport of the lasing photons is solved by the method of characteristics. The time dependent ASE is calculated in 3-D using a "local look-back" scheme with discrete ordinates and includes specular reflection off the side walls and rear mirror. Gain narrowing is treated by multi-frequency transport of the ASE. Calculations for the gain, saturation intensity, extraction efficiency, and laser output from the Orestes model will be presented and compared with available data from Electra operated as an oscillator. Potential implications for the difference in optimal F₂ concentration will be discussed along with the effects of window transmissivity at 248 nm.

*Supported by the U.S. Department of Energy, NNSA/DP

SRP 39 Small signal gain time measurements in the active medium of a pulsed CO laser in the wide spectral range (5.1-7.5 micron) ANDREI IONIN, YURI KLIMACHEV, ANDREI KOTKOV, LEONID SELEZNEV, DMITRIY SINITSYN, SERGEY VETOSHKIN, *P.N. Lebedev Physics Institute of Russian Academy of Sciences, Moscow, Russia* ALEXANDER KURNOSOV, ANATOLIY NAPARTOVICH, SERGEY SHNYREV, *Troitsk Institute for Innovation and Fusion Research, Troitsk, Moscow Region, Russia* Experimental investigations of small signal gain (SSG) time behavior in the active medium of a pulsed e-beam sustained discharge CO laser are presented. The experiments on study of the temporal behavior of the SSG were carried earlier but only for lower vibrational-rotational transitions (Bulletin Amer. Phys. Soc. 2002, v. 47, p. 71). Master oscillator laser amplifier system was used in our experiments. We applied two cryogenically cooled laser devices. The first one was tunable single-line continuous wave CO laser and the second one was the pulsed e-beam sustained discharge CO laser. SSG time behavior for pulsed CO laser on fundamental band from low transition 6-5 (~5.1 micron) up to high one 32-31 (~7.5 micron) was studied experimentally at different parameters of active medium. A recently developed complete kinetic model of pulsed CO laser was used for numerical simulations of the experimental measurements. A good agreement between theoretical data and experimental results are shown.

SRP 40 RF DISCHARGE IN ACTIVE MEDIUM OF SLAB CO LASERS YURI TEREKHOV, ANDREY IONIN, DMITRIY SINITSYN, *P.N. Lebedev Physical Institute of Russian Academy of Sciences* IGOR KOCHETOV, ANATOLIY NAPARTOVICH, *Troitsk Institute for Innovation and Thermonuclear Research* The experimental RF discharge facility of special design was developed for studying slab RF discharge properties in gas mixtures typical for carbon monoxide lasers. The dependencies of inter-electrode voltage on specific input power loaded into RF discharge were experimentally measured for gas mixtures with different content of CO in the total gas pressure range of 30 - 100 Torr at room temperature. The experimentally obtained voltage-power RF discharge characteristics were modeled theoretically using a one-dimensional model. Satisfactory agreement with the experiment was achieved for gas mixtures at a pressure of about 100 Torr, which is optimal for laser operation. With pressure decreasing to 30 Torr the calculated inter-electrode voltage was notably higher than the measured one. Explanation of this discrepancy requires additional studies to be performed within wide temperature range.

SRP 41 Pulse Compression of CO₂ laser in SF₆ and its Mixtures with Dymel Gas DECHANG YI, *Tennessee Technological University* SATISH MAHAJAN, *Tennessee Technological University* Laser pulse compression using OFID in ammonia, and CH₃F gases has been reported in the past. Recent work in dymel gas indicated a four times sharper pulse than that in vacuum [1]. In the present work, experiments were conducted in SF₆ gas to investigate the possibility of an OFID effecting a compressed CO₂ laser pulse. An average of fourty laser pulses was acquired at a typical gas pressure in the test cell. Pressure of SF₆ was varied from 0 to 2.5 torr while that of dymel (in a mixture with SF₆) was varied from 0 to 6 torr. Pressure of SF₆ was limited to a maximum of 2.5 torr due to strong absorption leading to weakening of output pulse. Results indicate that the addition of SF₆ to dymel led to a variation in sharpness (intensity divided by pulsewidth) of a pulse and also to a shift in pressure at which maximum compression in dymel normally occurs. [1]D. Yi, and S.Mahajan, "Pulse Compression of CO₂ laser by Optical Free Induction decay (OFID) Effect, Bulletin of APS, Vol.47, No.7, October 2002, pp.27,

trodes. The evolution of particle number depends on the gas composition. This means that the particle-growth mechanism changes in both the plasma-production and particle-levitation region. In this presentation, we discuss the particle-growth mechanism under changing plasma conditions.

*Professor Emeritus, Tohoku University

SRP 45 Fluid simulation of complex plasmas EDUARDO GONZALEZ, *MPE* BORIS KLUMOV, *CIPS* A fluid model is used for simulating the behavior of dust particles in a RF argon discharge. The fluid approach (mass, momentum and energy conservation) is used to simulate positive ions and electrons densities. The dust interaction is then calculated by using a molecular dynamic approach.

SRP 42 DUSTY PLASMAS

SRP 43 Sheath diagnostics using particles in a dusty plasma BIN LIU, JOHN GOREE, KHARE AVINASH, *The Department of Physics and Astronomy, The University of Iowa, Iowa City, IA 52242* A sensitive method of measuring the horizontal electric potential profile in a glow discharge plasma is developed. We introduce a small number of microsized polymer microspheres into a discharge, and they are levitated in the sheath above the lower electrode. The particles are negatively charged, and they are trapped by the radial electrical potential, which we can compute using measurements of the particle positions. This method also yields the Debye length inside the sheath and the particles charge. We verified the method using a molecular dynamics simulation. We demonstrate the method using a Xe rf plasma, obtaining the charge and the Debye length. Using these two parameters along with the particle positions, we calculated the radial profile of the electrical potential, verifying that it is parabolic above the center of the electrode. Work supported by NASA and DOE.

SRP 44 Particles Behavior in Methane-Hydrogen Plasmas TETSUJI SHIMIZU, WOLFGANG JACOB, HUBERTUS THOMAS, GREGOR MORFILL, NORIYOSHI SATO,* *Centre for Interdisciplinary Plasma Science (MPE and IPP)* TOSHIMI ABE, *Tohoku Institute of Technology* The behavior of particle clouds and particle growth in reactive plasmas is studied in a capacitively coupled rf discharge. We use a three electrode assembly. The electrodes, 10 cm in diameter, are oriented horizontally. The rf power is applied to the upper electrode. To change the plasma conditions around the particle cloud, a grid electrode is put between two rf electrodes. The particles are levitated between this grid and the lower electrode. In methane hydrogen plasmas at 20 Pa, we observed the formation of a particle cloud a few 10 minutes after igniting the plasma. Most of the particles levitated are amorphous carbon flakes, delaminated from the surface of the elec-

SRP 46 PLASMA-SURFACE INTERACTIONS

SRP 47 Effects of H⁺ kinetic energy on nano-particle formation due to interaction between H₂ plasma and carbon wall* RYUJI UEHARA, YASUHIRO KITaura, KAZUNORI KOGA, MASAHARU SHIRATANI, YUKIO WATANABE, *Dept. of Electronics, Kyushu University, Japan* AKIO KOMORI, *National Institute for Fusion Science, Japan* NATIONAL INSTITUTE FOR FUSION SCIENCE, JAPAN COLLABORATION Studies on particle formation due to interaction between H₂ plasma and carbon surface are important from viewpoints of safety operation of fusion devices and production of new functional materials. Recently we have studied nano-particle formation due to interaction between carbon fiber composite wall and ECR H₂ plasma of $n_i = 10^{11} \text{ cm}^{-3}$ and $T_e = 5 \text{ eV}$.¹⁾ With increasing the sheath voltage V_s from 14 V to 214 V, both average size and amount of particles decreases. Emission intensities of C, C⁺, C₂, and CH increase with V_s , whereas a rate of H absorption into the wall increases. Therefore, the smaller desorption rate of carbon-containing species for the higher V_s is considered to lead to the smaller size and amount of particles. Experimental results for graphite wall will be presented at the conference. 1) M. Shiratani, et. al., Proc. 20th Symp. on Plasma Processing (2003), pp.101.

*Work supported by JSPS and NIFS.

SRP 48 Fluorocarbon-based plasma etching: the role of the energy distribution of bombarding ions* RARDCHAWADEE SILAPUNT, SHUNTEL WILLIAMS, AMY WENDT, *University of Wisconsin - Madison* KAREN KIRMSE, LAURA LOSEY, *Texas Instruments* In fluorocarbon-based plasma etching of dielectrics, an overlying thin fluorocarbon film, deposited on the substrate during etching, strongly affects etch rate and etch selectivity (Oehrlein et al., JVSTA 15 (1997)). Recent results suggest that the energy distribution of bombarding ions (IED) has a significant effect on the thickness of this polymer layer, subsequently affecting etch rate and selectivity as well. Specifically, we have narrowed the IED while keeping other process conditions unchanged

by tailoring the shape of the RF voltage waveform used for substrate bias. Significant improvements in etch selectivity for SiO₂ over silicon, SiO₂ over photoresist and organosilicate glass (OSG) over silicon nitride and silicon carbide have been obtained by using a narrow IED compared to the broad IED resulting from a sinusoidal bias waveform. X-ray photoelectron spectroscopy (XPS) measurements of overlying fluorocarbon film thickness as a function of bias voltage for both narrow and broad IEDs show a strong inverse correlation between film thickness and etch rate. We conclude that the sensitivity of this polymer film to the IED is the key to observed improvements in selectivity.

*Supported by SRC (TI custom funding)

SRP 49 Ambient plasma for metal surface treatment PRASAD NUAMATHA, *Southern Illinois University* SHIRSHAK DHALI, *Southern Illinois University* The results of using ambient plasma for cleaning and treating metal surfaces are presented. Metal surfaces are cleaned with atmospheric pressure argon/hydrogen or argon/oxygen plasma. The cleaned surface was characterized by XPS and was found to consist of exposed metal with very low carbon content. Profilometry and optical imaging results show that plasma are very effective in removing oil and paint coatings from the surface of metals. This technique is a non-polluting alternative to surface treatments that currently use chemicals/solvents. In addition the plasma has been shown to improve the binding properties by uniformly hydroxylating the surface.

SRP 50 Investigation of a hyper-thermic atomic hydrogen beam source* TATIANA BABKINA, TIMO GANS, UWE CZARNETZKI, *Institut für Plasma- und Atomphysik, Ruhr-Universität Bochum, Germany* The design of and first investigations on a novel atomic hydrogen beam source are reported. The source is based on neutralisation and reflection of hydrogen ions at surfaces. Ions are produced in a pulsed inductively coupled hydrogen RF discharge with magnetic confinement at pressures in the Pascal range. A voltage pulse is applied to a small electrode inside the discharge volume. Ions are accelerated in the sheath potential in front of the electrode. A hydrogen atom beam is produced by neutralisation and reflection of impinging ions at the electrode surface. The atom beam traverses the plasma collisionless and is analysed by an energy resolved mass spectrometer opposite to the electrode. Influences of ion species, ion energy, and surface materials on the atomic beam characteristics can be studied. The atomic hydrogen beam with tunable energy in the range of 1eV to 100eV can be applied for detailed investigations of exothermic chemical reactions of hyper-thermic hydrogen atoms at metal surfaces.

*This work is supported by the DFG in the frame of the SFB 616

SRP 51 MATERIAL PROCESSING II

SRP 52 Etching mechanisms of new silicon containing copolymers for 157nm lithography DAVID EON, *IMN-LPCM* GILLES CARRY, *IMN-LPCM* VANESSA RABALLAND, *IMN-LPCM* CHRISTOPHE CARDINAUD, *IMN-LPCM* E. TEGOU, *IMEL* N. VOURDAS, *IMEL* V. BELLAS, *IMEL* P. ARGITIS, *IMEL* E. GOGOLIDES, *IMEL* We are involved in an European program, joining several national laboratories, to address resist challenges associated with 157 nm lithography. Particularly,

we are interested in the bilayer resist scheme. In such a scheme, a low absorbance silicon containing resist is imaged by a 157 nm optical source. Then, this material serves as a mask for pattern transfer, by oxygen plasma, into an usual carbon containing resist. During plasma development, control of etch rate, selectivity and roughness is of primary interest. Within the project, we developed a new class of inorganic (Si₈O₁₂ cage)-organic copolymers to be used as the top layer, and we extensively studied their behaviour during oxygen plasma in ICP source. Etch rate and selectivity have been determined by in-situ ellipsometry, and etch mechanisms have been investigated by quasi in-situ XPS, ellipsometry and ex-situ FTIR. In the present paper, we show results concerning etch mechanisms for several of these copolymers.

SRP 53 WITHDRAWN

SRP 54 Simulation of low-angle forward-reflected neutral beam for chargeup-free Si etching SUNG JIN KIM, SOON JUNG WANG, JAE KOO LEE, *Department of Electronic and Electrical Engineering, Pohang University of Science and Technology, Pohang, 790-784, S. Korea* DO HAING LEE, GEUN YOUNG YEOM, *Department of Material Engineering, SungKyunKwan University, Suwon, 440-746, Korea* As a device size shrinks toward nano-scale, a charge-up damage by using ion induced etching is a very serious problem. A neutral beam etching is one of the most popular techniques to reduce the charge-up damage. We have performed a neutral beam simulation[1] by a modified XOOPIE code, in order to obtain neutral energy and angle distributions. The neutral beam is generated by collisions between ions produced by an ion-gun and low angle reflectors. The ion-gun is composed of several grids with voltages applied. Positive ions are accelerated toward low angle reflectors by the potential between grids. We have optimized the condition of the ion-gun for high ion flux and better directionality. It is applied to the neutral beam simulation in order to calculate neutral beam characteristics such as neutral flux, energy and angle distributions which have an influence upon etch rate. As low energy neutral beam is used for Si etching, the ion-gun using two grids has low ion flux and broad angle distribution. Therefore, we propose a three-grid ion-gun which has one additional grid with positive voltage. The ion flux from the three-grid ion-gun is about three times larger than that from the two-grid ion-gun. Etch profile is calculated from neutral beam by the three-grid ion-gun at a shallow Si trench. It is verified by comparison with experiment. This work is supported by the national program for Tera-level nanodevices in Korea Ministry of Science and Technology. [1] M.S. Hur, S.J. Kim, H.S. Lee, J.K. Lee, and G.Y. Yeom, Particle in Cell Simulation of a Neutral Beam Source for Materials Processing, IEEE Trans. Plasma Science 30 (1) 110 (2002)

SRP 55 Future profile simulation of SiO₂ trench etching under topography charging TAKASHI SHIMADA, *Keio University, Yokohama, Japan* TOSHIKI MAKABE, *Keio University, Yokohama, Japan* In the next half-decade, multi-interconnect system with 10 or 11 layers will be realized to reduce RC signal delay in LSI under the technology node of 65 nm- 25 nm. Under these circumstances, the conventional trench or hole etching in the

multi-layers of SiO₂ will have to be much frequently processed. We will be faced practically with an electrical damage of the lower level gate oxide of MOS during the etching in each of trenches/holes in the multi-interconnect system. Linked design between the plasma equipment and future profile for etching is the hot issue as well as the control of the future geometrical variation across a wafer. We had an opportunity of proposing a prototyped CAD, VicAddress (Vertically integrated computer aided design for device processing) in 2000[1]. We have developed a future profile simulation of SiO₂ trench, considering a topographical charging by using the level set method in VicAddress. Here, we show and discuss our recent results of time- and space-development of the trench profile of SiO₂ in conjunction with the bottom and sidewall charging, under the high energy ions incident on the SiO₂ wafer in a two-frequency CCP in CF₄(5%)/Ar. The future profile is discussed as a function of aspect ratio and radial position on the SiO₂ wafer. [1]T.Makabe, edited, "Advances in Low Temperature RF Plasmas-basis for process design-" (Elsevier) 2002.

SRP 56 3-Dimensional Feature Profile Evolution Using Level Set Methods HELEN HWANG, T. R. GOVINDAN, M. MEYYAPPAN, *NASA Ames Research Center* Modeling 3-D feature profile evolution due to etching of semiconductor materials is a computationally expensive endeavor. Good resolution requires typical mesh sizes of the order 150×150×150 cells, with neutral and ion species flux integrals calculated at every cell. An additional challenge is that the self-shadowing calculation for the fluxes is not easily derived for arbitrary device shapes. For example, the allowable angular range of ions and neutrals at a given point inside the device can be solved for rectangular trenches, if the trench dimensions are known. For non-rectangular trenches, or if the mask erodes during the etch, the shadowing of the fluxes must be calculated at each time step. We have modified our existing Simulation of Profile Evolution using Level Sets (SPELS) to include a generalized shadowing routine in order to simulate features of arbitrary shapes in 3D. SPELS3D simulates etching of devices such as round via holes, L-shaped devices, etc., in addition to rectangular trenches. We will present sample animations of complete 3D geometries of silicon devices etching in chlorine plasmas.

SRP 57 Feature Profile Modeling of Silicon Etching in Chlorine-Containing Plasmas YUGO OSANO, ATSUSHI SANO, KOUICHI ONO, TAKAHASHI KAZUO, YUICHI SETSUHARA, *Department of Aeronautics and Astronautics, Kyoro University, Kyoto, Japan* Precise control of etched profiles, critical dimensions, and microscopic uniformity is still one of the most important issues to be addressed in plasma etching technology. This paper presents a modeling of the feature profile evolution during poly-Si gate etching in high-density chlorine-containing plasmas. A key component of the modeling is a full matrix approach with the volume density function in the entire computational domain for the materials being etched. This approach enables us to take into account surface reaction processes of enormous complexity that would occur during etching, particularly multilayer reaction kinetics on feature surfaces. The model includes the transport and surface reaction kinetics of ions and neutrals in microstructural features: neutral adsorption, geometrical shadowing, surface reemission or reflection of ions and neutrals, localized charging of feature surfaces, purely chemical etching, physical sputtering, ion-assisted reactions, and surface

inhibitor deposition and removal. The numerical results showed that a thin passivation layer of surface inhibitors on feature sidewalls, surface temperature, and charging of mask layers play an important role in precise control of the feature profile evolution in gate etch processes.

SRP 58 INNOVATIVE APPLICATIONS OF PLASMAS

SRP 59 Plasma neutralization models for intense ion beam transport in plasma IGOR D. KAGANOVICH, EDWARD A. STARTSEV, RONALD C. DAVIDSON, *Plasma Physics Laboratory, Princeton University, Princeton, NJ 08543* Plasma neutralization of an intense ion pulse is of interest for many applications, including plasma lenses, heavy ion fusion, cosmic ray propagation, etc. An analytical electron fluid model has been developed based on the assumption of long charge bunches. Theoretical predictions are compared with the results of calculations utilizing a particle-in-cell (PIC) code. The cold electron fluid results agree well with the PIC simulations for ion beam propagation through a background plasma. The analytical predictions for the degree of ion beam charge and current neutralization also agree well with the results of the numerical simulations. The model predicts very good charge neutralization (>99% during quasi-steady-state propagation, provided the beam pulse duration is much longer than the electron plasma period. In the opposite limit, the beam pulse excites large-amplitude plasma waves. The analytical formulas derived in this paper can provide an important benchmark for numerical codes, and provide scaling relations for different beam and plasma parameters. See <http://nonneutral.pppl.gov/> for more details.

SRP 60 ECR Plasma Immersion Implanter for SOI Technology MAHMUD RAHMAN, *Santa Clara University* YURI GLUKHOY, *American Advanced Ion Beam* ALEX USENKO, *American Advanced Ion Beam* GOTZE POPOV, *American Advanced Ion Beam* An attempt is made to improve Silicon-on-Insulator (SOI) wafer fabrication process that limits throughput and quality of this method SOI wafers with thickness of the top silicon layer under 25 nm next generations of CMOS technologies is addressed. The key element of PIII is a scalable antenna array for a large area plasma source. SCU proposes the ECR plasma source that consists of the array of the microwave coaxial lines with the distributed slots for leaking of microwaves. Each slot is in superposition with a magnetic gap between surrounded from both sides of slot the magnetic rings and serves as the elementary ECR antenna. The microwaves and magnetic field penetrate through the ceramic tubes enveloped each coaxial line in the gas chamber and develop the resonance plasma zones. According the simulation the density the downstream plasma is 10 E12 cm⁻² in area of the wafer for any size of wafer. The uniformity of the plasma density is also close to 99%. Another advantage of the ECR PIII is the high yield of the protons (90% used for the microbubble formation). But hydrogen implantation in required high dose often results in blistering To eliminate this problem, new Smart Cut-like

technology was suggested (US Pat 6,352,909). In the new process the one-step hydrogen implantation is replaced by two-step process (a) an ion-trap layer has to be formed with 10 E14 - 10 E15 cm⁻² implantation then (b) hydrogen is diffused by processing in hydrogen plasma.

SRP 61 POST-DEADLINE ABSTRACTS

SRP 62 WITHDRAWN

SRP 63 Comparison of kinetic calculation techniques for a pulsed Townsend discharge NUNO PINHÃO, *ITN, Estrada Nacional 10, 2686-953 Sacavém, Portugal* ZOLTAN DONKO, *KFKI, H-1525 Budapest, Hungary* DETLEF LOFFHAGEN, *INP, 17489 Greifswald, Germany* E.A. RICHLEY, *P.O. Box 64, Gaithersburg, MD 2084-0064 USA* MÁRIO PINHEIRO, *IST, 1049-01 Lisboa, Portugal* We present a comparison between the solutions of Boltzmann equation obtained from four different representations of the evdf and a Monte Carlo particle model and applied to the description of a pulsed Townsend discharge in the hydrodynamic regime. The comparison is made in neon at a constant and homogeneous electric field below 500 Td. The importance of non-conservative processes; of taking into account the electron density gradients and the order of the spherical harmonics expansion of the evdf on several transport parameters is analysed. For the isotropic component of the evdf we obtain an excellent agreement between the Boltzmann results from a density gradients expansion representation, a 8-term Legendre expansion, an elliptic

representation and the Monte Carlo results. However the results show that to obtain a correct description of the electron swarm and correct results for the drift velocity and diffusion tensor we need to take into account the non-conservative processes and the e-density gradients. In the conditions studied, it is found that although the two-term velocity expansion is less accurate than the other representations, the relative errors in the corresponding rate coefficients are below the typical experimental error.

SRP 64 Electron Impact Ionization of Diethylzinc* C. Q. JIAO, *Innovative Scientific Solutions, Inc., Dayton, OH* C. A. DEJOSEPH, JR., A. GARSCADDEN, *Air Force Research Laboratory, Wright-Patterson AFB, OH* Diethylzinc is of great interest because of its use as a precursor gas for plasma enhanced chemical vapor deposition of thin films of ZnO, which is one of the more promising materials for producing an ultraviolet laser due to its wide direct band gap and large excitonic binding energy. In this paper, Fourier-transform mass spectrometry (FTMS) is used to study the electron impact ionization of diethylzinc. The ionization of diethylzinc is found to produce the parent ion, $Zn(C_2H_5)_2^+$, and fragment ions including the metal containing ions, $ZnC_2H_5^+$, ZnH^+ and Zn^+ , as well as the organic moiety ions, $C_4H_5^+$, $C_3H_3^+$ and $C_2H_1^+$. At low electron energies (< 23 eV), the metal containing ions $ZnC_2H_5^+$ and $Zn(C_2H_5)_2^+$ dominate the ion population generated by electron impact. The partial ionization cross sections as a function of electron energy within the range 10-200 eV will be presented. If there is a correlation between the neutral dissociation and dissociative ionization, there are significant possible implications of the results on the preferred discharge conditions for efficient thin film deposition.

*This work supported by the Air Force Office of Scientific Research.

SRP 65 WITHDRAWN

SESSION TR1: HIGH PRESSURE DISCHARGES AND ARCS

Thursday afternoon, 23 October 2003; California Ballroom, Cathedral Hill Hotel at 15:30
C.H. Chang, Los Alamos National Laboratory, presiding

Invited Papers

15:30

TR1 1 Spatiotemporal Diagnostics of Excited and Reactive Species in High Pressure Discharges.

KUNIHIDE TACHIBANA, *Department of Electronic Science and Engineering, Kyoto University*

A convenient and effective method to generate glow discharge at around atmospheric pressure is the use of dielectric barrier discharge (DBD), in which the accumulated charge on the electrodes covered with dielectric material works to prevent automatically the over-current leading to filamentary or arc discharge. One of the typical examples is a microdischarge in a PDP (plasma display panel) cell operated at sub-atmospheric pressure in rare-gas mixture, in which VUV radiation from excited Xe atoms and dimmers is used for excitation of RGB phosphors. The dynamics of those species were diagnosed by optical emission spectroscopy (OES) and laser absorption spectroscopy (LAS) using a specially designed cell for the three-dimensional observation. In such a small space, the effects of accumulated charges on the surrounding surfaces become larger on the spatiotemporal behavior of microdischarge. We have been investigating the effects by applying additional pulsed potential onto the third electrode or the side wall for better production efficiency of excited species. As another example, we have been studying the transition between glow and filamentary discharges in a conventional DBD configuration with a gap of mm scale. On the way, we found a self-organization behavior of the

filaments. For understanding the mechanism, the spatiotemporal charge distribution on the dielectric surface is being measured by using the Pockels effect through a thin BSO crystal. Scale down of the DBD is being tried to see the change in the self-organizing behavior. The integration of large numbers of microdischarge is also effective for generating large area atmospheric pressure discharge for various material processing technologies. Such examples will be explained with some diagnostic results of excited and reactive species.

16:00

TR1 2 Neutral Gas Temperature Measurement by Incoherent and Coherent Rayleigh Scattering.

RICHARD MILES, *Princeton University*

The intensity and the spectral characteristics of Rayleigh scattering can be used in weakly ionized plasmas for local measurements of neutral gas density and temperature. Even in an equilibrium glow discharge, these quantities are otherwise difficult to measure due to the low density of the gas and the decoupling of electronic and vibrational modes from translational modes. Two approaches to Rayleigh measurements will be discussed in this talk. The first is the use of optically-thick, atomic and molecular vapor filters, together with tunable narrow linewidth lasers that operate in the vicinity of those optically-thick transitions. The second is the use of Coherent Rayleigh-Brillouin Scattering in a four-wave, nonlinear optical mixing configuration. In the first case, the sharp cut-off nature of the optically-thick filter permits Rayleigh scattering to be observed while background scattering is eliminated. If the gas pressure and species mole fractions are known, this can produce instantaneous, single pulse measurements of temperature. By scanning the laser, lineshape information can be extracted and fit to theory to give temperature, density, and velocity at a single point or in a cross-sectional plane. The Coherent Rayleigh-Brillouin Scattering produces a collimated coherent beam whose amplitude is proportional to the square of the number of molecules having a particular velocity. The density of scatterers is modulated by electric dipole forces from a pair of pump laser beams. A probe beam is coherently scattered and frequency shifted from the density modulated velocity subgroups to give a measurement of the Rayleigh-Brillouin spectral profile. The scattered light exits as a coherent beam, so background scattering is easily suppressed.

Contributed Papers

16:30

TR1 3 Two dimensional simulation of the structure of direct-current microdischarges

PRASHANTH KOTHNUR, *University of Texas at Austin* LAXMINARAYAN RAJA, *University of Texas at Austin*

Microdischarges have gained much attention in the plasma process community for a variety of applications. Proposed applications range from generation of intense UV radiation to maskless etching of thin films. For example, arrays of microhollow cathode discharges are being investigated for applications such as sources of flat panel light sources or electron sources. While some estimates of properties of microdischarges are available, a detailed understanding of the plasma dynamics and chemistry is lacking. The focus of this talk is to explore the fundamental characteristics of microdischarges using two-dimensional computational modeling. The model incorporates a self-consistent representation of the plasma that includes a description of multi-species transport and chemistry, electric field, electron and heavy species energy distributions in the microdischarge. The Poisson's equation is solved for the electric field and species conservation equations for generation and transport of species in the discharge. The electron energy equation is solved to determine the electron temperature distribution and the heavy species energy equation is used to determine the gas temperature. Our studies indicate that the structure of the microdischarge is highly inhomogeneous, and electron temperatures of order several tens of electron volts as well as gas temperatures of order of 1000's of Kelvin are possible. The talk also explores conditions under which the hollow cathode effect occurs in microdischarge geometries, and presents a detailed understanding of the overall microdischarge phenomena.

16:45

TR1 4 Gas and Electron Temperatures in Atmospheric Pressure High-Density Microdischarge Excited by Microwave A.

KONO, K. IWAMOTO, T. KANO, *Nagoya University* A stable high-density ($\sim 10^{15} \text{ cm}^{-3}$) non-equilibrium plasma can be produced in a microgap ($\sim 100 \mu\text{m}$) between two knife-edge elec-

trodes using microwave excitation (Jpn. J. Appl. Phys. 40, L238 (2001)). In an application of the microgap discharge to VUV excimer light sources, the gas temperature is an important parameter. In this study the effect of gas flow on the gas temperature as well as on the electron temperature and electron density in the microgap discharge in atmospheric pressure air and helium was studied using optical emission spectroscopy and laser Thomson scattering; for helium discharge, a small amount of N_2 was admixed to derive the gas temperature from N_2 optical emission. The helium discharge showed significant decrease in the gas temperature with increasing flow rate, whereas the air discharge did not. The optical emission from N_2 was much stronger in the helium discharge and it increased with increasing flow rate; this behavior can be attributed to the change in the electron temperature. Measurements are being extended to He/Ar and He/Xe mixture gases giving excimer emission. (Work supported by Grant 14658131 from Ministry of Education, Culture, Sports, Science and Technology in Japan)

17:00

TR1 5 Radio-Frequency Sustainment of Laser Initiated, High-Pressure Air Constituent Plasmas*

KAMRAN AKHTAR, JOHN SCHARER, SHANE TYSK, MARK DENNING, *Electrical and Computer Engineering Department, University of Wisconsin-Madison 53706*

We investigate the feasibility of creating a high-density $\sim 10^{12} - 10^{14} / \text{cc}$, large volume plasma in air constituents by laser (300 mJ, 20(2) ns) preionization of an organic gas. Tetrakis (dimethyl-amino) ethylene (TMAE) is seeded in high-pressure air constituent gases and then sustained by the efficient absorption of the radio-frequency (RF) power (1-25 kW pulsed) through inductive coupling of the wave fields, thereby reducing the rf initiation power budget. 1 A multi-turn helical antenna is used to couple rf power through a capacitive matching network to sustain the plasma. Plasma density and decay recombination mechanisms with and without the background gas are examined using a 105 GHz interferometer. 2 The effect of gas heating on plasma life-time enhancement through reduced formation of negative oxygen ions will also be presented. Optical emission

spectroscopy is employed to study the process of delayed ionization of the seed gas and RF creation of air constituent plasma and calculate the plasma temperature. RF wave penetration and projection of plasma away from the source region are also examined for different gas flow rates. 1. Kelly K, Scharer J, Paller E, and Ding G, *J. App. Phys.*, 92,698(2002). 2. Akhtar K, Scharer J, Tysk S., and Kho E., *Rev. Sci. Instrum.*, 74, 996 (2003).

*This research is supported by AFOSR Grant F49620-00-1-0181.

17:15

TR1 6 Three-Dimensional Modeling of Arc-Anode Attachments in Transferred Arcs* HE-PING LI, EMIL PFENDER, JOACHIM V. R. HEBERLEIN, *Department of Mechanical Engineering, University of Minnesota, Minneapolis, MN 55455* Studies of the complex non-equilibrium phenomena in the arc-anode attachment region are crucial for improving the performance of current plasma devices. In this paper, physical and mathematical models describing the kinetic and chemical non-equilibrium plasma in a transferred DC arc are presented, using quasi-steady, three-dimensional modeling of a deflected arc plasma exposed to transverse cold gas blowing along the anode surface. A non-commercial software FAST-3D is employed. The modeling results show that the arc will be deflected from its geometrical axis with increasing transverse cold gas flow rate, and the non-equilibrium effects are significant in the arc fringes. Qualitative comparisons with experimental data are also presented in this paper.

*Acknowledgement: The first author has been supported through a postdoctoral fellowship by the Department of Mechanical Engineering, University of Minnesota. The support through a super-computer grant by the University of Minnesota Supercomputing Institute is gratefully acknowledged.

SESSION TR2: FLUOROCARBON ETCH MECHANISMS

Thursday afternoon, 23 October 2003

International Ballroom, Cathedral Hill Hotel at 15:30

J.P. Booth, Ecole Polytechnique, presiding

15:30

TR2 1 Uncertainty analysis of C_4F_8 based plasma chemistry in the gas phase DEEPAK BOSE, *Eloret Corp.* SHAHID RAUF, *Motorola, Inc.* D.B. HASH, T.R. GOVINDAN, *NASA Ames Research Center* Octafluorocyclobutane ($c-C_4F_8$) based plasmas are widely used in the etching of dielectric films. The modeling of these plasmas is, however, severely limited by the uncertainties in the chemical kinetics data. The uncertainties are especially large in the cross sections of electron impact dissociation of C_4F_8 into neutral fragments, and their subsequent dissociation into smaller fluorocarbon radicals. Adequate tracking of these reaction pathways are critical in predicting the densities of CF_x radicals and C and F atoms that are primarily responsible for polymer formation and etching. In this work we assess the propagation of these rate uncertainties into the model outputs using a monte carlo analysis.

We also perform global sensitivity analysis to identify the largest sources of uncertainties and the dominant pathways in the C_4F_8 mechanism. Comparisons with experimental data available in the literature will be made to gain insight and possibly reduce some model uncertainties.

15:45

TR2 2 Etch mechanisms of low-k materials in Inductively Coupled Fluorocarbon Plasmas D. EON, V. RABALLAND, G. CARRY, MC. PEIGNON-FERNANDEZ, CH. CARDINAUD, IMN-LPC COLLABORATION Performances of new generation microelectronic circuits are now limited by the interconnection delay time. In order to reduce this delay time, SiO_2 usual interlevel dielectric ($k = 4.5$) is being replaced by $SiOC$ low-k material ($k = 2.8$) and in the future by porous $SiOC$ material. Control and understanding of their etching is needed for successful integration. We are particularly interested by the etching of these materials in Inductively Coupled Fluorocarbon Plasmas. Etch rate and selectivity are measured by in-situ ellipsometry. In order to determine etch mechanisms, we associate surface and plasma diagnostics. Ion flux is measured by Langmuir and planar probes, radical densities are evaluated by optical emission spectroscopy and mass spectrometry, and finally surface state is investigated by quasi in-situ XPS. Combination of these diagnostics allow us to draw a scheme of materials etching in several mixtures (C_2F_6 with H_2 , O_2 , or Ar) and different plasma conditions (flow rate, pressure, source power, bias power...).

16:00

TR2 3 Role of the fluorocarbon radical in silicon etching: Molecular dynamics simulations DAVID HUMBIRD, *Department of Chemical Engineering, University of California at Berkeley* DAVID B. GRAVES, *Department of Chemical Engineering, University of California at Berkeley* XUEFENG HUA, *Department of Materials Science and Engineering and Institute for Research in Electronics and Applied Physics* GOTTLIEB S. OEHRLEIN, *Department of Materials Science and Engineering and Institute for Research in Electronics and Applied Physics* Molecular dynamics (MD) simulations of inert and fluorocarbon (FC) ions and FC radicals impacting Si are compared to experimental measurements. During FC plasma etching of Si, Oehrlein and coworkers observe changes in surface chemistry as ion energy is increased above the threshold necessary for etching. The F/C ratio of the film decreases and Si-C, C-C, and Si-F bonds all increase in number with the onset of etching. These results were interpreted to mean that F is driven from the FC film into the underlying Si to initiate etching. In simulations of Si etching with CF_2 radicals and Ar^+ , we observe a change in the composition of the FC film as the ion energy increases from a depositing to an etching level. The FC film formed at lower energy consists almost entirely of $C-F_x$ groups. At higher energy (> 50 eV), Ar^+ efficiently separates F from C, mixing it with the underlying Si to create etch products. These results are in excellent agreement with experimental measurements of Si samples etched by FC plasmas. Oehrlein and co-workers concluded from their measurements that the FC film is the source of the etchant F. The simulations highlight the role of FC radicals in creating the FC film and confirm that ion-induced F transport to underlying Si occurs by way of this film.

16:15

TR2 4 Plasma parametric study in an ICP reactor and etching optimization REMI DUSSART, GREMI PHILIPPE LEFAUCHEUX, GREMI THOMAS TILLOCHER, GREMI PIERRE RANSON, GREMI PASCAL CHABERT, LPTP GREMI TEAM, LPTP COLLABORATION Silicon deep etching is investigated using the so-called cryogenic process in SF₆/O₂ plasma. An Alcatel 601 Etcher (ICP reactor) was used for the experiments. A new configuration was installed providing an injected power as high as 3000 W and an SF₆ flow as high as 1000 sccm. MEMS devices and power microelectronic components are structured with this process. The etching rate was measured in situ and optimized by using large mask patterns in SiO₂ and reflectometry setup. Langmuir probe measurements were performed indicating some different regimes as a function of the incident power. In low power conditions, the plasma seems very electronegative. In intermediate regime, the plasma is perturbed inducing some instabilities on the probe characteristic. Finally, in high power conditions, the characteristics is much more regular with a high electron current in the right part of the characteristic. Negative ion density is evaluated with a 2 Langmuir probe setup. Electron density was measured for different SF₆ flows. A maximum can be obtained at constant pressure. This maximum is shifted toward higher flow rates when the power is increased.

16:30

TR2 5 Etching of High Aspect Ratio Structures in Si using SF₆-O₂ Plasmas SERGI GOMEZ, JUN BELEN, ERAY S. AYDIL, *University of California Santa Barbara, Santa Barbara, CA* DAVID COOPERBERG, MARK KIEHLBAUCH, *Lam Research Corporation, Fremont, CA* There is increasing interest in plasma etching of high aspect ratio structures in Si for semiconductor processing. We have investigated etching of deep features (~ 10 μm) using low pressure (5-80 mTorr), high density, inductively coupled plasmas maintained in mixtures of SF₆ and O₂ gases, with a biased substrate. Various plasma diagnostics, scanning electron microscopy and feature profile evolution simulations were used to understand the key factors that control the anisotropy, selectivity and etch rate. Oxygen ionization and dissociation products (O and O⁺) oxidize the feature sidewalls and help achieve anisotropic etching through the sidewall passivation mechanism. F-to-ion flux ratio and F-to-O flux ratio are found to be the important internal plasma parameters that determine the etch rate and anisotropy. These internal plasma properties can be manipulated using the SF₆-to-O₂ ratio in the feed gas and the chamber pressure. In conjunction with experiments, we have developed a semi-empirical feature scale model of SF₆/O₂ plasma etching of Si to determine the phenomena that are important in feature profile evolution and to quantify etching kinetics.

16:45

TR2 6 Etching silicon by SF₆ in a continuous and pulsed power helicon reactor ANDREW HERRICK, ANDREW PERRY, ROD BOSWELL, *Australian National University* The etch rate of silicon by SF₆ in a helicon reactor has been measured along with simultaneous actinometric measurements of the concentration of atomic fluorine in the gas phase for a variety of gas flow rates resulting in pressures in the milli-Torr range. A bias rf power was applied to the substrate to investigate the effect of ion

energy on the etch rate. The etch rate was found to be proportional to the fluorine concentration and independent of the bias for the higher gas flow rates. However, at lower flow rates, the situation was more complicated and no simple model can explain the measurements. Measurements of the etch rate were also made in the afterglow of a repetitively pulsed discharge so that the ion energy would be reduced to the thermal motion after the rapid collapse of the plasma potential. A simple model was developed to explain the temporal etching phenomena in terms of the lifetime of the atomic fluorine.

17:00

TR2 7 Toward charging free plasma etching: Insitu measurement of negative charge injection and charge reduction in a contact hole TAKESHI OHMORI, *Keio University, Yokohama, Japan* TOSHIAKI MAKABE, *Keio University, Yokohama, Japan* It will be essential to develop in-situ diagnostics for damage free plasma etching in the interface under close and complementary cooperation between optical and electric procedure in a top-down nanoscale etching. In our previous paper[1], we have applied an emission selected computerized tomography close to the wafer exposed to plasma etching, in order to investigate the polarity and the phase of high energy charged particles incident on the wafer, biased deeply by a low frequency source in RIE. A reduction in charging voltage on a contact hole bottom of SiO₂ was validated in the pulsed plasma power source in the 2f-CCP in CF₄/Ar, by using a dual measurement system consisting of a temporal emission CT and a contact hole charging voltage. In the present work, detailed correlational results of the reduction in the charging voltage are shown as a function of phase and amplitude of the single bias pulse at 500 kHz. Discussion is focused both on the injection mechanism of energetic negative charges to the wafer and on the magnitude of the negative charges. As a result, during the off-period 10 us of VHF power source in the dual pulsed 2f-CCP, it is confirmed that; 1) the magnitude of the injected negative charge increases with increasing the on-time of the single bias pulse, and a strong reduction in the charging voltage is performed, 2) a strong negative self-bias-voltage is always kept to have an efficient RIE under energetic positive ion impact on the wafer except for the period of the single bias pulse. Some of predictive story will be also introduced by VicAddress. 1) T. Ohmori, T.K. Goto, T. Kitajima, and T. Makabe, Proc. of Dry Process Symposium 165(2002)Tokyo, and Appl. Phys. Lett. (submitted).

17:15

TR2 8 Validity of Binary Collision Theory in Ion-Surface Interactions at 50-500 eV MICHAEL GORDON, *California Institute of Technology* KOSTAS GIAPIS, *California Institute of Technology* Ion-surface interactions in the 50-500 eV regime have become increasingly important in plasma processing. Concerns exist in literature about the validity of the binary collision approximation (BCA) at low impact energies because peculiarities are frequently seen in the scattered ion energy distribution. Sub-surface processes, multiple bouncing, and super-elastic phenomena have all been hypothesized. This talk will explore the usefulness of BCA theory in predicting energy transfer during ion-surface collisions in the 50-500 eV energy range. Well-defined beams of rare gas ions (Ne, Ar, Kr) were scattered off semicon-

ductor (Si, Ge) and metal surfaces (Ag, Au, Ni, Nb) to measure energy loss upon impact. The ion beams were produced from a floating ICP reactor coupled to a small accelerator beamline for transport and mass filtering. Exit channel energies were measured using a 90 degree electrostatic sector coupled to a quadrupole mass filter with single ion detection capability. Although the BCA

presents an over-simplified picture of the collision process, our results demonstrate that it is remarkably accurate in the low energy range for a variety of projectile-target combinations. In addition, reactive ion scattering of O_2^+ and O^+ on inert and reactive surfaces (Au vs. Ag, Pt) suggests there may be rather high energy threshold processes which determine exit channel selectivity.

SESSION VF1: BIOLOGICAL APPLICATIONS OF PLASMAS II

Friday morning, 24 October 2003; California Ballroom, Cathedral Hill Hotel at 8:00

Thomas N. Rescigno, Lawrence Berkeley National Laboratory, presiding

*Invited Papers***8:00****VF1 1 Electron impact ionization of water molecules.**BIRGIT LOHMANN,* *Centre for Quantum Dynamics, Griffith University, Nathan, Queensland, Australia 4111*

Electron impact ionization is an important fundamental collision process which plays a significant role in areas as diverse as plasma physics, astrophysics, atmospheric modelling, discharge physics and radiobiology. Studies of the early stages of radiation damage in biological material, for example, reveal that low energy secondary electrons are responsible for much of the damage. Charged particle track structure analysis is a powerful tool for modelling the interaction of such electrons with matter in biological systems, but these techniques require reliable data on electron impact ionization cross sections. One of the most important species in biological systems is water, which constitutes about 80% of the body. In this talk I will discuss our recent measurements of electron impact ionization of single, gas phase, water molecules. The experiments have been performed with coincidence detection of the outgoing particles, enabling specification of a particular single ionization event. We have measured the probability for the ejected electron to be emitted at various angles, under conditions where the scattered electron is emitted at a fixed angle to the incident beam direction. Recent calculations of this process, originally developed for use in track structure analysis models, will be compared with the experimental data. These calculations represent the most sophisticated available to date for electron impact ionization of water molecules. The results indicate that the theoretical calculations completely neglect backward emission of the ejected electron, which has significant implications for charged particle track structure models relying on these calculated cross sections.

*D. Milne-Brownlie, S. J. Cavanagh.

8:30**VF1 2 Ultrafast reactions of energetic species produced by ionizing radiation.**SIMON PIMBLOTT, *Radiation Laboratory, University of Notre Dame, Notre Dame, IN 46556-0579*

As an ionizing radiation particle passes through water, it leaves in its wake clusters of low-energy electrons, and highly reactive molecular ions and excited states. The relative spatial distribution of these clusters depends upon the nature and the velocity of the ionizing radiation. For instance for energetic electrons the clusters are well separated (low-LET), while for alpha particles the clusters overlap (high-LET). The physical, physico-chemical and chemical processes that occur on a sub-picosecond time scale in the track of clusters are not well characterized. The principal questions concern (i) the attenuation, reaction, trapping, thermalization and solvation of low-energy electrons, and (ii) the fates of the excited states of water, the molecular cation, H_2O^+ , and the cluster anions, $(\text{H}_2\text{O})_n^-$, in the liquid phase. There is information on some of these processes in the gas phase, and limited data for water ice and water clusters, but essentially nothing is known for bulk liquid water: Photochemical studies of the dynamics of the precursors to the hydrated electron have identified several different states. In addition, radiation chemical studies have demonstrated that precursors to the hydrated electron play a dominant role in the sub-picosecond formation of H_2 in both low-LET and high-LET radiolysis. A dissociative electron recombination reaction involving a second radiation-induced transient, either the radical cation H_2O^+ or the pre-hydrated H_3O^+ ion, has been identified as the dominant source of sub-picosecond H_2 in high-LET radiolysis of water; however, other mechanisms cannot be discounted as contributing pathways in low-LET radiolysis. The chemistry of H_2O^+ , H_2O^* and $(\text{H}_2\text{O})_n^-$ in water is not only significant in the production of H_2 , these species also represent the precursors to the oxidizing radicals, OH (O^-), O and HO_2 , and the molecular species, O_2 and H_2O_2 . The yields of OH and other reactive oxygen species have been traditionally hard to quantify. To demonstrate the significance of the short-lived precursor species, their reactions in low- and high-LET radiolysis will be compared and contrasted and their influence on observed radiation effects will be discussed.

Contributed Papers

9:00

VF1 3 Ion Beam Bombardment of Biological Tissue S. SANGYUENYONGPIPAT, *Dept. of Physics, Chiang Mai University, Thailand* L. D. YU, *Dept. of Physics, Chiang Mai University, Thailand* T. VILAITHONG, *Dept. of Physics, Chiang Mai University, Thailand* B. PHANCHAISRI, *Institute for Science and Technology R&D, Chiang Mai University, Thailand* S. ANUNTA-LABHOCHAI, *Dept. of Biology, Chiang Mai University, Thailand* I. G. BROWN, *Lawrence Berkeley National Laboratory, Berkeley, CA* While ion implantation has become a well-established technique for the surface modification of inorganic materials, the ion bombardment of cellular tissue has received little research attention. A program in ion beam bioengineering has been initiated at Chiang Mai University, and the ion beam induced transfer of plasmid DNA molecules into bacterial cells (*E. coli*) has been demonstrated. Subsequent work has been directed toward exploration of ion beam bombardment of plant cells in an effort to understand the possible mechanisms involved in the DNA transfer. In particular, ion beam bombardment of onion cells was carried out and the effects investigated. Among the novel features observed is the formation of "microcraters" sub-micron surface features that could provide a pathway for the transfer of large molecules into the interior cell region. Here we describe our onion skin ion bombardment investigations.

9:15

VF1 4 Non-Equilibrium Modeling of Warm Dense Matter HYUN-KYUNG CHUNG, *LLNL* W. LOWELL MORGAN, *Kinema Research & Software* RICHARD W. LEE, *LLNL* The advent of high brightness femtosecond hard x-ray free electron lasers will provide a new and challenging regime for plasma research. Illumination of solid materials by such light sources will produce highly non-equilibrium plasmas on time scales of tens of femtosecond having mean electron energies in the 1-10 eV range, very non-thermal electron energy distributions, and cold ions at near solid state density. We will discuss our research on modeling the plasma spectroscopy of such warm dense matter [1,2] with emphasis on treating the electron interactions and non-Maxwell-Boltzmann energy distributions. 1. R. W. Lee, et al., *Laser and Particle Beams* 20, 527 (2002). 2. R. W. Lee, et al. *J. Opt. Soc. Am B* 20, 770 (2003).

SESSION VF2: MAGNETICALLY-ENHANCED PLASMAS

Friday morning, 24 October 2003

International Ballroom, Cathedral Hill Hotel at 8:00

E. Stamate, Nagoya University, presiding

8:00

VF2 1 Observation of Solitons in a Pulsed Magnetron Sputtering Discharge JON TOMAS GUDMUNDSSON, *Department of Electrical and Computer Engineering, University of Iceland, Hjardarhaga 2-6, IS-107 Reykjavik, Iceland* KRISTINN B. GYL-FASON, *Department of Electrical and Computer Engineering, University of Iceland, Hjardarhaga 2-6, IS-107 Reykjavik, Iceland*

JONES ALAMI, *Department of Physics and Measurement Technology, Linköping University, SE-581 83, Linköping, Sweden* JOHAN BÖHLMARK, *Department of Physics and Measurement Technology, Linköping University, SE-581 83, Linköping, Sweden* ULF HELMERSSON, *Department of Physics and Measurement Technology, Linköping University, SE-581 83, Linköping, Sweden* We report on the formation of multiple ion acoustic solitons in an unipolar pulsed magnetron plasma. A high density plasma ($\sim 10^{18} \text{ cm}^{-3}$) is created by applying a high power pulse (3 – 7 J) with pulse length 100 μs and repetition frequency 50 Hz to a planar magnetron discharge. The temporal behaviour of the electron density measured by a Langmuir probe shows oscillations as the plasma density decays. We relate these oscillations to solitons traveling away from the target. The velocity, width, and amplitude characteristics of the soliton are found to be in agreement with the basic properties of the soliton solutions of the Korteweg-de Vries equation. Furthermore, we demonstrate how the decay of the soliton along the axis indicates spherical symmetry of the soliton propagation. The speed of the soliton along the axis of the discharge decreases with increased gas pressure.

8:15

VF2 2 Developing electrical probes for measuring fast changes in plasma properties in pulsed low-pressure discharges S. K. KARKARI, A. M. VETUSHKA, J. W. BRADLEY, *UMIST* There has been much recent interest in the investigation of the plasma parameters in pulsed dc magnetron discharges, since these sources are now widely used in industry to produce engineering quality thin films and coatings, including optical materials. The quality of the depositing films can be related to the intrinsic plasma properties, such as the plasma potential V_p , the plasma density n_e , the electron temperature T_e , which vary as a function of time during pulsed period. These parameters determine the ion energy and ion flux arriving on the substrate. Simple diagnostic tools, such as electrical probes can give valuable information on the plasma properties, provided the probe is designed properly to respond at high frequency, for instance, in our bi-polar pulsed magnetron at pulsed repetition rates of 100 kHz with transients in discharge voltage and current occurring typically at 10MHz. In this study, we report on the technique of using the electrical probes, such as the emissive probes, double and single Langmuir probes, to obtain time-resolved measurements in such pulsed plasmas. The probes are capacitively coupled to the adjacent a.c. plasma potential fluctuation through a pickup metal foil. Using these probes we have obtained, for the first time, the temporal change in plasma potential and the complete probe characteristic during transient phases of the discharge. A time resolution of 100ns can be achieved with this technique. The time variation in plasma properties such as V_p , T_e , and n_e , obtained using these techniques, will be presented.

8:30

VF2 3 Characterisation of the diffusion chamber of a helicon source for materials processing CORMAC CORR, NICOLAS PLIHON, PASCAL CHABERT, *Laboratoire de Physique et Technologie des Plasmas, Ecole Polytechnique, 91128 Palaiseau, France* ROD BOSWELL, *Space Plasma and Plasma Processing Group, Plasma Research Laboratory, Research School of Physical Sciences and Engineering, The Australian National Laboratory, Canberra, Australia* Helicon plasma sources [1] have generated much interest due to their ability to produce high etch rates and high selectivity [2]. They are being studied not only for use in industrial applications such as plasma processing for micro-electronic circuits but also for the understanding of basic plasma

physics processes. Here, we present measurements of the basic plasma parameters in low-pressure electropositive and electronegative helicon plasmas. In the electropositive gas argon we have measured ion related instabilities with frequencies around 100 kHz near the edge of the plasma. Lower frequencies of 10 kHz are also often observed. Whether these instabilities are generated by gradients in plasma parameters at the edge or are a result of parametric decay from the helicon wave is being investigated. The introduction of negative ions complicates the discharge structure and chemistry. Attaching gases change the positive ion flux, can induce plasma instabilities and significantly alter plasma transport processes. These topics will also be discussed. [1] Boswell R W 1984 Plasma Phys. 26 1147 [2] Chabert P 2001 J. Vac. Sci. Technol. B 19 1339

8:45

VF2 4 Plasma beam generation from a helicon current-free double-layer CHRISTINE CHARLES,* ROD BOSWELL, *The Australian National University* A current-free electric double-layer has been experimentally observed in an expanding, high-density helicon sustained rf (13.56 MHz) discharge. The double-layer accelerates the ions to form a plasma beam which is characterized using a retarding field energy analyser. Axial and radial measurements of the ion energy distribution functions are obtained for various rf powers, operating pressures, magnetic field configurations and gases (Argon, Hydrogen...). This experiment differs from others in that the potentials are self-consistently generated by the plasma itself and there is no current flowing through an external circuit. Pulsed excitation is also used to get some insight into the double-layer formation during plasma breakdown and to study its temporal stability. This system can be applied to plasma propulsion.

*also at CNRS (Centre National de la Recherche Scientifique), France

9:00

VF2 5 Experimental Measurements and Modeling of a Helicon Plasma Source with Large Axial Density Gradients* SHANE TYSK, MARK DENNING, JOHN SCHARER, KAMRAN AKHTAR, *University of Wisconsin, Madison* Wave magnetic field, density and temperature profiles, electron distribution function and wave-correlated Argon optical emission are examined. The experimental facility is a 10 cm ID magnetized Pyrex tube and up to 1.3 kW of pulsed RF power is coupled to a half-turn, double-helix antenna with densities of 10^{11} - 5×10^{13} cm⁻³. The plasmas have different characteristics than the type-III coil and WOMBAT2 experiments. Wave-correlated optical emission and modulation is externally measured at Ar II 443 nm and phase-correlated with the 13.56 MHz source. The plasma, wave character and optical emission characteristics of the transition and helicon modes are examined. Helicon wave harmonic components of the antenna current driving frequency are also observed. The Ar II wave phase-correlated optical emission character is different for the transition and helicon regimes. The 2-D MaxEB and 1-D AntennaII codes and an ionization code are used to model the conditions present in the system and provide a comprehensive picture of wave field behavior and fast and thermal electron ionization processes in the source. 1 X. Guo, J.E. Scharer, Y. Mouzouris and L. Louis, *Physics of Plasmas* 6 (8), 3400 (1999). 2 J. Scharer, A. Degeling, G. Borg, and R. Boswell, *Physics of Plasmas* 9 (9), 3734 (2002). *Research supported by NSF and AFOSR

9:15

VF2 6 Particle Modeling of Plasma Confinement by a Multipolar Magnetic Field HIDEOTO TAKEKIDA, KENICHI NANBU, *Institute of Fluid Science* Multipolar plasma chambers have widely been used in basic and applied researches on low temperature plasmas. The multipolar confinement realizes enhanced plasma density, homogeneous plasma of a large volume, and quiescent plasmas. However, detailed theoretical studies on the multipolar confinement are few. Plasma confinement was studied using a self-consistent particle modeling of discharges in a cylinder sustained by electron emission from a heated filament at the central axis of the cylinder. The goal is to present design criteria of multipolar magnetic field. Use of the present method makes it possible to treat three effects of plasma confinement all together; (1) magnetic mirror effect near the cusp of two poles, (2) suppressed electron diffusion in the direction normal to magnetic field line, and (3) electron repelling in the sheath on the chamber wall. It was shown that electron number density for $B=0.1T$ is higher by 905mTorr. And also it was shown that as the pressure becomes lower than 10mTorr, the confinement is more effective. In addition, the plasma potential in plasma bulk has a negative value when the magnetic field confines plasma.

SESSION WF1: DIAGNOSTICS II

Friday morning, 24 October 2003

California Ballroom, Cathedral Hill Hotel at 10:00

Eric Hudson, Lam Research Corporation, presiding

10:00

WF1 1 Measurement of Electrical Fields Around Dissimilar Materials Exposed to a Discharge E. V. BARNAT, *Sandia National Laboratories* G. A. HEBNER, *Sandia National Laboratories* The nature of a surface/plasma boundary can have an important impact on the processes that occur both in the plasma and on the bounding surface. In this work, fluorescence-dip spectroscopy is used to study the surface dependant sheath structure at the boundary of an argon glow discharge. The two laser technique monitors the variation in the fluorescence from an intermediate state caused by laser excitation from this intermediate state to Stark-shifted Rydberg levels sensitive to the electric fields present in the sheath. To demonstrate the effectiveness of the dip-spectroscopy technique, half of a conducting electrode is covered with an insulating surface and both spatially and temporally resolved measurements of the structure of the sheath are made around both the conducting and the non-conducting surfaces. The fields through the sheath above the two surfaces, the potential drops across the sheath, and the fields near the surface along the electrode are discussed for various discharge conditions. This work was supported by the Division of Material Sciences, BES, Office of Science, U. S. Department of Energy and Sandia National Laboratories, a multiprogram laboratory operated by Sandia Corporation, a Lockheed Martin Company for the United States Department of Energy's National Nuclear Security Administration under contract DE-AC04-94AL85000.

10:15

WF1 2 Reactive Ion Etching of SiC in SF₆/He Plasmas RAMAKANTH ALAPATI, KAREN J. NORDHEDEN, *Plasma Research Laboratory, Chemical & Petroleum Engineering, University of Kansas, Lawrence, KS 66045* Etch rates of greater than 400 Å/min have been achieved for 6H SiC in a Plasma Therm 790 RIE system using SF₆/He gas mixtures. Both pressure and composition are strong determining factors in optimizing the etch rate. For an rf power of 175 W, the etch rate maximizes at a pressure of 125 mTorr and a composition of 50% SF₆. Microwave measurements indicate that the addition of helium results in an increase in the average electron density, although significant electron attachment is apparent. The electron density also exhibits a maximum at a pressure of 125 mTorr. Optical emission spectroscopy shows that the addition of helium results in increased emission of F and F₂, and these emissions also exhibit maxima at a pressure of 125 mTorr. The higher electron density and possibility of increased electron temperature, as a result of electron attachment heating, are believed to be responsible for an increase in the dissociation of SF₆ which results in an enhanced SiC etch rate.

10:30

WF1 3 Collisional Excitation and De-Excitation of N₂ and N₂⁺ in a High-Pressure Cylindrical Dielectric Barrier Discharge Plasma K. MARTUS, *William Paterson University* N. MASOUD, *Stevens Institute of Technology* K. BECKER, *Stevens Institute of Technology* The emissions from a high-pressure cylindrical Dielectric Barrier Discharges (DBDs) in a mixture of Ne and N₂ have been analyzed in this work. The discharge source consists of a 1/4" dielectric tube with two outer electrodes and the discharge is sustained by RF power at 13.56MHz. Emission spectroscopy using the 2nd positive system of N₂ and the 1st negative system of N₂⁺ was used to determine the translational, vibrational, and rotational temperatures of the plasma species. The rotational temperature is perhaps the most frequently determined quantity as its determination may reflect the gas temperature in the plasma and/or provide insight into the reaction kinetics of important plasma species. If the emitting species are in equilibrium with the bulk gas in the plasma, then this temperature can be interpreted as the gas kinetic temperature in the plasma. The rotational temperatures for N₂ and N₂⁺ in high-pressure discharges in mixtures in Ne with a trace admixture of N₂ will be presented and discussed. Work supported by the NSF and through the WPUNJ ART Program

10:45

WF1 4 Sensitive Detection of Singlet O₂ via the Noxon System SKIP WILLIAMS, *Air Force Research Laboratory* MANISH GUPTA, *Los Gatos Research, Inc.* THOMAS OWANO, *Los Gatos Research, Inc.* DOUG BAER, *Los Gatos Research, Inc.* ANTHONY O'KEEFE, *Los Gatos Research, Inc.* DAVID YARKONY, *Department of Chemistry, Johns Hopkins University* SPIRIDOULA MATSIKA, *Department of Chemistry, Johns Hopkins University* AIR FORCE RESEARCH LABORATORY COLLABORATION, LOS GATOS RESEARCH, INC. COLLABORATION, DEPARTMENT OF CHEMISTRY, JOHNS HOPKINS UNIVERSITY COLLABORATION A method for the practical determination of the absolute concentration of singlet oxygen is being developed as part of a collaboration between the Air Force Research Laboratory, Los Gatos Research, Inc. and Johns Hopkins University. The benefits of the development of such a singlet oxygen detection system include: Measuring the efficiency of singlet oxygen generators; analyzing electrically-driven COIL devices;

and studying singlet oxygen chemistry in air plasmas and plasma enhanced combustors. The method is based on sensitive off-axis integrated-cavity-output spectroscopy (ICOS). ICOS allows narrowband, continuous-wave lasers to be used in conjunction with optical cavities in a simple and effective manner. The absorption signal is obtained through the temporal integration of the laser intensity transmitted through the cavity in the same fashion as in conventional absorption measurements. The absolute transition probabilities are not known for the b¹Sg⁺-a¹Dg Noxon system and are being determined by chemical kinetic experiments and quantum chemistry theory. The details of the method as well as spectroscopic data confirming first ever observation of the (0,1) band of this system will be presented.

11:00

WF1 5 Attractive Interactions Between Negatively Charged Dust Particles in a Plasma GREG HEBNER, *Sandia National Laboratories* MERLE RILEY, *Sandia National Laboratories* Plasma dust particle interactions, charges, and screening lengths are derived from measurements of time-dependent particle positions in a simplified geometry. The magnitude and structure of the ion wakefield potential below a negatively-charged dust particle levitated in the plasma sheath region were measured as functions of the pressure and interparticle spacing. Attractive and repulsive components of the interaction force were extracted from a trajectory analysis of low-energy dust collisions between different mass particles in a well-defined electrostatic potential that constrained the dynamics of the collisions to be one dimensional. Typical peak attractions varied between 60 and 230 fN while the peak particle-particle repulsion was on the order of 60 fN. Random thermal motion of the particles contributed to observable rates for transitions between different equilibrium configurations of vertically separated particles. We also observed a slight potential barrier that impeded the formation of vertically aligned pairs. The influence of nearest- and non-nearest-neighbor interactions on calculated particle parameters are examined using several methods. Implications for plasma / surface interactions and plasma dielectric charging will be discussed. This work was supported by the Division of Material Sciences, BES, Office of Science, U. S. Department of Energy and Sandia National Laboratories, a multiprogram laboratory operated by Sandia Corporation, a Lockheed Martin Company for the United States Department of Energy's National Nuclear Security Administration under contract DE-AC04-94AL85000.

11:15

WF1 6 On Quantitative Detection of Methyl Radicals in Non-Equilibrium Plasmas by Absorption Spectroscopic Techniques J. RÖPCKE, G.D. STANCU, F. HEMPEL, *Institut für Niedertemperatur-Plasmaphysik, Greifswald, Germany* G. LOMBARDI, A. GICQUEL, *LIMHP-CNRS, Université Paris 13, Villetaneuse, France* Tuneable infrared diode laser absorption spectroscopy at 16.5 μm and broadband ultraviolet absorption spectroscopy at 216 nm have both been used to measure the ground state concentrations of the methyl radical in two different types of non-equilibrium microwave plasmas (f = 2.45 GHz), (i) in H₂-Ar plasmas of a planar reactor with small admixtures of methane or methanol, at a pressure of 1.5 mbar, and (ii) in H₂-CH₄ plasmas of a bell jar reactor, at pressures of 25 and 32 mbar under flowing conditions. For the first time, two different optical techniques have been directly compared to verify the available data about absorption cross sections and line strengths of the methyl radical. It was found, that the application of the CH₃ ab-

sorption cross section of the $B(^2A_1') \leftarrow X(^2A_2'')$ transition at 216 nm, reported by Davidson et al.¹, and of the line strength of the Q(8,8) line of the ν_2 fundamental band, given by Wormhoudt et al.², leads to satisfactory agreement.

¹Davidson et al. 1995 *J. Quant. Spectrosc. Radiat. Transfer* **53** 581

²Wormhoudt et al. 1989 *Chem. Phys. Lett.* **156** 47

11:30

WF1 7 Optical Time Modulation Spectroscopy in RF-Discharges UWE CZARNETZKI, VICTOR KADETOV, *Institut für Plasma- und Atomphysik, Ruhr-Universität Bochum, Germany*
In RF-discharges, the time varying electric fields within the dis-

charge cause a periodic modulation of the isotropic part of the electron energy distribution function. The modulation amplitude is proportional to the square of the electric field amplitude and increases with the electron energy. Highly excited states in atoms or molecules are excited by electrons in the tail of the distribution function where the modulation is particularly strong. Therefore, also the optical emission from these states is temporally modulated. Phase resolved detection of the emission and normalisation to the period average allows a simple and direct measurement of the modulation amplitude. If the measurement is performed also spatially resolved, one obtains a direct map of the relative electric field amplitude in the discharge. The complex conductivity of the plasma is linked to the field distribution by the Helmholtz equation. This allows in principle a direct determination of the plasma density distribution and the collision frequency without the need of a collision-radiative model. First measurements in an inductively coupled plasma in hydrogen where the Balmer-alpha line is observed are presented.

SESSION WF2: LIGHTING II

Friday morning, 24 October 2003; International Ballroom, Cathedral Hill Hotel at 10:00

Vikas Midha, GE Research Laboratory, presiding

Invited Papers

10:00

WF2 1 Low-Pressure Xenon Positive Column Plasmas for Lighting Purpose: A Model Investigation.

DIRK UHRLANDT,* *Institut für Niedertemperatur-Plasmaphysik, Greifswald, Germany*

For environmental reasons, the replacement of mercury in conventional fluorescent lamps by other components is highly desired. Column plasmas of low-pressure discharges in appropriate rare-gas mixtures including xenon can be used as alternatives for the generation of VUV radiation in specific cases. Light sources based on rare-gas glow discharges have favorable features like a temperature-independent and instant light output after ignition. Disadvantages are up to now the lower radiation efficiency and output power. Current research focusses on the replacement of the gas mixture in conventional fluorescent lamps with minimum changes in the lamp construction and technology and the maintenance of a stable discharge operation. This research is assisted by a theoretical study of the positive column plasma in such low-pressure glows. A self-consistent hybrid model of the cylindrical dc column plasma is used to analyse the plasma properties and their variation with the total gas pressure, the tube radius and the discharge current. Results for He/Xe mixtures are compared with probe and spectroscopic measurements. Operation conditions for an optimum efficiency and output power of the VUV radiation are predicted. The hybrid model comprises a self-consistent determination of the axial heating field and the radial space-charge field as well as a spatially resolved description of all important plasma components, in particular, a kinetic treatment of the electrons. It yields an improved understanding of the non-local power balance and the mechanisms of the radiation generation in the positive column plasma. Comprehensive balance descriptions of the excited states of the mixture components are included in the model. Therefore, the contributions of the different gas components and their excited states to the power balance and the radiation output can be studied in detail for complex rare-gas mixtures. Results are presented for mixtures of He/Xe and He/Ne/Xe. The impact of Xe admixtures as well as the role of the buffer gases are discussed.

*In collaboration with Serguei Gortchakov and supported by the Bundesministerium für Bildung und Forschung.

10:30

WF2 2 Calculations of Electron Collision Cross Sections for Lighting Applications.*

KLAUS BARTSCHAT, *Department of Physics and Astronomy, Drake University, Des Moines, IA 50311, USA*

In recent years, much progress has been achieved in calculating reliable cross-section data for electron scattering from atoms and ions. In particular, the "convergent close-coupling" (CCC) [1] and "R-matrix with pseudo-states" (RMPS) [2] methods have been extremely successful in describing elastic scattering as well as electron-impact excitation and ionization of light quasi-one and quasi-two electron targets, such as atomic hydrogen, helium, the alkalis, and the alkali-earth elements. Despite this progress in the numerical treatment of electron-atom collisions, there are still significant challenges that need to be addressed [3]. Specifically, the available data for electron collisions with noble gases other than helium (i.e., Ne, Ar, Kr, and Xe) are scarce and neither measurements nor theoretical predictions can realistically claim a high degree of accuracy. The same assessment holds for other heavy targets, such as Zn, Ba, or Hg,

particularly in the low-energy near-threshold resonance region. Finally, the field is wide open for truly complex targets such as Mo, which is a promising candidate for a mercury-free lighting concept, and other transition elements. In this talk, the current status of the theoretical treatment of electron collisions with heavy complex targets will be reviewed, with special emphasis on systems of interest for plasma processing and the lighting industry.

I. Bray, D.V. Fursa, A.S. Kheifets, and A.T. Stelbovics, *J. Phys. B* **35**, R117 (2002).

K. Bartschat, *Comp. Phys. Commun.* **114**, 168 (1998).

K. Bartschat, in *Atomic and Molecular Data and Their Applications*, D.R. Schultz, P.R. Krstic, and F. Owbny (eds.), AIP Conf. Proc. #636, 192 (2002).

*This work is supported by the National Science Foundation under grant PHY-0244470.

Contributed Papers

11:00

WF2 3 Measurement of the conductivity of the luminous high-pressure plasmoids generated by microwave discharges of molecular vapors* JIN JOONG KIM,[†] JUNG TAE KO, DONG HO WON, *Dept of Optical Engineering, Sejong University* JEONG WON KIM, *Taewon Lighting R&D Laboratory* We report on the measurement of the conductivity of the plasmoids in the pressure range of 100-400 kPa. The luminous high-pressure plasmoids are generated by microwave discharges of molecular vapors, including di-sulfur (S₂) and indium-monobromide (InBr), filled in a spherical ball of 3-cm-dia located in a cylindrical waveguide. Using a commercial microwave simulator (CST MWS) we designed and constructed a waveguide system that generates circularly polarized microwaves at 2.45 GHz. At the location of the highest electric field of TE₁₁ mode, we place a quartz ball filled with 10 Torr of argon gas and a few mg of a molecular fill at room temperature. When the microwave discharges are full-blown up to 1.2 kW, we move the ball to the position where the power absorption is a maximum. The effective conductivity of the plasmoid is then determined by iteration of the microwave simulator using the new position. We obtain the conductivity values in the range of 0.8-8.0 siemens/m, depending on the microwave input power. This is in good agreement with the results previously calculated by using a plasma modeling [1]. I. C. W. Johnston, et al., *J. Phys. D*: **35** (2002) 342-351

*Work supported by a contract from the Korean Ministry of Commerce, Industry, and Energy

[†]Also with Taewon Lighting R&D Laboratory

11:15

WF2 4 Numerical modelling of stability limit of diffuse discharge on thermionic cathodes* M. S. BENILOV, *Departamento de Fisica, Universidade da Madeira, Largo do Municipio, 9000 Funchal, Portugal* M. D. CUNHA, *Departamento de Fisica, Universidade da Madeira, Largo do Municipio, 9000 Funchal, Portugal* Steady-state current transfer from arc plasmas to axially symmetric cathodes is treated. An approach is developed to calculation of the limit of stability of the diffuse mode (the current below which the diffuse mode becomes unstable). Effect produced on the stability limit by variations of control parameters (cathode

dimensions, work function of the cathode material, plasma-producing gas and its pressure) is studied and found to conform to trends observed experimentally. The stability limit is found to be much more sensitive to variations of control parameters than characteristics of the diffuse mode are, the strongest effect being produced by variations of cathode dimensions and of the work function of the cathode material. This finding conforms to the fact that the diffuse-spot transition is difficult to reproduce in the experiment.

*The work was performed within activities of the project No. 2411/99 of FCT and of the project NumeLiTe and action COST-529 of the EC

11:30

WF2 5 Scaling of Microdischarge Devices: Pyramidal Structures* MARK J. KUSHNER, *Dept. of Electrical and Computer Engr., University of Illinois, Urbana, IL 61801* The development of microdischarge plasma sources is based on pd (pressure x dimensions scaling) scaling whereby devices 10s μm in size are realized by increasing the gas pressure. These scalings generally apply until the shrinking dimensions of the devices approach the Debye length or cathode fall thickness. At such times, the necessary plasma structures cannot be accommodated in the device, a condition which is particularly problematic for hollow cathode-like structures. The scaling of microdischarge devices was computationally investigated using a 2-dimensional plasma hydrodynamics model incorporating an unstructured mesh. An electron Monte Carlo simulation was interfaced to the model to provide excitation and ionization sources resulting from beam-like electrons produced by secondary emission into the cathode fall. Inverted pyramidal structures 15-50 μm in size operating in neon (400-1000 Torr) and other rare gas mixtures were examined. We found that negative-glow-like behavior, monitored by the ratio of double ionization to excitation, began at critically low values of pd (1 Torr-cm for these structures). At high operating voltages or with low values of ballast resistance, the electron density (10^{13} - 10^{14} cm^{-3}) is sufficiently large, and cathode fall thickness sufficiently small, that the discharge largely fits inside the cathode cavity.

*Work was supported by the National Science Foundation (CTS 99-74962) and the EPRI.

SESSION XF1: SCATTERING FROM MOLECULAR TARGETS

Friday afternoon, 24 October 2003; California Ballroom, Cathedral Hill Hotel at 13:15
Ann E. Orel, University of California, Davis, presiding

Invited Papers

13:15

XF1 1 New techniques in the study of ion processes in weak plasmas.

THOMAS M. MILLER,* *Air Force Research Laboratory, Space Vehicles Directorate*

The understanding of both natural and technical weak plasmas requires a detailed understanding of ion-molecule reaction dynamics, often under exotic conditions, including plasmas under nonequilibrium conditions. In modeling such plasmas it is not uncommon to make use of binary reaction rates measured at room temperature and low pressure, either directly or with some sort of extrapolation, to high temperatures and pressures. Measurements made at hyperthermal energies provide a guide. The Air Force Research Laboratory has made significant contributions to the understanding of these plasma environments over an unprecedented range of temperature (80-1800 K) and pressure (0.001 to 760 Torr). These results are provided by the laboratory's selected-ion flow-tube (SIFT), flowing-afterglow Langmuir-probe (FALP), guided ion-beam (GIB), high-temperature flowing-afterglow (HTFA), and turbulent ion flow tube (TIFT). In addition, state-selected ion-molecule reactions are being studied using the pulsed-field ionization photoelectron/secondary-ion coincidence method at the Advanced Light Source. Several examples of work carried out with these apparatuses will be described, e.g., online optical detection of labile reactants coupled with a flow tube reactor. We will also describe computational results for thermodynamic properties of hydrocarbon positive ions which appear as common products of reactions in our work.

*This presentation was prepared with S. T. Arnold, Y.-H. Chiu, R. A. Dressler, A. Fernandez, D. J. Levandier, A. J. Midey, A. A. Viggiano, and S. Williams.

Contributed Papers

13:45

XF1 2 Dissociative Recombination of Vibrationally-Excited Oxygen Molecular Ions P. C. COSBY, J. R. PETERSON, D. L. HUESTIS, *Molecular Physics Lab, SRI International* A. PETRIGNANI, *FOM-Institut* W. VAN DER ZANDE, *Nijmegen Univ.* M. LARSSON, R. THOMAS, F. HELLBERG, *Stockholm Univ.* Dissociative recombination (DR) is the primary mechanism for electron loss in ionized, low-pressure molecular gases and plasmas, such as planetary ionospheres. Through the use of heavy ion storage rings, there has been considerable progress in recent years in characterizing both the cross sections and the products produced by DR reactions. DR can in principle be strongly dependent on specific rotational, vibrational, and electronic states of the ion, but current work has allowed only investigating ground state species or uncharacterized internal state distributions. We report here the first experimental determination of cross sections and products produced in the DR of the oxygen molecular ion in its ground state vibrational levels $v = 0, 1, 2, 3,$ and $4,$ which are crucial to understanding the loss of this ion in the Venus ionosphere. In particular, our measurements show substantial variations (factors of 5) in the DR cross sections among these low levels. Our measurements were made at CRYRING using a variable pressure electron-impact ion source with the ion populations characterized by dissociative charge transfer in cesium vapor. This work is partially supported by the NASA Planetary Atmospheres Program under grant NAG5-11173.

14:00

XF1 3 An Assessment of Electron Collision Cross Sections for Tetrafluoroethylene W.L. MORGAN, *Kinema Research, Monument, Colorado* S.J. BUCKMAN, *Australian National University, Canberra, Australia* Electron collisions with C_2F_4 are of interest to the plasma processing community as it is used both as a feed gas in its own right and it is an important dissociative by-product

of processing plasmas which use $c-C_4F_8$ as a feed gas. There have been very few absolute scattering measurements for low energy electron collisions with C_2F_4 and a recently published cross section set [1] was based solely on a combination of theoretical estimates and analysis of electron transport parameters. In the light of recent, absolute measurements [2] for elastic scattering and vibrational excitation, this cross section set has been re-assessed and some significant differences are apparent. [1] K. Yoshida et al. *J. Appl. Phys.* 91, 2637 (2002) [2] R. Kajita et al. To be published (Collaborative measurements between ANU and Sophia University, Japan)

14:15

XF1 4 Ab Initio Study of Low-Energy Electron Collisions with Ethylene C. S. TREVISAN, *Department of Applied Science, UC Davis* A. E. OREL, *Department of Applied Science, UC Davis* T. N. RESCIGNO, *Lawrence Berkeley National Lab, Computing Science* We present the results of an investigation of elastic electron scattering by ethylene, C_2H_4 , with incident electron energies ranging from 0.5 to 20.0 eV, using the complex Kohn variational method. These *ab initio* calculations accurately reproduce, for the first time, experimental angular differential cross sections at electron-impact energies below 3 eV. Low-energy electron scattering by ethylene is sensitive to the inclusion of electronic correlation and target-distortion effects. We therefore report results that describe the dynamic polarization of the target by the incident electron and involve calculations over a range of different geometries, including the effects of nuclear motion by vibrationally averaging the T-matrices. We find that both the inclusion of dynamic polarization and the effect of nuclear motion are equally critical in obtaining accurate results. The calculated cross sections

are compared with recent experimental measurements. Work performed under the auspices of the US Department of Energy by the University of California Lawrence Berkeley National Laboratory, and supported by the US DOE Office of Basic Energy Science, Division of Chemical Sciences.

14:30

XF1 5 Electron transport in CF_4 in DC and RF fields ZORAN PETROVIĆ, SAŠA DUJKO, ZORAN RASPOPOVIĆ, *Institute of Physics, University of Belgrade* Electron transport coefficients were calculated for pure electric (E) and electric and magnetic (ExB) fields in CF_4 . A standard set of cross sections was used which allowed us to predict temporal relaxations, quasistationary and dc transport coefficients and swarm properties. A number of kinetic phenomena are observed such as rf negative differential conductivity, anomalous diffusion, negative diffusion, non-conservative effects and other. These effects are not properly taken into account if dc data are used for plasma modeling. We have studied the influence of the amplitude of electric and magnetic fields on electron transport, the effect of frequency and non-conservative effects in domain of E/N and B/N that is relevant for rf plasma modeling.

14:45

XF1 6 Selectivity in Threshold Vibrational Excitation of CO_2 by Electron Impact* W. VANROOSE, *LBNL* ZHIJONG ZHANG, *Lawrence Berk. National Lab.* C. W. MCCURDY, *LBNL* T. N. RESCIGNO, *LBNL* Vibrational excitation of the hydrogen halides by low energy electron impact has been a subject of continued interest ever since pronounced threshold peaks were observed in the vibrationally inelastic cross sections by Rohr and Linder some twenty-five years ago. More recently, similar structures were observed in non-polar triatomic molecules, but only for certain transitions. We present a non-empirical local potential model for studying threshold vibrational excitation by electron

impact. This work builds on the zero-range potential virtual state model of Gauyacq and Herzenberg (J. P. Gauyacq and A. Herzenberg, *Phys. Rev. A* 25, 2959 (1982)), using known analytic properties of the S-matrix to predict the analytic continuation of the negative ion potential curve into the continuum. We derive an equation that determines the nuclear dynamics which can be solved without the need for an expansion in target vibrational states. The model is applied to CO_2 vibrational excitation and provides, for the first time, a quantitatively accurate description of the observed excitation cross sections at energies below 1 eV.

*This work was performed under the auspices of the US Department of Energy by the University of California Lawrence Berkeley Laboratory under contract DE-AC03-76SF00098. The work was supported by the US DOE Office of Basic Energy Science, Division of Chemical Sciences.

15:00

XF1 7 Resonant Scattering of Low Energy Electrons from NO MILICA JELISAVCIC, RADMILA PANAJOTOVIC, STEPHEN BUCKMAN, *RSPHysSE, Australian National University, Canberra* NO is a molecule of significant interest because of its importance in areas as diverse as the chemistry of our atmosphere and many human biological processes. In particular NO plays an important role in the energy balance of the atmosphere through its IR emissions from fundamental and first and higher order overtones in its ground electronic state. Despite this there exist no definitive measurements of absolute cross sections for these scattering processes at energies below 5 eV. We present measurements of absolute elastic scattering and vibrational excitation (0-1, 0-2) cross sections for NO at energies between 0.4 and 5 eV. This region is of particular interest as the scattering cross sections are dominated by negative ion resonances.

SESSION XF2: MATERIAL PROCESSING II

Friday afternoon, 24 October 2003; International Ballroom, Cathedral Hill Hotel at 13:15
Bert Ellingboe, Dublin City University, presiding

Invited Papers

13:15

XF2 1 Plasma Parameter Control Mechanism in plasma sources.

HONG-YOUNG CHANG,* *Department of Physics, KAIST, Yusong-Gu, Daejeon, South Korea*

We have studied to control the plasma parameters such as electron temperature and electron density for next generation etching process. In this paper, three methods for controlling plasma parameters such as electron temperature and electron density have been suggested. And some etch results by these methods will be presented. The mechanism of controlling electron temperature with grid-biased voltage is studied experimentally and relevant physics is discussed in an inductively coupled plasma. With the grid method, etching selectivity of oxide to photo-resist is 74, which is ten times higher than that of without the grid. The electron energy distribution function and plasma parameters in various gas mixture ($N_2, O_2, CF_4/He, Ar, Xe$) discharges are measured. When He is mixed, the electron temperature increases but the electron density is almost constant. In He mixture discharge, the electron temperature is almost constant; the electron density increases rapidly near a mixing ratio of 1. Mixing Xe increases the electron density and decreases the electron temperature. Electron temperature decreases to 1.8 eV as driving frequency increases up to 100 MHz by using modified parallel resonance antenna and the plasma uniformity by controlling current of the outer antenna connected to the capacitor is achieved within 5%.

*D.S. Lee, K.H. Bai, G.C. Kwon, and Buil Jeon.

13:45

XF2 2 Understanding pulsed magnetron plasma processes through time-resolved measurement.J.W. BRADLEY, *UMIST*

Asymmetric bi-polar DC magnetron pulsing [1] has become an important technique in the reactive sputter-deposition of high quality dielectric thin films and coatings [2]. In this technique, the magnetron cathode voltage is typically modulated between 20 and 350 kHz with duty cycles ranging from 50-90%. In our studies, we have used an emissive probe [3] to determine the temporal and spatial evolution of plasma potential V_p in such a pulsed discharge, relevant to industrial thin film deposition. The initial measurements were made along a line above the racetrack, for a fixed frequency (100 KHz), duty cycle (50%) argon pressure (0.74 Pa,) and discharge power (583W). This will be extended to map V_p throughout the whole of the bulk plasma. During the pulse cycle, V_p is found to follow the large changes in the cathode voltage V_d , and in the downstream plasma remains at least several volts above the most positive surface in the discharge. In the driven on phase, the results show an axial electric field generated in the plasma bulk, with potential drop ~ 20 V over 40 mm from plasma to sheath-edge, consistent with that observed in the DC magnetron. During the stable reverse period of the discharge this axial electric field is found to collapse. The temporal evolution of V_p confirms a simple picture of the evolution of V_p , predicted from previously made time-resolved mass spectroscopic measurements of the ionic component in the pulsed magnetron. The results presented here are also compared to time-resolved Langmuir probe measurements of the discharge plasma. Some implications of the form of the transient potential profile on the operation of the magnetron discharge are discussed, in particular the particle drifts and the potential for ion sputtering of the anode and walls. [1] RA Scholl, *Surf. Coat Technol.* 98 (1998) 823, [2] PJ Kelly and RD Arnell, *J. Vac. Sci. Technol. A* 17 (3) (1999) 945, [3] J.W. Bradley, SM Thompson and Y Aranda Gonzalvo, *Plasma Sources Sci Technol.* 10 (2001) 490.

Contributed Papers

14:15

XF2 3 Non-equilibrium Ion and Neutral Transport in Low-pressure Plasma Processing Reactors: Applications of Ionized Metal PVD*

VIVEK VYAS, *Dept. of Materials Science and Engr., University of Illinois, Urbana, IL 61801* MARK J. KUSHNER, *Dept. of Electrical and Computer Engr., University of Illinois, Urbana, IL 61801* Low pressure (< 1 mTorr), partially ionized plasmas are used extensively for materials processing. At these pressures, conventional fluid or continuum simulations are of questionable validity as transport is highly non-equilibrium and a kinetic approach may be warranted. In principle, continuum equations of motion are simply moments of Boltzmann's equation. If the distribution functions are known, the equations, with appropriate boundary conditions, should be applicable at arbitrarily low pressures. In this regard, a hybrid modeling approach has been developed for ion and neutral transport in which velocity distribution functions are directly computed and used to obtain transport coefficients for a continuum model. The ion and neutral velocity distributions are obtained using Monte Carlo simulations. These modules have been incorporated into a 2-dimensional plasma equipment model and applied to the analysis of low pressure, ionized metal physical vapor deposition. Comparisons will be made between conventional continuum techniques and this hybrid method, and with experiments.

*Work was supported by the National Science Foundation (CTS99-74962) and the Semiconductor Research Corp.

14:30

XF2 4 Self-consistent simulation of N_2/H_2 gas plasma for low-k material etching CHAE-HWA SHON, TOSHIKI MAKABE, *Keio University at Yokohama, Japan* We have developed a self-consistent modeling tool for H_2/N_2 gas in two-frequency capacitively coupled plasma (2f-CCP) [1], based on the relaxation continuum (RCT) model [2]. As the resistance-capacitance (RC) delay of signals through interconnection materials becomes important, low-k materials have been proposed to solve the problem. H_2/N_2 gas is a promising candidate for the etching of future low-k dielectric materials because of high selectivity and environmentally

friendly process. There are many reactions among the vibrationally excited states, electronically excited states, and ionized plasma in the N_2/H_2 gas, that have to be considered self-consistently. In this model, plasma and neutrals are calculated self-consistently by iterating the simulation of both species till a spatiotemporal periodic steady state profile could be obtained. The spatiotemporal profiles and reactions of plasma and neutrals are discussed as a simulation results of the model. [1] C. H. Shon and T. Makabe, Submitted to *Phys. Rev. E*. [2] T. Makabe, "Advances in Low Temperature RF plasmas" (Elsevier, 2002).

14:45

XF2 5 Gas temperature monitoring in plasma reactors.

A.A. BOL'SHAKOV,* B.A. CRUDEN,† S.P. SHARMA, *NASA Ames Research Center, Moffett Field, CA 94035*. A VCSEL diode laser was used for determination of the radial-averaged gas temperature inside an inductively coupled plasma reactor. The data were derived from Doppler-broadened absorption by excited Ar atoms at 763.51 nm in argon and argon/nitrogen plasmas (3, 45, and 90% N_2 in Ar). The results were compared to rotational temperature determined by fitting the N_2 emission profiles of the (0,0) transition in the $C^3\Pi_u-B^3\Pi_g$ system. A space-homogeneous plasma model was applied to distinguish trends of the gas heating mechanisms in dependence on power deposition and pressure. The differences in measured rotational and Doppler temperatures were attributed to nonuniform spatial distributions of both temperature and thermometric species (Ar^* and N_2^*) that varied depending on conditions (power 100-300 W; pressure 0.5-70 Pa). Development of a miniature diode-based sensor for *insitu* nonintrusive monitoring of the gas temperature during plasma processing of materials should be possible, thus enabling the diagnostic-assisted continuous optimization and advanced control over the processes.

*NRC/NASA Senior Research Associate.

†Also at Eloret Corp.

15:00

XF2 6 Charging of dielectrics during VUV exposure*

J.L. LAUER, J.L. SHOHET, R.W. HANSEN, R.D. BATHKE, *U. of Wisconsin-Madison* Dielectric charging plays a key role in processing damage of semiconductor devices during plasma processing. Radiation emitted in the VUV energies of 4-30 eV can induce

charge on a dielectric. Charge on Si wafers coated with 3000Å of SiO₂, Si₃N₄ and PMMA from synchrotron VUV exposure with photon flux from 10⁹-10¹³ photons/sec cm⁻² was measured with a Kelvin probe (KP). Photoemission current (IPE) and substrate voltage (VS) were monitored during exposure. The integral of IPE was compared to the net charge measured with the KP for various substrate biases. The photoemission charge depends on photon flux, wafer bias, dielectric thickness, and photon energy. The net dielectric charge results from both photoemission (which saturates

for long exposure times) as well as from charge carriers generated within the dielectric. A Charm-2 wafer was exposed to 5, 10, 15 and 20 eV photons at various locations on the wafer, as VS was measured. We find that positive-charge generation by VUV photoemission result in CHARM2 wafers may measure charge that is higher than that produced by charged particle bombardment alone.

*Supported by NSF under grants DMR-0306582 and DMR-0084402

Author Index

A

- Aanesland, Ane **NWP 71**
 Abada, Hana **HW1 6**
 Abdur, R **NWP 31**
 Abe, Toshimi **SRP 44**
 Abramzon, Nina **SRP 15**
 Adamovich, Igor **GTP 74**
 Adams, Steven **SRP 24**
 Adibzadeh, Mehrdad
SRP 22
 Adler, H. G. **GTP 35**
 Ahmed, Belasri **FT1 7**,
SRP 2, SRP 32
 Aiura, Y. **NWP 19**,
NWP 20
 Akashi, Haruaki **MW1 6**
 Akatsuka, Hiroshi **GTP 52**,
NWP 52
 Akhtar, Kamran **TR1 5**,
VF2 5
 Akishev, Yuri **QR2 5**
 Alami, Jones **VF2 1**
 Alapati, Ramakanth **WF1 2**
 Albrecht, R.M. **SRP 28**
 Aldea, Eugen **BT2 6**
 Alexandrovich, Benjamin
ET2 5, SRP 16
 Anderson, Curtis **BT2 1**,
BT2 2
 Anderson, L W **QR1 2**
 Andruczyk, D. **NWP 2**
 Ankiewicz, Adrian **FT1 2**
 Ansari, J. **GTP 36**
 Anuntalabhochai, S. **VF1 3**
 Aoi, Tatsufumi **CT2 1**
 Apruzese, J. **GTP 39**
 Aramaki, M. **GTP 65**,
PR2 4, QR2 2, SRP 14
 Arthritis, P **SRP 52**
 Arndt, S. **PR2 6**
 Arslanbekov, Robert
ET2 6, FT2 3, GTP 4,
GTP 59, SRP 3
 Avinash, K. **BT1 2**
 Avinash, Khare **BT1 1**,
SRP 43
 Aydil, Eray S. **TR2 5**
- B
- Babicky, Vaclav **GTP 67**
 Babkina, Tatiana **SRP 50**
 Baer, Doug **WF1 4**
 Baik, Hong Koo **NWP 37**
 Bailey, William **SRP 4**
 Barnat, E. V. **WF1 1**
 Barnes, Mike **MW2 3**
 Barthélemy, Olivier **FT2 4**
 Bartschat, K. **SRP 19**
- Bartschat, Klaus **QR1 5**,
SRP 21, WF2 2
 Basner, Ralf **NWP 16**
 Bathke, R.D. **SRP 28**,
XF2 6
 Becker, Kurt H. **FT2 2**,
GTP 37, GTP 76,
NWP 16, NWP 33,
PR2 5, QR2 4, SRP 15,
WF1 3
 Behnke, J.F. **GTP 15**,
NWP 34, NWP 35,
NWP 35, NWP 67,
NWP 67, NWP 68,
NWP 69
 Belen, Jun **TR2 5**
 Belich, T. J. **HW2 5**
 Belkind, Abe **PR2 5**
 Bellas, V **SRP 52**
 Benck, Eric **HW1 2**
 Benilov, M. S. **NWP 42**,
WF2 4
 Bhoj, Ananth **MW1 3**
 Bilyk, O. **NWP 68**,
NWP 69
 Blackwell, D.D. **GTP 13**
 Bletzinger, Peter **GTP 26**,
NWP 30
 Boeuf, J.-P. **NWP 29**
 Boffard, John B **QR1 2**
 Bogaerts, Annemie **BT1 5**,
BT2 4
 Bhlmark, Johan **VF2 1**
 Bol'shakov, A.A. **XF2 5**
 Bonvallet, G. A. **NWP 19**,
NWP 21
 Booth, Jean-Paul **CT2 2**,
HW1 1, HW1 6
 Borysov, Jacek **SRP 17**
 Bose, Deepak **CT1 5**,
TR2 1
 Boswell, Rod **FT1 2**,
NWP 71, TR2 6, VF2 3,
VF2 4
 Boyle, P. C. **FT1 4**,
NWP 49
 Bradley, J.W. **NWP 66**,
XF2 2
 Bradley, J. W. **VF2 2**
 Braithwaite, Nicholas
CT2 3, GTP 20
 Bratescu, Maria-Antoaneta
NWP 6, NWP 7
 Bray, Igor **QR1 3, QR1 5**
 Brown, I. G. **VF1 3**
 Brown, Michael **SRP 13**
 Brunger, Michael **GTP 75**
 Buchberger, Dog **HW1 5**

- Buckley, Mark **NWP 3**
 Buckman, S.J. **XF1 3**
 Buckman, Stephen **XF1 7**
 Buckman, Stephen J.
QR1 1
 Bulcourt, Nicolas **HW1 1**,
HW1 6
 Bulkin, Pavel **CT2 5**
 Bussiahn, René **GTP 41**
- C
- Campbell, Laurence
GTP 75
 Cardinaud, C.H. **TR2 2**
 Cardinaud, Christophe
SRP 52
 Carew, Alex **NWP 3**
 Carman, Robert **GTP 38**,
MW1 7
 Carter, C. B. **HW2 4**,
HW2 5
 Cartry, G. **TR2 2**
 CARTRY, GILLES
SRP 52
 Cartwright, David **GTP 75**
 Chabert, Pascal **CT2 2**,
HW1 6, TR2 4, VF2 3
 Chafin, Mike **HW1 5**
 Chaker, Mohamed **FT2 4**
 Chang, Hong-Young
GTP 55
 Chang, HongYoung
GTP 63
 Chang, Hong-Young **XF2 1**
 Chang, Hong Young
NWP 65
 Charles, Christine **NWP 71**,
VF2 4
 Chau, Foo-Tim **HW1 1**
 Chen, Guangye **CT2 4**
 Chen, Wan-lin **GTP 56**
 Chen, Weiwei **NWP 56**
 Chen, Zhangjin **GTP 6**,
NWP 11
 Chi, Kyeong-Koo **MW2 4**
 Childers, James Gregory
LW1 2, SRP 20
 Childers, J.G. **SRP 19**
 Choi, Jai Hyuk **NWP 37**
 Choi, Joon-Sik **NWP 24**
 Cho, Sung-II **MW2 4**
 Chou, T. **QR2 4**
 Christodoulatos, C. **QR2 4**
 Chung, ChinWook **GTP 9**
 Chung, Hyun-Kyung
VF1 4
 Clupek, Martin **GTP 67**
 Coates, Don **FT2 5**
- Coburn, John W. **JW 1**
 Collaboration, AFRL **FT2 8**
 Collaboration, Air Force
 Research Laboratory
WF1 4
 Collaboration, Department
 of Chemistry, Johns
 Hopkins University
WF1 4
 Collaboration, Drake
 University **SRP 21**
 Collaboration, IMN-LPC
TR2 2
 Collaboration, ISAS
 Dortmund **LW2 3**
 Collaboration, Lebedev
FT2 8
 Collaboration, Los Gatos
 Research, Inc. **WF1 4**
 Collaboration, LPTP **TR2 4**
 Collaboration, Moscow
 State University **SRP 21**
 Collaboration, National
 Institute for Fusion
 Science, Japan **SRP 47**
 Collaboration, Naval
 Research Laboratory
SRP 21
 Collaboration, Plasma
 Diagnostics **SRP 13**
 Collaboration, TRINITY
FT2 8
 Collaboration, University of
 Missouri-Rolla **SRP 21**
 Collins, George **NWP 31**,
SRP 27
 Cooperberg, David **TR2 5**
 Corporation, Lam Research
GTP 56
 Corr, Cormac **GTP 7**,
VF2 3
 Cosby, P. C. **LW1 5**,
XF1 2
 Craig, Gary **ET2 2, GTP 7**
 Crowe, R. **QR2 4**
 Cruden, B.A. **XF2 5**
 Cunge, Gilles **MW2 2**
 Cunha, M. D. **WF2 4**
 Curry, J. J. **GTP 35**
 Czarnetzki, Uwe **SRP 50**,
WF1 7
- D
- Dabringhausen, Lars
NWP 23
 Dai, Xin **GTP 25**
 Dasgupta, Arati **SRP 21**

- Dateo, Christopher E. **NWP 17**
 Davidson, Ronald C. **NWP 15, SRP 58**
 Davies, P.B. **FT2 1, SRP 33**
 De Bleecker, Kathleen **BT1 5**
 DeJoseph, Charles **SRP 24**
 DeJoseph, Jr., C. A. **SRP 62**
 Denning, Mark **TR1 5, VF2 5**
 Denysenko, I. B. **BT1 3, NWP 55**
 Deshmukh, Shashank **DTW 2**
 Detrick, Troy **HW1 5**
 Deutsch, H. **GTP 76**
 Dhali, Shirshak **NWP 36, SRP 49**
 Dias, Francisco M. **GTP 49**
 Dietz, D. **QR2 4**
 Döbele, H.-F. **NWP 62, NWP 63**
 Donkó, Zoltan **PR2 1**
 Donk, Zoltan **SRP 61**
 Dorf, Leonid **NWP 48**
 Dragan, Podlesnik **DTW 2**
 Dujko, Saša **XF1 5**
 Dussart, Remi **TR2 4**
 Du, Yan **MW2 5**
 Dyke, John **HW1 1**
- E**
- Ebihara, Takashi **QR2 3**
 Ellingboe, A. R. **FT1 4, NWP 49**
 Eon, D. **TR2 2**
 Eon, David **SRP 52**
 Esnault, S. **SRP 28**
 Et-touhami, E.-S. **GTP 43**
- F**
- Fernsler, R.F. **GTP 13, LW2 5**
 Fernsler, R. F. **LW2 2**
 Ferreira, Carlos M. **GTP 49, SRP 6**
 Ferreira, CM. **GTP 50**
 Figus, Margaret **SRP 15**
 Fisch, Nathaniel **NWP 48, NWP 53, NWP 72**
 Flagan, Richard C. **HW2 2**
 Flannery, M. Raymond **GTP 73, PR1 4**
 Fletcher, Graham **NWP 17**
 Foest, R. **NWP 34**
- Fontes, C. J. **SRP 19**
 Forlines, Robert **SRP 13**
 Foster, M. **NWP 14**
 Fox, Allen **HW1 5**
 Franke, St. **NWP 25**
 Frank, Leopold **NWP 39**
 Franklin, Raoul **FT1 8, GTP 20**
 Franzke, Joachim **LW2 3**
 Fredriksen, Aashild **NWP 71**
 Friedmann, Peretz **NWP 58**
 Frolov, Mikhail **FT2 8**
 Fruchtman, Amnon **NWP 70**
 Fursa, Dmitry **QR1 5**
- G**
- Gallagher, Alan **BT1 4**
 Ganguly, Biswa N. **GTP 26, NWP 30, SRP 13**
 Gani, Nicolas **MW2 5**
 Gans, Timo **SRP 50**
 Garner, Richard **SRP 16**
 Garscadden, A. **SRP 62**
 Garscadden, Alan **GTP 26**
 Gerberich, W. **HW2 4**
 Giapis, Konstantinos P. **HW2 2**
 Giapis, Kostas **TR2 8**
 Gicquel, A. **WF1 6**
 Gidwani, A. **HW2 4**
 Gijbels, Renaat **BT1 5, BT2 4**
 Girshick, S. **HW2 4**
 Girshick, Steven **HW2 3**
 Giuliani, J.L. **GTP 39, GTP 40, SRP 38**
 Glukhoy, Yuri **SRP 59**
 Godyak, V. **ET2 6**
 Godyak, Valery **ET2 4, ET2 5, FT1 3, NWP 41, SRP 16**
 Goedheer, Wim **BT1 5**
 Gogolides, E. **SRP 52**
 Golubovskii, Yu.B. **NWP 34, NWP 67**
 Golubovskii, Yu. B. **NWP 35**
 Gomez, Sergi **GTP 7, TR2 5**
 Gonzalez, Eduardo **SRP 45**
 Gonzalvo, Yolanda A. **NWP 3, PR2 5**
 Goodyear, Alec **CT2 3, GTP 20**
 Gordiets, Boris F. **SRP 6**
- Gordon, Michael **TR2 8**
 Goree, J. **BT1 2**
 Goree, John **BT1 1, SRP 43**
 Gortchakov, Serguei **GTP 41**
 Goto, Toshio **GTP 68**
 Gottscho, Richard **MW2 1**
 Gould, Phillip **PR1 2**
 Govindan, T.R. **TR2 1**
 Govindan, T. R. **CT1 5, SRP 55**
 Graham, Bill **ET2 2, GTP 7, GTP 72**
 Graham, William **BT2 5**
 Graves, David B. **HW1 6, PR2 2, TR2 3**
 Greenwood, Claire **NWP 3**
 Grum-Grzhimailo, Alexie **SRP 21**
 Gudmundsson, Jon Tomas **VF2 1**
 Guerra, Vasco **GTP 49, GTP 51**
 Guillon, Jean **CT2 2**
 Gupta, Manish **WF1 4**
 Gylfason, Kristinn B. **VF2 1**
- H**
- Hafiz, J. **HW2 4**
 Hager, Gordon **FT2 8**
 Hammel, Jeff **SRP 7**
 Hammond, Edward **CT2 6, LW2 7**
 Hansen, R.W. **XF2 6**
 Han, Woo-Sung **MW2 4**
 Han, W.S. **MW2 6**
 Harmon, Nicholas **SRP 22**
 Harris, Lawson **NWP 46**
 Hartmann, Peter **PR2 1**
 Hash, D.B. **TR2 1**
 Hash, D. B. **CT1 5**
 Hassouni, Khaled **CT2 5**
 Hattori, Yosuke **GTP 28**
 Hayashi, Nobuya **GTP 30, GTP 31, SRP 35, SRP 36**
 Heberlein, J. **HW2 4**
 Heberlein, Joachim V. R. **BT2 1, BT2 2, CT1 4, TR1 6**
 Hebert, Michael **ET2 3**
 Hebner, G. A. **WF1 1**
 Hebner, Greg **WF1 5**
 Hegeler, F. **SRP 38**
 Hellberg, F. **XF1 2**
 Helmersson, Ulf **VF2 1**
- Hempel, F. **FT2 1, WF1 6**
 Henriques, J. **GTP 50**
 Herrick, Andrew **TR2 6**
 Hershkowitz, Noah **FT1 1, GTP 66, NWP 44, NWP 47**
 Hippler, R. **GTP 15**
 Hirochi, Yuuki **GTP 46**
 Hisano, Taishi **NWP 5**
 Hitzschke, L. **GTP 35**
 Hoffman, Daniel **GTP 60, HW1 5**
 Holik, M. **NWP 68, NWP 69**
 Holland, John **DTW 2, HW1 5, MW2 3, MW2 5**
 Holunga, Dean **HW2 2**
 Hori, Masaru **GTP 68**
 Horiuchi, Yasuhiro **ET1 3, SRP 29**
 Horner, D. A. **LW1 3**
 Hoshimiya, Katsumi **NWP 31**
 Houston, E. **QR2 4**
 Howlader, Mostofa **SRP 12**
 Huang, S. Y. **GTP 11**
 Hua, Xuefeng **TR2 3**
 Hudson, Eric **HW1 1**
 Hudson, Eric A. **DTW 3, GTP 56**
 Huestis, D. L. **LW1 5, XF1 2**
 Humbird, David **TR2 3**
 Huo, Winifred M. **NWP 17**
 Hur, Min **BT2 1, BT2 2**
 Hwang, Helen **SRP 55**
- I**
- Ihara, Satoshi **GTP 30, GTP 31, SRP 35, SRP 36**
 Ikematsu, Tomokazu **SRP 36**
 Ikuma, Soichi **GTP 68**
 Ionin, Andrei **SRP 39**
 Ionin, Andrey **FT2 8, SRP 40**
 Ishigaki, Takuya **GTP 46**
 Ishii, Shozo **GTP 32**
 Itoh, Haruo **LW2 6**
 Ito, Hiroaki **NWP 57, NWP 59**
 Ivanova, O. **GTP 15**
 Iwamoto, K. **TR1 4**
 Iwata, S. **GTP 69, NWP 4**
- J**
- Jacob, Wolfgang **SRP 44**
 James, B.W. **NWP 2**

- Jelisavcic, Milica **XF1 7**
 Jeon, Buil **GTP 55**
 Jeon, Yong-Seog **NWP 24**
 Jesih, Adolf **SRP 31**
 Jiao, C. Q. **SRP 62**
 Johnston, Tudor W. **FT2 4**
 Jolly, Jacques **CT2 2**
 Jones, S. **NWP 14**
 Jones, Steve **LW1 4**
 Joyce, G. **LW2 2**
 Jung, R O **QR1 2**
 Jung, Y.J. **MW2 6**
 Jun, Sanghyun **NWP 65**
- K**
 Kadetov, Victor **WF1 7**
 Kaganovich, Igor D.
 GTP 3, NWP 15, PR2 3, SRP 58
 Kakalios, J. **HW2 5**
 Kalache, Billel **CT2 5**
 Kaneda, Shunichi **GTP 31**
 Kane, Deborah **GTP 38, MW1 7**
 Kang, Chang-Jin **MW2 4**
 Kang, C.J. **MW2 6**
 Kaning, M. **GTP 35**
 Kano, T. **TR1 4**
 Kanuma, Toshiaki **NWP 52**
 Karalnik, Vladimir **QR2 5**
 Karkari, S. K. **NWP 66, VF2 2**
 Karpenko, Oleh **GTP 6**
 Kato, T. **GTP 69, NWP 4**
 Katsch, H.-M. **NWP 62, NWP 63**
 Kawamura, Kazutaka
 NWP 61, SRP 25
 Kazuo, Takahashi **SRP 56**
 Kedzierski, Wladyslaw
 QR1 3
 Keidar, Michael **NWP 53, NWP 58**
 Keil, Douglas **GTP 56**
 Keller, John H **GTP 12**
 Kepple, P. **SRP 38**
 Kessaratikoon, P. **HW1 4**
 Kettlitz, Manfred **NWP 22, NWP 23, NWP 26**
 Khakoo, M. A. **SRP 19**
 Khakoo, Murtadha A.
 LW1 2, SRP 20
 Khelifa, Yanallah **SRP 2**
 Khudik, Vladimir **SRP 8, SRP 9**
 Kiehlbauch, Mark **TR2 5**
 Kim, HyunChul **CT2 7, GTP 63**
- Kim, Hyun-Jung **NWP 24**
 Kim, Jeong Won **MW1 5, WF2 3**
 Kim, Jin Joong **MW1 5, WF2 3**
 Kim, Jisoo **GTP 57**
 Kim, Sungjin **GTP 2**
 Kim, Sung Jin **SRP 53**
 Kimura, Takashi **GTP 28**
 Kim, W. K **GTP 9**
 Kim, Yong-Ki **NWP 13**
 Kirmse, Karen **SRP 48**
 Kitaura, Yasuhiro **SRP 47**
 Klimachev, Yuri **FT2 8, SRP 39**
 Klumov, Boris **SRP 45**
 Kobayashi, J. **SRP 14**
 Kobayashi, M. **GTP 65**
 Kochetov, Igor **FT2 8, QR2 5, SRP 40**
 Ko, Eunsuk **FT1 1, GTP 66, NWP 44, NWP 47**
 Koga, Kazunori **SRP 47**
 Ko, Jung Tae **MW1 5, WF2 3**
 Kolobov, Vladimir **ET2 6, FT2 3, GTP 4, GTP 59, SRP 3**
 Komori, Akio **SRP 47**
 Kono, A. **FT1 6, PR2 4, SRP 14, TR1 4**
 Korfiatis, G. **QR2 4**
 Kortshagen, U. **HW2 5**
 Kortshagen, Uwe **BT2 1, BT2 2, CT1 4, ET2 3, HW2 3**
 Kothnur, Prashanth **TR1 3**
 Kotkov, Andrei **SRP 39**
 Kotkov, Andrey **FT2 8**
 Kozakov, R. **PR2 6**
 Kralj, Bogdan **SRP 31**
 Kriha, Vitezslav **GTP 29**
 Kroesen, Gerrit **MW1 1**
 Kroesen, G.M.W. **BT1 6**
 Kruger, Charles H. **LW2 4**
 Krylova, Olga **NWP 22**
 Kuba, Shiro **QR2 3**
 Kudrna, P. **NWP 68, NWP 69**
 Kumita, Kentaro **NWP 61**
 Kunihide, Tachibana
 NWP 27
 Kunze, Kerstin **LW2 3**
 Kurakane, H. **QR2 2**
 Kurnosov, Alexander
 SRP 39
 Kurunczi, Peter **NWP 33**
- Kushner, Mark J. **ET2 7, FT2 7, MW1 3, MW1 4, WF2 5, XF2 3**
- L**
 Lampe, M. **LW2 2**
 Lampe, Martin **SRP 11**
 Lange, Hartmut **GTP 41**
 Langenscheidt, Oliver
 NWP 23
 Laroussi, Mounir **NWP 39**
 Larsson, M. **XF1 2**
 Lauer, J.L. **SRP 28, XF2 6**
 Lauro-Taroni, Laura
 GTP 20
 Laux, Christophe O.
 LW2 4
 Laville, Stéphane **FT2 4**
 Lawler, J. E. **MW1 2, NWP 19, NWP 20, NWP 21**
 Leahey, Patrick **DTW 2, MW2 5**
 Le Drogoff, Boris **FT2 4**
 Lee, Do Haing **SRP 53**
 Lee, Edmond **HW1 1**
 Lee, JaeKoo **CT2 7**
 Lee, Jae Koo **SRP 53**
 Lee, JaeKu **GTP 63**
 Lee, Ji-Young **NWP 24**
 Lee, Richard W. **VF1 4**
 Lee, Robert **SRP 24**
 Lee, Se-Jong **NWP 37**
 Lee, W. **FT2 2**
 Lee, Wonchul **NWP 8**
 Lefaucheux, Philippe
 TR2 4
 Lehmberg, R.H. **SRP 38**
 Lempert, Walter **NWP 8**
 Leonhardt, D. **GTP 13, LW2 5**
 Lichtenberg, A.J. **GTP 2, GTP 57, GTP 58**
 Lieberman, M.A. **GTP 2, GTP 57, GTP 58**
 Li, He-Ping **TR1 6**
 Lill, Thorsten **DTW 2**
 Lima, Paulo **CT2 3**
 Lin, Chun C **QR1 2**
 Liu, B. **BT1 2**
 Liu, Bin **BT1 1, SRP 43**
 Lockwood, Nathaniel
 SRP 4
 Loffhagen, D. **FT2 1**
 Loffhagen, Detlef **GTP 45, SRP 61**
 Lohmann, Birgit **VF1 1**
 Lombardi, G. **WF1 6**
- Long, J. D. **CT1 3, GTP 11, NWP 55**
 Lopez, Jose **PR2 5**
 Losey, Laura **SRP 48**
 Loureiro, Jorge **GTP 51**
 Luo, Gang **MW1 3**
 Luque, Jorge **HW1 1**
 Lu, XinPei **NWP 39**
- M**
 MacAdam, K.B. **GTP 71, PR1 3**
 MacAskill, John **QR1 3**
 Machala, Zdenko **LW2 4**
 Mackey, D. **GTP 18**
 Madani, Myriam **BT2 4**
 Madhan, Raja Chandra
 Mohan **GTP 24**
 Madison, D.H. **NWP 12, SRP 19**
 Madison, D. H. **NWP 14**
 Madison, Don H **LW1 4, NWP 11, SRP 21**
 Maerk, T. **GTP 76**
 Mahajan, Satish **SRP 41**
 Maiorov, V. A **NWP 35**
 Maiorov, V.S. **NWP 34**
 Makabe, Toshiaki **ET1 3, HW1 3, SRP 29, SRP 54, TR2 7, XF2 4**
 Makrinich, Gennady
 NWP 70
 Malović, Gordana **GTP 44**
 Malter, J.S. **SRP 28**
 Manheimer, W. M. **LW2 2**
 Manthey, C. **NWP 63**
 Marco, Redwitz **NWP 26**
 Marek, A. **NWP 68, NWP 69**
 Margot, Joëlle **FT2 4**
 Marić, Dragana **PR2 1**
 Marler, J.P. **LW1 6**
 Martines, E. **NWP 68**
 Martus, K **FT2 2, GTP 37, WF1 3**
 Masahiro, Yamaji **NWP 10**
 Mashima, Hiroshi **CT2 1**
 Masoud, N **GTP 37, WF1 3**
 Matsika, Spiridoula **WF1 4**
 Matsui, H. **GTP 69**
 Matsuura, Haruaki **GTP 52, NWP 52**
 Matsuzaki, Mitsuo **NWP 52**
 Mays, Brad **HW1 5**
 McConkey, William **QR1 3**
 McCurdy, C. W. **LW1 3, XF1 6**

- McGrath, Cormac QR1 3
 McMurry, P. HW2 4
 Mechold, L. FT2 1
 Medina, Christina LW1 2,
SRP 20
 Meyyappan, M. **CT1 1**,
 CT1 5, SRP 55
 Miclea, Manuela LW2 3
 Mildren, Richard GTP 38,
 MW1 7
 Miles, Richard **TR1 2**
 Miller, Thomas M. **XF1 1**
 Min, K.J. MW2 6
 Mirpuri, Chandru **GTP 11**
 Mishra, Lekha Nath
 NWP 57, **NWP 59**
 Miyauchi, Masaru HW1 3
 Miyazaki, Koichi NWP 5
 Miyoshi, Yasufumi **HW1 3**
 Mogzina, O. QR2 4
 Mohamed, A.H. **NWP 32**
 Moin, Parviz CT2 6,
 LW2 7
 Mok, Daniel HW1 1
 Monich, Anton QR2 5
 Mook, W. HW2 4
 Moon, Joo-Tae MW2 4
 Moon, J.T. MW2 6
 Morfill, Gregor SRP 44
 Morgan, W.L. **XF1 3**
 Morgan, W. Lowell VF1 4
 Morrow, Tom BT2 5,
 ET2 2
 Mosbach, Th. **NWP 62**
 Moselhy, M.M. **GTP 36**,
 GTP 53
 Mui, David DTW 2
 Mukherjee, R. HW2 4
 Muraoka, Katsunori
NWP 5, QR2 3
 Murata, Masayoshi CT2 1
 Muratore, C. GTP 13
 Myers, M.C. SRP 38
- N**
 Nafarizal, N. NWP 4
 Nagesha, K. **GTP 71**,
PR1 3
 Nakao, S **GTP 48**, PR2 4
 Namba, S. NWP 2
 Nanbu, Kenichi **GTP 61**,
 VF2 6
 Naoi, Koichi **GTP 52**
 Napartovich, Anatoliy
 SRP 39, SRP 40
 Napartovich, Anatoly
FT2 8, QR2 5
 Neale, Ian NWP 3
- Nersisyan, Gagik **BT2 5**
 Nguyen, Hoan MW2 5
 Nguyen, T. D. GTP 15
 Niazi, Kaveh **GTP 6**
 Niemax, Kay LW2 3
 Nierode, Mark PR2 2
 Nikitivić, Željka **GTP 44**
 Nishida, Yasushi NWP 57,
 NWP 59
 Noda, Matsuhei GTP 62
 Nordheden, Karen J WF1 2
 Nosenko, V. **BT1 2**
 Novikova, Tatiana **CT2 5**
 Nozaki, Tomohiro **CT1 4**
 Nuamatha, Prasad **SRP 49**
- O**
 O'Connell, D. M. **NWP 49**
 Oda, Akinori GTP 28,
 MW1 6
 Oda, T. NWP 2
 Oehrlein, Gottlieb S TR2 3
 Ogawa, Hironori NWP 61,
 SRP 25
 Ohgo, T. NWP 2
 Ohmori, Takeshi **TR2 7**
 Okazaki, Ken CT1 4
 O'Keefe, Anthony WF1 4
 O., Minayeva NWP 39
 Ono, Kouichi NWP 51,
 SRP 56
 Ono, Masataka NWP 61,
 SRP 25
 Orel, A. E. XF1 4
 Osano, Yugo **SRP 56**
 Ostrikov, K. **BT1 3**,
 CT1 3, ET2 1, **GTP 5**,
 GTP 11, NWP 55
 Ostrovsky, Valentine PR1 4
 Owano, Thomas WF1 4
- P**
 Paduraru, Cristian **PR2 5**
 Panagopoulos, Theodoros
 HW1 5
 Panagopoulos, Theodoros
 MW2 5
 Panajotovic, Radmila
 XF1 7
 Panda, Siddhartha DTW 1
 Park, Byeong-Ju **NWP 24**
 Pashaie, Bijan NWP 36
 Paterson, Alex DTW 2,
 HW1 5, **MW2 3**
 Pau, Wilfred MW2 5
 Peignon-Fernandez, M.C.
 TR2 2
 Pekarek, Stanislav **SRP 34**
- Perret, Amelie **CT2 2**
 Perrey, C. R. HW2 4,
 HW2 5
 Perry, Andrew TR2 6
 Peterson, J. R. XF1 2
 Petrignani, A. XF1 2
 Petrov, G. GTP 39,
GTP 40, SRP 38
 Petrović, Zoran **ET1 4**,
 PR2 1, **XF1 5**
 Pfender, Emil TR1 6
 Pham, G. V. GTP 15
 Phanchaisri, B. VF1 3
 Phelps, A.V. GTP 43
 Phelps, A. V. **SRP 5**
 Piejak, Robert ET2 5,
SRP 16
 Pimblott, Simon **VF1 2**
 Pinho, Nuno **SRP 61**
 Pinheiro, Mrio SRP 61
 Pinheiro, Mário J. SRP 6
 Pitchford, L.C. GTP 43,
 NWP 29, SRP 5
 Plantie, L. GTP 18
 Platts, David FT2 5
 Plihon, Nicolas VF2 3
 Plummer, Dirk **GTP 17**
 Plusquellic, David HW1 2
 Podmarkov, Yuri FT2 8
 Polomarov, Oleg **GTP 3**,
 PR2 3
 Popov, Gotze SRP 59
 Popović, S. **HW1 4**
 Porokhova, I.A. **NWP 67**
 Pospisil, Milan SRP 34
 Pratoomtong, C. SRP 28
 Prideaux, A. **NWP 12**
 Pruden, Amy, SRP 27
 Prudov, N PR1 4
- Q**
 Qui, Hongwei **FT2 2**
- R**
 Raballand, V. TR2 2
 Raballand, Vanessa SRP 52
 Rahel, Jozef GTP 24,
GTP 25
 Rahman, Mahmud **SRP 59**
 Raitses, Yevgeny NWP 48,
NWP 53, **NWP 72**
 Raja, Laxminarayan L.
 BT2 3, CT2 4, TR1 3
 Rajaraman, Kapil **MW1 4**
 Ranson, Pierre TR2 4
 Raspopović, Zoran XF1 5
 Rauf, Shahid TR2 1
 Redwitz, Marco NWP 23
- Rees, Alan **NWP 3**
 Remskar, Maja SRP 31
 Remy, J. **BT1 6**
 Renault, T. HW2 4
 Rescigno, T. N. LW1 3,
 XF1 4, XF1 6
 Ricard, A. GTP 50
 Ricatto, P.J. QR2 4
 Richley, E.A. SRP 61
 Richley, Edward **GTP 22**
 Rich, William GTP 74
 Riley, Merle WF1 5
 Robertson, Scott NWP 43,
 SRP 11
 Robiche, J. FT1 4
 Roca i Cabarrocas, Pere
 CT2 5
 Röpcke, J. FT2 -1, SRP 33,
WF1 6
 Rosocha, Louis **FT2 5**
 Roth, J. Reece SRP 12
 Roth, J. Reece **GTP 24**,
 GTP 25, NWP 56
 Rousseau, Antoine **QR2 1**
 Rutkevych, P. NWP 55
- S**
 Sabsabi, Mohamad FT2 4
 Sadjadi, Reza GTP 56
 Sakai, Yosuke GTP 46,
 MW1 6, **NWP 6**,
NWP 7, QR1 4
 Sakamoto, Takeshi GTP 92
 Sakura, Nobukazu NWP 6
 Sanden, Richard van de
 BT2 6
 Sangyuenyongpipat, S.
VF1 3
 Sankaran, R. Mohan
HW2 2
 Sano, Atsushi SRP 56
 Sansonetti, C. J. GTP 35
 Sá, Paulo A. GTP 51
 Sasaki, K. **FT1 6**, GTP 65,
 GTP 69, NWP 4, QR2 2
 Satake, Koji CT2 1,
GTP 62
 Satoh, Saburoh GTP 30,
 GTP 31, SRP 35,
 SRP 36
 Sato, Noriyoshi SRP 44
 Saxena, S SRP 19
 Schalk, B. GTP 35
 Scharer, John TR1 5,
 VF2 5
 Scheier, P. GTP 76
 Schmidt, M. NWP 34
 Schneidenbach, H. NWP 25

- Schneidenbach, Hartmut
NWP 22, NWP 23,
NWP 26
- Schoenbach, K.H. GTP 36,
GTP 53, NWP 32
- Schöpp, H. NWP 25
- Schow, Eric LW1 2,
SRP 20
- Schrauwen, Cor BT2 6
- Schulz, M. NWP 14
- Schulz, Michael LW1 1
- Seleznev, Leonid FT2 8,
SRP 39
- Sergeyev, Aleksandr
SRP 17
- Servern, Greg FT1 1
- Sethian, J.D. SRP 38
- Setsuhara, Yuichi NWP 51,
SRP 56
- Severn, Greg NWP 47
- Shannon, Steven HW1 5
- Sharma, Ashish SRP 27
- Sharma, S.P. XF2 5
- Sharpee, B. D. LW1 5
- Shastri, S. D. GTP 35
- Shen, Meihua DTW 2,
MW2 5
- Shibagaki, K. GTP 69,
NWP 4
- Shibata, Kanetoshi
NWP 57, NWP 59
- Shimada, Takashi SRP 54
- Shimizu, Tetsuji SRP 44
- Shimosaki, Mitsuaki
GTP 30
- Shin, Jichul BT2 3
- Shiratani, Masaharu
HW2 1, SRP 47
- Shnyrev, Sergey SRP 39
- Shohet, J.L. SRP 28,
XF2 6
- Shohet, S.B. SRP 28
- Shon, Chae-Hwa XF2 4
- Shon, JongWon CT2 7
- Shvydky, Alex SRP 8,
SRP 9
- Sieg, Michael NWP 23,
NWP 26
- Siegrist, Karen HW1 2
- Sigeneger, F. PR2 6
- Silapunt, Rardchawadee
SRP 48
- Simek, Milan GTP 67
- Sinitzyn, Dmitriy SRP 39,
SRP 40
- Sinitzyn, Dmitry FT2 8
- Skapin, Tomaz SRP 31
- Slanger, T. G. LW1 5
- Slinker, S. P. LW2 2
- Smirnov, Artem NWP 72
- Sobolewski, Mark GTP 8
- Somiya, Satoru GTP 14
- Song, Ki Moon NWP 37
- Sonnenfeld, A. GTP 15
- Sorokin, M. BT1 6
- Sosov, Yuriy GTP 21,
GTP 34
- Srivastava, R SRP 19
- Stafford, D. Shane FT2 7
- Stalder, Kenneth R. ET1 2,
FT2 6, GTP 72, NWP 38
- Stamate, E. GTP 48,
PR2 4, SRP 14
- Stancu, G.D. SRP 33,
WF1 6
- Stange, Sy FT2 5
- Stan, Ovidiu NWP 31
- Startsev, Edward A.
NWP 15, SRP 58
- Stauffer, A.D. SRP 19
- Steen, Philip BT2 5,
ET2 2, GTP 7
- Sternberg, Natalia FT1 3,
NWP 41
- Sternovsky, Zoltan
NWP 43, SRP 11
- Stoffels, Eva ET1 1
- Stoffels, W.W. BT1 6
- Stone, Tom QR1 2
- Storer, R CT1 3
- Strinić, Aleksandra GTP 44
- Suda, Yoshiyuki NWP 6,
NWP 7
- Suddala, S. NWP 32
- Sugai, H BT1 3, GTP 48
- Sugai, H. GTP 69
- Sugai, H NWP 4, PR2 4,
SRP 14
- Sugai, Hideo GTP 14
- Sugawara, Hirotake
GTP 46, NWP 6, QR1 4
- Sullivan, J. P. LW1 6
- Sunka, Pavel GTP 67
- Surko, C.M. LW1 6
- Surla, Vijay NWP 31
- Sutherland, Orson FT1 2
- Su, T.L. QR2 4
- Suzuki, Susumu LW2 6
- T**
- Tachibana, Kunihide
TR1 1
- Takahashi, Kazuo NWP 51
- Takakura, Yasushi MW2 3
- Takao, Yoshinori NWP 51
- Takekida, Hideto GTP 61,
VF2 6
- Takeuchi, Yoshiaki CT2 1
- Takiyama, K. NWP 2
- Takizawa, K. FT1 6
- Tatarova, E. GTP 50
- Tatarova, Elena GTP 49
- Team, Department of Pulse
Plasma Systems GTP 67
- Team, Energy and
Environmental NWP 57,
NWP 59
- Team, FOM Institute for
Plasmaphysics
'Rijnhuizen', The
Netherlands BT1 5
- Team, GREMI TR2 4
- Team, Group of Electrical
Discharges SRP 34
- Team, Kaist GTP 63
- Team, Plasma Sciences
Lab, Department of ECE,
Univ. of Tennessee,
Knoxville SRP 12
- Team, plasma simulations
group (UA) BT2 4
- Team, PLT (VITO) BT2 4
- Team, Postech GTP 63
- Team, Process Development
MW2 6
- Team, Semiconductor
Research and
Development Center
DTW 1
- Team, Sheath NWP 47
- Team, Subsonic Plasma
Aerodynamics GTP 24
- Team, Tokai University
Plasma Group NWP 61,
SRP 25
- Team, University of
Antwerp, Belgium BT1 5
- Teeuwen, Justin QR1 3
- Tegou, E SRP 52
- Teranishi, Kenji LW2 6
- Terekhov, Yuri SRP 40
- Testrinch, H. PR2 6
- Teubner, Peter GTP 75
- Theodosiou, Constantine
GTP 3, GTP 21,
GTP 34, SRP 22
- Thomas, Hubertus SRP 44
- Thomas, R. XF1 2
- Thompson, S. HW2 5
- Tichy, M. NWP 68,
NWP 69
- Tillocher, Thomas TR2 4
- Toader, Emil GTP 72
- Todorow, Valentin MW2 5
- Tonegawa, Akira NWP 61,
SRP 25
- To, T. X. H. GTP 15
- Toyoda, H. GTP 69,
NWP 4
- Toyoda, HIROTAKA
GTP 14
- Trevisan, C. S. XF1 4
- Trushkin, Nikolay QR2 5
- Tsai, Peter P.-Y. NWP 56
- Tsakadze, E ET2 1
- Tsakadze, Z. L. CT1 3,
ET2 1, NWP 55
- Tsunashima, S. GTP 69,
NWP 4
- Turner, M. M. FT1 4,
GTP 18, NWP 49
- Tuszewski, Michel LW2 1
- Tysk, Shane TR1 5, VF2 5
- U**
- Uchino, Kiichirou NWP 5
- Uchiyama, Taro CT2 1
- Uehara, Ryuji SRP 47
- Uhrlandt, Dirk ET2 3,
GTP 41, WF2 1
- Usenko, Alex SRP 59
- Utkin, Yuri GTP 74
- V**
- Vaccari, D. QR2 4
- Vagin, Nikolay FT2 8
- van der Zande, W. XF1 2
- Vandeventer, P. SRP 19
- Van Dijk, Jan ET1 3,
SRP 29
- Vangeneugden, Dirk BT2 4
- Vanroose, W. XF1 6
- Vasenkov, Alex ET2 7
- Verboncoeur, John SRP 7
- Verboncoeur, J.P. GTP 58
- Vetoshkin, Sergey SRP 39
- Vetushka, A. M. NWP 66,
VF2 2
- Vidal, Francois FT2 4
- Vidmar, Robert FT2 6,
NWP 38
- Vilaithong, T. VF1 3
- Vladimirov, S. V. BT1 3
- von Andrian, U.H. SRP 28
- Vourdas, N SRP 52
- Vrinceanu, Daniel GTP 73,
PR1 1, PR1 4
- Vu, K. O. GTP 15
- Vušković, L. HW1 4
- Vyas, Vivek XF2 3

W

Waelbroeck, Frank.L.
 FT1 5
 Waldorff, Erik **NWP 58**
 Walters, H R J **NWP 11**
 Walton, S.G. **GTP 13**,
LW2 5
 Wang, J.Q. **NWP 29**
 Wang, Soon Jung **SRP 53**
 Wang, X. **HW2 4**
 Wang, Xu **FT1 1**, **GTP 66**,
NWP 44, **NWP 47**
 Ward, Barry **GTP 38**,
MW1 7
 Warthesen, Sarah **HW2 3**
 Wass, Anthony **NWP 58**
 Watanabe, Yukio **SRP 47**
 Wendt, Amy **SRP 48**
 Wendt, Martin **NWP 22**,
NWP 23, **NWP 26**
 Whelan, Colm T **NWP 11**
 White, Robert **LW2 1**
 Wieman, S. **QR2 4**
 Wilke, C. **PR2 6**

Wilkinson, Stephen P.
GTP 24
 Williamson, James M.
NWP 30, **SRP 24**
 Williams, Shuntel **SRP 48**
 Williams, Skip **WF1 4**
 Winkler, Rolf **GTP 45**
 Wise, Richard **DTW 1**
 Wolford, M. **SRP 38**
 Won, Dong Ho **MW1 5**,
WF2 3
 Wu, Alan **GTP 58**

X

Xiang, Nong **FT1 5**,
NWP 45
 Xu, S. **BT1 3**, **CT1 3**,
ET2 1, **GTP 5**, **GTP 11**,
NWP 55

Y

Yadav, Manish **GTP 24**
 Yalin, Azer **NWP 31**

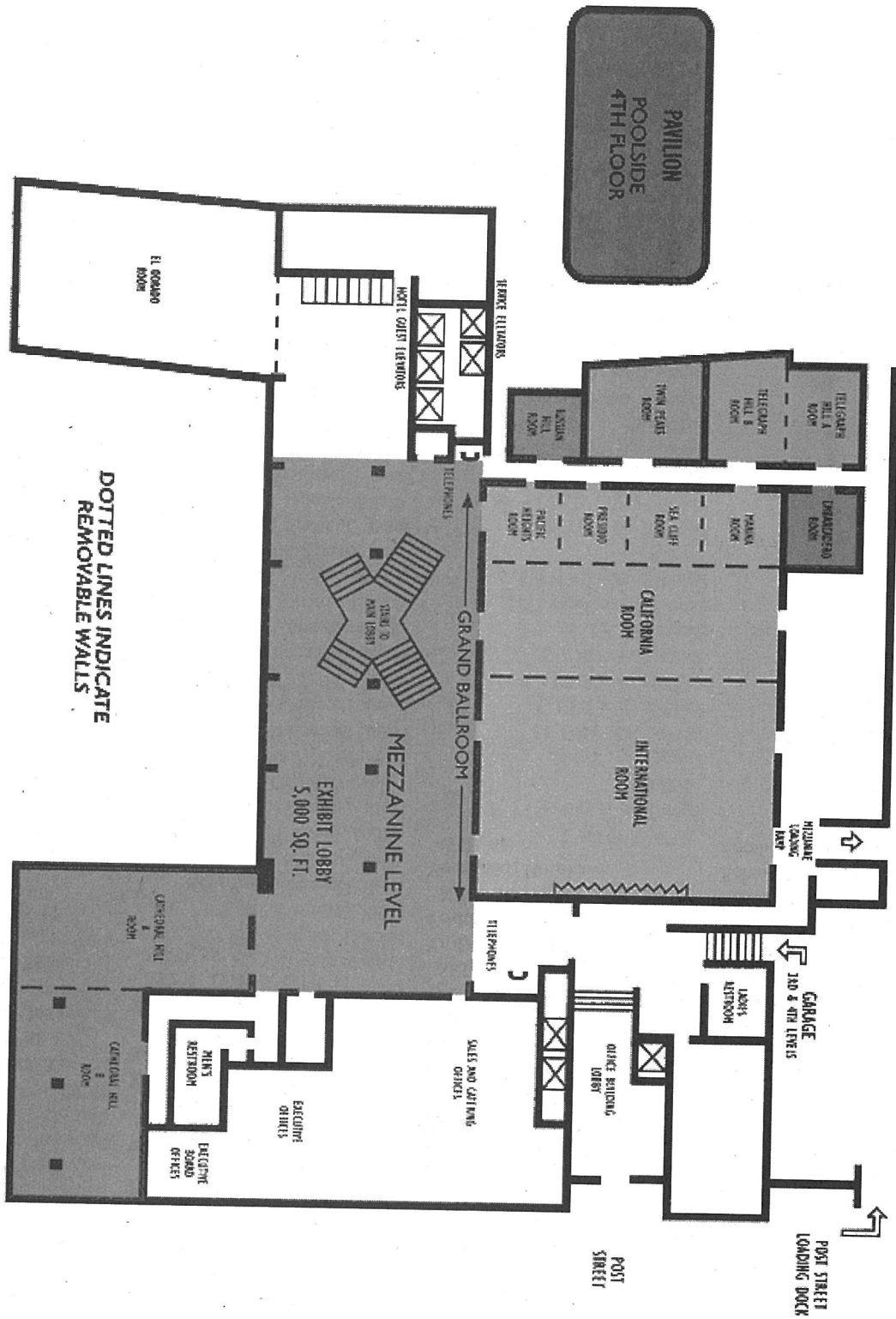
Yamabe, Chobei **GTP 30**,
GTP 31, **SRP 35**,
SRP 36
 Yamagata, Yukihiko
NWP 5, **QR2 3**
 Yamakoshi, Hideo **CT2 1**,
GTP 62
 Yamartino, John **MW2 3**
 Yamatake, Atsushi **GTP 32**
 Yang, Jang-Gyoo **HW1 5**
 Yang, Yunqiang **SRP 12**
 Yan, Wendy **DTW 1**
 Yarkony, David **WF1 4**
 Yasuoka, Koichi **GTP 32**
 Yasuo, Komukai **HW1 3**
 Yazawa, Hiroyuki **SRP 25**
 Yellina, Rayan **NWP 36**
 Yeom, Geun Young
SRP 53
 Yi, Dechang **SRP 41**
 Yoshiharu, Nakamura
NWP 10
 Yoshiyuki, Hosokawa
GTP 61

Yoshizaki, Yasunao
NWP 7
 Youichi, Shintani **NWP 27**
 You, K.-I **GTP 9**
 You, ShinJae **GTP 63**
 Yugami, Noboru **NWP 57**,
NWP 59
 Yu, L. D. **VF1 3**
 Yu, M. Y. **BT1 3**
 Yuryshv, Nikolay **FT2 8**
 Yu, Zengqi **NWP 31**,
SRP 27

Z

Zhang, Peng **BT2 2**
 Zhang, Zhijong **XF1 6**
 Zheng, Wengang **BT1 4**
 Zhou, N. **ET2 6**
 Zhou, Ning **FT2 3**,
GTP 4, **GTP 59**
 Zhou, Otto **CT1 2**
 Zigon, Dusan **SRP 31**
 Zoheir, Harrache **SRP 32**
 Zoran, Petrović **GTP 44**

Cathedral Hill Hotel



DOTTED LINES INDICATE
REMOVABLE WALLS

On the Cover: From left to right: Simulated wave plasma current and magnetic field in a helicon discharge, Deepak Bose, Eloret Corporation; Modified GEC reference cell used at NASA Ames Research Center, M. Meyyappan; Carbon nanofibers grown in a dc plasma with a hot filament pre-treatment, Brett A. Cruden, Alan M. Cassell, Eloret Corporation, Qi Ye, Integrated Nanosystems, Inc., and M. Meyyappan, NASA Ames Research Center. Photo layout courtesy of Jay Nuez.

Epitome of the 56th Gaseous Electronics Conference of the American Physical Society

19:00 MONDAY EVENING
20 OCTOBER 2003

AM Reception and Registration
Mezzanine Lobby, Cathedral Hill Hotel

8:00 TUESDAY MORNING
21 OCTOBER 2003

BT1 Dusty Plasmas
California Ballroom, Cathedral Hill Hotel

BT2 Atmospheric Pressure Glow
Discharges
International Ballroom, Cathedral Hill Hotel

10:00 TUESDAY MORNING
21 OCTOBER 2003

CT1 Carbon Nanotube Growth
Meyyappan, Zhou
California Ballroom, Cathedral Hill Hotel

CT2 Capacitively Coupled Plasmas
International Ballroom, Cathedral Hill Hotel

11:45 TUESDAY MORNING
21 OCTOBER 2003

DTW Special Session: Trends in Plasma Etching
International Ballroom, Cathedral Hill Hotel

13:15 TUESDAY AFTERNOON
21 OCTOBER 2003

ET1 Biological Applications of
Plasmas I
Stoffels, Stalder, Petrović
California Ballroom, Cathedral Hill Hotel

ET2 Inductively Coupled Plasmas
International Ballroom, Cathedral Hill Hotel

15:30 TUESDAY AFTERNOON
21 OCTOBER 2003

FT1 Plasma Sheaths
California Ballroom, Cathedral Hill Hotel

FT2 Plasma Chemistry
International Ballroom, Cathedral Hill Hotel

19:15 TUESDAY EVENING
21 OCTOBER 2003

GTP Poster Session I
El Dorado, Cathedral Hill Hotel

8:00 WEDNESDAY MORNING
22 OCTOBER 2003

HW1 Diagnostics I
California Ballroom, Cathedral Hill Hotel

HW2 Nanostructures and
Nanoparticles
Shiratani
International Ballroom, Cathedral Hill Hotel

10:00 WEDNESDAY MORNING
22 OCTOBER 2003

JW GEC Foundation Talk
Coburn
International Ballroom, Cathedral Hill Hotel

11:15 WEDNESDAY MORNING
22 OCTOBER 2003

KW Business Meeting
International Ballroom, Cathedral Hill Hotel

13:15 WEDNESDAY AFTERNOON
22 OCTOBER 2003

LW1 Atomic Ionization
Schulz
California Ballroom, Cathedral Hill Hotel

LW2 Innovative Applications of
Discharges
International Ballroom, Cathedral Hill Hotel

15:30 WEDNESDAY AFTERNOON
22 OCTOBER 2003

MW1 Lighting I
Kroesen
California Ballroom, Cathedral Hill Hotel

MW2 Material Processing I
Gottscho, Cunge
International Ballroom, Cathedral Hill Hotel

19:15 WEDNESDAY EVENING
22 OCTOBER 2003

NWP Poster Session II
El Dorado, Cathedral Hill Hotel

8:00 THURSDAY MORNING
23 OCTOBER 2003

PR1 Rydberg Plasmas and Highly
Excited Atoms
Vrinceanu, Gould
California Ballroom, Cathedral Hill Hotel

PR2 Glows
International Ballroom, Cathedral Hill Hotel

10:00 THURSDAY MORNING
23 OCTOBER 2003

QR1 Electron Scattering
Buckman
California Ballroom, Cathedral Hill Hotel

QR2 Environmental Applications
Rousseau
International Ballroom, Cathedral Hill Hotel

11:30 THURSDAY MORNING
23 OCTOBER 2003

RRW Thermal Plasma Workshop
International Ballroom, Cathedral Hill Hotel

13:30 THURSDAY AFTERNOON
23 OCTOBER 2003

SRP Poster Session III
El Dorado, Cathedral Hill Hotel

15:30 THURSDAY AFTERNOON
23 OCTOBER 2003

TR1 High Pressure Discharges and Arcs
Tachibana, Miles
California Ballroom, Cathedral Hill Hotel

TR2 Fluorocarbon Etch Mechanisms
International Ballroom, Cathedral Hill Hotel

18:00 THURSDAY EVENING
23 OCTOBER 2003

UR Reception and Banquet
Mezzanine/Pavilion, Cathedral Hill Hotel

8:00 FRIDAY MORNING
24 OCTOBER 2003

VF1 Biological Applications of
Plasmas II
Lohmann, Pimblott
California Ballroom, Cathedral Hill Hotel

VF2 Magnetically-Enhanced Plasmas
International Ballroom, Cathedral Hill Hotel

10:00 FRIDAY MORNING
24 OCTOBER 2003

WF1 Diagnostics II
California Ballroom, Cathedral Hill Hotel

WF2 Lighting II
Uhrlandt, Bartschat
International Ballroom, Cathedral Hill Hotel

13:15 FRIDAY AFTERNOON
24 OCTOBER 2003

XF1 Scattering from Molecular
Targets
Miller
California Ballroom, Cathedral Hill Hotel

XF2 Material Processing II
Chang, Bradley
International Ballroom, Cathedral Hill Hotel



0003-0503(200310)48:6;1-W